

Complex Simplicity

Towards reconstituting Cdc42-based polarity establishment

Tschirpke, S.

DOI

[10.4233/uuid:0b046c92-2aeb-4260-94ec-3e13876e1712](https://doi.org/10.4233/uuid:0b046c92-2aeb-4260-94ec-3e13876e1712)

Publication date

2022

Document Version

Final published version

Citation (APA)

Tschirpke, S. (2022). *Complex Simplicity: Towards reconstituting Cdc42-based polarity establishment*. [Dissertation (TU Delft), Delft University of Technology]. <https://doi.org/10.4233/uuid:0b046c92-2aeb-4260-94ec-3e13876e1712>

Important note

To cite this publication, please use the final published version (if applicable). Please check the document version above.

Copyright

Other than for strictly personal use, it is not permitted to download, forward or distribute the text or part of it, without the consent of the author(s) and/or copyright holder(s), unless the work is under an open content license such as Creative Commons.

Takedown policy

Please contact us and provide details if you believe this document breaches copyrights. We will remove access to the work immediately and investigate your claim.

The background of the cover is an abstract, marbled pattern. The top half features swirling, organic shapes in shades of light blue, pink, and white. The middle section is dominated by a dark blue field filled with intricate, colorful patterns of red, yellow, and green, resembling a microscopic view of a cell or a complex biological structure. The bottom edge is a horizontal band of vibrant, multi-colored patterns, including green, yellow, and red, suggesting a cross-section of a biological tissue or a highly detailed cellular structure.

Complex Simplicity

**Towards reconstituting Cdc42-based
polarity establishment**

Sophie Tschirpke

Complex Simplicity

Towards reconstituting Cdc42-based polarity establishment

Complex Simplicity

Towards reconstituting Cdc42-based polarity establishment

Dissertation

for the purpose of obtaining the degree of doctor
at Delft University of Technology
by the authority of the Rector Magnificus prof. dr. ir. T. H. J. van der Hagen
chair of the Board of Doctorates
to be defended publicly on
Friday 2 December 2022 at 10:00 o'clock

by

Sophie TSCHIRPKE

Master of Science in Chemistry,
Ludwig Maximilian University of Munich, Germany,
born in Bautzen, Germany.

The dissertation has been approved by the promotor

promotor: Dr. ir. L. Laan

copromotor: Dr. A. Jakobi

Composition of the doctoral committee:

Rector Magnificus,	chairman
Dr. ir. L. Laan	Delft University of Technology
Dr. A. Jacobi,	Delft University of Technology

Independent members:

Prof. dr. C. Dekker,	Delft University of Technology
Prof. dr. G. H. Koenderink,	Delft University of Technology
Prof. dr. E. Frey,	Ludwig Maximilian University Munich, Germany
Prof. dr. M. Loose,	Institute of Science and Technology Austria, Austria

Other member:

Dr. R. Eelkema,	Delft University of Technology
-----------------	--------------------------------



Keywords: Cdc42, reconstitution, minimal systems, *in vitro*, prenylation, protein kinetics

Printed by: Gildeprint

Front & Back: by Shazia Farooq (2022)

Copyright © 2022 by S. Tschirpke

ISBN 978-94-6384-393-5

An electronic version of this dissertation is available at <http://repository.tudelft.nl/>.

The moment that you feel that, just possibly, you're walking down the street naked, exposing too much of your heart and your mind and what exists on the inside, showing too much of yourself. That's the moment you may be starting to get it right.

— Neil Gaiman

Contents

Summary	ix
Samenvatting	xi
Zusammenfassung	xiii
Preface	xv
1 Introduction: Minimal systems shed light on cell polarity	1
Graphical abstract	3
Abstract	5
1.1 The Min protein system in <i>E. coli</i>	6
1.2 A minimal system for polarity establishment in <i>S. cerevisiae</i>	12
1.3 Thesis aim and outline	19
Contributions and acknowledgements.	20
2 Materials and methods	21
Graphical abstract	23
2.1 Protein constructs	25
2.2 Buffer composition	32
2.3 Protein expression and purification	32
2.4 Flag pulldown assay	33
2.5 GTPase activity assay	35
2.6 Synthesis of H ₂ N-Gly ₃ -cysteamine-farnesyl ('farnesyl peptide')	36
2.7 Sortase-mediated reactions	37
2.8 Preparation of farnesylated protein for mass-spectroscopy	39
2.9 Total internal reflection fluorescence (TIRF) microscopy	39
3 Cdc42 construct design for <i>in vitro</i> studies	43
Graphical abstract	45
Abstract	47
3.1 Introduction	47
3.2 Results	49
3.3 Discussion	60
3.4 Appendix	64
Contributions and acknowledgements.	68
4 Synergistic regulation of the Cdc42 GTPase cycle	69
Graphical abstract	71
Abstract	73
4.1 Introduction	73
4.2 Results	74

4.3 Discussion	91
4.4 Appendix	92
Contributions and acknowledgements.101
5 Approaches for Cdc42 with membrane-binding capabilities	103
Graphical abstract105
Abstract107
5.1 Introduction107
5.2 Results109
5.3 Discussion122
5.4 Appendix125
Contributions and acknowledgements.130
6 The effect of buffer components on protein functionalities	131
Graphical abstract133
Abstract135
6.1 Introduction135
6.2 Results137
6.3 Discussion138
Contributions and acknowledgements.140
7 Preliminary data and outlook	141
Graphical abstract143
Abstract145
Results and discussion.145
Contributions and acknowledgements.151
8 Conclusion and discussion: <i>why, how, and what?</i>	153
Bibliography	159
Acknowledgements	173
Curriculum Vitæ	179
List of Publications	181

Summary

How do cells create their internal order? According to the second law of thermodynamics, any system of particles maximises its entropy, thereby increasing the system's disorder. Cells counteract this natural process through expending energy; dynamic interactions between molecules that consume energy lead to intracellular structures and organisation. What are these interactions?

In this thesis I explore this question using the example of Cdc42-based polarity establishment: The yeast *Saccharomyces cerevisiae* proliferates through budding, where a daughter cell grows by budding off one side of the mother. The first step towards budding is polarity establishment; here the cell goes from a state of having the protein Cdc42 uniformly distributed towards one where it is accumulated in one spot on the cell membrane, marking the site of bud-emergence. Cdc42 accumulation arises through interconnected regulatory feedback loops that are based on a reaction-diffusion mechanism and the actin cytoskeleton. The exact molecular mechanisms underpinning Cdc42 accumulation remain controversial, because of both the parameter sensitivity of the system and the high level of observed redundancy and interdependence within and between the feedback loops.

I present our work towards building a minimal *in vitro* system for Cdc42-based polarity establishment. Minimal systems follow the Richard Feynman saying "what I cannot create, I do not understand". They are a subgroup of the *in vitro* methodology in which a particular cellular function is reconstituted with a minimal number of required components. Minimal systems allow a high level of control over the system and the components involved: for example, proteins can be added and removed at will, and protein concentrations and their ratios, the temperature, and the compartment shape of the system can easily be modified. This facilitates mechanistic studies and can help us understand how molecular functions necessary for polarity establishment are distributed within a protein network. I start by focusing on our methodology through asking *why*: *Why* are minimal systems useful? I explore this question on the example of the Min protein system in *Escherichia coli*, for which a minimal system was established in 2008. I discuss what led to its establishment and what this system and follow-up investigations taught us (Chapter 1).

I then show our progress towards establishing a minimal system for Cdc42-based polarity establishment, which is based on the three proteins Cdc42, Cdc24, and Bem1:

We explore how additions to Cdc42, such as purification tags, affect the protein behaviour. Purification tags are needed to isolate the protein from its expression host. We observe that most purification tags, with the exception of the Twin-Strep-tag placed at the protein's N-terminus, do not influence Cdc42's expression level and activity. We further show that the T7-lead, a peptide tag aiding protein expression, is needed for expressing Cdc42 (a *S. cerevisiae* gene) in *E. coli*. We use the case of Cdc42 as an example to discuss general criteria relevant for protein construct design in *in vitro* studies (Chapter 3).

We continue by investigating the dynamic properties of Cdc42. Cdc42 is a GTPase and part of a complex network of polarity proteins, including GDP/GTP exchange factors (GEFs), GTPase activating proteins (GAPs), guanine nucleotide dissociation inhibitors, scaffold proteins, and other

regulatory proteins, that all interact with each other and with Cdc42 in particular. We study the kinetic properties of Cdc42's GTPase activity and the effect of molecular crowding, GEF Cdc24, GAP Rga2, scaffold protein Bem1, and combinations thereof, on it. We observe that all four increase the GTPase activity of Cdc42, and that Cdc24 synergises with Rga2 (Chapter 4).

We then address a big obstacle for using Cdc42 in *in vitro* experiments. In yeast cells, Cdc42 gets post-translationally modified: a hydrophobic tail is appended to the protein's C-terminus. This hydrophobic tail is responsible for binding Cdc42 to membranes. Obtaining post-translationally modified Cdc42 remains a challenge and available methods are not accessible for scientists from many backgrounds. We set out to explore three more accessible methods for producing membrane-binding Cdc42: (1) one that appends the hydrophobic tail in an *in vitro* reaction, (2) one that adds the machinery responsible for the modification to *E. coli* cells, and (3) one that is based on adding an alternative membrane-binding domain to Cdc42. Our investigations indicate that method (1) is most promising, as the produced protein remains fully active and binds strongly to membranes (Chapter 5).

Next, we investigate how buffer components affect protein properties. Most *in vitro* assays are conducted in a buffer, and some of the added components can be required for, while others inhibit, protein functioning. We find that calcium ions, contrary to previous findings, do not disrupt binding of the proteins Bem1 and Cdc24. Furthermore, magnesium ions decrease the Cdc42 GTPase activity, but are required for the GTPase cycle boosting effect of Cdc24 on Cdc42 (Chapter 6). Lastly, we add the three proteins Cdc42, GEF Cdc24, and scaffold Bem1 to a supported lipid bilayer and observe their behaviour with total internal fluorescence microscopy. Theoretical work proposes that these proteins can lead to Cdc42 accumulation on the membrane. However, we did not observe Cdc42 accumulation and suspect that this is due to the parameter regime (protein concentrations and ratios, experimental setup) we used. We believe that further experiments, screening wider parameter ranges, are required to establish the minimal system (Chapter 7).

Taken together, our work builds a solid foundation for establishing a minimal system for Cdc42-based polarity establishment. We explored in-depth the fundamentals required and addressed the obstacles that needed to be overcome.

Samenvatting

Hoe creëren cellen hun interne orde? Volgens de tweede wet van de thermodynamica maximaliseert elke systeem van deeltjes zijn entropie, waardoor de wanorde van het systeem toeneemt. Cellen werken dit natuurlijke proces tegen door energie te verbruiken; dynamische interacties tussen moleculen die energie verbruiken leiden tot intracellulaire structuren en organisatie. Wat zijn deze interacties?

In dit proefschrift onderzoek ik deze vraag aan de hand van het voorbeeld van op Cdc42 gebaseerde polariteitsvestiging: De gist *Saccharomyces cerevisiae* prolifereert door knopvorming, waarbij een dochtercel groeit aan één kant van de moeder. De eerste stap in de richting van knopvorming is het bevestigen van polariteit; hier gaat de cel van een toestand waarin het eiwit Cdc42 gelijkmatig is verdeeld naar één waar het zich op één plek op het celmembraan verzamelt en de plaats van de celdeling markeert. Cdc42-accumulatie ontstaat door onderling verbonden regelgevende feedback-lussen die gebaseerd zijn op een reactie-diffusiemechanisme en het actine-cytoskelet. De exacte moleculaire mechanismen die Cdc42-accumulatie onderliggen blijven controversieel, vanwege zowel de parametergevoeligheid van het systeem en de hoge mate van waargenomen redundantie en onderlinge afhankelijkheid binnen en tussen de feedback-lussen.

Ik presenteer ons werk aan het bouwen van een minimaal *in vitro* systeem voor op Cdc42 gebaseerde polariteitsvestiging. Minimale systemen volgen wat Richard Feynman heeft gezegd: "wat ik niet kan creëren, begrijp ik niet". Ze vormen een subgroep van de *in vitro*-methodologie waarin een bepaalde cellulaire functie wordt gereconstitueerd met een minimaal aantal benodigde componenten. Minimale systemen geven een hoge mate van controle over het systeem en de betrokken componenten: eiwitten kunnen bijvoorbeeld worden toegevoegd en verwijderd, en eiwitconcentraties, hun verhoudingen, de temperatuur, en de compartimentvorm van het systeem kan eenvoudig worden gewijzigd. Dit vergemakkelijkt mechanistische onderzoek en kan ons helpen te begrijpen hoe moleculaire functies, die nodig zijn voor het vaststellen van polariteit, zijn verdeeld binnen eiwitnetwerken. Ten eerste focus ik op onze methodologie en vraag *waarom?*: *Waarom* zijn minimale systemen nuttig? Ik onderzoek deze vraag aan de hand van het voorbeeld van het Min-eiwit systeem in *Escherichia coli*, waarvoor in 2008 een minimaal systeem is opgezet. Ik bespreek wat tot de oprichting ervan heeft geleid en wat dit systeem en vervolgonderzoek ons hebben geleerd (hoofdstuk 1).

Vervolgens laat ik onze vooruitgang zien bij het opzetten van een minimaal systeem voor op Cdc42 gebaseerde polariteitsvestiging, die is gebaseerd op de drie eiwitten Cdc42, Cdc24, en Bem1:

We onderzoeken hoe het aanbrengen van zuiveringstags aan Cdc42 het eiwitgedrag beïnvloeden. Zuiveringstags zijn nodig om het eiwit te isoleren van zijn gastheer. We merken dat de meeste zuiveringstags, met uitzondering van de Twin-Strep-tag die aan het N-uiteinde van het eiwit is geplaatst, geen invloed op de expressieniveau en activiteit van Cdc42 hebben. We laten verder zien dat de T7-lead, een peptide-tag die eiwitexpressie helpt, nodig is voor de expressie van Cdc42 (een *S. cerevisiae*-gen) in *E. coli*. Wij gebruiken Cdc42 als voorbeeld voor het bespreken van alge-

mene criteria voor het ontwerp van eiwitconstructen voor *in vitro* onderzoek (hoofdstuk 3). We gaan vervolgens in op het onderzoeken van de dynamische eigenschappen van Cdc42. Cdc42 is een GTPase en onderdeel van een complex netwerk van polariteitseiwitten, inclusief GDP/GTP-uitwisselingsfactoren (GEFs), GTPase-activerend eiwitten (GAPs), guanine-nucleotide- dissociatieremmers, scaffold-eiwitten, en andere regulerende eiwitten, die allemaal met elkaar en met Cdc42 in het bijzonder interacteren. We onderzoeken de kinetische eigenschappen van de GTPase-activiteit van Cdc42 en het effect van moleculaire crowding, de GEF Cdc24, GAP Rga2, scaffold-eiwit Bem1, en combinaties daarvan, erop. We zien dat alle vier factoren de GTPase-activiteit van Cdc42 toe laten nemen, en dat Cdc24 met Rga2 synergiseert (hoofdstuk 4).

Vervolgens pakken we een groot obstakel aan voor het gebruik van Cdc42 in *in vitro*-experimenten. In gistcellen wordt Cdc42 post-translationeel gemodificeerd: een hydrofobe groep wordt toegevoegd aan de C-terminus van het eiwit. Deze hydrofobe groep is verantwoordelijk voor het binden van Cdc42 aan membranen. Post-translationeel gemodificeerde Cdc42 in handen krijgen blijft een uitdaging en beschikbare methoden zijn niet toegankelijk voor wetenschappers uit vele achtergronden. We gingen op zoek naar drie meer toegankelijke methoden om membraanbindend Cdc42 te produceren: (1) een die de hydrofobe groep toevoegt in een *in vitro* reactie, (2) een die het systeem, dat verantwoordelijk is voor de modificatie, toevoegt aan *E. coli*-cellen, en (3) een die is gebaseerd op het toevoegen van een alternatief membraanbindend domein aan Cdc42. Onze onderzoek toont aan dat methode (1) meest veelbelovend is, omdat het geproduceerde eiwit volledig actief blijft en sterk aan membranen bindt (hoofdstuk 5).

Vervolgens onderzoeken we hoe buffercomponenten de eiwiteigenschappen beïnvloeden. De meeste *in vitro*-assays zijn uitgevoerd in een buffer, en sommige van de toegevoegde componenten kunnen nodig zijn voor eiwitwerking, terwijl andere deze remmen. We vinden dat calciumionen, in tegenstelling tot eerdere bevindingen, niet de binding van de eiwitten Bem1 en Cdc24 verstoren. Verder verlagen magnesiumionen de Cdc42 GTPase-activiteit, maar zijn vereist voor het GTPase-cyclus verhogende effect van Cdc24 op Cdc42 (hoofdstuk 6).

Ten slotte voegen we de drie eiwitten Cdc42, GEF Cdc24, en scaffold Bem1 toe op een ondersteund lipide dubbellaag en observeren hun gedrag met behulp van totale interne reflectie fluorescentiemicroscopie. Theoretisch werk suggereert dat deze eiwitten kunnen leiden tot Cdc42-accumulatie op het membraan. Echter, hebben we geen Cdc42-accumulatie waargenomen. We vermoeden dat dit te wijten is aan het parameterregime (eiwitconcentraties en -verhoudingen, experimentele opstelling) die we gebruikten. Wij geloven dat verdere experimenten, die grotere parameterbereiken screenen, nodig zijn om het minimale systeem op te zetten (hoofdstuk 7).

Tot slot vormt ons werk een stevige basis voor het opzetten van een minimaal systeem voor Cdc42- gebaseerde polariteitsvestiging. We hebben de vereiste basisprincipes grondig onderzocht en hebben de obstakels, die overwonnen moesten worden, aangepakt.

Zusammenfassung

Wie schaffen Zellen ihre innere Ordnung? Nach dem zweiten Hauptsatz der Thermodynamik maximiert jedes Teilchensystem seine Entropie und erhöht dadurch die Unordnung des Systems. Zellen wirken diesem natürlichen Prozess entgegen, indem sie Energie verbrauchen; dynamische Wechselwirkungen zwischen Molekülen, die Energie verbrauchen, führen zu intrazellulären Strukturen und zur Organisation. Was sind das für Wechselwirkungen?

In dieser Arbeit gehe ich dieser Frage am Beispiel der Cdc42-basierten Polaritätsherstellung nach: Die Hefe *Saccharomyces cerevisiae* vermehrt sich durch Knospung - die Tochterzelle wächst als Knospe aus einer Seite der Mutter heraus. Der erste Schritt zum Knospen ist die Herstellung der Polarität: Hier geht die Zelle von einem Zustand, in dem das Protein Cdc42 gleichmäßig verteilt ist, zu einem über wo es sich an einer Stelle auf der Zellmembran ansammelt und dort den Ort der Knospenbildung markiert. Die Cdc42-Akkumulation entsteht durch miteinander verbundene regulatorische Rückkopplungsschleifen, die auf einem Reaktions-Diffusions-Mechanismus und dem Aktin-Zytoskelett beruhen. Die genauen molekularen Mechanismen die zur Cdc42-Akkumulation führen bleiben umstritten. Der Grund dafür ist die Parametersensitivität des Systems und das hohe Maß an beobachteter Redundanz und Interdependenz innerhalb und zwischen der Rückkopplungsschleifen.

Ich stelle unsere Arbeit zum Aufbau eines Minimalen *In-vitro*-Systems für die Cdc42-basierte Polaritätsherstellung vor. Minimale Systeme folgen dem Ausspruch von Richard Feynman: „Was ich nicht erschaffen kann, das verstehe ich nicht“. Sie sind eine Untergruppe der *In-vitro*-Methodik, bei der eine bestimmte zelluläre Funktion mit der minimalen Anzahl an erforderlichen Komponenten rekonstituiert wird. Minimale Systeme ermöglichen ein hohes Maß an Kontrolle über das System und über die beteiligten Komponenten: Proteine können nach Belieben hinzugefügt und entfernt werden, und die Proteinkonzentrationen und ihre Verhältnisse, die Temperatur, und die Form des Systems kann leicht verändert werden. Dies ermöglicht mechanistische Studien und kann unserem Verständnis über die Verteilung von molekularen Funktionen (die für die Polaritätsherstellung notwendig sind) in Proteinnetzwerken zuträglich sein. Zu Beginn fokussiere ich mich auf unsere Methodik und frage *warum?*: *Warum* sind Minimale Systeme sinnvoll? Ich gehe dieser Frage am Beispiel des Min-Protein Systems in *Escherichia coli* nach, für das ein Minimales System in 2008 etabliert wurde. Ich diskutiere was zu seiner Erschaffung notwendig war und was uns dieses System und seine Nachfolger gelehrt haben (Kapitel 1).

Anschließend zeige ich unsere Arbeit an einem Minimalen System für die Cdc42-basierte Polaritätsherstellung, welches auf den drei Proteinen Cdc42, Cdc24, und Bem1 basiert:

Wir untersuchen wie Zusätze an Cdc42, z.B. Aufreinigungs-Tags, das Proteinverhalten beeinflussen. Aufreinigungs-Tags werden benötigt um das Protein aus seinem Expressionswirt zu isolieren. Wir beobachten, dass die meisten Aufreinigungs-Tags, mit Ausnahme des am N-Terminus des Proteins platzierten Twin-Strep-Tags, das Expressionsniveau und die Aktivität von Cdc42 nicht beeinflussen. Wir zeigen, dass der T7-Lead, ein Peptid-Tag, der die Proteinexpression unterstützt, für die Expression von Cdc42 (ein *S. cerevisiae*-Gen) im Bakterium *E. coli* benötigt wird. Wir nehmen Cdc42 als Beispiel um allgemeine Kriterien für das Design von Proteinkonstrukten

für *In-vitro*-Studien zu diskutieren (Kapitel 3).

Wir fahren fort indem wir die dynamischen Eigenschaften von Cdc42 untersuchen. Cdc42 ist eine GTPase und Teil eines komplexen Netzwerks von Polaritätsproteinen. Zu diesen gehören GDP/GTP-Austauschfaktoren (GEFs), GTPase-Aktivierungs Proteine (GAPs), Guaninnukleotid-Dissoziationsinhibitoren, Gerüstproteine, und andere regulatorische Proteine. All diese Proteine interagieren miteinander, und insbesondere mit Cdc42. Wir studieren die kinetischen Eigenschaften der GTPase-Aktivität von Cdc42 und den Effekt von molekularem Crowding, dem GEF Cdc24, dem GAP Rga2, dem Gerüstprotein Bem1, und Kombinationen davon, darauf. Wir beobachten, dass alle vier die GTPase-Aktivität von Cdc42 steigern, und dass Cdc24 mit Rga2 synergisiert (Kapitel 4).

Wir wenden uns dann einem großen Hindernis zu, dass der Verwendung von Cdc42 in *In-vitro*-Experimenten entgegensteht. In Hefezellen wird Cdc42 posttranslational modifiziert: An dem C-Terminus des Proteins wird eine hydrophobe Gruppe angehängt. Diese hydrophobe Gruppe ist dafür verantwortlich, dass Cdc42 an Membranen binden kann. Der Erwerb von posttranslational modifiziertem Cdc42 ist eine Herausforderung und die verfügbaren Methoden sind für Wissenschaftler vieler Felder nicht zugänglich. Wir haben drei zugänglichere Herstellungsmethoden für membranbindendes Cdc42 erforscht: (1) eine, die die hydrophobe Gruppe in einer *In-vitro*-Reaktion anhängt, (2) eine, die die für die Modifikation verantwortliche Maschinerie zu *E. coli*-Zellen hinzufügt, und (3) eine, die auf dem Hinzufügen einer alternativen membranbindenden Domäne zu Cdc42 basiert. Unsere Untersuchungen weisen darauf hin, dass Methode (1) am vielversprechendsten ist, da das produzierte Protein komplett aktiv bleibt und stark an Membranen bindet (Kapitel 5).

Wir untersuchen als nächstes wie Pufferkomponenten Proteineigenschaften beeinflussen. Die meisten *In-vitro*-Experimente werden in einem Puffer durchgeführt, und einige der hinzugefügten Komponenten können für Proteinfunktionen notwendig sein, während andere diese hemmen können. Unsere Untersuchungen zeigen, dass Calciumionen - im Gegensatz zu früheren Erkenntnissen - die Bindung zwischen den Proteinen Bem1 und Cdc24 nicht hemmt. Magnesiumionen verringern die Cdc42 GTPase-Aktivität, sind aber für die GTPase-Zyklus verstärkende Wirkung von Cdc24 auf Cdc42 erforderlich (Kapitel 6).

Letztendlich fügen wir die drei Proteine Cdc42, den GEF Cdc24, und das Gerüstprotein Bem1, einer Lipid Doppemembran hinzu, und beobachten ihr Verhalten mit totaler interner Fluoreszenzmikroskopie. Eine theoretische Studie zeigte dass diese Proteine zur Cdc42-Akkumulation auf der Membran führen können. Jedoch konnten wir keine Cdc42-Akkumulation beobachten und vermuten, dass dies auf das von uns verwendete Parameterregime zurückzuführen ist (Proteinkonzentrationen und -verhältnisse, Versuchsaufbau). Wir glauben dass weitere Experimente, die die größere Parameterbereiche erforschen, erforderlich sind um das Minimale System zu etablieren (Kapitel 7).

Zusammenfassend bildet unsere Arbeit eine solide Grundlage für die Etablierung eines Minimalen Systems für Cdc42- basierte Polaritätsherstellung. Wir haben die erforderlichen Grundlagen vertiefend erforscht und die Hindernisse, die es zu überwinden galt, adressiert.

Preface

Simple and Complex

... make a spot, make a stripe, a square, a circle – multiply, multiply, multiply. Change, destroy, rebuild, and multiply! Call it zebra! Call it cloud! Call it leaf! Kiwi! Sunflower! Giraffe! Snowflake!

What?

Full of shapes, they're multiplied!

A pattern?

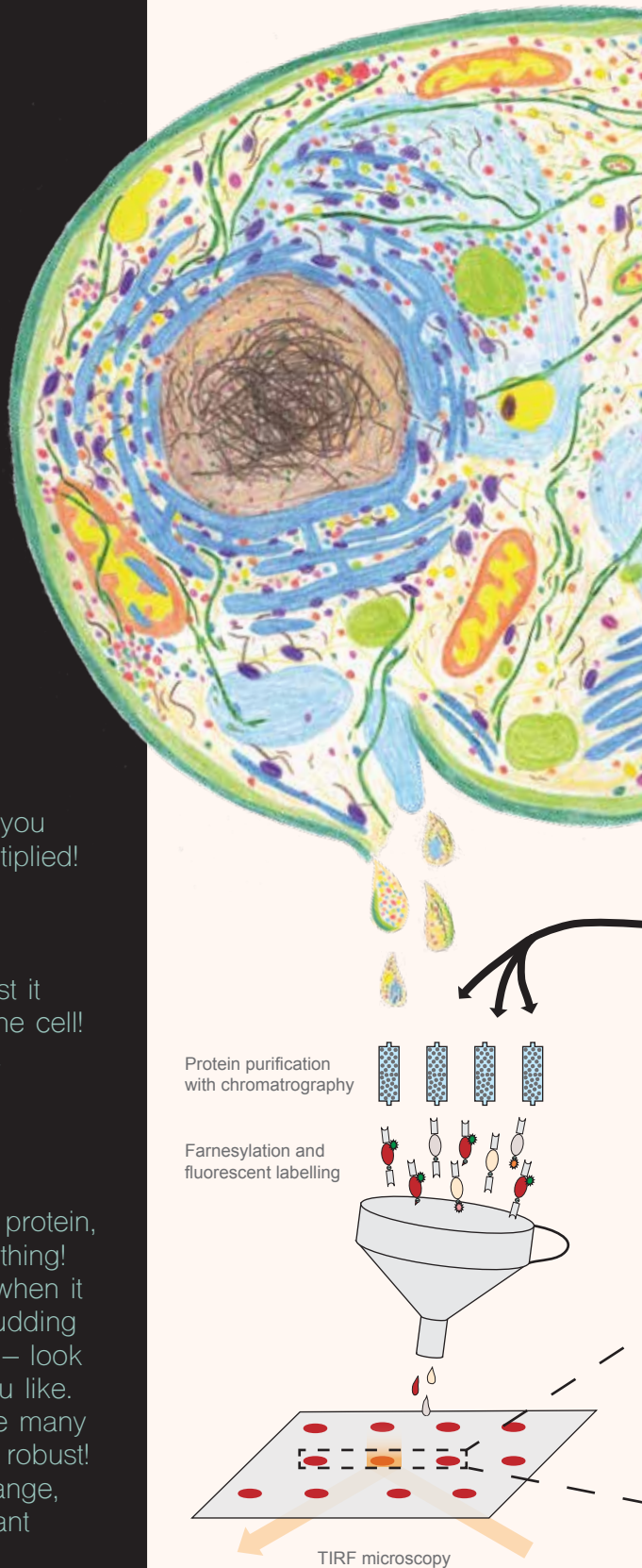
Call it pattern, if you like! In big and small, long and wide, it grows endlessly, it's multiplied! I give you landscapes, give you mammals, give you cells – spots and shapes, forever multiplied!

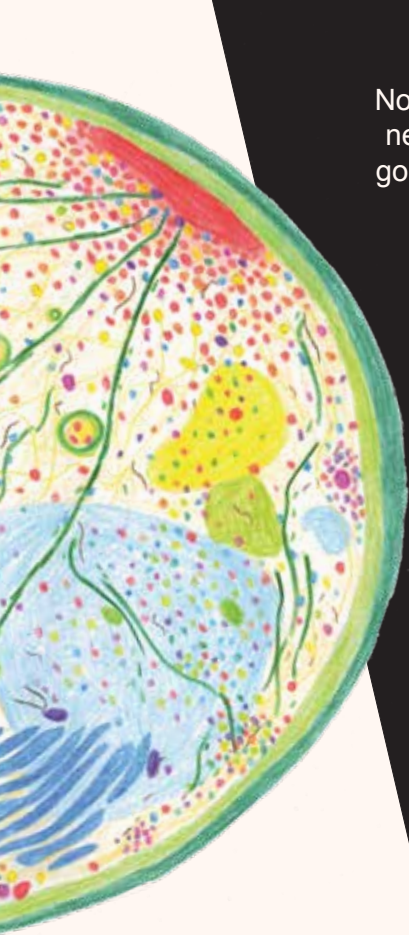
Yeas?

Yeast? Yest? Yeast? Does as well! First it grows, then it buds – divides itself! One cell! Two cells! Four cells! Look how fast it multiplies!

You said spots – there are no spots!

Spots there are – look inside! Take a protein, make it king, give it power over everything! Let it regulate the cell; how it grows, when it grows! Recruit it to a spot – let the budding start! Take its servants, actin, proteins – look it's getting there! Call it feedback if you like. One feedback loop, two loops, maybe many more! Make interconnections! Make it robust! Make it sensitive – adaptable! We change, environment changes, the king's servant network changes. Yeast stays!





Now I get you! I take apart, I purify, I label your king! I give it a new crown – small and bright – shine light on it, look where it goes! I take some of its servants – not all, only the essential – teach your king humility! I put them together, shall they live in a new home – make a membrane on a slide!
 I model and investigate! I make it general!
 I know how spots work: take a membrane, a protein switch, a redistribution process, mass conservation, a Turing instability! Observe a pattern – yes or no?
 Change conditions – observe again!
 I make a model and go on!

Conquered. Taken apart. Broken life – artificially.

But understood!

Do you?! Make a change – it won't match your prediction. Toss your model, it's not right!

Do not fear me – trust me.

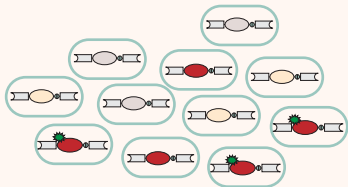
But why?

I'm here to understand you, not to break you.
 To admire you. To let you show me the world.

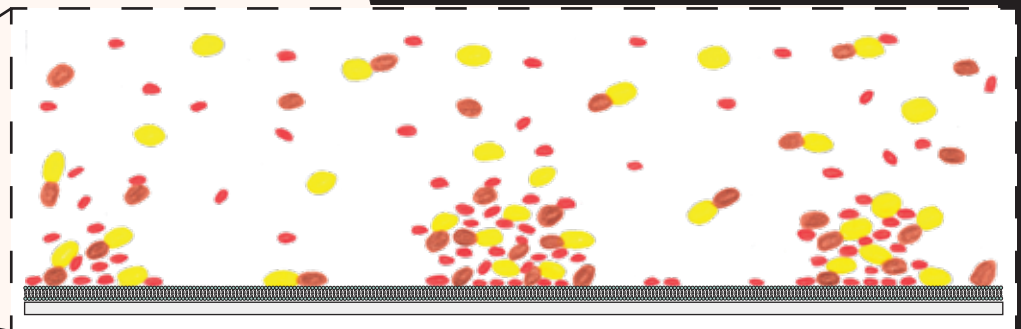
Who are you?

Simplicity, on behalf of science. Who are you?
 Whom did I fell in love with?

Complexity, on behalf of nature.



Protein expression in *E. coli*



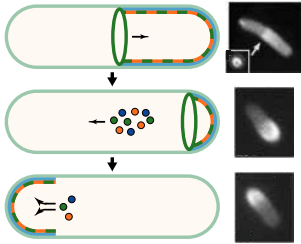
Protein pattern formation on a supported lipid bilayer

1

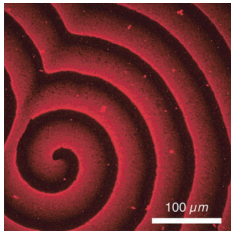
Science gets reality itself to collaborate with us, because our intuitions are all off.

— Rebekka Goldstein

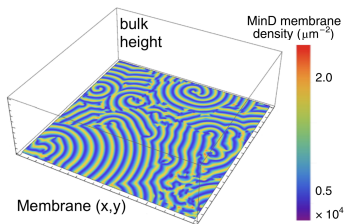
Sources and Copyright statements of images used in the graphical abstract



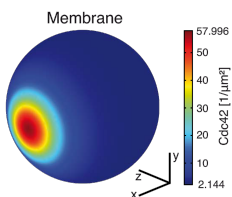
The schematic illustration on the left is adapted from *Loose et al. (2011b)* with permission conveyed through Copyright Clearance Center. The microscopy image on the top right is taken from *Raskin and de Boer (1997)* with permission conveyed through Copyright Clearance Center. The microscopy images on the middle and bottom right are taken from *Raskin and de Boer (1999b)*, Copyright (1999) National Academy of Sciences.



Taken from *Loose et al. (2008)*, reprinted with permission from AAAS (conveyed through Copyright Clearance Center).



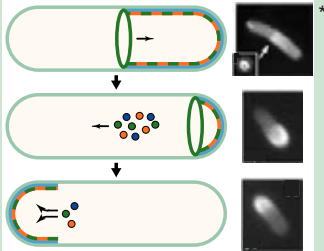
Reprinted with permission from the Licensor (conveyed through Copyright Clearance Center): Springer Nature, [Nature Physics](#) [Rethinking pattern formation in reaction-diffusion systems, J. Halatek *et al.*] Copyright (2018) (*Halatek et al. (2018)*).



Taken from *Klünder et al. (2013)*.

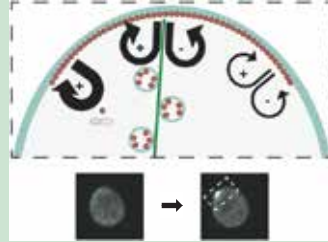
Introduction: Minimal systems shed light on cell polarity

In vivo



The Min proteins oscillate between the cell poles of *E. coli* (Raskin and de Boer, 1997, 1999)

In vivo



Multiple feedback loops lead to Cdc42 accumulation in one spot on the membrane (e.g. reviewed in Chiou *et al.* 2017)

In vitro

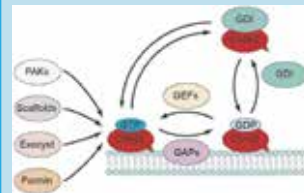
Minimal systems



Reconstitution of Min protein waves (Loose *et al.* 2008)

+ follow-up investigations
+ extension of the system

In vitro



Protein-protein and protein-membrane interaction studies of polarity proteins centering Cdc42

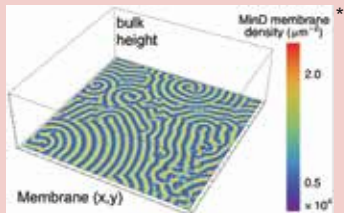
(e.g. Zheng *et al.* 1993,1994; Zhang *et al.* 1999; Johnson *et al.* 2009, 2012; Rapali *et al.* 2017; Golding *et al.* 2019)

Combination of *in vitro* and *in silico* findings

Minimal systems

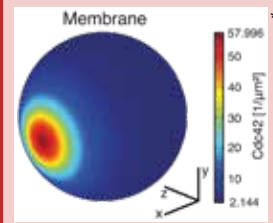
In silico

Many mechanisms for Min oscillations; refinement through minimal system data:



e.g. formation of Min waves *in vitro* (Halatek *et al.* 2018)
[Reprinted with permission from Springer Nature]

In silico



e.g. Cdc42 accumulation *in vivo* is driven by positive feedback of Cdc24 and Bem1 (Klünder *et al.* 2013)



Timeline

MinCDE system in *E. coli*



Cdc42-based polarity in *S. cerevisiae*

Introduction: Minimal systems shed light on cell polarity

Abstract Cell polarity refers to the morphological and functional differentiation of cellular compartments in a directional manner. It is required for processes such as orientation of cell division, directed cellular growth and motility. How the interplay of components within the complexity of a cell leads to cell polarity is still heavily debated. Here, I focus on one specific aspect of cell polarity: the non-uniform accumulation of proteins on the cell membrane. In cells, this is achieved through reaction-diffusion and/or cytoskeleton-based mechanisms. In this thesis I show our progress towards establishing a minimal system for Cdc42-based cell polarity in *Saccharomyces cerevisiae*. Minimal systems are *in vitro* reconstitutions of a particular cellular function with a minimal number of components. In this chapter I first examine the question: *why* do minimal systems matter? I explore this question on the example of the Min protein system from *Escherichia coli*, which represents a reaction-diffusion system with a well-established minimal system. I use this system (1) to show how the minimal system contributed to our understanding this protein systems, and (2) to showcase that efforts towards building minimal systems are worthwhile. I then introduce the processes that lead to polarity establishment in *S. cerevisiae*, discuss how a minimal system for this process could look like, and describe our attempt to realising one. I close by giving an outline of this thesis.

According to the second law of thermodynamics, any system of particles naturally tends to maximise its entropy, increasing the disorder of the system. How is it then possible that cells are intracellularly structured and organised? Spatial organisation in cells – the non-uniform distribution of cellular components – is the result of dynamic interactions between molecules under dissipation of energy (*Karsenti (2008)*). Cell polarity is a special form of spatial organisation that refers to the morphological and functional differentiation of cellular compartments in a directional manner (*Thery et al. (2006)*), which is important for processes where spatial separation is necessary (e.g. growth, division, differentiation and motility). Here, I focus on one specific aspect of cell polarity: the non-uniform accumulation of proteins at the cell membrane. An example is the accumulation of the cell division control protein Cdc42 at the location of the bud-site in

Abbreviations:

BC	basic cluster
GAP	GTPase activating protein
GDI	guanine nucleotide dissociation inhibitor
GEF	GDP/GTP exchange factor
SLB	supported lipid bilayer
TIRF	total internal reflection fluorescence (microscopy)

Saccharomyces cerevisiae cells, acting as a division precursor (**Mazel (2017)**). Cells employ reaction–diffusion and cytoskeleton-based mechanisms to distribute and accumulate proteins (i.e. establish polarity). In reaction–diffusion systems, components are transformed into each other by chemical reactions and are moving in space by diffusion. Under specific conditions, these systems can establish polarity (Box 1.1). In cytoskeleton-based processes, cellular components (e.g. proteins) are actively transported by microtubules and actin filaments to specific locations in the cell.

Cells are complex systems, and combinations of *in vivo*, *in vitro* and *in silico* approaches are required to elucidate the principles of polarity establishment (Box 1.2). In this chapter I discuss the role and importance of *in vitro* approaches in general, and minimal system approaches in particular. Minimal systems are a subgroup of the *in vitro* methodology in which a particular cellular function is reconstituted with a minimal number of required components. I start by examining the Min protein system in *E. coli* - a reaction–diffusion system. Here three proteins (MinC, MinD and MinE) oscillate between the cell poles (i.e. accumulate alternately at the membrane of one of the cell poles). These oscillations result in a time-averaged protein gradient that differentiates the cell centre from the cell poles. The protein oscillations were reconstituted in a minimal system in 2008 (**Loose et al. (2008)**). I use this system to explore the question: *Why* do minimal systems matter? On the example of the Min protein system I discuss what leads to their establishment and what we can learn from them and from follow-up investigations. I then introduce Cdc42-based polarity in *S. cerevisiae*, which is based on reaction–diffusion and cytoskeleton-based mechanisms. I discuss how a minimal system for this system could look like and which steps need to be taken towards establishing it. I close by giving an outline of this thesis.

1.1. The Min protein system in *E. coli*

1.1.1. The Min protein system

E. coli cells divide by binary fission, a process in which the cell divides in its centre into two equally sized daughter cells. Two mechanisms that are independent from each other – nucleoid occlusion to prevent chromosome bisection and the Min system – ensure together that this occurs at the right time and place (**Wu and Errington (2012)**; **Rico et al. (2013)**; **Laloux and Jacobs-Wagner (2014)**). The Min system consists of three proteins, MinC, MinD and MinE (**de Boer et al. (1989)**), which oscillate due to reaction–diffusion processes between the cell poles (**Hu and Lutkenhaus (1999)**; **Raskin and de Boer (1999a,b)**). These oscillations create a time-averaged protein gradient of all three Min proteins with the maxima at the cell poles (Fig. 1.1a). In presence of a membrane, only MinD and MinE are required for oscillations (**Raskin and de Boer (1999a)**) whereas MinC inhibits polymerisation of the protein filamenting temperature- sensitive mutant Z (FtsZ) (**Bi and Lutkenhaus (1991)**; **De Boer et al. (1992)**). Thus, the polymerisation of FtsZ into the Z-ring only occurs at middle of the cell, where it establishes the cell division protein complex, the divisome (**Vicente and Rico (2006)**).

1.1.2. Towards a minimal Min protein system

The reconstituted Min system was not the result of a single methodology, but was established by the synergy of findings from *in vivo*, *in vitro* and *in silico* approaches (Box 1.2). *In vivo* approaches showed which proteins are responsible for the oscillations, what their oscillation patterns look like and which protein domains are required for the oscillations to occur (**de Boer et al. (1989, 1991)**; **Hu and Lutkenhaus (1999, 2001)**; **Raskin and de Boer (1999a,b)**; **Rowland et al. (2000)**; **Fu**

Box 1.1. Polarity establishment through reaction–diffusion processes

In reaction–diffusion systems, components are transformed into each other by chemical reactions and are moving through space owing to diffusion. Systems subject to diffusion are generally spatially uniform (i.e. unordered). However, the unordered state can become unstable if a small perturbation (i.e. a small local deviation from the well-mixed uniform state) gets amplified and thus drives the system towards a non-uniform (i.e. ordered) state. This concept is called a dynamic instability, and hereby cell polarity can be established.

One biologically relevant example is the so-called Turing instability (**Turing (1952)**). In this case, the reaction–diffusion system consists of components whose diffusion constants are of different orders of magnitudes. Order emerges from the combination of molecular diffusion and feedback loops in the reaction system, as diffusive coupling can lead to an instability that gets amplified through the feedback loops.

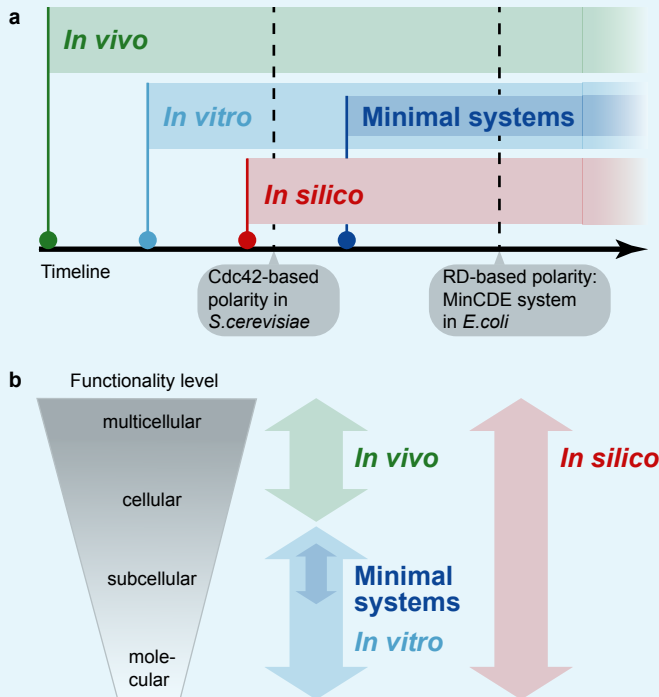
et al. (2001); *Hale et al. (2001)*). Furthermore, they allowed the elucidation of processes involved in the assembly of the global structure of the division machinery, like the polymerisation of FtsZ into a Z-ring (**Bi and Lutkenhaus (1991)**) or those of MinE into the E-ring (**Raskin and de Boer (1997)**). *In vitro* investigations refined this picture by adding mechanistic details; the oscillation mechanism was found through insights on which protein–protein interactions take place (**Huang et al. (1996)**) and further elaborated through the addition of knowledge on domain specificity (**Hu and Lutkenhaus (2000)**; **Szeto et al. (2001)**; **Dajkovic et al. (2008)**). Importantly, *in vitro* experiments revealed the biochemical basis of the oscillations; they showed that MinD exhibits ATPase activity (**de Boer et al. (1991)**) and binds in an ATP- dependent (**Hu et al. (2002)**; **Suefuji et al. (2002)**) and cooperative (**Lackner et al. (2003)**; **Mileykovskaya et al. (2003)**) fashion to the membrane. It forms dimers (**Hu et al. (2002, 2003)**; **Suefuji et al. (2002)**; **Hu and Lutkenhaus (2003)**; **Mileykovskaya et al. (2003)**), recruits MinC and MinE (**Hu et al. (2003)**; **Lackner et al. (2003)**) and is displaced from the membrane upon MinE-stimulated ATP hydrolysis (**Hu and Lutkenhaus (2001)**; **Hu et al. (2002)**; **Hu and Lutkenhaus (2003)**; **Suefuji et al. (2002)**; **Lackner et al. (2003)**) (Fig. 1.1a). These observations of the mechanistic details of molecular events represent the core element for the development of mathematical models, defining which specific reactions take place. Furthermore, *in vitro* experiments contributed to the accuracy of model predictions (that depend on the used parameters) through quantification of the involved reactions, for example, the analysis of reaction kinetics (**de Boer et al. (1991)**). *In silico* work suggested that the Min oscillations can be reconstituted *in vitro* (**Kruse (2002)**) and in an open geometry (**Fischer-Friedrich et al. (2007)**) – proposing an experimentally easily accessible setup.

1.1.3. What did we learn from the minimal Min protein system?

The first reconstitution of the Min dynamics showed that, in presence of ATP, MinD and MinE spontaneously self-organise on a flat, supported lipid bilayer into traveling waves and spirals (**Loose et al. (2008)**) (Fig. 1.1b). This observation revealed the minimal requirements for Min patterns: MinD, MinE, a membrane and ATP. Furthermore, the reconstitution established a highly controlled and adjustable environment for the dissection of the molecular mechanism and the systematic manipulation of the system. Mechanistic insights that were gained are: (1) that the proteins self-organise from a homogeneous state into protein patterns (i.e. require no spatial

Box 1.2. Interplay of *in vivo*, *in vitro* and *in silico* approaches

In vivo experiments deal with complex living systems, reveal the components behind cellular functionalities and characterise their interplay within an organism. Traditionally, this is how biological experiments are conducted. In addition, *in vitro* experiments play an increasingly important role. *In vitro* experiments use purified components to dissect exact molecular mechanisms and obtain more quantitative information. Both *in vivo* and *in vitro* results contribute to the design of *in silico* models. Based on the knowledge from *in vivo* and *in vitro* experiments and guided by model predictions, minimal systems can be established. Minimal systems are specific types of *in vitro* systems that contain enough complexity to reconstitute a specific cellular function (e.g. the formation of a protein gradient), while still using a minimal number of components. Ideally, this allows the conclusive comparison of theoretical predictions and experimental results. The figure below is a schematic representation of the development of *in vivo*, *in vitro* and *in silico* approaches and the functionality levels the different methodologies deal with, including an indication of the current state of the two systems discussed.



markers), (2) that ATP is required for the oscillations to occur, and (3) that the emerging protein waves are based on reaction–diffusion processes, namely the attachment and detachment of proteins on a membrane. Next to this qualitative information, the reconstituted system also facilitated investigations on how features of the system quantitatively influence the protein dynamics, revealing that the MinE to MinD ratio influences the wave velocity and wavelength. The Min oscillations have also been studied intensively *in silico* (Meinhardt and de Boer (2001); Howard et al. (2001); Kruse (2002); Huang et al. (2003); Howard and Rutenberg (2003); Meacci and Kruse (2005); Drew et al. (2005); Kerr et al. (2006); Pavin et al. (2006); Tostevin and Howard (2006); Fange and Elf (2006); Cytrynbaum and Marshall (2007); Fischer-Friedrich et al. (2007); Arjunan and Tomita (2010); Halatek and Frey (2012); Bonny et al. (2013); Hoffmann and Schwarz (2014)). However, the proposed models differed in some fundamental properties, such as the origin of the dynamic instability (Fischer-Friedrich et al. (2007)). The establishment of the minimal system provided a tool to experimentally test the model predictions and the validity of their assumptions. For example, the first Min reconstitution experiment pointed out one source of the dynamic instability: the reversible, cooperative and energy-dependent membrane-binding of proteins and their subsequent detachment (Loose et al. (2008)). Interestingly, although the reconstituted Min waves had a great resemblance to the observations made *in vivo* (Hale et al. (2001)), they displayed an $\approx 10 \times$ greater length scale than those in bacterial cells (Loose et al. (2008)). As it turned out, this discrepancy became one of the strongest driving forces for future investigations.

1.1.4. What insights were gained from further reconstitution experiments?

The development and details of the Min reconstitution experiments are reviewed plentifully (Loose et al. (2011b); Rowlett and Margolin (2015); Kretschmer and Schwille (2016); Halatek et al. (2018); Kretschmer et al. (2018); Wettmann and Kruse (2018)). In the following I use the example of the Min reconstitutions to show the diversity of minimal system investigations and the knowledge that can be gained from it.

Dissecting the influence of single factors on the properties of the system

Minimal systems are ideal environments to inspect the contribution of single factors to the properties of the system, as they facilitate highly controlled, adaptable and reproducible experimental conditions. As mentioned above, the main property that distinguished the reconstituted (Loose et al. (2008)) and the *in vivo* situation was the specific length scale of the Min protein patterns. Many investigations explored factors that could cause this difference, thereby contributing to the characterisation of modulators of the Min dynamics (Fig. 1.2a). The role of geometrical confinement was investigated most, since theoretical models (Varma et al. (2008); Fischer-Friedrich et al. (2010); Halatek and Frey (2012)) and *in vivo* investigations (Raskin and de Boer (1999b); Varma et al. (2008); Corbin et al. (2002); Shih et al. (2005)) had already shown that the Min oscillations are influenced by compartment geometry. The aim to reconstitute the Min oscillations in cell-shaped *in vitro* environments stimulated the development of systems with defined shapes, both *in vitro* and *in vivo* (Mannik et al. (2009); Männik et al. (2012); Wu et al. (2015, 2016)). Experiments in these setups elaborated on how confinement influences the Min dynamics: confinement length and width affects the orientation and period of the oscillations (Schweizer et al. (2012); Zieske and Schwille (2013, 2014); Caspi and Dekker (2016)). In addition, the specific length scale, which is $10 \times$ bigger on flat membranes (Loose et al. (2008)) than *in vivo*, is brought closer to the *in*

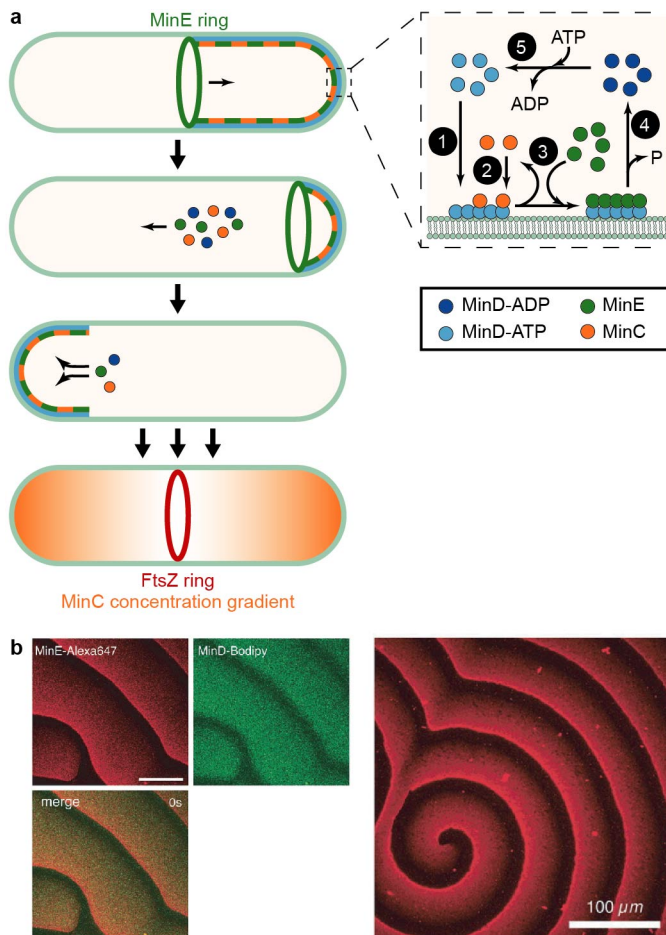


Figure 1.1. Schematic of Min dynamics in *E. coli* and *in vitro* reconstitution of Min dynamics. (a) Schematic of Min dynamics in *E. coli*. Left, MinD-ATP (blue) binds to the membrane and recruits MinC (orange) and MinE (green). A high MinE concentration (MinE ring) diffuses from the middle of the cell towards the poles, causing protein displacement from the membrane. All three proteins diffuse through the cytoplasm and rebind to the plasma membrane. These oscillations result in a MinC concentration gradient that directs FtsZ ring formation to the middle of the cell. Right, the biochemical reactions near and at the membrane. The ATPase MinD (*de Boer et al. (1991)*), in its ATP-bound form (*Hu et al. (2002)*; *Suefuji et al. (2002)*), binds cooperatively (*Lackner et al. (2003)*; *Mileykovskaya et al. (2003)*; *Loose et al. (2011a)*; *Renner and Weibel (2012)*; *Miyagi et al. (2018)*) to the cell membrane (1), dimerises (*Hu et al. (2002, 2003)*; *Suefuji et al. (2002)*; *Hu and Lutkenhaus (2003)*; *Mileykovskaya et al. (2003)*) and recruits MinC (2), forming a MinC–MinD complex (*Hu et al. (2003)*; *Lackner et al. (2003)*). Concomitantly, MinD recruits the ATPase-activating protein MinE, which displaces MinC (3) and subsequently triggers ATP hydrolysis that results in the detachment of ADP-bound MinD (dark blue) from the membrane (*Hu and Lutkenhaus (2001)*; *Hu et al. (2002, 2003)*; *Suefuji et al. (2002)*; *Lackner et al. (2003)*) (4). MinD undergoes nucleotide exchange, diffuses through the cytoplasm and rebinds to the membrane of the opposite cell pole (*Raskin and de Boer (1999b)*) (5). (b) *In vitro* reconstitution of Min protein dynamics. MinD, supplemented with Bodipy-labelled MinD (green), and MinE, supplemented with Alexa Fluor 647-labelled MinE (red), form dynamic surface waves and rotating spirals on a supported lipid bilayer in presence of ATP (*Loose et al. (2008)*). Scale bar: 50 μm , if not indicated otherwise. The images in (a) have been adapted from *Loose et al. (2011b)* with permission conveyed through Copyright Clearance Center; the images in (b) are adapted from *Loose et al. (2008)*, reprinted with permission from AAAS (conveyed through Copyright Clearance Center).

vivo situation through confinement in 3D (**Caspi and Dekker (2016)**). Furthermore, these studies elucidated another feature of the Min dynamics – their adaptability and variety: depending on the chosen confinement, different dynamics and Min patterns occurred (**Ivanov and Mizuchi (2010)**; **Zieske and Schwille (2013, 2014)**; **Caspi and Dekker (2016)**; **Vecchiarelli et al. (2016)**; **Zieske et al. (2016)**). Reaction–diffusion systems are sensitive to parameter changes. Therefore, factors such as temperature (**Touhami et al. (2006)**; **Caspi and Dekker (2016)**), membrane composition (**Mileykovskaya and Dowhan (2000)**; **Koppelman et al. (2001)**; **Mileykovskaya et al. (2003)**; **Szeto et al. (2003)**; **Hsieh et al. (2010)**; **Renner and Weibel (2011, 2012)**; **Shih et al. (2011)**; **Vecchiarelli et al. (2014)**; **Zieske and Schwille (2014)**), diffusion in the cytosol (**Meacci et al. (2006)**; **Schweizer et al. (2012)**; **Martos et al. (2015)**; **Caspi and Dekker (2016)**) and on the membrane (**Meacci et al. (2006)**; **Martos et al. (2013)**), the concentration ratio of MinD to MinE (**Raskin and de Boer (1999b)**; **Shih et al. (2002)**; **Loose et al. (2008)**; **Vecchiarelli et al. (2016)**; **Kretschmer et al. (2017)**; **Miyagi et al. (2018)**) and interaction of MinE with the membrane (**Hsieh et al. (2010)**; **Loose et al. (2011a)**; **Park et al. (2011)**; **Shih et al. (2011)**; **Zieske and Schwille (2014)**; **Vecchiarelli et al. (2016)**; **Kretschmer et al. (2017)**) can also modulate the Min behaviour and cause a difference in the specific length scale in *in vivo* and reconstituted systems. Reconstitution experiments helped, for example, to characterise the role of the membrane- targeting sequence of MinE; **Kretschmer et al.** showed that membrane binding of MinE is not a requirement for Min oscillations, but that it modulates the length scale of the pattern (**Kretschmer et al. (2017)**). Experiments with higher diffusion constants, representing the absence of molecular crowding in the cytosol and on the membrane, showed that these factors account for the increased length scale *in vitro* (**Martos et al. (2013, 2015)**; **Caspi and Dekker (2016)**). By contrast, cardiolipin, which has been speculated to act as a structural cue for MinD membrane binding (**Drew et al. (2005)**; **Mileykovskaya and Dowhan (2005)**; **Cytrynbaum and Marshall (2007)**; **Shih et al. (2011)**), is not required for oscillations (**Vecchiarelli et al. (2014)**; **Zieske and Schwille (2014)**). In summary, the reconstituted environment has been a powerful tool for dissecting which factors are responsible for altering the dynamic behaviour of the Min proteins.

Quantitative characterisation and mechanistic details

Reconstitution experiments have helped to disentangle the molecular mechanisms underlying MinC, MinD and MinE propagation. **Loose et al.** showed that MinD binds cooperatively to the membrane and that MinE can persist on it even after MinD is released. At the rear of the protein wave, MinE does not inhibit binding of MinC to MinD, but collectively displaces it from membrane-bound MinD (**Loose et al. (2011a)**). **Miyagi et al.** elaborated on the MinD association and dissociation processes; MinD binds as a monolayer to the membrane but detaches in supramolecular structures from large membrane subareas (**Miyagi et al. (2018)**). The details and the kinetic characterisation are given in **Miyagi et al. (2018)**.

Exchange with theoretical investigations

Owing to defined and adjustable conditions, minimal systems provide an experimental setup in which model assumptions from *in silico* approaches can be tested. Several models assumed that MinD binds cooperatively to the membrane (**Hale et al. (2001)**; **Huang et al. (2003)**) and that the underlying instability leading to protein patterns *in vivo* as well as *in vitro* is of the Turing type (Box 1.1) (**Meinhardt and de Boer (2001)**; **Huang et al. (2003)**; **Meacci and Kruse (2005)**; **Fange and Elf (2006)**; **Loose et al. (2008)**). However, reconstitution experiments could verify the cooperativity of MinD membrane binding (**Loose et al. (2011a)**), but brought to notion that *in vitro*

Min protein patterns might be based on a different kind of instability (*Caspi and Dekker (2016)*) – thereby influencing *in silico* approaches (*Halatek and Frey (2018)*). At the same time, theoretical knowledge of the dynamics of a system did improve experiments. The mathematical description of reaction–diffusion systems implies that these systems are parameter-sensitive. Earlier Min reconstitutions only investigated the influence of one parameter and were carried out under different conditions each time, meaning the results could not be compared. Only in the past few years has the sensitivity of the system to parameter changes been considered as a factor itself, and systematic variations of geometry in interplay with other parameters were investigated (*Caspi and Dekker (2016)*; *Kretschmer et al. (2017)*; *Miyagi et al. (2018)*) (Fig. 1.2a). These studies experimentally illustrated the significance of parameter interplay, created comprehensive datasets for comparisons with simulations, and clarified, for example, the highly discussed role of membrane binding for MinE (*Kretschmer et al. (2017)*).

Expanding the system

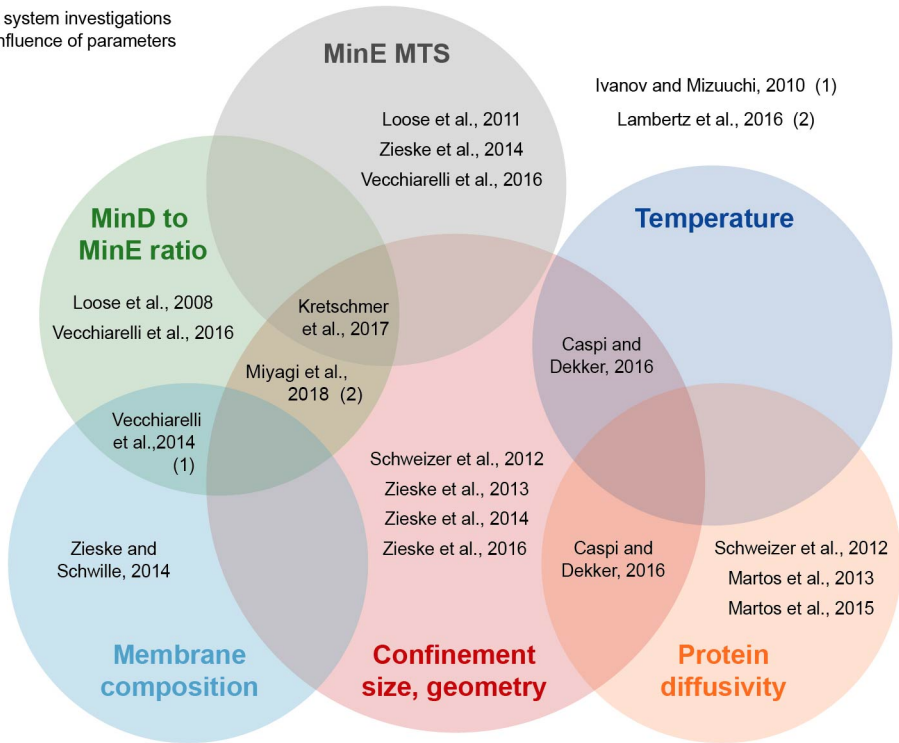
Reconstituted systems facilitate the functional characterisation of a component in a system through their ‘plug and play’ property, by which the components of the system can be added or removed at will. Min oscillations ensure the positioning of the Z-ring at the middle of the cell (*Wu and Errington (2012)*; *Rico et al. (2013)*; *Laloux and Jacobs-Wagner (2014)*). Although the assembly of FtsZ into the Z-ring was already reconstituted *in vitro* (*Osawa et al. (2008)*), the influence of Min oscillations on this process, as well as the mechanism of FtsZ inhibition by MinC, were poorly understood. Reconstitutions containing all Min proteins, FtsZ and the protein ZipA helped to clarify these processes (*Arumugam et al. (2014)*; *Zieske and Schwille (2014)*; *Martos et al. (2015)*; *Zieske et al. (2016)*). It showed, for example, that the Min oscillations alone are sufficient to position FtsZ (*Zieske et al. (2016)*). An overview of which components have been added is given in Fig. 1.2b.

1.2. A minimal system for polarity establishment in *S. cerevisiae*

1.2.1. Polarity establishment in *S. cerevisiae*

Polarity establishment in *S. cerevisiae* is a classical system for pattern formation (*Bi and Park (2012)*; *Martin (2015)*) (Fig. 1.3a), where a Cdc42-based protein pattern on the cell membrane marks the site of bud emergence ((*Bi and Park (2012)*). Cdc42 - the cell division control protein 42 - is a highly conserved membrane-bound small GTPase (*Diepeveen et al. (2018)*) with a GTP- and a GDP-bound state. Switching between the two states is highly regulated and only Cdc42-GTP signaling towards the downstream processes is sufficient for bud formation. The genes and proteins that contribute to Cdc42 regulation in *S. cerevisiae* have been identified. Four different molecular functions – typically shared between several different proteins – are relevant for Cdc42 regulation *in vivo*. First, GDP/GTP exchange factor (GEF) activity, which leads to Cdc42-GTP by enhancing nucleotide exchange. GEFs for Cdc42 are cell division cycle protein 24 (Cdc24) and bud site selection protein 3 (Bud3) (*Hartwell et al. (1973)*; *Sloat et al. (1981)*; *Chant and Herskowitz (1991)*; *Zheng et al. (1994)*; *Kang et al. (2014)*). Second, GTP-activating protein (GAP) activity, which leads to deactivation of Cdc42 by enhancing GTP hydrolysis. GAPs for Cdc42 are bud emergence protein 2 (Bem2), Bem3, Rho-type GTPase-activating protein 1 (Rga1) and Rga2 (*Bender and Pringle (1991)*; *Zheng et al. (1993, 1994)*; *Stevenson et al. (1995)*; *Smith et al. (2002)*). Third, guanine nucleotide dissociation inhibitor (GDI) activity; this enhances dissociation of Cdc42 from the membrane, and promotes retention in the cytosol. The single GDI for Cdc42 is Rho GDP-dissociation inhibitor (Rdi1) (*Dovas and Couchman (2005)*; *Dransart et al. (2005)*; *Slaughter et al.*

a Minimal system investigations on the influence of parameters



b Expansion of the minimal system

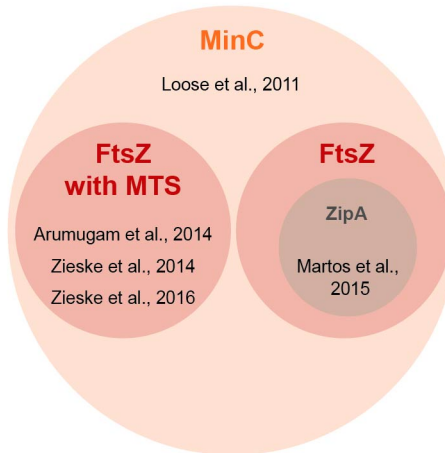


Figure 1.2. Overview of established minimal Min protein systems. Studies illustrating the investigated parameters in the minimal Min protein systems (a) and components added to expand the system (b). (1) The experiment in this publication was conducted under constant flow of proteins. (2) Label-free methods were used in this publication. Abbreviations: MTS: membrane-targeting sequence.

(2009b); *Boulter et al. (2010)*; *Woods et al. (2016)*). Finally, a scaffolding function is needed; for example, binding through Bem1 strengthens the interaction between Cdc42 and Cdc24 (*Bose et al. (2001)*; *Irazoqui et al. (2003)*; *Smith et al. (2013)*; *Rapali et al. (2017)*) (Fig. 1.3b).

Pattern formation of Cdc42-GTP on the membrane arises from local accumulation of Cdc42 through interconnected regulatory feedback loops (Fig. 1.3a) (*Howell et al. (2012)*; *Freisinger et al. (2013)*; *Wu and Lew (2013)*). Through a combination of quantitative cell biological and theoretical approaches, at least three partially independent feedback loops have been identified (*Bose et al. (2001)*; *Wedlich-Soldner and Li (2003)*; *WEDLICHOLDNER and LI (2004)*; *Slaughter et al. (2009a)*; *Howell et al. (2012)*; *Rubinstein et al. (2012)*; *Freisinger et al. (2013)*; *Klünder et al. (2013)*; *Wu and Lew (2013)*; *Martin (2015)*): a feedback loop based on a reaction–diffusion system, the so-called GDI-based mechanism, another one based on the actin cytoskeleton (*Wedlich-Soldner and Li (2003)*) and a third (weak) feedback loop, which is at least partly independent from both the GDI and actin (*Bendezú et al. (2015)*). In brief, in the GDI-based reaction–diffusion mechanism, Cdc42 accumulation is suggested to be achieved by double-positive feedback through Cdc42-GTP-dependent recruitment of the GEF Cdc24 and the scaffold protein Bem1 to the membrane (*Goryachev and Pokhilko (2008)*; *Kozubowski et al. (2008)*; *Klünder et al. (2013)*; *Wu and Lew (2013)*; *Witte et al. (2017)*). Localised concentrations of Cdc24 can lead to enhanced nucleotide exchange rates of Cdc42, thus increasing the local Cdc42-GTP concentration, which – together with Cdc42 recycling from the membrane to the cytosol through Rdi1 – can lead to pattern formation (*DerMardirossian and Bokoch (2005)*) (Fig. 1.3a). However, the exact role of the different components is still to be determined. How the actin cytoskeleton-based pathway contributes to pattern formation is heavily debated (*Martin (2015)*). Several possible mechanisms have been proposed, but their relative importance and interaction is unclear. For example, Cdc42-GTP activates formins (*Evangelista et al. (1997)*; *Dong et al. (2003)*; *Bi and Park (2012)*; *Chen et al. (2012)*), which nucleate actin cables, through which vesicles that contain Cdc42 are transported towards the membrane (*Slaughter et al. (2013)*). The influx of membrane material and Cdc42 might result in a net dilution of the Cdc42 concentration at the membrane (*Layton et al. (2011)*; *Savage et al. (2012)*; *Watson et al. (2014)*). Nevertheless, the formation of microdomains of Cdc42 on the membrane might counteract this dilution effect (*Slaughter et al. (2013)*). Hence, both GDI-based reaction–diffusion mechanisms and actin cytoskeleton-dependent delivery and internalisation of Cdc42 vesicles affect pattern formation, most likely combined with other, weaker, feedback loops. Whether they contribute to positive and/or negative feedback and what the exact molecular mechanisms are remains to be determined. Dissecting the molecular mechanisms and coupling between the different feedback loops is to date very controversial because of both parameter sensitivity and the high level of observed redundancy and interdependence within and between the feedback loops (*WEDLICHOLDNER and LI (2004)*; *Howell et al. (2012)*; *Woods et al. (2016)*; *Witte et al. (2017)*). This calls for the development of a minimal system for pattern formation in *S. cerevisiae*.

1.2.2. Towards reconstituting Cdc42-based polarity establishment

Currently, we are far from establishing a minimal system that combines reaction–diffusion-based and cytoskeleton-based feedback. The first step towards this goal is reconstituting pattern formation through a single minimal feedback loop (Fig. 1.3c). At least three interconnected regulatory feedback loops are predicted to lead to the accumulation of Cdc42 on the plasma membrane (Fig. 1.3a). Because of this redundancy, several ways of building a minimal system for Cdc42-

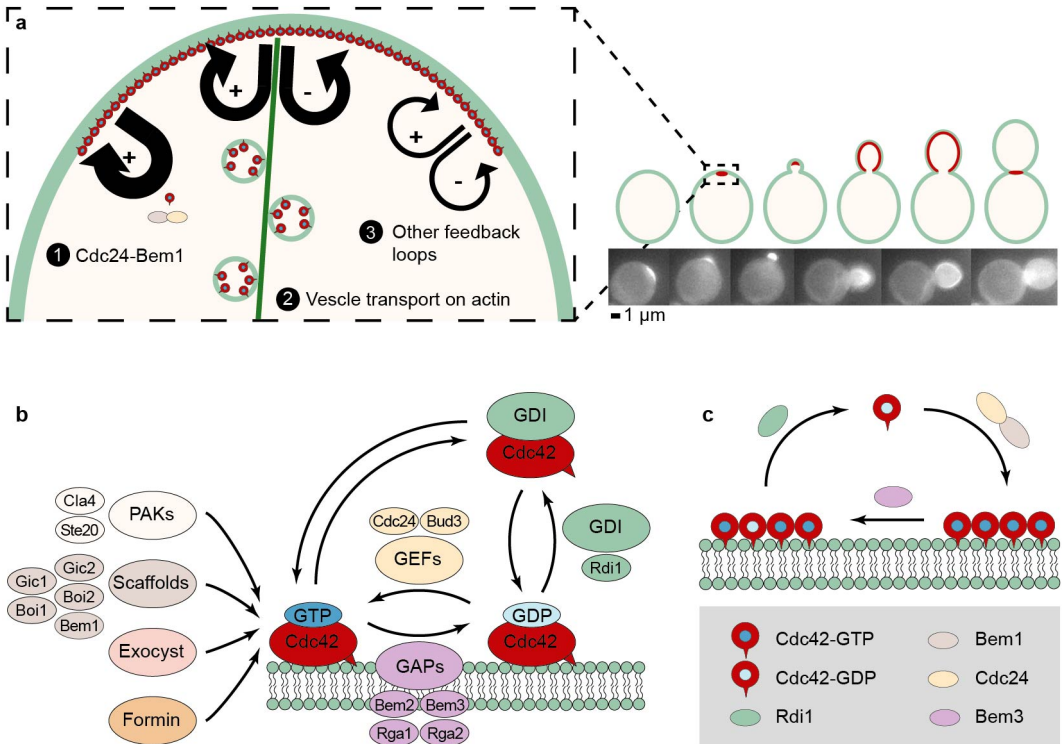


Figure 1.3. Polarity establishment in *Saccharomyces cerevisiae* *in vivo* and *in vitro*. (a) The illustration on the right shows polarity establishment in the yeast cell cycle and a montage of live cell spinning disk microscopy images of *sfGFP-Cdc42^{SW}*. On the left, the different feedback loops that establish a Cdc42 protein pattern on the cell membrane are depicted. (1) The reaction-diffusion feedback depends on double-positive feedback between Cdc42 and the scaffold protein Bem1 and the GEF Cdc24; (2) the cytoskeleton-based feedback loop is based on directed transport of vesicles along actin cables; (3) and a recently discovered (weak) feedback loop, which is at least partially independent from the other two depicted feedback loops. (b) Illustration of the polarity interaction network around Cdc42: Cdc42's nucleotide state is regulated by GEFs and GAPs. It can be extracted from membranes by the RhoGDI Rdi1, and also interacts with p21 activated kinases (PAKs), scaffold proteins, exocysts and formins. (c) Depiction of a schematic for a hypothetical minimal system for Cdc42 pattern formation by a reaction-diffusion mechanism. This is based on the recruitment and activation of Cdc42 to the membrane by the GEF Cdc24 and the scaffold protein Bem1 and possibly depending on the GDI Rdi1 for a high enough recycling rate, and on the GAP Bem3 for a high enough deactivation rate.

based polarity establishment should exist (**Goryachev and Leda (2017)**).

Theoretical work based on quantitative *in vitro* and *in vivo* experiments predicts that Cdc42, Bem1, and Cdc24 are sufficient to form Cdc42-based patterns on a spherical lipid membrane (e.g. a vesicle or water-in-oil emulsion droplet) through a reaction-diffusion mechanism (**Goryachev and Pokhilko (2008)**; **Klünder et al. (2013)**). However, fine tuning of the reaction rates might require the addition of GAPs such as Bem3 and/or the GDI Rdi1 (**Altschuler et al. (2008)**) (Fig. 1.3c). *In vitro* work has revealed that recombinant Bem3 shows GAP activity and that Cdc24 shows GEF activity (**Zheng et al. (1993, 1994)**). Rdi1 can extract Cdc42-GDP *in vitro* (and to a lesser extent Cdc42-GTP) from a lipid membrane (**Johnson et al. (2009)**; **Das et al. (2012)**), and Bem1 binds Cdc24 (**Peterson et al. (1994)**) and enhances Cdc24 GEF activity (**Rapali et al. (2017)**). Since the individual components have been characterised, the next step will be to combine them to investigate whether pattern formation will occur as predicted by theory.

Which steps need to be taken to establish such a minimal system?

We worked towards creating a minimal system that is based on the theoretical model by Klünder *et al.*. The model assumes double-positive feedback (Fig. 1.4) (**Klünder et al. (2013)**): GTP-bound Cdc42 is recruiting Bem1 to the membrane. Membrane-bound Bem1 recruits the GEF Cdc24 to the membrane and forms a heterodimeric complex with it. The resulting localised concentrations of Cdc24 can lead to enhanced nucleotide exchange rates of Cdc42, thus increasing the local Cdc42-GTP concentration. The model implicitly includes the effects of GAPs and the GDI as well. GAPs increase Cdc42's GTP hydrolysis rate and the GDI extracts Cdc42 from the membrane. Both thus reduce the local Cdc42-GTP concentration and counterbalance the positive feedback of Cdc24-Bem1, thereby leading to pattern formation of membrane-bound Cdc42.

To realise such a system, we started by focusing on the main components - Cdc42, Cdc24, and Bem1 - as they are the main drivers of Cdc42 accumulation. If the model predictions are true, a system of these three proteins should lead to the accumulation of Cdc42 on the membrane. The addition of a GAP and the GDI might then be necessary to drive it sufficiently off the membrane to get into a regime of pattern formation. To further simplify the experimental approach, and in line with the route taken for Min protein reconstitution (**Loose et al. (2008)**), we first aim to reconstitute the system on a flat membrane (supported lipid bilayer, SLB) before encapsulating it in lipid droplets (that are experimentally more challenging to realise). By using fluorescently labelled proteins, the protein dynamics are observed using total internal reflection fluorescence (TIRF) microscopy (Fig. 1.4).

Even though the reconstituted system contains only three proteins and might appear simple, an outline of all the steps required to get there reveals the systems inherent complexity (Fig. 1.5):

1. Cdc42, Cdc24, and Bem1 are purified from an *E. coli* expression system.
2. Their interactions are tested to assure proper protein functionality.
3. Bem1 and Cdc24 are fluorescently labelled with a chemical dye using a Sortase-mediated reaction.
4. The protein Cdc42 requires special attention; (1) a membrane-binding moiety, and (2) a fluorophore needs to be added. (1) In yeast, Cdc42 is post-translationally modified; a hydrophobic prenyl-group is attached to its C-terminus. It is responsible for Cdc42's membrane binding ability (**Caplin et al. (1994)**; **Coxon and Rogers (2003)**). Standard *E. coli* expression systems do not possess the proteins that are carrying out this modification and can therefore

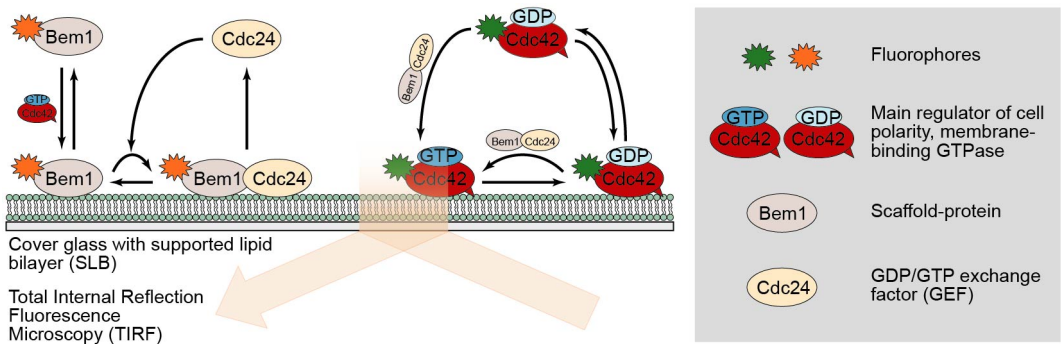


Figure 1.4. Illustration of the reactions and feedback loops that could comprise the minimal system for Cdc42-based polarity establishment (based on and modified from Klünder *et al.* (2013)).

not produce prenylated Cdc42. We explored three methods to attach a membrane-binding moiety to Cdc42, including a Sortase-mediated reaction. (2) A fluorophore can neither be attached to Cdc42's C-terminus (because of the post-translational modification), nor its N-terminus (*in vivo* data revealed that these fusions are not fully functional). It therefore needs to be inserted internally, via one of Cdc42's solvent-exposed loops (Bendezú *et al.* (2015)). We adopted the by Bendezu *et al.* published route to obtain sfGFPs and mNeogreen-Cdc42 fusions, to which also a prenyl-group was added in a second step.

5. The protein-membrane interaction is assessed with co-floitation assays or quartz crystal microbalance with dissipation monitoring experiments (for not fluorescently labelled proteins) or by using microscopy (for fluorescently labelled proteins). For this SLBs whose composition mimics the yeast plasma membrane are created.
6. Cdc42 accumulation in the Klünder *et al.* model is based on two feedback/recruitment loops: Cdc42-GTP recruits Bem1 to the membrane, and the Bem1-Cdc24 complex recruits Cdc42-GTP to the membrane (Klünder *et al.* (2013)). They can be experimentally verified by tethering Strep-tagged proteins to biotinylated SLBs, and observing if the other proteins are recruited from the cytosol.
7. Using the model to find optimal parameter regimes, all three proteins can be put together (creating a minimal system). At first, parameters should be tuned so that all Cdc42 is recruited to the membrane. Next, the system should be modified in such a way (e.g. through altered protein concentrations or addition of a GDI and/or GAP) to achieve pattern formation.

Cdc42 accumulation in yeast cells is driven by several feedback loops (Martin (2015)). This redundancy makes yeast cells robust against random mutations that can perturb protein interactions. In reconstitutions, especially in minimal systems, (almost) no redundancy is present. This allows a higher level of control over the system, but makes them also more fragile; if only one or a few assumed interactions are not taking place, or only to a lesser extent than expected, the functionality of the entire system can break down. In the case of a minimal system for Cdc42 polarity establishment, this would lead to no Cdc42 accumulation and/or pattern formation. Therefore all interactions need to be carefully assessed and verified. In the next section I outline our progress towards establishing this minimal system.

1

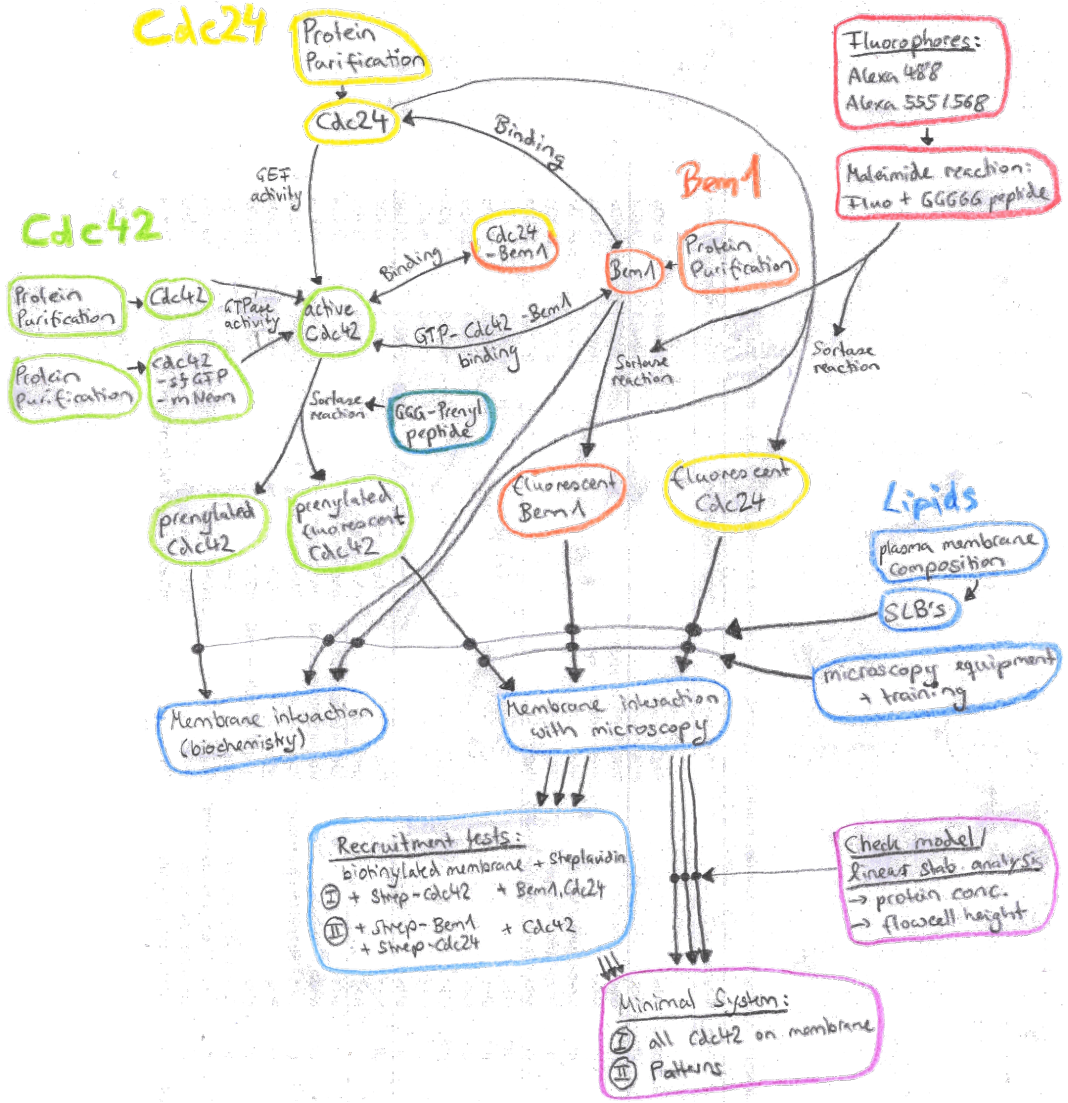


Figure 1.5. Bubble-diagram with the steps that need to be taken to establish a minimal system that is based on the three proteins Cdc42, Cdc24, and Bem1 (based on the model by Klünder *et al.* (Klünder *et al.* (2013))); Proteins need to be purified and their interactions need to be verified (green, yellow, orange). In a Sortase-mediated reaction, Bem1 and Cdc24 are fluorescently labelled and to Cdc42 a prenyl moiety is added (red and green-blue). SLBs need to be produced that mimic in their composition those of the yeast plasma membrane, and the membrane-binding capacity of proteins needs to be tested. Using the Streptavidin-Biotin system and Strep-tagged proteins, proteins can be tethered to the membrane to test the feedback/recruitment loops from the model (Klünder *et al.* (2013)) (blue). Using the model to find optimal parameter regimes, all three proteins can be put together (creating a minimal system). At first, parameters should be tuned so that all Cdc42 gets recruited to the membrane. Next, the system should be modified to achieve pattern formation (purple).

1.2.3. What can we learn from a minimal system for pattern formation?

Polarity establishment in *S. cerevisiae* is a highly regulated and precisely tuned process. Nevertheless, yeast can show evolutionary adaption of protein composition to compensate for the deletion of Bem1 through the stepwise deletion of Bem2, Bem3 and Nrp1 (*Laan et al. (2015)*). How the functions of Bem1 are redistributed by removing the three other proteins remains to be discovered. How molecular functions are rearranged is also relevant beyond this specific experiment: comparative studies on 298 fungal strains and species showed that redistribution of functions over different proteins in the polarisation network happens regularly over the fungal tree of life (*Diepeveen et al. (2018)*), and theoretical work suggested that small changes in reaction rates or the topology of the polarisation network can dramatically rearrange functions within the polarity network (*Goryachev and Leda (2017)*). A minimal system for pattern formation, where proteins can be selectively added and removed, might help the understanding of how molecular functions necessary for pattern formation can be redistributed during evolution.

1.3. Thesis aim and outline

In this thesis I describe our steps towards reconstituting Cdc42-based polarity establishment. I highlight the obstacles that needed to be addressed, including our efforts on new methods for Cdc42 prenylation and the effect of purification tags on Cdc42 dynamics. I describe our findings on the dynamics of the Cdc42 GTPase cycle, and the effect of the scaffold Bem1, GEF Cdc24, GAP Rga2, and molecular crowding, on it. I close with dissecting the effects of buffer components on the proteins and show our preliminary results of the reconstitution with all three proteins on an SLB.

Chapter 2: Materials and methods

In this chapter I describe all materials and methods used in this thesis.

Chapter 3: Cdc42 construct design for *in vitro* studies

In order to make *in vitro* studies more accessible to non-biochemists, we explore the effect of protein construct design and purification tags on the *S. cerevisiae* protein Cdc42. We show that the T7 lead is a requirement for Cdc42 expression in the *E. coli* expression system and that purification tags can influence the expression and degradation levels of Cdc42-sfGFP and Cdc42-mNeonGreen sandwich fusions. Cdc42's GTPase activity, interaction with the GEF Cdc24 and scaffold Bem1 are largely unaffected by Cdc42's N- and C-terminal purification tags. The exception is Cdc42 tagged with an N-terminal Twin-Strep-tag, which shows precipitation issues and a decreased GTPase activity and Cdc24 interaction. Further, Cdc42 seems to be quite robust: it can be stored in a buffer with 10% glycerol at -20°C for at least 12 weeks, and samples can even go through at least five freeze/thaw cycles without activity loss. We close with using the case of Cdc42 as an example for discussing criteria relevant for protein construct design in general.

Chapter 4: Synergistic regulation of the Cdc42 GTPase cycle

The small Rho-type GTPase Cdc42 is the main regulator of polarity establishment in *S. cerevisiae*. To shed more light on emergent properties of highly regulated yeast polarity protein system, we investigate a process at the centre of Cdc42 - its GTPase cycle. We studied the entire GTPase cycle of Cdc42 *in vitro* and the effect of molecular crowding, the GEF Cdc24, GAP Rga2, scaffold protein Bem1, and combinations thereof, on it. We developed a mathematical model to describe the GTPase cycle and show that Cdc42 exhibits cooperativity, which is likely not due to dimerisation.

1

The GEF Cdc24 shows cooperativity as well, and our data suggests that it synergises with Rga2. Surprisingly, we also found that molecular crowding, even at μM concentrations, positively affects the Cdc42 GTPase cycle and interactions with its effector proteins.

Chapter 5: Approaches for Cdc42 with membrane-binding capabilities

Cdc42 binds to membranes through a lipid tail that it acquires through post-translational prenylation at its C-terminus. This prenylation presents a challenge for *in vitro* studies, as the purification of prenylated Cdc42 is non-trivial. We here show and compare three complementary approaches for producing membrane-binding Cdc42 for *in vitro* experiments; (1) Sortase-mediated *in vitro* farnesylation of Cdc42, (2) *E. coli*-based farnesylation of Cdc42, and (3) Cdc42 with Bem1 basic cluster membrane binding (BC) domains (*Meca et al. (2019)*). We show that Sortase-mediated farnesylation of Cdc42 works robustly. The reaction product can easily be separated from the other reaction components through a purification-tag based strategy. The farnesylation does not interfere with the protein's GTPase activity and GEF interaction and preliminary data suggests that this protein binds strongly to membranes. *E. coli*-based farnesylation of Cdc42 works, but leads to $<1\%$ farnesylated protein. We are currently exploring further optimisation steps to increase the yield. Addition of BC domains to the C-terminus of Cdc42 encompasses the easiest approach, Cdc42 can be purified in a high yield in a single purification step. BC domains do not alter Cdc42's GTPase activity nor interaction with the GEF Cdc24, but only bind weakly to membranes.

Chapter 6: The effect of buffer components on protein functionalities

We discuss our considerations for creating the buffer in which the experiments are conducted, and explore the effects of magnesium and calcium ions on the protein-protein interactions of Cdc42, Cdc24, and Bem1. We show that, contrary to previous findings (*Zheng et al. (1995)*), Ca^{2+} does not disrupt the Bem1-Cdc24 interaction. It also does not influence the GTPase activity of Cdc42 or the Cdc42-Bem1 interaction. Mg^{2+} , on the other hand, reduces Cdc42's intrinsic GTPase activity and is required for the GEF activity of Cdc24 (*Zhang et al. (2000)*).

Chapter 7: Preliminary data and outlook

We show preliminary microscopy data of the three protein system in combination with lipid membranes: Cdc24, fluorescently labelled Bem1, and fluorescently labelled, and prenylated Cdc42 are added on an SLB and their behaviour is observed by TIRF microscopy and fluorescence recovery after photobleaching. We discuss our considerations regarding the membrane composition and the state of the current system, as we do not observe an accumulation of Cdc42 on the membrane. We close by discussing our next steps towards the reconstitution.

Contributions and acknowledgements

Parts of this chapter were published in the Journal of Cell Science (2019) as *Vendel et al. (2019)* (<https://doi.org/10.1242/jcs.217554>). Permission for reprint was conveyed through Copyright Clearance Center.

S. Tschirpke and K. Vendel wrote the abstract, boxes, and introductory section. S. Tschirpke wrote the section about the Min protein system and prepared all figures. L. Laan and S. Shamsi wrote the section about yeast polarity. These parts were edited and extended upon by S. Tschirpke to fit the scope of this chapter.

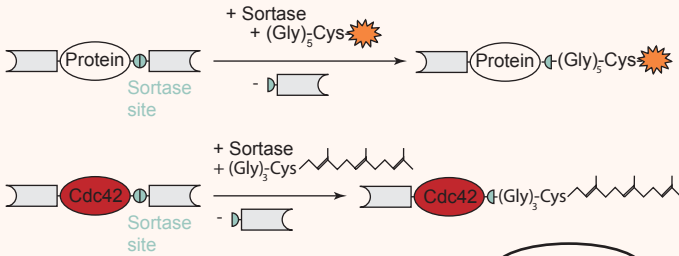
2

Nothing ever goes according to plan. Sometimes I hear new filmmakers talk down about their film; nothing worked and it was a disappointment. They don't realise yet that that's the job. The job is that nothing is going to work at all.

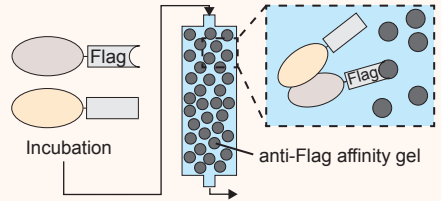
— Robert Rodriguez

Materials and methods

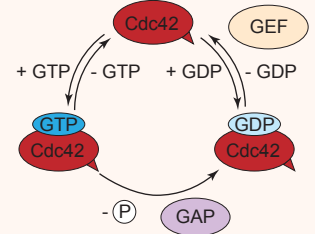
Sortase-mediated labelling reactions



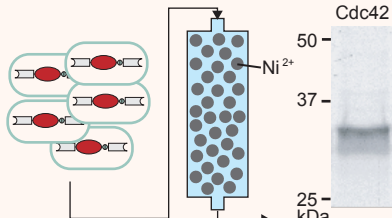
Flag-pulldown assay



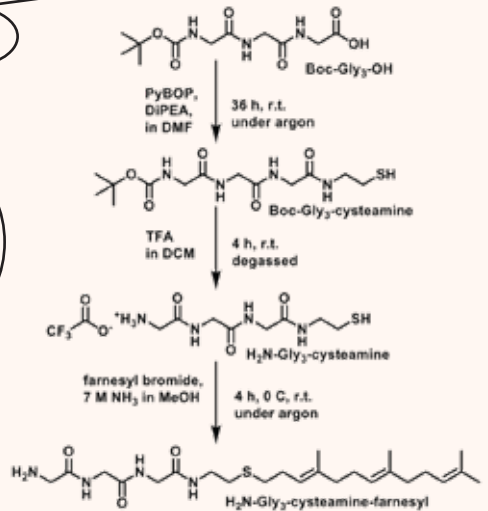
GTPase assay



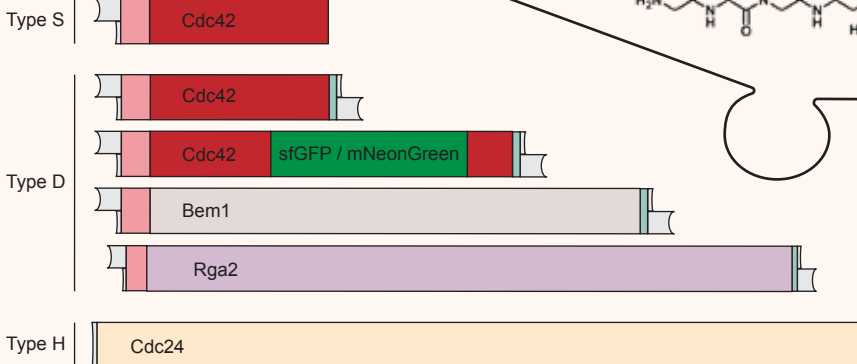
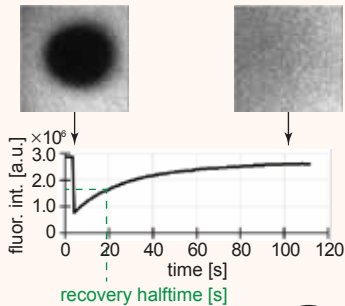
Protein expression, purification



Synthesis of farnesyl peptide



Fluorescence recovery after photobleaching



Protein construct design

2.1. Protein constructs

2.1.1. General design of protein constructs

We used three types of protein constructs (Fig. 2.1a):

Type H: Here only a single 6His-tag is directly appended to the N- or C-terminus of the protein.

Type S, single-tagged constructs: After an N-terminal purification tag an additional thrombin site, T7 lead, and Enterokinase site is added (Fig. 2.1b). Thrombin and Enterokinase sites allow the cleavage of the N-terminal region, thus allowing for the removal of the purification tag and T7 lead. The T7 lead, also known as T7 tag, is an 11-residue peptide from the leader sequence of the T7 bacteriophage gene 10 (*Studier and Moffatt (1986)*). It was added because it aids protein expression in *E. coli*.

Type D: It contains all N-terminal additions from type S plus a C-terminal Sortase site followed by a second purification tag (Fig. 2.1b). The Sortase site allows the removal of the C-terminal tag and the ligation of a peptide probe, for example a fluorophore or prenylation moiety, to the protein in a single reaction step (*Popp and Ploegh (2011)*). The C-terminal purification tag can be used for an additional affinity chromatography step during protein purification, and to separate labelled from unlabelled protein after a Sortase-mediated labelling reaction.

We constructed fluorescent Cdc42-fusions by attaching the fast-folding fluorescent proteins mNeonGreen or sfGFP (*Pédelacq et al. (2006)*; *Shaner et al. (2013)*) to the protein via one of its solvent exposed loops (*Bendezú et al. (2015)*), and created a Cdc42 version with an alternative membrane-binding domain by inserting the basic cluster regions 1 and 2 (BC) of Bem1 into Cdc42's C-terminus, in between its polybasic region (PBR) and CAAX box (*Meca et al. (2019)*).

Illustrations of these constructs are given in Fig. 2.1, where (a) shows the general design of the constructs and (b) gives an more detailed view of the N- and C-terminal tag-region, including an illustration of the size-difference of the purification tags. An overview of the protein constructs and their abbreviations is given in Tab. 2.3 and 2.2. Tab. 2.1 states the sequences of the purification tags.

2.1.2. Plasmid construction

Genes of interest were obtained from the genome of *Saccharomyces cerevisiae* W303, or in the case of mNeonGreen and sfGFP from plasmids, and were amplified through PCR. The target vector was also amplified through PCR. Additionally, each PCR incorporated a small homologous sequences needed for Gibson assembly (*Gibson et al. (2009)*). After Gibson assembly, the resulting mixture was used to transform chemically competent Dh5 α cells and plated out onto a Petri dish containing Lysogeny broth agar and the correct antibiotic marker. The primers used for each PCR can be found in Fig. 2.4.

Gibson assembly resulted in plasmids found Tab. 2.3 and 2.2. All 'pRV' plasmids were created as part of this work and are based on the plasmid pET28a-His-mcm10-Sortase-Flag, which we received from N. Dekker (TU Delft) (Tab. 2.2). This plasmid contains is a ribosome-binding-site sequence prior to the gene of interest (i.e. protein construct) that hugely improves the translation efficiency of genes foreign to *E. coli* (*Olins et al. (1988)*).

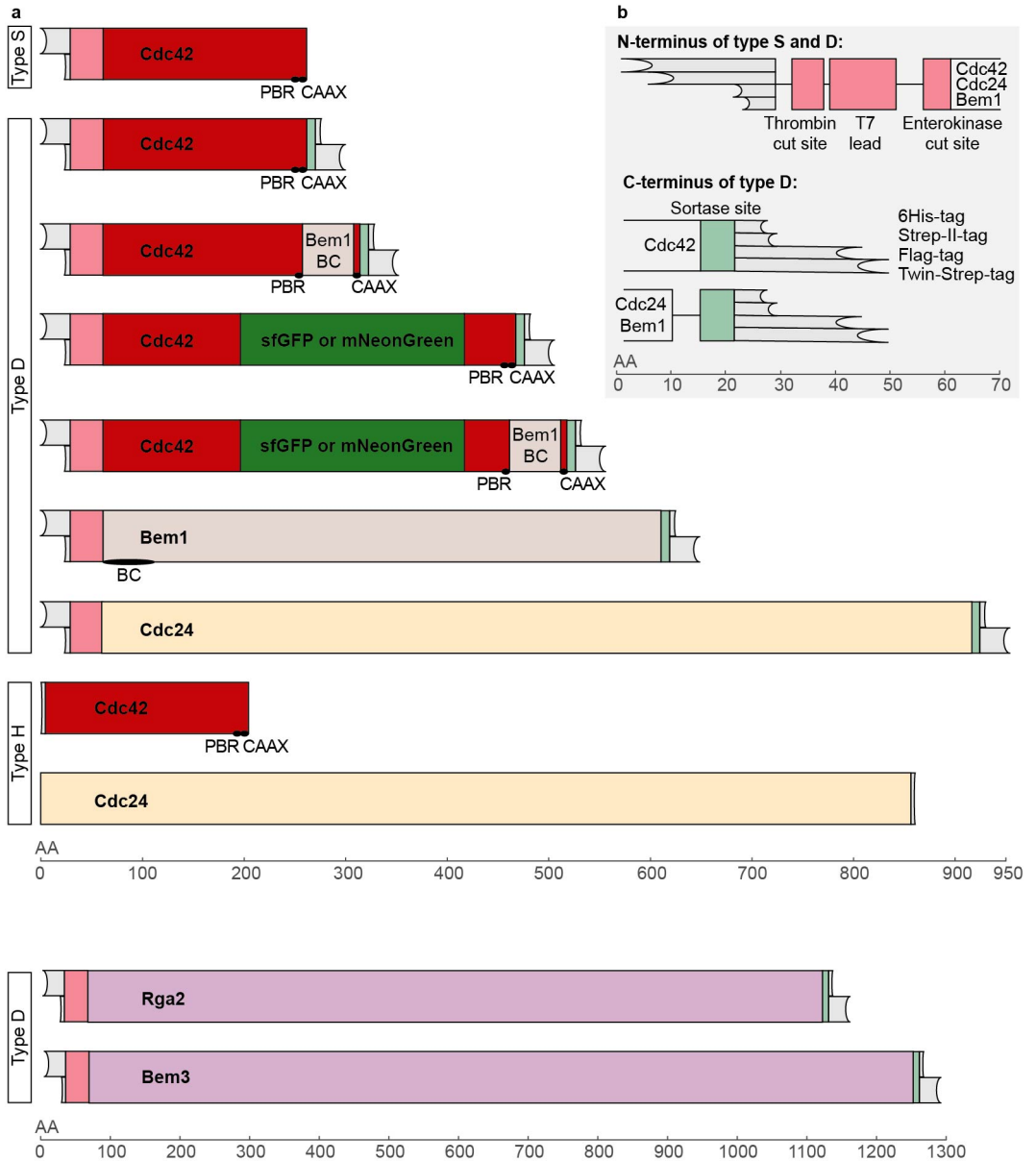


Table 2.1. Purification tag specifications. For more information regarding the Strep-II®-tag and Twin-Strep®-tag see *Schmidt et al. (2013)*, and regarding the Flag®-tag see *Hopp et al. (1988)*.

Tag	Amino acid sequence	Length [AA]	Size [kDa]
H: 6His	HHHHHH	6	0.8
F: Flag®	DYKDHDGDYKDHDIDYKDDDDK	22	2.7
S: Strep-II®	WSHPQFEK	8	1.1
SS: Twin-Strep®	WSHPQFEKGGGSGGGSGGGWSHPQFEK	28	2.9
H-SS: 6His + Twin-Strep®	HHHHHHWSHPQFEKGGGSGGGSGGGWSHPQFEK	34	3.7

Table 2.2. List of additional protein constructs/plasmids used throughout this publication.

Plasmid	Description	Source
pWKD011a	Cdc42-sfGFP ^{SW}	this work
pWKD017	Cdc42-mNeonGreen	this work
pAJLD0035	pCDFDuet FNTA/B	received from A. Jacobi (TU Delft)
pAJLD0063	pCDFDuet His-FNTA/B	received from A. Jacobi (TU Delft)
pET28a-His-mcm10-Sortase-Flag	template for 'pRV' plasmids made in this work	received from N. Dekker (TU Delft), based on pBP6 (<i>Douglas and Diffley (2016)</i>)

Table 2.3. List of protein constructs and specification of their attributes, including purification tags, added modifications, plasmid name, size, and abbreviation used throughout the publication. If not stated otherwise, Cdc42 constructs contain the proteins natural CAAX sequence (CAL). All 'pRV' plasmids were created as part of this work and are based on the plasmid pET28a-His-mcm10-Sortase-Flag we received from N. Dekker (TU Delft) (Tab. 2.2). ; pDM272 was received from D. McCusker (University of Bordeaux) and was published as *Rapali et al. (2017)*.

Abbreviation	Type	N-term. tag	C-term. tag	Other modification	Plasmid	Protein size
Cdc42						
H-Cdc42-F	D	6His	Flag		pRV007	29 kDa
F-Cdc42-H	D	Flag	6His		pRV073	29 kDa
H-Cdc42-S	D	6His	Strep-II		pRV024	28 kDa
H-Cdc42-SS	D	6His	Twin-Strep		pRV068	29 kDa
S-Cdc42-H	D	Strep-II	6His		pRV030	28 kDa
SS-Cdc42-H	D	Twin-Strep	6His		pRV058	29 kDa
H-SS-Cdc42-F	D	6His + Twin-Strep	Flag		pRV087	32 kDa
H-Cdc42:CAIA	S	6His		CAAX sequence = CAIA	pRV050	26 kDa
H-Cdc42:CTIS	S	6His		CAAX sequence = CTIS	pRV086	26 kDa
H-Cdc42:CSIM	S	6His		CAAX sequence = CSIM	pRV082	26 kDa
H-Cdc42:CAIM	S	6His		CAAX sequence = CAIM	pRV084	26 kDa
H-Cdc42:CALQ	S	6His		CAAX sequence = CALQ	pRV085	26 kDa
H-Cdc42	H	6His		CAAX sequence = CAIA	pRV035	22 kDa
H-Cdc42-mNeon-F	D	6His	Flag	+ mNeonGreen	pRV010	55 kDa
F-Cdc42-mNeon-H	D	Flag	6His	+ mNeonGreen	pRV074	55 kDa
H-Cdc42-mNeon-S	D	6His	Strep-II	+ mNeonGreen	pRV052	54 kDa
H-Cdc42-mNeon-SS	D	6His	Twin-Strep	+ mNeonGreen	pRV067	56 kDa
S-Cdc42-mNeon-H	D	Strep-II	6His	+ mNeonGreen	pRV057	54 kDa
H-SS-Cdc42-mNeon-F	D	6His + Twin-Strep	Flag	+ mNeonGreen	pRV090	58 kDa
F-Cdc42-sfGFP-H	D	Flag	6His	+ sfGFP	pRV101	57 kDa
H-Cdc42-sfGFP-SS	D	6His	Twin-Strep	+ sfGFP	pRV100	56 kDa
S-Cdc42-sfGFP-H	D	Strep-II	6His	+ sfGFP	pRV099	55 kDa
H-SS-Cdc42-sfGFP-F	D	6His + Twin-Strep	Flag	+ sfGFP	pRV102	59 kDa

S-Cdc42-BC-H	D	Strep-II	6His	+ BC from Bem1	pRV051	33 kDa
S-Cdc42-mNeon-BC-H	D	Strep-II	6His	+ BC from Bem1 + mNeonGreen	pRV093	61 kDa
Cdc24						
Cdc24-H	H		6His		pDM272 ¹	98 kDa
H-Cdc24-F	D	6His	Flag		pRV008	105 kDa
H-Cdc24-SS	D	6His	Twin-Strep		pRV065	103 kDa
S-Cdc24-H	D	Strep-II	6His		pRV031	105 kDa
SS-Cdc24-H	D	Twin-Strep	6His		pRV060	105 kDa
H-SS-Cdc24-F	D	6His + Twin-Strep	Flag		pRV088	108 kDa
Bem1						
H-Bem1-F	D	6His	Flag		pRV009	70 kDa
S-Bem1-H	D	Strep-II	6His		pRV032	68 kDa
SS-Bem1-H	D	Twin-Strep	6His		pRV061	70 kDa
H-SS-Bem1-F	D	6His + Twin-Strep	Flag		pRV089	73 kDa
GAPs						
H-Rga2-F	D	6His	Flag		pRV014	121 kDa
H-Bem3-F	D	6His	Flag		pRV013	133 kDa

Table 2.4. List of primers used to generate plasmids of Tab 2.3 and 2.2. Abbreviations: ins: insertion; add: addition; fwd: forward; rev: reverse.

Designed purpose	Primer	Sequence
oRV39 ins. of Cdc42	gene fw	Gcaaatgggt cgcggatccg aattcGATGA CGACGATAA ATGCAAAACGC TAAAGT-GTGT TGTTG
oRV40 ins. of Cdc42	gene rev	CACCGTCGTG GTCCTTGTAG TCACCGCCGG TTTCCGGTAA CAAAATTGCA CTTTTTAC TTTTCTTGAT AACAGG
oRV41 ins. of Cdc42	vector fw	TTACCGAAA CCGCGGGT
oRV42 ins. of Cdc42	vector rev	TTATCGTCG TCATCgaatt cggatcc
oRV43 ins. of Cdc24	gene fw	caGcaaatgg gtccggatc cgaattcGAT GACGACGATA AAATGGCGAT CCAAACCCG
oRV44 ins. of Cdc24	gene rev	CTTGTAGTCA CCGCCGGTTT CCGGTAAGCT TCCTCCGCCA CCATACAGAC GAAT-GTTCAA GAAATTTCTCA TTG
oRV45 ins. of Cdc24	vector fw	GGTGGCGGAG GAAAGCT
oRV46 ins. of Cdc24	vector rev	TTTATCGTCG TCATCgaatt cggat
oRV47 ins. of Bem1	gene fw	caGcaaatgg gtccggatc cgaattcGAT GACGACGATA AAATGCTGAA AAACCTTCAA CTCTCAAAAA GAGA
oRV48 ins. of Bem1	gene rev	CTTGTAGTCA CCGCCGGTT CCGGTAAGCT TCCTCCGCCA CCGAGTCTAA TATCGTGAAC GGAAATTTTC AGT
oRV49 ins. of Bem1	vector fw	GGTGGCGGAG GAAAGCT
oRV50 ins. of Bem1	vector rev	TTTATCGTCG TCATCgaatt cggatcc
oRV102 add. of mNeogreen to Cdc42	gene fw	GGTAATCATC GAGAAGTTC AAAGACAAAG ATTAAGCGGC GGTTCTGCTA TGG
oRV103 add. of mNeogreen to Cdc42	gene rev	CCTTGTCTG ATGTAATCG ACGACCAGGA GGCCACTAC ATTTG
oRV104 add. of mNeogreen to Cdc42	vector fw	CAAATGTAGT GGGCCTCCTG GTCGTCCGAT TACATCAGAA CAAGG
oRV105 add. of mNeogreen to Cdc42	vector rev	CCATAGCAGA ACCCGCGTT AATCTTTGTC TTTGCAACT CTCGATGATT ACC
oRV145 add. of a C-term. 6His tag	vector fw	catcatc atcatcaCTA Agaattcag ctccgtcgac aagc
oRV146 add. of a N-term. Strep-II tag	vector rev	TTTTTCAAAC TCGGATGG ACCAGtgct gcccatggta tatctct
oRV147 add. of a N-term. Strep-II tag	gene fw	TGGTCCCATC GCAGTTTGA AAAAagcagc ggctctggtc cg
oRV148 add. of a C-term. 6His tag	gene rev	gtgatgata tgatgatgAC CGCCGGTTTC CGG
oRV149 add. of a C-term. Strep-II tag	gene rev	TGGTCCCATC GCAGTTTGA AAAATAAGaa ttcgagctcc gtcgacaagc
oRV150 add. of a C-term. Strep-II tag	vector fw	TTTTTCAAAC TCGGATGG ACCAACCCGCC GGTTCCTCCGGT AAGC

oRV224	add. of a N-term. Twin-Strep tag	gene fw	TTGAAAAAG GTGGAGGTTT CGGAGGTGGA TCGGGAGGTG GATCGTGGAG CCACCCGCAG TTCGAGAAAa gcagcggcct ggtgccc
oRV225	add. of a N-term. Twin-Strep tag	vector rev	CACCUCCGGA ACCUCCACCU UUUUCGAACU GCGGGUUGGCU CCAGCCCCGCC AUgguaa <u>u</u> ccU <u>l</u> uc <u>u</u> aa aguu <u>u</u> aa <u>u</u> ca <u>u</u> a
oRV227	add. of a C-term. Twin-Strep tag	gene rev	ggtggctcca cgatccacct cccgatccac ctccggaacc tccaccttt tgaactgcg ggtggctcca ACCGCCGGTT TCCGGTAA
oRV228	add. of a C-term. Twin-Strep tag	vector fw	ggaggtccg gagtggatc gggaggtaga tcgtggagcc acccgagtt cgagaaataa gaattc- gagc tcgctgaca agcttgagg
oRV250	add. of N-term. 6His-Twin-Strep tag	gene fw	tggaggttcc ggaggtggat cgggaggtgg atcgtggagc caccgcagt tcgagaaaaag cagcggc- ctg g'tgcc
oRV251	add. of N-term. 6His-Twin-Strep tag	vector rev	Ccgatccacc tccggaacct ccacctttt cgaactgcgg g'tggctcca t'gatgatgat gatgatggct gctg
oRV258	add. of sfGFP to Cdc42	vector fw	CACTCACGGC ATGGATGAGC TTTATAAGAG TGGGCCTCCT GGTCGTCC
oRV259	add. of sfGFP to Cdc42	vector rev	CCTGTGAACA GCTCTTCTCC TTTTGACATA GCAGAACC GCCTTAATCT TTGTC
oRV260	add. of sfGFP to Cdc42	gene fw	GACAAAAGATT AAGCGGCGGT TCTGCTATGT CAAAAGGAGA AGAGCTGTT ACAGG
oRV261	add. of sfGFP to Cdc42	gene rev	GGACGACCAG GAGGCCACT CTTATAAAGC TCATCCATGC CGTGAGTG

2.2. Buffer composition

If not mentioned otherwise, the buffers in this thesis are of the composition stated in Tab. 2.5.

2.3. Protein expression and purification

2.3.1. Protein expression and expression tests

Proteins were expressed in BL21::DE3 pLysS cells, which carry the gene for the bacteriophage T7 RNA polymerase under the regulation of a lactose dependent promoter. Expression of the T7 RNA polymerase, which for example can be induced by IPTG, results in the transcription and therefore expression of the genes of interest that are placed under the T7 promoter. This system is of advantage, as the T7 RNA polymerase transcribes 5-10× faster than E. coli RNA polymerase (*Studier and Moffatt (1986); Dubendorf and Studier (1991)*). Four conditions were used:

1. Cells were grown in Lysogeny broth at 37°C until an OD₆₀₀ of 0.7, the expression was induced through addition of 1.0 mM IPTG, after which cells were grown for 3 h at 37°C.
2. Cells were grown in Lysogeny broth at 37°C until an OD₆₀₀ of 0.7, the expression was induced through addition of 0.2 mM IPTG, after which cells were grown for 18 h at 18°C.
3. Cells were grown in Lysogeny broth at 37°C until an OD₆₀₀ of 0.7, the expression was induced through addition of 0.2 mM IPTG, after which cells were grown for 18 h at 10°C.
4. Cells were grown in Studier Induction ZYP-5052 Medium for 3 h at 37°C, followed by 18 h at 18°C, and in accordance to the recommended protocol (*Studier (2005)*).

Condition 1 was mainly used for Cdc42 and Cdc42-mNeon-BC constructs, condition 2 was used for Cdc24, Bem1, Cdc42-BC constructs, condition 3 was used for Bem3 and Rga2. For Cdc42-mNeon and Cdc42-sfGFP constructs, condition 1 or 2 was used, as the amount of obtained protein and degradation-related side products was influenced by the N- and C-terminal purification tags and showed an optimum in one of the two conditions. Cells were harvested through centrifugation and pellets were stored at -80°C.

Cell samples were resuspended in SDS loading buffer (Laemmli buffer, *Laemmli (1970)*) and expression levels were analysed through SDS-Page and Western Blotting.

2.3.2. Protein purification

Cdc24, Cdc42, and Bem1 were purified in a similar fashion as described previously for Cdc24 (*Rapali et al. (2017)*). In brief, cell pellets were resuspended in lysis buffer A and lysed with a high pressure homogenizer at 4°C (French press cell disruptor, CF1 series Constant Systems). The cell lysate was centrifuged at 37000× g for 30 min and the supernatant was loaded onto a HisTrap™ excel column (Cytiva). After several rounds of washing with His-AC washing buffer A, the protein was eluted with His-AC elution buffer A.

If the protein was not sufficiently clean and contained a Twin-Strep-tag®, it was further purified by Strep affinity chromatography using Strep washing buffer, Strep elution buffer, and a StrepTrap™ HP column (Cytiva).

Samples that required more clean-up steps were further purified by size exclusion chromatography using SEC buffer (and a Superdex 75 Increase 10/300 GL, Superdex 200 Increase 10/300 GL, or HiPrep 16/60 Sephacryl S-300 HR column (Cytiva)).

For Cdc42-mNeonGreen, Cdc42-sfGFP, and Cdc42-mNeonGreen-BC constructs, all buffers were

Table 2.5. Buffer composition.

Buffer	Composition
Lysis buffer A	50 mM Tris-HCl (pH=8.0), 1 M NaCl, 5 mM imidazole, 1 mM 2-Mercaptoethanol, supplemented with EDTA-free Protease inhibitor cocktail (Roche) and 1 mM freshly prepared PMSF.
Lysis buffer B	20 mM Tris-HCl (pH=8.0), 150 mM NaCl, 10% Glycerol, 5 mM 2-Mercaptoethanol, supplemented with EDTA-free Protease inhibitor cocktail (Roche).
His-AC washing buffer A	50 mM Tris-HCl (pH=8.0), 1 M NaCl, 5 mM imidazole, 1 mM 2-Mercaptoethanol.
His-AC washing buffer B	20 mM Tris-HCl (pH=8.0), 150 mM NaCl, 10% glycerol, 5 mM 2-Mercaptoethanol.
His-AC elution buffer A	50 mM Tris-HCl (pH=8.0), 100 mM NaCl, 500 mM imidazole, 1 mM 2-Mercaptoethanol.
His-AC elution buffer B	20 mM Tris-HCl (pH=8.0), 150 mM NaCl, 1 M imidazole, 10% glycerol, 5 mM 2-Mercaptoethanol.
Strep-AC washing buffer	50 mM Tris-HCl (pH=8.0), 100 mM NaCl, 1 mM 2-Mercaptoethanol.
Strep-AC elution buffer	50 mM Tris-HCl (pH=8.0), 100 mM NaCl, 10 mM Desthiobiotin, 1 mM 2-Mercaptoethanol.
SEC buffer	50 mM Tris-HCl (pH=7.5), 100 mM NaCl, 10 mM MgCl ₂ , 1 mM 2-Mercaptoethanol.

supplemented with 0.1% Tween-20, 0.1% NP40, and 0.1% Triton-X.

All proteins were dialysed twice in SEC buffer. After the addition of 10% glycerol, samples were flash frozen in liquid nitrogen for storage.

Fig. 2.2 shows all purified proteins on SDS-Page.

2.3.3. Purification of prenylated Cdc42 from *E. coli*

BL21 DE::3 pLysS was transformed with pAJLD0035, expressing the α and β subunits of the human FTase (genes FNTA/FNTB) (as described previously (*Fres et al. (2010)*)), and H-Cdc42-CTIS (pRV082) or H-Cdc42-CSIM (pRV086). Cells were grown in Studier Induction ZYP-5052 Medium for 3 h at 37°C, followed by 18 h at 18°C, and in accordance to the recommended protocol (*Studier (2005)*). Cells were harvested by centrifugation and pellets were stored at -80°C. Cell pellets were resuspended in lysis buffer B and lysed with a high pressure homogenizer at 30 MPa and 4°C (French press cell disruptor, CF1 series Constant Systems). The process was repeated thrice and the soluble fraction was isolated by centrifugation (37000×g for 30 min) and loaded onto a HisTrap™ excel column (Cytiva). After several rounds of washing with His-AC washing buffer B, the protein was eluted with His-AC elution buffer B. The peak fractions were pooled and flash frozen in liquid nitrogen for storage.

2.4. Flag pulldown assay

In this assay, two proteins were mixed; one contained a Flag®-tag and the other one did not. For each experiment, 0.2 nmol Bem1, 0.2 nmol Cdc24, 1.0 nmol Cdc42, or 0.6-1.4 nmol Ovalbumin

2

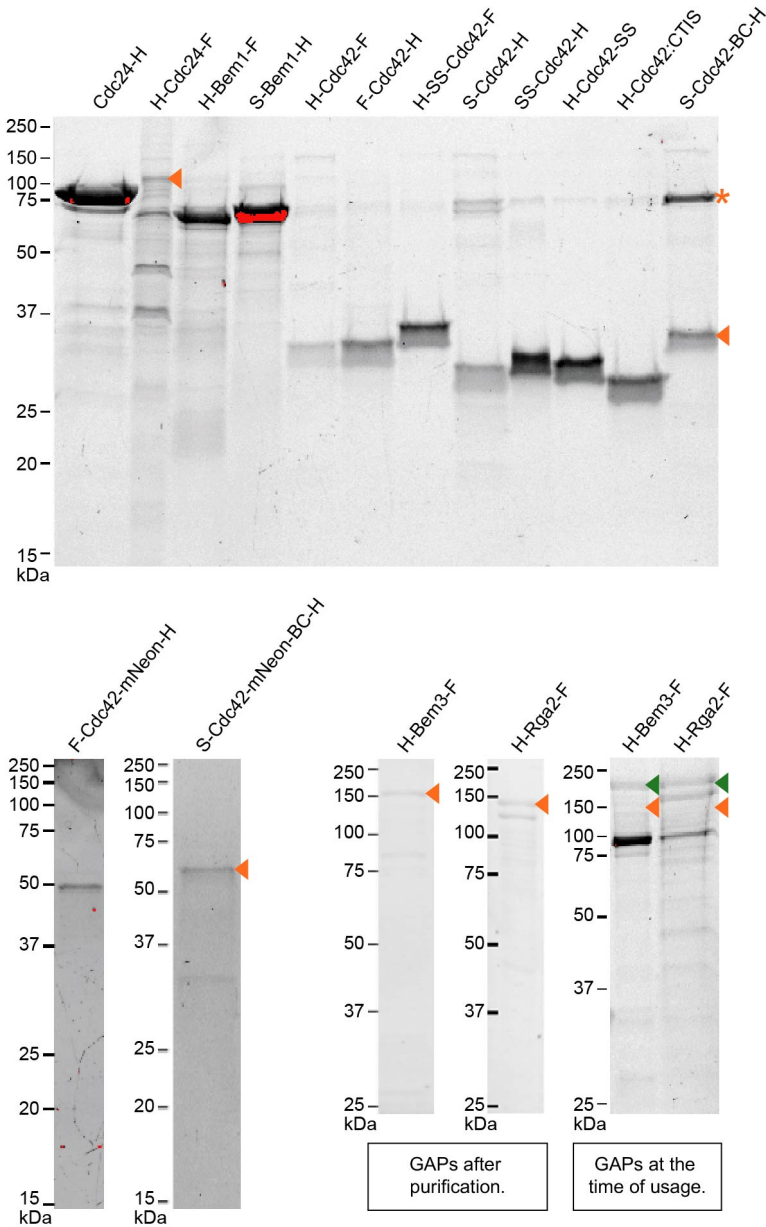


Figure 2.2. SDS-Page with purified protein constructs. Oversaturated pixels are shown in red. If the protein was not entirely clean, the band of the full-length protein is indicated by an orange arrow. The asterisk indicates the height of SDS-Page induced dimers of Cdc42. For GAPs (Bem3 and Rga2, ~120-130 kDa) SDS-Page of the proteins after purification and at the time of usage is shown. At the time of usage a significant portion of GAPs was degraded and no band at ~130 kDa could be observed (orange arrow). However, higher bands were present (green arrow). In the SDS-Page gels showing the proteins after purification, Bem3 has one band and Rga2 has two bands at ~130 kDa. This pattern also shows up in the SDS-Page at the time of usage, but at a bigger size (~200 kDa, green arrow). It is possible that in this SDS-Page these are the full-length proteins that run at a bigger size than expected.

(neg. control) were used. If Cdc42 was used, 1.0 nmol got first pre-loaded with either no nucleotide, 100 nmol GDP, or 100 nmol GTP γ S (Sigma Aldrich) for 30 min at room temperature. Two proteins (one containing a Flag-tag and one that does not) were incubated for 1 h at 30 °C. 100 μ L anti-Flag[®] M2 affinity gel (Sigma Aldrich) was added and incubated for another 30 min at room temperature. The reaction mixture was added onto a Poly-Prep Chromatography column (Bio-rad) and was washed 3 \times with 1 mL of assay buffer (25 mM Tris-HCl (pH=7.2), 300 mM NaCl, 10% Glycerol, 0.01% NP40; supplemented either with no nucleotide, 10-100 μ M GDP, or 10-100 μ M GTP γ S). Proteins were eluted with 200 μ L assay buffer supplemented with 0.6 mg/mL 3 \times Flag[®] peptide (Sigma Aldrich), and analysed by SDS-Page and Western Blotting.

2.5. GTPase activity assay

GTPase activity was measured using the GTPase-Glo[™] assay (Promega) as described previously (*Mondal et al. (2015)*). In brief, 5 μ L protein in SEC buffer (Tab. 2.5) was mixed with 5 μ L of a GTP-solution (10 μ M GTP, 50 mM Tris-HCl (pH=7.5), 100 mM NaCl, 10 mM MgCl₂, 1 mM 2-Mercaptoethanol, 1 mM DTT) in 384-well plates (Corning) to initiate the reaction. The reaction mixture got incubated at 30°C on an Innova 2300 platform shaker (New Brunswick Scientific) (120 rpm), before the addition of 10 μ L Glo buffer and another 30 min incubation. The Glo buffer contains a nucleoside-diphosphate kinase that converts remaining GTP to ATP. Addition of 20 μ L detection reagent, containing a luciferase/luciferin mixture, makes the ATP luminescent, which was read on a Synergy HTX plate reader (BioTek) in luminescence mode. The amount of hydrolysed GTP inversely correlates with the measured luminescence. Wells without protein ('buffer') were used for the normalisation and represent 0% GTP hydrolysis (Eq. 2.1). Reactions were carried out with at least 4 replicates (wells) per assay, and the average ('Lum.>') and standard deviation (' Δ Lum.>') of each set was used to calculate the activity and error of each set.

$$\text{hydrolysed GTP} = 1 - \text{remaining GTP} = \left(1 - \frac{\text{Lum. protein}}{\text{Lum. buffer}}\right) \times 100\% \quad (2.1)$$

Error bars were calculated using error propagation:

$$\Delta \text{hydrolysed GTP} = \sqrt{\left(\frac{\Delta \text{Lum. protein}}{\text{Lum. protein}}\right)^2 + \left(\frac{\Delta \text{Lum. buffer}}{\text{Lum. buffer}}\right)^2} \times \frac{\text{Lum. protein}}{\text{Lum. buffer}} \times 100\% \quad (2.2)$$

For determining the GTPase cycling rates k , the amount of remaining GTP at the time of reaction termination ($t_{\text{term.}}$) was calculated

$$[\text{GTP}]_{t_{\text{term.}}} = \left(\frac{\text{Lum. protein}}{\text{Lum. buffer}}\right) \times 100\% \quad (2.3)$$

and fitted with an exponential

$$\begin{aligned} [\text{GTP}]_t &= [\text{GTP}]_0 \exp(-K[\text{Cdc42}]t) \\ &\text{with } [\text{GTP}]_0 = 100\%, \\ &\text{and } K = k'_1[\text{Cdc42}] + k'_2[\text{Cdc42}]^2 + k'_{3,X}[\text{Cdc42}][X] \end{aligned} \quad (2.4)$$

where X is any potential binding partner of Cdc42. A more detailed description of the model is given in Chapter 4.

2.6. Synthesis of H₂N-Gly₃-cysteamine-farnesyl ('farnesyl peptide')

Abbreviations:

Boc	tert-butoxycarbonyl protecting group
Gly	glycine
DCM	dichloromethane
DMF	N,N-dimethylformamide
PyBOP	benzotriazol-1-yl-oxytripyrrolidinophosphonium hexafluorophosphate
DiPEA	N,N-diisopropylethylamine
TFA	trifluoroacetic acid
MeOH	methanol
NMR	nuclear magnetic resonance
DMSO	dimethylsulfoxide

General Information

Boc-Gly₃-OH was purchased from Bachem. DCM, DMF, PyBOP, DiPEA, Cysteamine hydrochloride, farnesyl bromide, TFA, 7 M NH₃ in MeOH, MeOH were purchased from Sigma Aldrich. DMSO-*d*₆ was purchased from Eurisotop. Deionised (milliQ) water was made in our laboratory. Unless stated otherwise, all chemicals were used as received. For all synthetical steps anhydrous solvents were used. NMR spectra were recorded on an Agilent-400 MR DD2 (399.67 MHz) instrument. Measurements were taken at 298 K.

Synthesis

An overview of the synthesis steps is given in Fig. 2.3.

It was proceeded according to a modified procedure of Agarwal *et al.* (Agarwal *et al.* (2015)). Boc-Gly₃-cysteamine was prepared by dissolving 579.0 mg (2.0 mmol, 1.0 eq.) in 7 mL anhydrous DMF. Then, 1561.0 mg PyBOP (3.0 mmol, 1.5 eq.) and 1293.0 mg (1750 μL, 10.0 mmol, 5.0 eq) DiPEA were added to the clear solution under argon. The solution was stirred for 10 min at room temperature upon which it turned yellow. 455.0 mg (2.0 mmol, 2.0 eq.) cysteamine hydrochloride were added upon which the solution turned colourless again. The reaction mixture was stirred under argon for 36 h at room temperature. The solvent was removed under reduced pressure and the crude, yellow oil was purified via flash column chromatography (DCM/MeOH 9/1) to yield 644.3 mg (93%, 1.85 mmol) compound as a colourless solid. ¹H-NMR (400 MHz, DMSO-*d*₆) δ 8.11 (dt, *J* = 11.9, 5.9 Hz, 2H, NH), 7.92 (q, *J* = 7.2, 5.9 Hz, 1H, NH), 7.01 (t, *J* = 6.1 Hz, 1H, NH-Boc), 3.73 (d, *J* = 5.6 Hz, 2H, CH₂-Gly), 3.67 (d, *J* = 5.9 Hz, 2H, CH₂-Gly), 3.59 (dd, *J* = 12.0, 6.2 Hz, 2H, CH₂-Boc), 3.21 (q, *J* = 6.5 Hz, 2H, CH₂CH₂SH), 2.54 (m, 2H, CH₂SH, Note: partly overlapping with DMSO signal), 2.39 (t, *J* = 8.2 Hz, 1H, SH), 1.38 (s, 9H, Boc).

H₂N-Gly₃-cysteamine was prepared by first degassing DCM and TFA separately by spraging with argon for 30 min. 644.0 mg of Boc-Gly₃-cysteamine (1.85 mmol, 1.0 eq.) were dissolved in 7.4 mL degassed, anhydrous DCM under argon. 1.86 mL degassed TFA were then added at 0°C over the course of 5 min. The solution was then stirred for 4 h at room temperature. The solvent was removed via cold-distillation by subjection the mixture to a fine vacuum at 0°C while stirring to yield the NH₂-Gly₃-cysteamine TFA salt. The crude was then subjected to a full analysis without further purification. A full conversion was assumed due to the disappearance of the Boc-signal. Note: We found the use of degassed solvents and the removal under reduced pressure at lower temperatures to be essential to avoid oxidation of the free thiol group! Furthermore, it is crucial

to remove the Boc-group before introducing the farnesyl residue due to its high lability towards acids (*Naider and Becker (1997)*) ¹H-NMR (400 MHz, DMSO-d₆) δ 8.63 (t, J = 5.6 Hz, 1H, NH), 8.26 (t, J = 5.9 Hz, 1H, NH), 8.00 (m, 4H, NH, NH₃⁺), 3.85 (d, J = 5.7 Hz, 2H, CH₂-Gly), 3.70 (d, J = 5.7 Hz, 2H, CH₂-Gly), 3.61 (m, 2H, CH₂-Gly), 3.26 – 3.16 (m, 2H, CH₂CH₂SH), 2.58 – 2.51 (m, 2H, CH₂SH, Note: partly overlapping with DMSO signal), 2.37 (t, J = 8.2 Hz, 1H, SH).

H₂N-Gly₃-cysteamine-farnesyl was synthesised according to a modified procedure of Cini *et al.* (*Cini et al. (2009)*). 1.85 mmol of H₂N-Gly₃-cysteamine were used without further purification. 6.0 mL MeOH were added to dissolve H₂N-Gly₃-cysteamine. 7.9 mL of 7M NH₃ in MeOH were added dropwise at 0°C under nitrogen while stirring. Subsequently, 428.0 mg farnesyl bromide (407 μL, 1.5 mmol, 1.0 eq.) were added. It was stirred for 3 h at 0°C and for 1 h at room temperature. The solvent was removed under reduced pressure at room temperature. The yellow residue was suspended in 15 mL H₂O and washed with 1-butanol three times (15 mL + 5 mL + 5 mL). The combined organic phases were dried over MgSO₄ and filtered under a stream of argon. The solvent was removed under reduced pressure at room temperature. Note: The compound was directly subjected to analysis and no further purification was attempted due to the labile nature of the farnesyl residue which is well studied (*Naider and Becker (1997)*). The spectra showed some impurities of residual 1-butanol, water and a minor impurity in the aromatic region of unknown origin. ¹H-NMR (400 MHz, DMSO-d₆) δ 8.55 (s, 1H, NH), 8.22 (d, J = 6.4 Hz, 1H, NH), 7.96 (s, 1H, NH), 5.24 – 5.13 (m, 1H, CH=C), 5.06 (d, J = 5.9 Hz, 2H, CH=C), 3.80 (d, J = 3.9 Hz, 2H, CH₂-Gly), 3.68 (d, J = 5.7 Hz, 2H, CH₂-Gly), 3.48 (s, 2H, CH₂-Gly), 3.22 (q, J = 6.9 Hz, 2H, CH₂CH₂S), 3.14 (d, J = 7.7 Hz, 2H, CHCH₂CH₂S), 2.47 (m, 2H, CH₂SH, Note: partly overlapping with DMSO signal), 2.10 – 1.97 (m, 6H, CH₂-farnesyl), 1.91 (dd, J = 15.6, 7.9 Hz, 2H, CH₂-farnesyl), 1.65 (s, 6H, CH₃-farnesyl), 1.56 (s, 6H, CH₃-farnesyl).

2.7. Sortase-mediated reactions

2.7.1. Sortase-mediated fluorescent labelling of Bem1 and Cdc42

Proteins were labelled at the N-terminus with Alexa-peptides in a Sortase-mediated reaction (*Guimaraes et al. (2013)*). To obtain 'Alexa-peptide', Alexa Fluors (Alexa FluorTM 568 C₅ Maleimide, Alexa FluorTM 555 C₂ Maleimide, Alexa FluorTM 488 C₅ Maleimide (Invitrogen)) were ligated to Gly-Gly-Gly-Gly-Gly-Cys peptide (Biomatik) in a 1:2 molar ratio, as described previously (*Nanda and Lorsch (2014)*; *Liu et al. (2018)*).

Sortase A (Octamutant, BPS Bioscience) was incubated with Bem1 (S-Bem1-H) and Alexa-peptide at a 2:100:2000 molar ratio in labelling buffer (115 mM Tris-HCl (pH=7.5), 150 mM NaCl, 10 mM CaCl₂, 1 mM 2-Mercaptoethanol) for 73 h at 4°C. The sample was spun for 5 min at 13000×g and gel-filtrated on a Superdex 200 Increase 10/300 (Cytiva) equilibrated with SEC buffer. Peak fractions were pooled and after the addition of 10% glycerol flash frozen in liquid nitrogen for storage. SDS-Page of the peak fractions, including images showing only the fluorescent signal, are shown in Fig. 2.4.

For reaction condition screens, Sortase A was incubated with Bem1 (S-Bem1-H, H-Bem1-F), or Cdc42 (S-Cdc42-H), and Alexa488-peptide at stated molar ratio in labelling buffer and incubated for stated time points at 4°C or room temperature. The labelling efficiency was analysed by SDS-Page and imaging using a Cy2 filter (Amersham Typhoon Biomolecular Imager (Cytiva)).

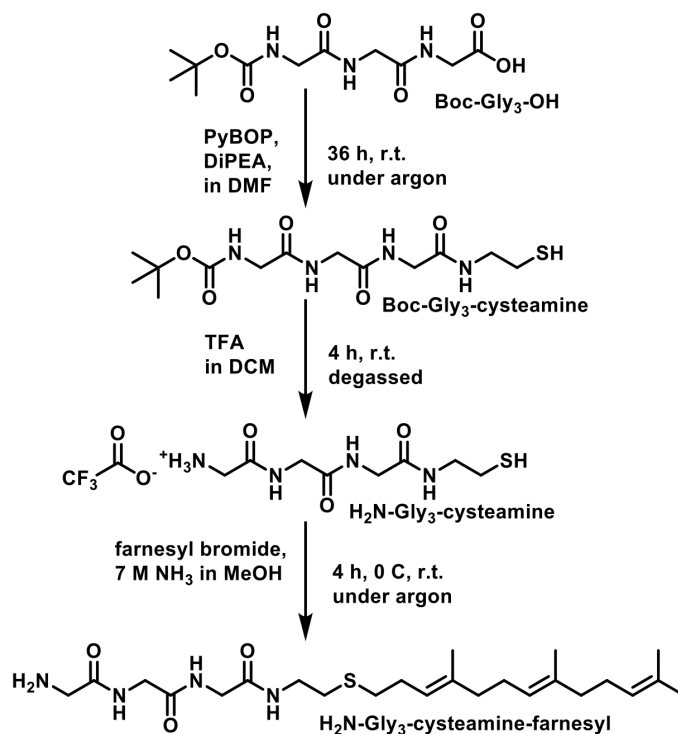


Figure 2.3. General synthetic procedure going from Boc-Triglycine to the C-terminally farnesylated triglycine derivative ('farnesyl peptide'). Abbreviations: r.t.: room temperature.

2.7.2. Sortase-mediated *in vitro* prenylation of Cdc42

Cdc42 (F-Cdc42-H, H-Cdc42-F) and Cdc42-mNeon (F-Cdc42-mNeon-H) got labelled at the N-terminus with farnesyl peptide in a Sortase-mediated reaction (*Guimaraes et al. (2013); Golding et al. (2019)*). In brief, Sortase A (Octamutant, BPS Bioscience) was incubated with Cdc42/Cdc42-mNeon and farnesyl peptide (dissolved in DMSO) at a 2:100:2000 or 4:100:20000 molar ratio in labelling buffer (200 mM Tris-HCl (pH=7.5), 100 mM NaCl, 10 mM MgCl₂, 20 mM CaCl₂, 1 mM 2-Mercaptoethanol, 100 μM GDP/GTP, 2% CHAPS, supplemented with 2 mM freshly prepared DTT; with a final DMSO content of 6-26%) for 72 h at 4°C. The sample was spun for 5 min at 13000×g.

Reaction mixtures containing F-Cdc42-H or F-Cdc42-mNeon-H got gel-filtrated on a HiPrep 16/60 Sephacryl S-300 HR column (Cytiva) equilibrated with SEC buffer (Tab. 2.5) that was supplemented with 0.5% CHAPS. Peak fractions were pooled and immediately loaded onto a HisTrap™ excel column (Cytiva). The flow-through got loaded again and this cycle was repeated for a total of three times. After the last cycle the flow-through, containing the final product, was dialysed twice in SEC buffer and was flash frozen in liquid nitrogen for storage.

Reaction mixtures containing H-Cdc42-F got gel-filtrated on a Superdex 75 Increase 10/300 column (Cytiva) equilibrated with HIC loading buffer (50 mM Tris-HCl (pH=8.0), 1 M NH₄(SO₄)₂, 2 mM MgCl₂, supplemented with 2 mM freshly prepared DTT). Peak fractions were pooled and immediately loaded onto a HiTrap™ Butyl HP column (Cytiva) equilibrated with HIC loading buffer. After several rounds of washing (50 mM Tris-HCl (pH = 8.0), 1.5 M NH₄(SO₄)₂, 2 mM MgCl₂, supplemented with 2 mM freshly prepared DTT), the protein was eluted (50 mM Tris-HCl (pH=8.0), 2 mM

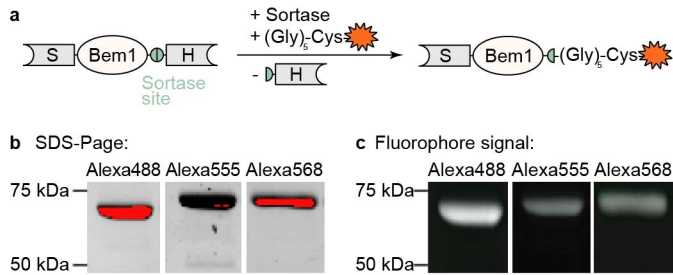


Figure 2.4. Fluorescent labelling of Bem1 (S-Bem1-H) with Alexa-peptides. (a) Schematic illustration of the labelling reaction. (b) SDS-Page of the labelled protein fraction after size exclusion chromatography. Oversaturated pixels are shown in red. (c) SDS-Page the labelled protein fraction after size exclusion chromatography showing only the signal of the fluorophores (Cy2 filter for Alexa488, Cy3 filter for Alexa555 or Alexa568).

MgCl₂, supplemented with 2 mM freshly prepared DTT). After the addition of 10% glycerol the peak fractions were flash frozen in liquid nitrogen for storage.

2.8. Preparation of farnesylated protein for mass-spectroscopy

Proteins were precipitated with chloroform methanol and digested with GluC (*in vivo* farnesylation of Cdc42) or Trypsin (Sortase-mediated farnesylation of Cdc42), as described previously (Wessel and Flügge (1984); Fres *et al.* (2010)).

Precipitation with chloroform methanol: 0.8 mL of methanol was added to 0.2 mL of protein sample. The sample was vortexed and centrifuged (10 s at 9000×g). 0.2 mL of chloroform was added and the sample was vortexed and centrifuged again. 0.3 mL of water was added and the sample was vortexed vigorously and centrifuged for 1 min at 9000×g. The upper phase was carefully removed and discarded. 0.3 mL methanol was added and the sample was mixed and centrifuged again for 2 min at 9000×g to pellet the protein. The supernatant was removed and the protein pellet was dried under a stream of air.

Digestion with GluC or Trypsin: The dried protein pellet was resuspended in 8 M urea, 50 mM Tris-HCl (pH=8.0), 10 mM DTT, and reduced by incubation at 60°C for 45 min. To S-alkylate reduced cysteine residues, iodoacetamide was added to a final concentration of 25 mM, and the reaction was allowed to proceed for 30 min in the dark at room temperature. The sample was diluted 1:4 in 50 mM Tris-HCl (pH=8.0) and Endoproteinase GluC (New England Biolabs) or Serine protease Trypsin (New England Biolabs) was added (sample to protease ratio = 1:50). The sample was digested at 37°C overnight.

2.9. Total internal reflection fluorescence (TIRF) microscopy

2.9.1. Supported lipid bilayers

Abbreviations:

DOPC	1,2-dioleoyl-sn-glycero-3-phosphocholine
DOPS	1,2-dioleoyl-sn-glycero-3-phosphoserine
PIP2	phosphatidylinositol 4,5-bisphosphate
SLB	supported lipid bilayer
SUV	small unilamellar vesicle

Procedure

An SLB was prepared by using (1) DOPC or (2) a mixture of DOPC:DOPS:PIP2 lipids (Avanti Polar Lipids) in the molar ratio 75:25:5 (*Meca et al. (2019)*). All lipids were stored in chloroform as instructed by the manufacturer. The lipids were transferred into a glass vial by using a gastight syringe and mixed by vortexing. To make fluorescent lipids, 1 nM fluorescent lipid dye Cy5-DOPC (Avanti Polar Lipids) was added and mixed by vortexing. Nitrogen was used to evaporate the chloroform, then the glass vial was placed into a vacuum desiccator overnight to make sure that all chloroform evaporated. The dried lipid film was resuspended in NaCl buffer (50 mM citrate, 50 mM KCL, 0.1 mM EDTA, pH=4.8). Then, the solution was vortexed for 15 min to form giant unilamellar vesicles. To prepare SUVs the lipid mixture was sonicated (10% amplitude, 5 s off, 5 s on) for 1 h.

The SLBs are formed by spreading the SUVs on the glass slides. Since the process is very sensitive to the surface properties of glass we used acid piranha to clean the glass slides before use. In short, a 3:1 mixture of sulfuric acid : 30% hydrogen peroxide was freshly prepared. The dry glass slides were kept in that solution for 7 min, after which they were rinsed with copious amounts of MilliQ, and sonicated in MilliQ for 5 min. Glasses treated in this way are highly positively charged and useable for up to four days (storage in MilliQ).

The experiments were performed in a 25 μ L well which was prepared by placing a 25 μ L well silicon gasket on top of acid piranha cleaned microscopy slides. SUVs were added into the well and incubated the membrane for 20 min at room temperature. Then the wells were washed for 6x with SEC buffer (Tab. 2.5) to remove the SUVs from the solution.

2.9.2. Protein sample preparation

The protein sample for microscopy imaging was prepared by mixing proteins, GTP (1 mM), imaging buffer 1 mM (0.8%, dextrose (Sigma), 1 mg/mL glucose oxidase (Sigma), 170 mg/mL catalase (Merck), and 1 nM Trolox ((\pm)-6-hydroxy-2,5,7,8-tetramethylchromane-2-carboxylic acid, Sigma) and SEC buffer (Tab. 2.5). All proteins were spun down for 5 min at 30 kPSI using an Airfuge Centrifuge (Beckman) prior to sample preparation to remove any protein aggregation.

2.9.3. TIRF image acquisition and analysis

TIRF microscopy

To image protein-membrane and protein-protein interaction, TIRF microscopy on an inverted microscope (Nikon Ti2-E), equipped with a 100x oil immersion objective (Nikon Apo TIRF 1.49 NA) which is upgraded with an azimuthal TIRF/ FRAP illumination module (Gata systems iLAS 2), was used. To investigate the mobility of proteins on a lipid membrane, fluorescence recovery after photobleaching (FRAP) experiments were performed on the above-mentioned setup. A laser power of 10 mW at 488 nm, or 561 nm respectively, was used to excite the fluorescently-labelled protein for the full duration of each camera frame (50 ms). Further, dual-color imaging with alternate laser excitation at wavelengths 488 nm, and 561 nm (Cairn Research Optosplit II ByPass EM-CCD Andor iXONUltra 897) was used to simultaneously monitor the recovery/mobility behaviour of different proteins and their impact on each other.

Image analysis

ImageJ was used to extract the intensity profile of the bleached area for FRAP experiments. For this, first the microscope's background noise was subtracted and then the intensity was nor-

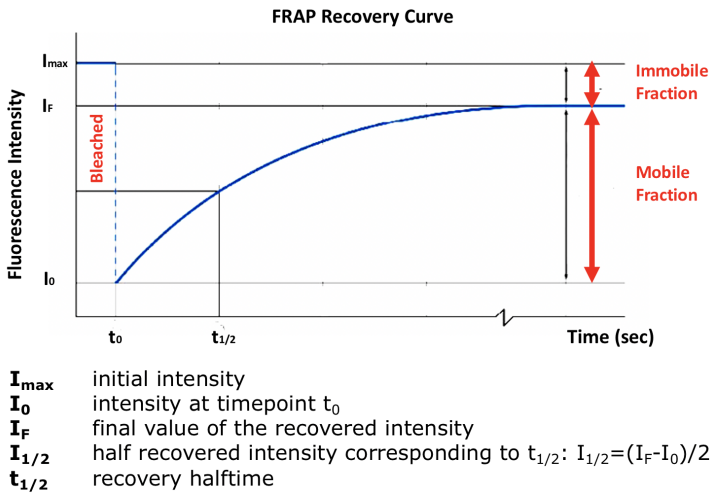


Figure 2.5. A schematic illustration of a FRAP curve.

malised to the initial unbleached intensity.

Quantitative analysis of FRAP

FRAP uses a high-intensity laser source to bleach fluorescent molecules in a region of interest within the lipid membrane. If the fluorescent molecules are mobile, then the bleached molecules will be replaced by fluorescent molecules over time. By monitoring the recovery of fluorescent intensity the fraction of mobile molecules and the recovery half-time can be determined. Here the recovery half-time ($t_{1/2}$) is the time from the bleaching to the time where the fluorescent intensity reaches the half ($I_{1/2}$) of the final recovered intensity (I_F). We assume that in our experiments the molecules are freely diffusing. Therefore, to determine $t_{1/2}$ the fluorescence recovery data to a simple exponential equation was fitted:

$$I_{norm} = A(1 - e^{-\tau t}) \quad (2.5)$$

Where A is a constant and accounts for final recovered intensity (I_F), t is the time after photobleaching, τ is the fitted parameter and I_{norm} is the detected fluorescence signal normalised with respect to the intensity before bleaching. After determining the characteristic time τ for the fluorescence intensity recovery after photobleaching, the recovery half-time ($t_{1/2}$) was calculated:

$$t_{1/2} = \frac{\ln(0.5)}{-\tau} \quad (2.6)$$

A schematic illustration of a FRAP curve is given in Fig. 2.5.

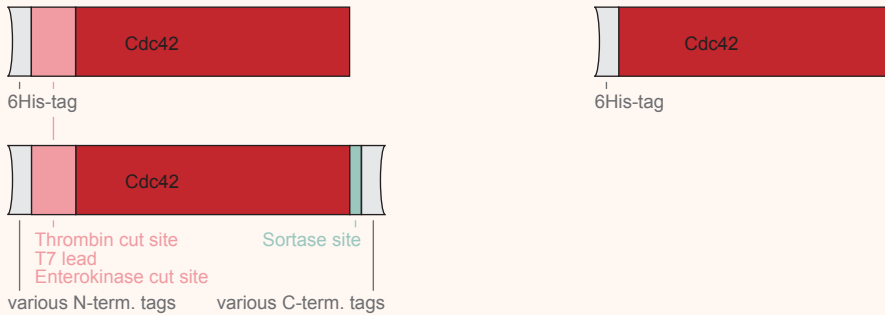
3

Before you've noticed important details they are, of course, basically invisible. It's hard to put your attention on them because you don't even know what you're looking for. But after you see them they quickly become so integrated into your intuitive models of the world that they become essentially transparent. [...] This means it's really easy to get stuck. Stuck in your current way of seeing and thinking about things. Frames are made out of the details that seem important to you. The important details you haven't noticed are invisible to you, and the details you have noticed seem completely obvious and you see right through them. This all makes makes it difficult to imagine how you could be missing something important.

— John Salvatier

Cdc42 construct design for *in vitro* studies

Cdc42 construct types



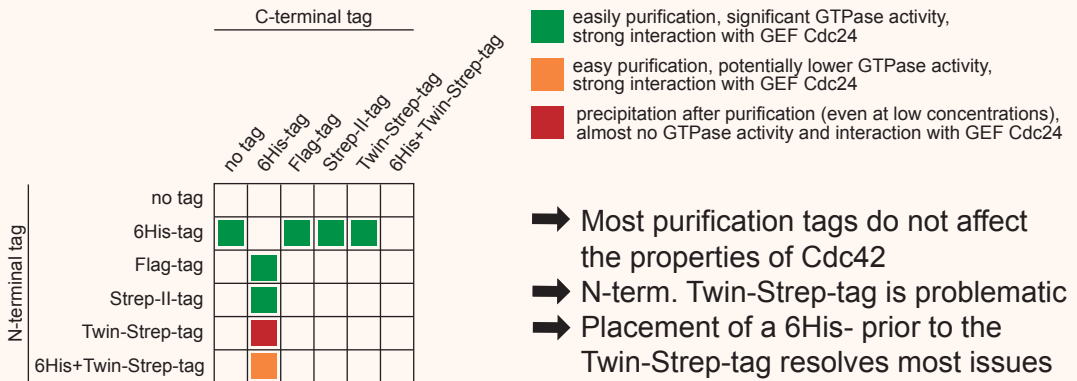
Expression in *E. coli*?

yes

no

➔ T7 lead is required for expression of Cdc42 in *E. coli*

Effect of purification tags



Cdc42 construct design for *in vitro* studies

Abstract Biological systems are complex by nature. To shine light on their inner workings, the multi-faceted lens of interdisciplinary research is required. One lens is the *in vitro* approach, in which the physical and biochemical properties and interactions of isolated components are investigated in detail. If the components are proteins, they need to be purified. This is generally done by attaching an N- or C-terminal purification tag to the protein of interest. The rationale behind the placement of purification tags and their effect on the protein's properties is rarely discussed, making *in vitro* studies less accessible to non-biochemists. Here, we explore the effect of protein construct design and purification tags on the *S. cerevisiae* protein Cdc42. Cdc42 is an essential small GTPase and the main regulator of polarity establishment and cell division in budding yeast. It's part of a complex polarity protein network and highly regulated, making it an attractive target for *in vitro* studies. We show that the T7 lead is a requirement for the Cdc42 expression in the *E. coli* expression system and that purification tags can influence the expression and degradation levels of Cdc42-sfGFP and Cdc42-mNeonGreen sandwich fusions. Cdc42's GTPase activity, interaction with the GEF Cdc24 and scaffold Bem1 are largely unaffected by Cdc42's N- and C-terminal purification tags. The exception is Cdc42 tagged with an N-terminal Twin-Strep-tag, which shows precipitation issues and a decreased GTPase activity and Cdc24 interaction. Further, Cdc42 seems to be quite robust and can be stored in a buffer with 10% glycerol at -20°C for at least 12 weeks, and samples can even go through at least five freeze/thaw cycles without activity loss. We close with using the case of Cdc42 as an example for discussing criteria relevant for protein construct design in general.

3.1. Introduction

Cdc42 is a small GTPase and the main regulator of polarity establishment and cell division in eukaryotes (*Diepeveen et al. (2018)*). It's part of a complex network of polarity proteins, including GDP/GTP exchange factors (GEFs), GTPase activating proteins (GAPs), guanine nucleotide dissociation inhibitors (GDIs), scaffold proteins, and other regulatory proteins, that all interact with each other and with Cdc42 in particular (*Gao et al. (2011)*; *Costanzo et al. (2016)*; *Daalman et al. (2020)*). In order to understand the regulation of cell division, detailed understanding of the complex protein network around Cdc42 is needed. This requires not only a biological, but also a biochemical, physical, and network perspective, and calls for interdisciplinary research. One approach is to conduct *in vitro* experiments. Here isolated components and their physical and biochemical properties as well as interactions with other components are studied in detail (*Vendel et al. (2019)*). For these proteins need to be purified, which is generally done by attaching an N- or C-terminal purification tag to the protein of interest (POI). The rationale behind the placement of purification tags and their effect on the protein's properties is rarely discussed, making *in vitro* studies less accessible to non-biochemists. A simple solution would be to always cleave off purification tags. In practice, this is not always possible or desirable. To cleave off a tag a recognition site for a cleavage enzyme needs to be placed in-between the POI and purification tag. Cleavage

enzymes have a relatively high sequence specificity, but can also cleave within the POI causing degradation products. The enzyme's cleavage behaviour and efficiency would need to be tested for every POI to ensure proper matching. After the cleavage reaction the tagged, untagged, degraded POI species and the cleavage enzyme need to be separated, adding another undesirable and yield-reducing purification step. In other cases the cleavage of the purification tag is not possible. For example when the tag is used to bind the POI to beads or a modified surface to study protein-protein interactions. Microscopy studies require fluorescent POIs, which can be achieved by attaching a fluorophore of choice to the N- or C-terminus. A fluorophore, similar to purification tags, is a modification of the protein. Knowledge on the effect of tags can help on deciding if and on which terminus the fluorophore should be placed. Hence, the effect of purification tags on the POI's properties should be considered, as tag cleavage is not always desirable or possible.

So-far, only *in vitro* studies with N-terminally tagged Cdc42 were conducted: a 6His-tag (**Zhang and Zheng (1998)**; **Zhang et al. (2000)**; **Kozminski et al. (2003)**; **Johnson et al. (2012)**; **Golding et al. (2019)**), GST-tag (**Zheng et al. (1995)**; **Bose et al. (2001)**; **Kozminski et al. (2003)**; **Das et al. (2012)**), and 6His-Strep-II-tag (**Rapali et al. (2017)**) was used. Of these references, only one reported to have cleaved off the tag (**Zhang and Zheng (1998)**). It stands out that all of these constructs have the purification tag placed on the N-terminus. It is likely the case because *in vivo* Cdc42 is post-translationally modified at its C-terminus. Cdc42 has a CAAX-box, a four amino acid (AA) sequence at its C-terminus, to which a prenyl group gets appended allowing the protein to bind to membranes (**Cox and Der (1992)**). Even though not all mentioned studies used prenylated Cdc42, all left the C-terminus unmodified. This only leaves the N-terminus for the addition of a purification tag. The N-terminus, however, is also not entirely unproblematic: N-terminal fusions of Cdc42 with fluorescent proteins have been shown to lead to not fully functional proteins *in vivo* (**Bendezú et al. (2015)**). The placement of a linker between the fluorophore and Cdc42 seemed to restore protein functionality (**Sartorel et al. (2018)**). It is thus not fully clear if N-terminal purification tags indeed do not affect Cdc42's properties, especially if large tags, like the 26 kDa GST-tag, are used.

In order to make the use of Cdc42 more accessible to a broader experimental audience, we shed light on the effect of purification tags on Cdc42's properties by conducting experiments with single- and double-tagged Cdc42. We explored the effect of the purification tags and other additions on (1) protein expression levels in *E. coli*, (2) Cdc42's GTPase activity, (3) the ability and extend to which the GEF Cdc24 can boost Cdc42's GTPase activity, and (4) the interaction of Cdc42 with the scaffold protein Bem1. Additionally, we explored Cdc42's stability under unideal storage conditions (at -20°C).

We show that the T7 lead is necessary for Cdc42 expression in *E. coli* and that purification tags can influence the expression and degradation levels of Cdc42-sfGFP and Cdc42-mNeonGreen sandwich fusions. Cdc42's GTPase activity, interaction with the GEF Cdc24 and scaffold Bem1 are largely unaffected by Cdc42's N- and C-terminal purification tags. The only exception is Cdc42 tagged with an N-terminal Twin-Strep-tag, which shows precipitation issues and a decreased GTPase activity and Cdc24 interaction. Further, Cdc42 seems to be quite robust and can be stored in a buffer with 10% glycerol at -20°C for at least 12 weeks, and samples can even go through at least five freeze/thaw cycles without activity loss. We close with using the case of Cdc42 as an example for discussing general criteria for protein construct design.

Abbreviations:

AA	amino acid
GAP	GTPase activating protein
GDI	guanine nucleotide dissociation inhibitor
GEF	GDP/GTP exchange factor
PBR	polybasic region
POI	protein of interest
SEC-MALS	size-exclusion chromatography - multi-angle light scattering

3.2. Results

3.2.1. Design of Cdc42 constructs

To test the effect of purification tags on the properties of Cdc42, we explored three types of constructs that mainly differ in their placement of purification tags:

Type H: Here only a single 6His-tag is directly appended to the N-terminus of the protein (Fig. 3.1b). This construct has the least amount of N- and C-terminal additions and therefore is expected to be least influenced by them.

Type S: After an N-terminal purification tag an additional thrombin site, T7 lead, and Enterokinase site is added (Fig. 3.1a). Thrombin and Enterokinase sites allow the cleavage of the N-terminal region, thus allowing for the removal of the purification tag and T7 lead. The T7 lead, also known as T7 tag, is an 11-residue peptide from the leader sequence of the T7 bacteriophage gene 10 (*Studier and Moffatt (1986)*). It was added because it aids protein expression in *E. coli*.

Type D: It contains all N-terminal additions from type S plus a C-terminal Sortase site followed by a second purification tag (Fig. 3.1a). The Sortase site allows the removal of the C-terminal tag and the ligation of a peptide probe to the protein in a single reaction (*Popp and Ploegh (2011)*). With this, a protein prenylation moiety could be added (see Chapter 5). The C-terminal purification tag can be used for an additional affinity chromatography step during protein purification, and to separate labelled from unlabelled protein after a Sortase-mediated labelling reaction.

Protein dynamics and interactions are often studied using microscopy. In principle, a fluorophore could be attached to either the N- or C-terminus. However, protein fusions with N-terminal fluorophores have been controversial (*Bendezú et al. (2015); Sartorel et al. (2018)*), and the attachment of a C-terminal amphipathic helix to Cdc42 resulted in folding issues of the protein *in vitro* (data (in preparation) by P. Schwillie group (MPI Martinsried)), casting also the C-terminus as unattractive for fluorophore attachment. It has been shown that fast-folding fluorophores can be inserted into a solvent-exposed loop of Cdc42 (*Bendezú et al. (2015)*). We used this approach to create sandwich-fusions of Cdc42 and sfGFP or mNeonGreen, two proteins that are known to fold quickly (*Pédrelacq et al. (2006); Shaner et al. (2013)*).

An overview of the specific constructs and their abbreviations is given in Tab. 3.1, and specifications of purification tags are given in Tab. 3.2.

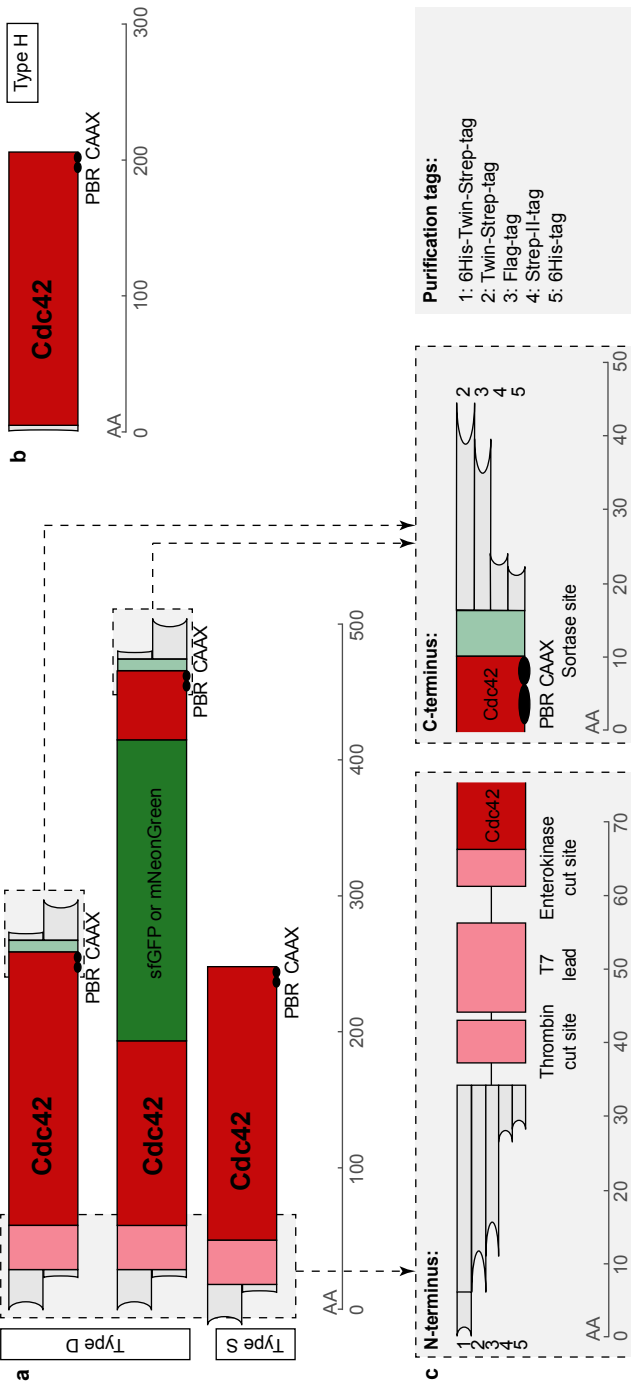


Figure 3.1. Schematic overview of the protein constructs. Illustration of the general size and outline of double-tagged (type D) and single-tagged constructs (type S) and of constructs to which only a single 6His-tag was added N-terminally (type H) (b). (c) Zoom-in of the N- and C-terminal tag regions from (a) and illustration of the size difference of the purification tags. Please note, the T7 lead illustrated here is also commonly known as the T7 tag. All constructs are drawn roughly up to scale, in terms of their number of amino acids (AA). The position of domains of interest are indicated. An overview of the specific constructs is given in Tab. 3.1.

Table 3.1. List of protein constructs and specification of their attributes, including purification tags, added modifications, plasmid name, size, and abbreviation used throughout the publication. If not stated otherwise, Cdc42 constructs contain the proteins natural CAAX sequence (CAI).

Construct	Type	N-term. tag	C-term. tag	Other modification	Plasmid	Protein size
H-Cdc42-F	D	6His	Flag		pRV007	29 kDa
F-Cdc42-H	D	Flag	6His		pRV073	29 kDa
H-Cdc42-S	D	6His	Strep-II		pRV024	28 kDa
H-Cdc42-SS	D	6His	Twin-Strep		pRV068	29 kDa
S-Cdc42-H	D	Strep-II	6His		pRV030	28 kDa
SS-Cdc42-H	D	Twin-Strep	6His		pRV058	29 kDa
H-SS-Cdc42-F	D	6His + Twin-Strep	Flag		pRV087	32 kDa
H-Cdc42:CAIA	S	6His		CAAX sequence = CAIA	pRV050	26 kDa
H-Cdc42:CTIS	S	6His		CAAX sequence = CTIS	pRV086	26 kDa
H-Cdc42	H	6His		CAAX sequence = CAIA	pRV035	22 kDa
H-Cdc42-mNeon-F	D	6His	Flag	+ mNeonGreen	pRV010	55 kDa
F-Cdc42-mNeon-H	D	Flag	6His	+ mNeonGreen	pRV074	55 kDa
H-Cdc42-mNeon-S	D	6His	Strep-II	+ mNeonGreen	pRV052	54 kDa
H-Cdc42-mNeon-SS	D	6His	Twin-Strep	+ mNeonGreen	pRV067	56 kDa
S-Cdc42-mNeon-H	D	Strep-II	6His	+ mNeonGreen	pRV057	54 kDa
H-SS-Cdc42-mNeon-F	D	6His + Twin-Strep	Flag	+ mNeonGreen	pRV090	58 kDa
F-Cdc42-sfGFP-H	D	Flag	6His	+ sfGFP	pRV101	57 kDa
H-Cdc42-sfGFP-SS	D	6His	Twin-Strep	+ sfGFP	pRV100	56 kDa
S-Cdc42-sfGFP-H	D	Strep-II	6His	+ sfGFP	pRV099	55 kDa
H-SS-Cdc42-sfGFP-F	D	6His + Twin-Strep	Flag	+ sfGFP	pRV102	59 kDa

Table 3.2. Purification tag specifications. For more information regarding the Strep-II[®]-tag and Twin-Strep[®]-tag see *Schmidt et al. (2013)*, and regarding the Flag[®]-tag see *Hopp et al. (1988)*.

Tag	Amino acid sequence	Length [AA]	Size [kDa]
H: 6His	HHHHHH	6	0.8
F: Flag [®]	DYKDHDGDYKDHDIDYKDDDDK	22	2.7
S: Strep-II [®]	WSHPQFEK	8	1.1
SS: Twin-Strep [®]	WSHPQFEKGGGSGGGSGGGSWHPQFEK	28	2.9
H-SS: 6His + Twin-Strep [®]	HHHHHHWSHPQFEKGGGSGGGSGGGSWHPQFEK	34	3.7

3.2.2. Effect of purification tags on Cdc42 expression levels and dimerisation

First, we tested if the purification tags have an effect on the expression levels of Cdc42. Cdc42 was placed under an IPTG inducible promoter so that its expression can be induced through addition of that chemical. We tested three expression conditions: 'f' - a strong and fast expression at elevated temperatures, induced by a high amount of IPTG (3 h at 37°C with 1 mM IPTG); 's' - a low and slow expression at lower temperatures, induced by a smaller amount of IPTG (18 h at 18°C with 0.2 mM IPTG); and 'AI' a self-inducing combined approach, called auto-induction (3 h at 37°C + 18 h at 18°C) (*Studier (2005)*).

All Cdc42 constructs contained a 6His-tag, therefore expression levels could be analysed by anti-His Western Blotting (Fig. 3.2a-c). Both type S and D expressed at all conditions in roughly equal amounts (Fig. 3.2a). The presence of a C-terminal tag or variations in Cdc42's CAAX box, a four amino acid sequence directly at Cdc42's C-terminus (Fig. 3.1), did also not alter the expression levels. Type H did not express in any condition. Cdc42 is a foreign gene in *E. coli* and might therefore not be well expressed. Constructs of type S and D, but not of type H, contain the T7 lead (also known as T7 tag), a peptide tag shown to aid protein expression in *E. coli* (*Studier and Moffatt (1986)*). We therefore conclude that the T7 lead is required for Cdc42 expression in *E. coli*.

We further tested the expression levels of proteins with combinations of N- and C-terminal 6His- (H), Flag- (F), Strep-II- (S), and Twin-Strep- (SS) tags. The Strep-II- and Twin-Strep-tag differ only in so far from each other as the Twin-Strep-tag is made from two repeats of the Strep-II-tag that are spaced with a linker (Tab. 3.2). The Twin-Strep-tag binds by an order of magnitude tighter to Strep-Tactin and is therefore more effective when used for purification purposes (*Schmidt et al. (2013)*). All explored tag combinations did not affect the Cdc42 expression (Fig. 3.2b), and all constructs could be purified in a high yield using His affinity chromatography. We observed that after purification only one construct, SS-Cdc42-H, was highly unstable and precipitated even at low concentrations (0.5 mg/mL). This was only the case for the N-terminal Twin-Strep-tag, constructs with an N-terminal Strep-II-tag, C-terminal Twin-Strep-tag, or N-terminal 6His-Twin-Strep-tag (6His-tag proceeded by a Twin-Strep-tag) showed no precipitation and were stable up to at least 4 mg/mL. We observed a similar trend for the expression of two other yeast proteins; Cdc24 and Bem1. Cdc24 and Bem1 constructs, that were double-tagged in the same fashion as described for Cdc42, expressed when tagged with an N-terminal Strep-II-tag, C-terminal Twin-Strep-tag, or N-terminal 6His-Twin-Strep-tag, but did not, or only to greatly reduced level, express when tagged with an N-terminal Twin-Strep-tag (Fig. 3.2b). This suggests that the N-terminal Twin-Strep-tag destabilises proteins. Taken together, we show that Cdc42 expression and purification are unaffected by N-

and C-terminal tags, with the exception of an N-terminal Twin-Strep-tag.

Further, we observed two other tag-related effects: (1) Strep-tagged Cdc42 constructs of type D run slightly lower on SDS-Page than their Flag-tagged counterparts. A discussion is given in Appendix 3.4.1. (2) The anti-His and anti-Cdc42 Western Blots show, in addition to the 25-30 kDa Cdc42 band, a 50-60 kDa band for almost every construct (Fig. 3.2b). Its presence in the anti-Cdc42 Western Blot confirms that this band is also Cdc42, suggesting that Cdc42 forms dimers. Even though *in vivo* data indicates that yeast Cdc42 does not dimerise (*Kang et al. (2010)*), *in vitro* data of human Cdc42 and of other small GTPases (*Zhang and Zheng (1998)*; *Zhang et al. (2001)*) suggests that it could. To further investigate this possibility, we ran purified Cdc42 sample on a size-exclusion chromatography (SEC) column and used multi-angle light scattering (MALS) to determine the molecular weight of the protein in each peak (Fig. 3.2c). Cdc42 ran in one peak and the SEC-MALS molecular weight corresponded to that of a monomer, independent of construct type or added nucleotide. We subsequently analysed the protein of these peak fractions by anti-His and anti-Cdc42 Western Blotting. Again, the blots showed bands of the size of a dimer. Taken together, we conclude that Cdc42 does not dimerise *in vitro*, but can form dimers in its denatured state (e.g. during SDS-Page conditions)¹. Interestingly, the presence of dimers on SDS-Page was again influenced by the Strep-tag. Constructs with an N-terminal Twin-Strep-tag (SS-Cdc42-H, H-SS-Cdc42-F) formed no dimers (Fig. 3.2b), and S-Cdc42-H showed dimers in the anti-His, but not in the anti-Cdc42 Western Blot (both in the expression test (Fig. 3.2b) and SEC-MALS samples (Fig. 3.2c)). C-terminal tags did not induce or influence dimer formation; type S constructs, and type D constructs with all possible C-terminal tags (6His, Flag, Strep-II, Twin-Strep) formed dimers (Fig. 3.2b). Thus, N-terminal Strep-II and Twin-Strep-tags seem to interfere with Cdc42 dimerisation. The origin of this remains elusive.

As double-tagged Cdc42 was mostly unaffected by its specific N- and C-terminal tags (with the exception of an N-terminal Twin-Strep-tag), we tested if this was also true for sandwich-fusions of Cdc42 and sfGFP or mNeonGreen (*Bendezú et al. (2015)*). We conducted expression tests (condition 'r' and 's'), and analysed them by Western Blotting. Most, but not all, N- and C-terminal tag combinations lead to full-size fusion products. Degradation bands were present in all cases but to different degrees, and we could not determine a relation between used tags and expression behaviour. Experimental data and a more in-depth discussion is given in Appendix 3.4.2.

3.2.3. Effect of purification tags on Cdc42's GTPase activity

Cdc42 is a small GTPase and can therefore hydrolyse GTP. To test if and how strongly purification tags can influence or interfere with Cdc42's GTPase activity, we performed GTPase assays using the Promega GTPase Glo™ assay. Here serial dilutions of Cdc42 were incubated with GTP for a certain time, after which the reactions were stopped and the amount of remaining GTP was measured (see materials and methods). Thus, how much GTP got hydrolysed by Cdc42 proteins in a certain amount of time was measured. To quantitatively compare the effect of tags on Cdc42's GTPase activity, we determined GTP hydrolysis cycling rates k . These rates encompass the entire GTPase cycle, which can be described in three steps (Fig. 3.3a): (1) Cdc42 binds to a free GTP. (2) GTP gets hydrolysed by Cdc42. (3) Cdc42 releases GDP.

If one construct shows decreased rates k it would indicate that at least one of these steps is happening at a slower speed - likely because the purification tags of this construct are interfering with it. This GTPase assay is very effective for investigating if and how strong purification tags

¹A more detailed discussion of Cdc42 dimerisation is given in Chapter 4.

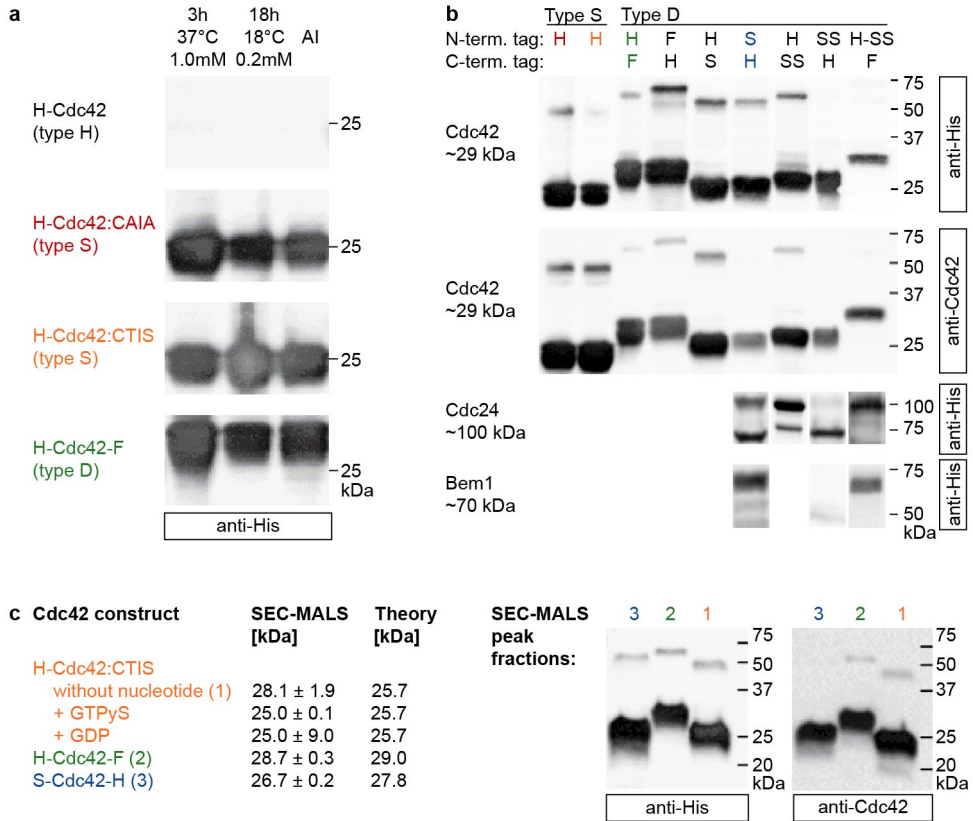


Figure 3.2. Effect of purification tags on Cdc42 expression levels and dimerisation. (a) Expression levels of Cdc42 under three expression conditions, assessed by anti-His Western Blotting. (b) Expression levels of variously tagged Cdc42, Cdc24, and Bem1 constructs, assessed by anti-His and anti-Cdc42 Western Blotting. Cdc42 constructs were expressed in condition ‘f’ (3 h 37°C 1.0mM IPTG) and Cdc24 and Bem1 constructs were expressed in condition ‘s’ (18 h 18°C 0.2mM IPTG). (c) Molecular weight of purified Cdc42 constructs determined by SEC-MALS in comparison to the expected mass based on the amino acid sequence (Theory) (left). Anti-His and anti-Cdc42 Western Blots of the peak fractions from SEC-MALS runs (right).

can influence GTPase activities, as it not only assesses the GTP hydrolysis step, but also the GTP binding and GDP release steps of the GTPase cycle.

First, we examined how the GTP concentration changed for different Cdc42 concentrations over time. We performed experiments to measure the amount of remaining GTP after incubation times of 1.5 h, 3 h, and 5 h. The graph of the amount of remaining GTP over time (Fig. 3.3b) shows that the GTP hydrolysis process can be described by an exponential decline (Eq. 3.1).²

We fitted the Cdc42 GTP hydrolysis data with

$$\begin{aligned}
 [\text{GTP}]_t &= [\text{GTP}]_{t_0} \exp(-K[\text{Cdc42}]t) \\
 &\text{with } [\text{GTP}]_{t_0} = 100\%, \\
 &\text{and } K = k'_1[\text{Cdc42}] + k'_2[\text{Cdc42}]^2
 \end{aligned}
 \tag{3.1}$$

²We subsequently only performed measurements using incubation times of about 1.5 h.

Here k'_1 describes the GTP hydrolysis cycling rate of a single Cdc42 molecule and k'_2 includes any effects due to crowding, cooperativity, and Cdc42 dimerisation³.

We performed several assays to determine the rates of the Cdc42 constructs (Fig. 3.3c, Appendix 3.4.3 Tab. 3.3). Rates are not very intuitive to interpret. To make their interpretation more accessible, we used the rates and Eq. 3.1 to calculate how much GTP would remain in a simulated GTPase assay with equimolar amounts of each Cdc42 construct (Fig. 3.3d). The less GTP remains, the more active Cdc42 is. To ensure that any observed rate differences reflect the effect of purification tags, we assessed how much the rates of the same protein construct vary (1) within separate assays, and (2) between batches obtained from different protein purifications. We observed that values of k'_1 and k'_2 obtained from separate assays (Fig. 3.3c, blue dots) can vary quite a bit, but that they all describe a similar GTPase behaviour: in the simulated assay 0-15% GTP remains (Fig. 3.3d, blue bars with blue dot). Possible reasons for this variation include small concentration differences introduced through pipetting of small volumes (as are required for this assay), temperature and shaker speed fluctuations during the incubation, and/or intrinsic changes in the Cdc42 protein due to other external conditions. Even bigger rate-affecting factors are protein changes that originate from purification-related steps. Distinct symbols of the same colour in Fig. 3.3c,d indicate that different purification batches were used. The variability for F-Cdc42-H purification batches is about as big as that observed for different assays: 15-35% GTP remain in the simulated assay (Fig. 3.3d green circle/ triangle/ rhombus). A part of the variability could also be due to the variability between assays. A more significant case is H-Cdc42-F (Fig. 3.3d blue circle/ triangle): 0-15% GTP remain for one purification batch whereas ~60% remain for the other, indicating that protein of the batch has a less active state or consists of a mixed pool of active and inactive protein. When taking these variability into account, the difference in GTPase activity between the different constructs is minor: single-tagged Cdc42 (H-Cdc42:CTIS) is roughly equally active as most double-tagged variants (H-Cdc42-F, F-Cdc42-H, H-Cdc42-SS, S-Cdc42-H). Exceptions are SS-Cdc42-H and H-SS-Cdc42-F, which hydrolyse less GTP and are therefore less active/ contain a bigger fraction of inactive protein (Fig. 3.3d). This data suggests that C-terminal tags do not interfere with Cdc42's GTPase activity, but that the N-terminal Twin-Strep-tag does. SS-Cdc42-H showed already precipitation issues during the purification process. This assay confirms that the protein is barely functional⁴. H-SS-Cdc42-F shows a reduced GTPase activity, similar to the outlier H-Cdc42-F purification batch (blue triangle). It is possible that this is due to the same purification-related reason that lead to less active H-Cdc42-F, or that the 6His-tag upstream of the Twin-Strep-tag partially restores Cdc42 functionality. H-SS-Cdc42-F showed no precipitation issues, indicating that a problem induced by the N-terminal Twin-Strep-tag got resolved. Measurements on different purification batches would be required to resolve if the reduced GTPase activity is due to protein damage during the purification process or because of the N-terminal tag.

Taken together, the GTPase activity of Cdc42 is mostly unaffected by N- and C-terminal purification tags, with the exception of the N-terminal Twin-Strep-tag, which impedes protein functionality.

³A more in-depth description of the fitting model is given in Chapter 4.

⁴Only one data point/one assay is shown for this construct. However, several additional assays were performed to ensure that the observed behaviour is not an artefact. A similar behaviour was observed repeatedly; in most assays no GTPase activity was observed. The rates could only be extract from one assay where a significantly longer incubation time was used.

3.2.4. Effect of purification tags on Cdc42-Cdc24 and Cdc42-Bem1 interaction

Next, we assessed if the different protein constructs are still capable of interacting with other proteins from the yeast polarity protein network. We conducted tests with Cdc24 and Bem1.

The Cdc42-Cdc24 interaction

Cdc24 is a GEF, meaning it boosts the release of GDP from Cdc42 (GTPase cycle step (3), Fig. 3.3a) and thereby increases the cycling speed of the GTPase cycle.

Cdc42:Cdc24 mixtures, as well as samples containing only Cdc42, were incubated with GTP for 1-1.5 h and the amount of remaining GTP was measured. We had observed that rates for Cdc42 can vary slightly between assays (Fig. 3.3c,d). Possible reasons for this include small concentration differences introduced through pipetting of small volumes (as are required for this assay), temperature and shaker speed fluctuations during the incubation step, and/or intrinsic changes in the Cdc42 activity due to other external conditions. To account for this variance, we introduced the parameter c_{corr} that maps all factors that lead to variations between assays onto the Cdc42 concentration. The assay data, including samples containing only Cdc42 and Cdc42 - effector protein mixtures, were fitted with Eq. 3.1 using

$$K = k'_1 c_{corr} [\text{Cdc42}] + k'_2 (c_{corr} [\text{Cdc42}])^2 + k'_3 c_{corr} [\text{Cdc42}] [\text{Cdc24}]^2 \quad (3.2)$$

to determine c_{corr} and k'_3 (using k'_1 and k'_2 values determined earlier (Eq. 3.1 and Fig. 3.3c)). Values of c_{corr} are 1.0 - 1.6 (Fig. 3.3e, Appendix 3.4.3 Tab. 3.4), illustrating that the assay variability was not severe.

The GEF activity rates of Cdc24 range from 20 to 120 $\mu\text{M}^{-2}\text{h}^{-1}$ for H-Cdc42-F in different assays (Fig. 3.3f blue dots, Appendix 3.4.3 Tab. 3.4). They are a factor of 1000 larger than k'_1 or k'_2 , displaying how strong the effect of Cdc24 on the GTPase cycle is. A factor of six in k'_3 variation seems thus reasonable. It likely reflects small changes in Cdc24's activity that affect the GTPase cycle significantly stronger than any Cdc42 intrinsic changes do. The variability in k'_3 between assays also accounts for all the difference in k'_3 values between purification batches (F-Cdc42-H: Fig. 3.3f green circle/ triangle/ rhombus) and between distinct constructs: rates k'_3 of single and most double-tagged Cdc42 constructs (H-Cdc42-F, F-Cdc42-H, H-Cdc42-SS, S-Cdc42-H, H-SS-Cdc42-F) are 20 to 120 $\mu\text{M}^{-3}\text{h}^{-1}$. The only exception is again SS-Cdc42-H, which shows almost no interaction with Cdc24 ($k'_3=0.19 \mu\text{M}^{-3}\text{h}^{-1}$ (Appendix 3.4.3 Tab. 3.4)). Surprisingly, H-SS-Cdc42-F, despite having a significantly reduced GTPase activity (Fig. 3.3d), interacted with Cdc24 to the same extend as the other constructs (Fig. 3.3f). Together with the observed loss in precipitation this indicates that the N-terminal 6His-tag restores functionality. Further experiments with other purification batches and GAPs are nonetheless recommended to ensure proper protein functionality, as the origin and the extend of N-terminal Twin-Strep-tag interference are unknown. In conclusion, we show that, with the exception of SS-Cdc42-H, the presence of N- and C-terminal purification tags does not influence the GTPase activity of Cdc42 or its interaction with the GEF Cdc24.

The Cdc42-Bem1 interaction

We then tested the interaction with the scaffold protein Bem1. We conducted Flag-pulldown experiments, in which Flag-tagged Bem1 (H-Bem1-F) and Cdc42 constructs that don't contain a Flag-tag, were incubated and mixed with anti-Flag affinity gel. Flag-tagged Bem1 binds to the gel but Cdc42, as it does not contain a Flag-tag, does not. After several rounds of washing, the

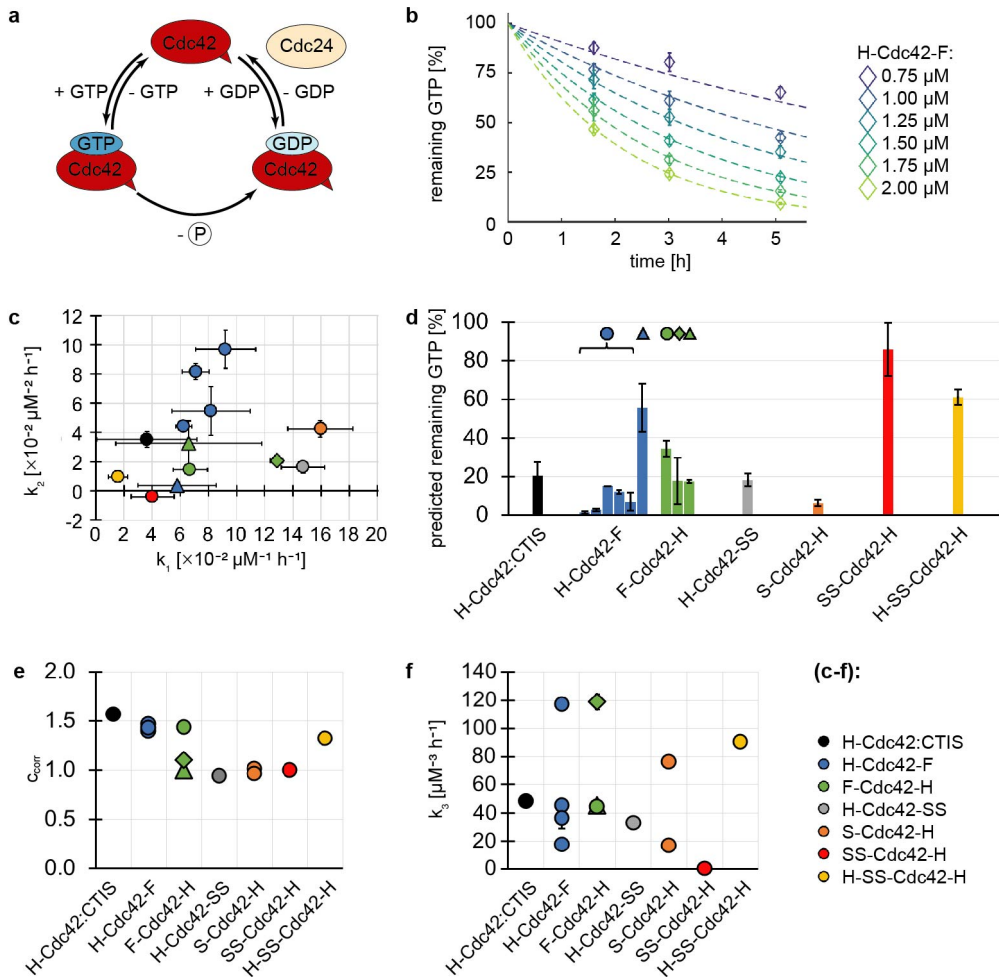


Figure 3.3. Cdc42's GTPase activity and interaction with Cdc24. (a) Schematic illustration of the GTPase cycle. (b) GTPase assay: The amount of remaining GTP ($[GTP]_{t=0h} = 5 \mu\text{M}$) declines exponentially over time. Dashed lines are fits (Eq. 3.1). (c) GTP hydrolysis cycling rates (k'_1 , k'_2) of different Cdc42 constructs. Data points of the same colour refer to the rates obtained from separate measurements. Data points of the same colour but a distinct shape (circle, triangle, rhombus) represent different purification batches of the same construct. Values are given in Appendix 3.4.3 Tab. 3.3. (d) Predicted amount of remaining GTP for Cdc42 constructs ($5 \mu\text{M}$) after an incubation time of 1.5 h. Symbols indicate if a specific purification batch was used. The data was calculated using k'_1 , k'_2 shown in (c) and Eq. 3.1. (e) C_{corr} values (Eq. 3.2) of Cdc42-Cdc24 interaction assays. Values are given in Appendix 3.4.3 Tab. 3.4. (f) Cdc42-Cdc24 interaction rate (k'_3 , determined using Eq. 3.2). Values are given in Appendix 3.4.3 Tab. 3.4.

proteins were eluted. If Cdc42 was eluted as well, it must have been because it was bound to Bem1.

The data of these experiments are shown in Fig. 3.4: We observed that binding between Bem1 and Cdc42 occurred, but that it was so weak that Cdc42 could only be detected using Western Blotting. In comparison, pulldown experiments with the same Bem1 construct and Cdc24, another binding partner of Bem1, showed so high amounts of Cdc24 in the elution fraction that it was visible on SDS-Page. This indicates stronger binding (see Chapter 4).

3

We observed an interaction between Flag-tagged Bem1 and all Strep-tagged Cdc42 versions. The blotting signal for H-Cdc42-SS was weaker in comparison to S-Cdc42-H and SS-Cdc42-H. This could indicate that this construct interacts less strongly with Bem1 because of the purification tags, or that in this particular pulldown set less protein interacted with Bem1 for an external reason. Favouring the latter is the observation that in different pulldown experiments different amounts of S-Cdc42-H bound to Bem1 (Fig. 3.4). It is therefore questionable if any quantitative conclusions can be drawn from this data. We also tested the interaction between Flag-tagged Cdc42 and Strep-tagged Bem1, but Strep-tagged Bem1 (S-Bem1-H), for some reason whatsoever, was sticking to the anti-Flag affinity gel by itself (data not shown). We tested if Strep-tagged Cdc42 (S-Cdc42-H) would also stick to the anti-Flag affinity gel. In absence of H-Bem1-F, a small amount of S-Cdc42-H was binding to the anti-Flag affinity gel. Its signal in the Western Blot however was significantly weaker than when Cdc42 was incubated with anti-Flag affinity gel in presence of H-Bem1-F (Fig. 3.4).

Bem1 was shown to specifically bind to GTP-bound, but not GDP-bound, Cdc42 (**Bose et al. (2001)**). We conducted Flag-pulldown experiments in which 1 nmol Cdc42 got pre-loaded with no nucleotide, 100 nmol GDP, or 100 nmol GTP γ S (a non-hydrolysable variant of GTP). Surprisingly, no significant effect of the nucleotide state on the Cdc42-Bem1 interaction could be observed: Cdc42-GDP and Cdc42-GTP γ S bound equally strong to Bem1. We also found that Cdc42 that was not incubated with any nucleotide bound to Bem1. If the observations of Bose *et al.* are correct (**Bose et al. (2001)**), this would indicate that most of our Cdc42 was "naturally" in its GTP-bound conformation. It is therefore possible that our nucleotide pre-loading step was not sufficient, and that even in presence of GDP most Cdc42 still was in the GTP-conformation, resulting in its binding to Bem1. Experiments with the addition of more nucleotide, the use of longer incubation times, or in which only Cdc42 is used that was purified already in a specific nucleotide state (**Rapali et al. (2017)**), could verify or falsify this hypothesis. It is also possible that the contradicting experimental results are explained by the differences in the experimental setups: Bose *et al.* conducted similar pulldown experiments as shown here, but used GST-tagged (26 kDa) instead of a Flag-tagged (3 kDa) proteins (and subsequently GST agarose instead of anti-Flag affinity gel). Given the size of the GST-tag, it can not be excluded that this tag is destabilising the Bem1-Cdc42 interaction, thereby exaggerating the effect of a conformational state of Cdc42 on Bem1 binding. Pulldowns with (1) GST-Cdc42 and Bem1, and (2) GST-Bem1 and Cdc42, both showed the same result. Thus, the GST-tag would need to be positioned in both cases in such a way that it destabilises the interaction, questioning this hypothesis. Nonetheless, pulldown experiments with Bem1 and Cdc24 indicate that the GST-tag can indeed destabilise protein-protein interactions: Zheng *et al.* reported that 2 mM CaCl₂ disrupt the interaction between GST-Bem1 and Cdc24 (**Zheng et al. (1995)**), whereas our experiments show that even in presence of 20 mM CaCl₂ Cdc24 still binds to Flag-Bem1 (see Chapter 6). Another experimental difference is the way in which Cdc42 was locked in one nucleotide state: We pre-loaded Cdc42 with excess GDP or

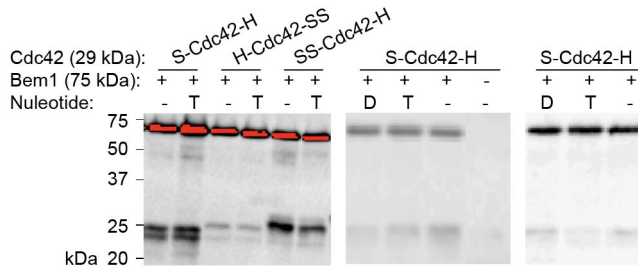


Figure 3.4. Cdc42 - Bem1 interaction. Anti-His Western Blots of Cdc42-Bem1 Flag-pulldown experiments.

GTP γ S, Bose *et al.* used Cdc42-mutants that are locked in a GDP- or GTP-state. One interpretation is that GDP/GTP-loaded Cdc42 and Cdc42 mutants are structurally distinct in a way that affects Cdc42-Bem1 binding. Alternatively, it could indicate that our pre-loading was insufficient and that it did not bring the majority of Cdc42 into its GDP-bound conformation.

Taken together, we show that all Strep-tagged Cdc42 constructs can bind to Bem1. The binding occurs independent of if a nucleotide is added and also in presence of GDP (contradicting *Bose et al. (2001)*). Further experiments are needed to fully understand the Bem1-Cdc42 interaction and the contradicting experimental results.

3.2.5. Cdc42 storage at -20°C

So-far, Cdc42 seemed to be very stable and mostly unaffected by any added tag. We further investigated if this robustness also applies to less ideal storage conditions. Proteins are usually flash-frozen in liquid nitrogen and stored at -80°C, as this impedes the formation of ice-crystals that damage protein folding. Not every laboratory, including those in more physics-oriented fields, has always easy access to these. Protein storage at -20°C would allow for a larger field to study aspects of Cdc42. *Zhang et al. (2000)* already reported that Cdc42 stored in 30% glycerol was stable at -20°C for up to two weeks without activity loss. We explored if and how storage at -20°C affects Cdc42's GTPase activity.

First, one Cdc42 batch (H-Cdc42-F, in SEC buffer supplemented with 10% glycerol) got divided into six small sub-batches. One was flash-frozen with liquid nitrogen and kept at -80°C until use. The other five batches were kept at -20°C (without flash-freezing), and up to four additional freeze/thaw cycles were performed. After seven days the GTPase activity of Cdc42 was measured. (Fig. 3.5a). It remained the same for all samples, independent of the storage location (-80°C/-20°C) and amount of freeze/thaw cycles.

Next, we assessed if longer-term storage at -20°C affects Cdc42's GTPase activity. Again, one Cdc42 batch got divided and one sample was kept at -80°C for the entire time (12 weeks). The other samples were kept for a certain amount of time at -80°C, after which they were moved to -20°C (with one additional thaw/freeze cycle). At week 12 a GTPase assay was performed (Fig. 3.5b). Again, the GTPase activity of all Cdc42 samples remained the same.

Taken together, Cdc42 can be stored in a buffer with 10% glycerol at -20°C for at least 12 weeks, and samples can even go through at least five freeze/thaw cycles without activity loss.

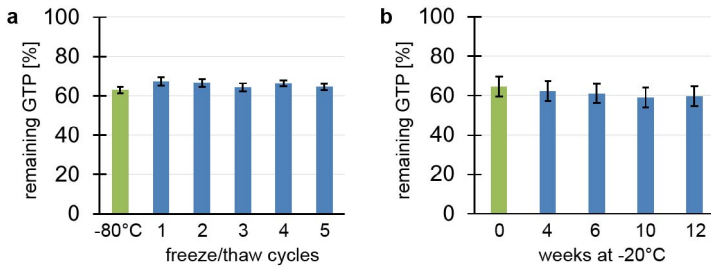


Figure 3.5. Cdc42 at non-ideal storage conditions. (a) GTPase activity of Cdc42 (9 μ M H-Cdc42-F, 1.5 h incubation with 5 μ M GTP) after 7 days of storage at -80°C (green) or -20°C (blue). Samples stored at -20°C underwent 1-5 freeze/thaw cycles. (b) GTPase activity of Cdc42 (9 μ M H-Cdc42-F, 1.5 h incubation with 5 μ M GTP) in relation to the amount of weeks the sample was stored at -20°C . The total storage time was 12 weeks, of which samples were stored for 0, 4, 6, 10, or 12 weeks at -20°C and the time prior at -80°C .

3.3. Discussion

Here, we explored if and how purification tags can influence Cdc42's properties. We show that Cdc42's GTPase activity and interaction with the GEF Cdc24 and scaffold Bem1 is largely unaffected by Cdc42's N- and C-terminal purification tags. The only exception is Cdc42 tagged with an N-terminal Twin-Strep-tag, which showed precipitation issues and a decreased GTPase activity and interaction with Cdc24. We also observed negative effects of the N-terminal Twin-Strep-tag for Cdc24 and Bem1 constructs, which did not express well or at all. These two proteins are larger and less tightly folded than Cdc42, making them more susceptible to degradation and/or folding issues. We think that these early and easily detectable expression issues already indicate a general problem with the construct design: in the case of the bigger and less stable Cdc24 and Bem1 it already showed up on the expression level. In the case of the smaller and more stable Cdc42 it was only observable after purification. We suggest to not use an N-terminal Twin-Strep-tag. Instead, tagging proteins with an N-terminal Strep-II-tag (although this tag is less suitable than the Twin-Strep-tag, as it has an order of magnitude lower affinity for Strep-Tactin than the Twin-Strep-tag (*Schmidt et al. (2013)*)), a C-terminal Twin-Strep-tag, or an N-terminal 6His-Twin-Strep-tag is a more suitable approach.

We observed Cdc42 dimerisation in denaturing conditions, but not in *in vitro* conditions. Our results are in accordance with previous *in vivo* findings (*Kang et al. (2010)*). The question if Cdc42 can dimerise is of interest, because Cdc42 dimerisation constitutes a possible feedback mechanism for its recruitment to the polarity spot during cell division (*Goryachev and Leda (2017)*). Our data indicates that this is not the case. It is, however, possible that very transient and weakly bound Cdc42 dimers form. Such complexes would not sustain themselves under the constant flow under which SEC is performed. Interestingly, we consistently observed Cdc42 dimers under denaturing conditions. This could be an artefact of the denaturing conditions that has no translation to the behaviour of the folded protein, or could mean that Cdc42 has some, still unexplored, potential to dimerise. Cdc42 belongs to the group of small GTPases, of which some (e.g. Rsr1, human Cdc42, Rac1 and Rac2) have been shown to dimerise or oligomerise *in vitro* or *in vivo* (*Zhang and Zheng (1998)*; *Zhang et al. (1999, 2001)*; *Kang et al. (2010)*). The dimerisation capacity was linked to the polybasic region (PBR) of these GTPases, which is a five AAs long C-terminal region consisting of mostly basic AAs. The dimerising GTPases all have similar, but distinct PBR sequences and a partial removal of the PBR impedes dimerisation. For example, human Cdc42

has the PBR sequence KKSRR, Rac1 has KRKRK, Rac2 has QQKRA, and Rsr1 has KKKKK. Mutation of the PBR of Rac1 to KKSRR does not affect its oligomerisation, but a change to QQQQQ inhibits it. The same holds true for Rsr1: changing its PBR to SSSSS inhibits dimerisation. Not all mutations, however, affect dimerisation: human Cdc42 with the altered PBR KKSQR still dimerises (**Zhang and Zheng (1998); Zhang et al. (1999, 2001)**). Yeast Cdc42 has the PBR KKSQR. As the direct relation between the PBR sequences and protein dimerisation is still largely unknown, it is difficult to say, based on the PBR sequence, if Cdc42 in principle can dimerise, and if the dimers on SDS-Page are of biological relevance. We observed that the presence of an N-terminal Twin-Strep-tag disrupted the formation of dimers on SDS-Page (SS-Cdc42-H, H-SS-Cdc42-F). This is yet another effect of the N-terminal Twin-Strep-tag, indicating that it affects the protein in an odd fashion. Here, in contrast to its other effects, the prior placement of a 6His-tag (H-SS-Cdc42-F) did not neutralise it. We observed a dimer band for S-Cdc42-H in the anti-His, but not in the anti-Cdc42 Western Blot (both for expression test fractions and for SEC-MALS peak fractions), suggesting that the tag interferes with the unfolded Cdc42 structure in such a way that the dimer still forms, but that the Cdc42 antibody can not bind anymore. The double repeat of that tag (= Twin-Strep-tag) interferes much more, resulting in no dimerisation. It is very surprising that an N-terminal tag influences dimerisation at all, because the PBR, which sits on the protein's C-terminus, is directly linked to dimerisation. As this dimerisation is observed in denaturing conditions, we can not exclude that it's based on an entirely different mechanism and biologically irrelevant. Nevertheless, the role of the proteins' N-terminus on dimerisation has not yet been explored, and it could be a binding partner of the PBR. In fact, the PBR consists of mostly positively charged AAs. It likely binds not to itself but to another protein part, which could be an N-terminal region. Adding other positively charged AAs to the N-terminus could inhibit this interaction. The 6His- (6 AA), Strep-II- (8 AA), and Twin-Strep-tag (28 AA) contain positively charged AAs. Given the significant size difference between the 6His-/Strep-II- and Twin-Strep-tag, we suspect that the Twin-Strep-tag's charge in combination with its size hinders the interaction required for dimerisation. We show that the T7 lead is necessary for Cdc42 expression in *E. coli* and that purification tags don't influence the expression and degradation levels of Cdc42, but those of Cdc42-sfGFP and Cdc42-mNeonGreen sandwich fusions. Cdc42 is a rather small and tightly folded protein. The sandwich-fusions of Cdc42 and sfGFP, or mNeonGreen, (**Bendezú et al. (2015)**) consist of two folded proteins parts. Because the sequence of sfGFP/mNeonGreen is inserted into that of Cdc42, Cdc42 can only completely fold if the fluorophore is fully folded. As long as both protein parts are not full folded, the entire construct is more susceptible to degradation. It is therefore not surprising to see almost no degradation bands in the Cdc42 expression tests, but many degradation bands in the Cdc42-sfGFP/mNeonGreen expression tests. We had already observed that Cdc42, Cdc24, and Bem1 constructs with an N-terminal Twin-Strep-tag don't behave well. Therefore we did not test such Cdc42-mNeonGreen/sfGFP constructs. Among the purification tag combinations tested, it was surprising to see that the purification tags do not influence the expression of Cdc42, but that of the sandwich fusions: H-Cdc42-F and H-Cdc42-S expressed as full-size protein, but no full-length H-Cdc42-mNeon-F and H-Cdc42-mNeon-S could be obtained. Here, the N- or C-terminal tag, or the tag combination could be the problem. The expression of full-sized H-Cdc42-mNeon-SS suggests that the N-terminal 6His-tag is not the origin of the issue, but that C-terminal Strep-II- and Flag-tag are. However, H-SS-Cdc42-mNeon-F expressed well, suggesting that the reason behind the expression issue is not purely the C-terminal tag. The fact that H-Cdc42-mNeon-SS, but not H-Cdc42-mNeon-S, expressed, is especially surprising. The Twin-

Strep-tag is made of a double repeat of the Strep-II-tag, and is therefore in its properties very similar to the Strep-II-tag. Further, constructs with the same tags on opposite termini (S-Cdc42-mNeon-H and F-Cdc42-mNeon-H) expressed well. The reasons behind these observations are still unknown to us. When constructing Cdc42 sandwich fusions, we suggest to design and test a few variants to check which express and purify well.

In conclusion, we observe that most purification tags, including C-terminal tags, don't affect Cdc42's properties. The only exception is the N-terminal Twin-Strep-tag, which negatively affects Cdc42. This negative effect is exaggerated for larger and lesser folded proteins. N-terminal Strep-II- and Twin-Strep-tags further influence Cdc42 dimerisation in denaturing conditions. In addition, Cdc42-mNeonGreen and -sfGFP sandwich fusions are further affected by two additional tag combinations. We suspect that the less tightly folded a protein is, the more purification tags can negatively affect protein folding and/or expression and degradation.

So-far, we discussed how purification tags influence the properties of Cdc42. Zooming out from this example to protein construct design, and the relevance of purification tags in general, two questions emerge: Do we need to care about purification tags? And do we, for every protein, need to test them all?

The answer is two-fold: Do we need to care? Yes! And do we need to try them all? No! The results shown here illustrate that protein construct design matters, but testing all tag combinations for every protein is not feasible. When planning to use a protein for *in vitro* studies, one should spend a significant amount of thought on the construct design. Which criteria should be considered?

Scientific studies often don't explain or even explicitly mention the construct design, nor state which tag plus POI combinations did not work. It can therefore be difficult to find evidence for or against a certain construct design. A thorough study of the POI constructs in scientific literature can reveal which constructs do work, and give hints on how to solve existing issues with certain protein constructs. For example, for SS-Cdc42-H we observed precipitation, a decreased GTPase cycling and Cdc42-Cdc24 interaction rate. Rapali *et al.* used H-S-Cdc42⁵ (Rapali *et al.* (2017)), which indicated that the placement of a 6His-tag in front of the Twin-Strep-tag could resolve the observed issues. Indeed, H-SS-Cdc42-F showed no precipitation and GTP hydrolysis cycling rates more closely to those of the other constructs. At the same time, the accumulation of a certain construct or tag placement in scientific literature also has to be viewed critically, as it could represent a bias towards what has been tried before. We here show that small C-terminal tags do not affect the GTPase properties of Cdc42. C-terminal tags on Cdc42 have not been reported before, but are a viable option if Cdc42 prenylation is not required.

An important criterion for the construct design is the POI shape and size. Larger proteins and proteins made from protein domains that are connected by flexible linkers tend to show more degradation than smaller and compact proteins. The placement of a purification tag on both the N- and C-terminus can then be helpful for the purification process. If, however, one terminus is essential for protein functionality, a purification tag should not be placed there. If Cdc42 membrane binding is of interest, constructs with an unmodified C-terminus of Cdc42 ought to be used. Cdc42 binds to membranes via a prenyl moiety that gets appended to its C-terminus. A C-terminal tag would inhibit the prenylation process and thus lead to protein that can't bind to

⁵It could also have been a H-SS-Cdc42 construct. Sometimes the distinction between a Twin-Strep and a Strep-II-tag is omitted, thus classifying both as Strep-II-tags.

membranes.

Protein labelling and consequent clean-up steps should also be considered in the initial construct design. In this thesis we use double-tagged Cdc42 with an C-terminal Sortase labelling site. This site can be used to append a moiety of interest and cleave the C-terminal tag in one step. Afterwards, the labelled protein needs to be separated from unlabelled protein and the Sortase enzyme used for this reaction. Cdc42 and Sortase enzyme both are about 30 kDa in size. If labelled Cdc42 is not significantly bigger, then the three protein species can not be separated by size. In this case, the positioning of the tags can be of use. Constructs with a C-terminal His-tag, such as F-Cdc42-H, result in the labelling product F-Cdc42-Label. After the labelling step, the reaction mixture contains F-Cdc42-H, F-Cdc42-Label, and H-Sortase. The labelling product can easily be purified by His affinity chromatography, as it is the only species that does not have a His-tag and thus can not bind to the column material. This clean-up strategy, however, is not possible if Cdc42 with the opposite tag orientation (H-Cdc42-F) is used (see Chapter 5).

Further, the application itself can guide the tag choice. Applications in structural biology generally require only small amounts (ng – µg) of protein but strive for constructs that are only minimally modified or in which tags and other appendices are at least cleavable. Biochemical applications tend to require more protein (µg – mg), but can accommodate more heavily tagged constructs, given the tag is not interfering with the studied protein function. If the POI should be tethered to a membrane or other object, the Twin-Strep-tag can be used to achieve this goal. Using biotinylated lipids coated with Streptavidin, Twin-Strep-tagged proteins can be tethered to the lipids, as the Twin-Strep-tag binds with high affinity to Streptavidin (*Schmidt et al. (2013)*). If protein-protein interactions are of interest, big tags like the GST-tag (26 kDa) might want to be avoided, as they could sterically hinder the protein-protein interaction and destabilise the interaction. The much smaller Flag-tag, that generally shows a high specificity towards the anti-Flag affinity gel, might then be a better option. The amount of protein needed plays a role in itself, too. Protein purification is a time-consuming activity, and in each purification step protein gets lost. Chromatography techniques that use POI inherent properties (such as hydrophobicity) require prior knowledge of protein properties and screening experiments. Techniques based on protein size limit the sample volume that can be applied. Both can be fine choices if knowledge of POI properties exists or if only small amounts of POI are needed. If, however, higher amounts of POI are needed, techniques that can easily be scaled up are of advantage. The protein should ideally be pure after one or two purification steps, both of which are fast and allow for a high sample volume⁶. Most affinity-purification techniques fall in this category. Of the tags mentioned in this chapter, the 6His- and Twin-Strep-tag are ideal, as both bind with high affinity and capacity to the column materials. In contrast, the Strep-II-tag and Flag-tag are less ideal for protein purification purposes. The Strep-II-tag has a low affinity for its column material, and anti-Flag affinity gel is expensive and can not be regenerated after a single usage.

If an *E. coli* expression system ought to be used, and the POI is not from this bacterium, the N-terminal placement of the T7 lead (T7 tag) is advisable. Here we show that Cdc42 expresses in high amounts independent of the used purification tags, but only if the T7 lead is included. The T7 lead might not always be required, but is generally advisable if small additions to the N-terminus

⁶To achieve larger amounts of POI, the expression levels of the POI can be optimised. Further up-scaling then involves increasing the expression volume. This leads to larger volumes of sample during the purification process (especially after cell lysis). Samples can be concentrated using spin-concentrators, but one loses (in our experience) about 30% of protein during the process. Additionally, not all proteins stay soluble at high concentrations. Purification techniques that allow for higher flow rates in the sample application process and that can handle larger sample volumes are thus advantageous.

are not interfering with protein or assay functionality.

Lastly, placing cleavage sites after N- and before C-terminal tags is preferable, as this allows the removal of the purification tag, T7 lead, or other additions. Thereby a tag-free version of the POI can be generated, which can be used if the tag unexpectedly interferes with the protein functionality or to generally test if or how strong the tag affects it. The type of cleavage site and enzyme has to be considered as well - not all cleavage enzymes are suitable for all POIs! We placed an N-terminal Enterokinase cleavage site on most constructs, to be able to cleave the N-terminal additions. Enterokinase cleaves after the lysine of the recognition sequence DDDDK (with D: aspartic acid and K: lysine). However, it has been reported to also cleave after any sequence of one to four acidic AAs plus one basic AA (*Shahravan et al. (2008)*). Cdc42 contains three sequences that fit these requirements (EDYDR, DDK, EK) and initial tests showed non-specific cutting (data not shown). We replaced the enterokinase cut site with a TEV protease cut site. Further tests still have to be conducted to test if the TEV protease is more suitable than Enterokinase to remove N-terminal tags from Cdc42.

Taken together, construct designs published in literature, POI shape and size, protein labelling and consequent clean-up steps, applications, amount of protein needed, and compatibility of the POI with the *E. coli* expression system and with cleavage enzymes are factors that should be considered when designing a protein construct. If many factors are unknown, it can be advisable to design a few construct variations (that all fit the mentioned criteria) in parallel and check with expression tests if, how strongly, and with how much degradation, the POI expresses. Thereby constructs that are either not suitable for the desired application or are difficult to purify can be avoided. To make working with protein more accessible for a broader spectrum of scientists, it will also necessary that publications state and explain the used construct designs and their effects on the protein behaviour, as well as show data of constructs that "failed".

3.4. Appendix

3.4.1. Appendix: Twin-Strep- and Strep-II-tagged Cdc42

All double-tagged Cdc42 constructs (type D) are 28-32 kDa and single-tagged constructs (type S) are 25 kDa in size (Tab. 3.1). The expression tests (Fig. 3.2b) show that type S constructs run at their expected size, but that type D constructs only partially do: constructs containing a Flag-tag (H-Cdc42-F, F-Cdc42-H, H-SS-Cdc42-F) run at their expected size (29-32 kDa). Constructs containing combinations of a His-tag and Strep-II/Twin-Strep-tag, however, run at a size that is a bit smaller than expected (closer to 25 kDa than to 28/29 kDa). This is the case for both constructs with N- or C-terminal Strep-II/Twin-Strep-tag. We determined the exact protein size by size-exclusion chromatography - multi-angle light scattering (SEC-MALS). Here a sample of purified protein is run on a SEC column and the protein size is determined through the light scattering properties of the protein. Again, the size of constructs of type S and of Flag-tagged Cdc42 is as expected, but Strep-II-tagged Cdc42 is about 1 kDa smaller than expected (26.7 vs. 27.8 kDa) (Fig. 3.2c). Strep-II-tag is about 1 kDa in size. It is theoretically possible that during the expression the Strep-II-tag is cleaved from all constructs. However, anti-His and anti-Strep Western Blotting of S-Cdc42-H show the presence of both tags (Fig. 3.6). The general origin of this apparent size-reduction is therefore unknown.

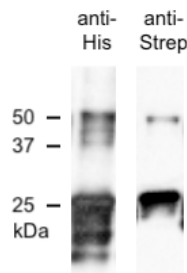


Figure 3.6. Anti-His and anti-Strep Western Blots of S-Cdc42-H.

3.4.2. Appendix: Cdc42-mNeon/sfGFP expression tests

Double-tagged Cdc42 was mostly unaffected by its specific N- and C-terminal tags (with the exception of an N-terminal Twin-Strep-tag). We assessed if this was also true for sandwich-fusions of Cdc42 and sfGFP or mNeonGreen (*Bendezú et al. (2015)*). We conducted expression tests (condition 'f' and 's') and analysed them by anti-His Western Blotting (Fig. 3.7).

Most fusion-constructs show bands at the expected size of 55 kDa (Fig. 3.7, green arrow). Only H-Cdc42-mNeon-F and H-Cdc42-mNeon-S constructs do not express as the full-size protein (lane 2, 3, 10, 11). This is surprising as their Cdc42 equivalents show no expression problems at all (black arrow, lane 1 and 9). In contrast to Cdc42, most Cdc42-mNeon/sfGFP fusions show additional lower bands, that can originate from degradation or translation processes that terminated prematurely. This is not surprising, as the fluorophore sequence was inserted into the Cdc42 sequence, potentially making the fusion more susceptible to degradation.

In most cases both Cdc42-mNeon and Cdc42-sfGFP fusions expressed with roughly the same amount and to same level of degradation, through significantly less strong than Cdc42. An exception is F-Cdc42-sfGFP-H (lane 7 and 8), that expressed at way higher amount than its mNeonGreen equivalent (lane 5 and 6). It also shows higher amounts of degradation, even though it could be the case that the degradation bands are only more pronounced due to the generally higher expression levels.

In most cases no big difference between the slow ('s') and fast ('f') expression condition can be observed; the fast condition leads to slightly more protein than the slow condition, but also shows a higher amount of degradation bands. An exception is S-Cdc42-sfGFP-H (lane 20 and 21), where less degradation is present in the fast condition (when compared to the slow condition). This, however, is not true for the mNeonGreen equivalent (S-Cdc42-mNeon-H, lane 18 and 19). Here the slow condition expressed roughly the same amount of protein with less degradation.

Taken together, fluorescent Cdc42 fusions can be produced both with sfGFP and mNeonGreen and with several, but not all, N- and C-terminal tag combinations. Degradation bands are observed in all cases but to different degrees, but no apparent relation between used tags and expression behaviour can be drawn.

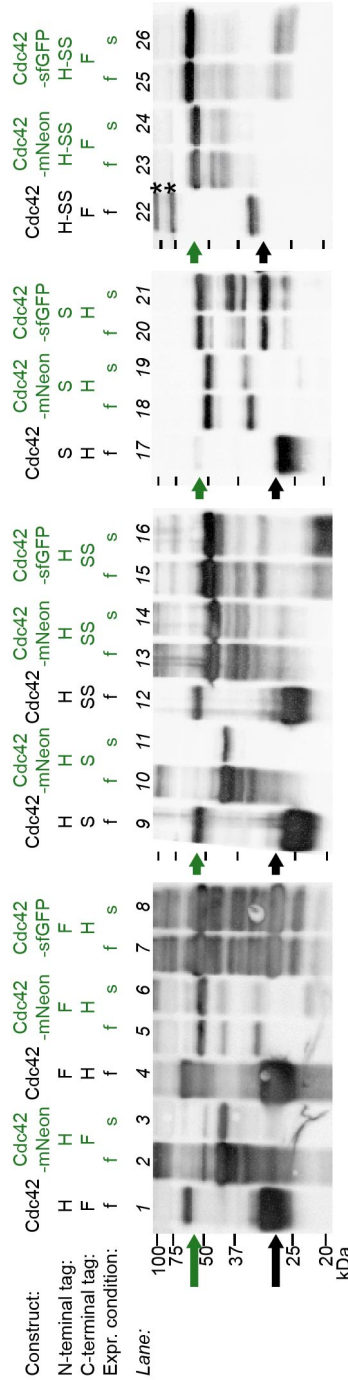


Figure 3.7. Effect of purification tags on Cdc42-sfGFP and -mNeonGreen expression levels ('f' and 's' expression condition), analysed by anti-His Western Blotting. The black arrow indicates the size of monomeric Cdc42 and the green arrow indicates that of the fluorescent Cdc42 fusions. Bands annotated with an asterisk (lane 22) are not from the protein in that lane, but bands of the protein standard that migrated to this lane during the Blotting process.

3.4.3. Appendix: GTP hydrolysis cycling rates

Table 3.3. GTP hydrolysis cycling rates k'_1 and k'_2 of Cdc42 (Fig. 3.3c).

Cdc42 construct	Purif. batch	k'_1 [$\times 10^{-2} \mu\text{M}^{-1} \text{h}^{-1}$]	k'_1 std. err.	k'_2 [$\times 10^{-2} \mu\text{M}^{-2} \text{h}^{-1}$]	k'_2 std. err.
H-Cdc42-F	2	6.23	0.56	4.41	0.15
H-Cdc42-F	2	7.10	0.94	8.16	0.56
H-Cdc42-F	2	9.22	2.13	9.70	1.31
H-Cdc42-F	2	8.18	2.80	5.47	1.66
H-Cdc42-F	1	5.79	2.79	0.38	0.22
S-Cdc42-H	1	15.95	2.30	4.25	0.58
H-Cdc42-SS	1	14.73	1.53	1.63	0.39
F-Cdc42-H	1	6.60	5.17	3.26	1.53
F-Cdc42-H	2	12.85	0.45	2.09	0.08
F-Cdc42-H	3	6.72	1.21	1.46	0.19
H-Cdc42:CTIS	1	3.64	3.55	3.52	0.56
H-SS-Cdc42-F	1	1.58	0.70	0.97	0.10
SS-Cdc42-H	1	4.03	1.53	-0.39	0.30

Table 3.4. Correction factors c_{corr} and Cdc42-Cdc24 interaction rate k'_3 (Fig. 3.3d.e). Abbreviations: N.A.: not available (there were not enough data points to determine an error).

Cdc42 construct	Purif. batch	c_{corr}	c_{corr} std. err.	k'_3 [$\mu\text{M}^{-3} \text{h}^{-1}$]	k'_3 std. err.
H-Cdc42-F	2	1.46	0.54	44.12	N.A.
H-Cdc42-F	2	1.40	0.54	117.31	4.16
H-Cdc42-F	2	1.43	0.63	36.39	7.38
H-Cdc42-F	2	1.39	0.60	17.46	N.A.
S-Cdc42-H	1	1.01	0.98	16.66	N.A.
S-Cdc42-H	1	0.97	0.98	76.28	2.90
H-Cdc42-SS	1	0.94	1.08	32.79	N.A.
F-Cdc42-H	1	1.00	1.75	45.30	N.A.
F-Cdc42-H	2	1.10	0.10	118.84	5.71
F-Cdc42-H	3	1.43	0.41	44.25	N.A.
H-Cdc42:CTIS	1	1.57	1.38	48.30	N.A.
H-SS-Cdc42-F	1	1.33	0.31	90.52	N.A.
SS-Cdc42-H	1	1.00	0.00	0.38	0.21

Contributions and acknowledgements

R. van der Valk constructed the plasmids of protein constructs. Proteins were expressed and purified by S. Tschirpke and F. van Opstal. S. Tschirpke conducted GTPase assays, Flag-pulldown experiments, expression tests, Western Blots, and analysed the data thereof. The modelling and fitting of the GTPase data was done by W. Daalman. F. van Opstal conducted expression tests and Western Blots. Figure preparation and writing of this chapter was done by S. Tschirpke.

We thank C. de Agrela Pinto for conducting SEC-MALS with our samples and analysing the data thereof. We thank D. McCusker (University of Bordeaux) for the plasmid pDM272 and N. Dekker (TU Delft) for the plasmid pET28a-His-mcm10-Sortase-Flag.

4

Emergence is one of the founding principles of agility, and is the closest one to pure magic. Emergent properties aren't designed or built in, they simply happen as a dynamic result of the rest of the system. "Emergence" comes from middle 17th century Latin in the sense of an "unforeseen occurrence." [...] A classic example of emergence lies in the flocking behaviour of birds. A computer simulation can use as few as three simple rules and suddenly you get very complex behaviour as the flock wends and wafts its way gracefully through the sky, reforming around obstacles, and so on. None of this advanced behaviour is specified by the rules; it emerges from the dynamics of the system. Simple rules, as with the birds simulation, lead to complex behaviour. Complex rules, as with the tax law in most countries, lead to stupid behaviour. [...] Keep it small. Keep it simple. Let it happen.

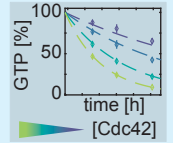
— Andrew Hunt

Synergistic regulation of the Cdc42 GTPase cycle

A Cdc42 GTPase activity model

➔ Coarse-grain GTPase cycle:
 $[GTP] + n [Cdc42] \rightarrow [GDP] + n [Cdc42]$

➔ Amount of remaining GTP in the reaction mixture declines exponentially with time: $[GTP]_t = [GTP]_{t=0} e^{-Kt}$



$$\text{with } K = K'_1[Cdc42] + K'_2[Cdc42]^2 + K'_{3,x}[Cdc42][X]$$

monomeric Cdc42

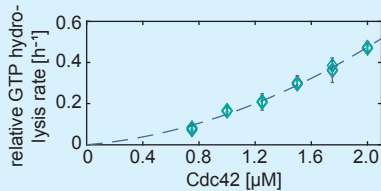
Cdc42 cooperativity dimerisation + crowding

Cdc42 - effector protein interaction + crowding

Crowding, Cooperativity, & Dimerisation in Luminescence Experiments



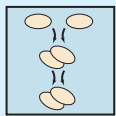
Cdc42



➔ The GTP hydrolysis rate depends non-linearly on the Cdc42 concentration

➔ Due to...

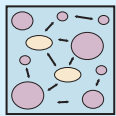
Dimerisation?



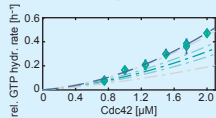
SEC-MALS:
Cdc42 is monomeric

➔ Dimerisation is unlikely

Crowding?

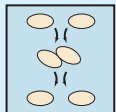


Cdc42 + BSA (crowding agent):
BSA/crowding increases the rate



Contribution of crowding to the total rate

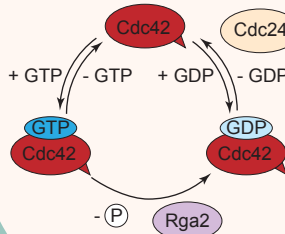
Cooperativity?



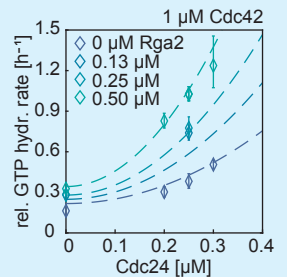
Possible, but not verified

Can be facilitated by crowding (Kuznetsova *et al.* 2014)

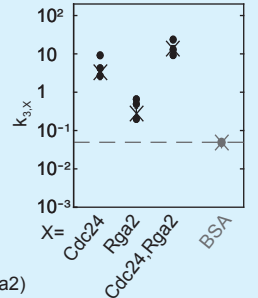
Cdc42 GTPase cycle



Regulation of Cdc42 through Cdc24 and Rga2



$$-\frac{d \ln[GTP]}{dt} = K'_1[Cdc42] + K'_2[Cdc42]^2 + K'_{3,Cdc24}[Cdc42][Cdc24] + K'_{3,Rga2}[Cdc42][Rga2] + K'_{3,Cdc24,Rga2}[Cdc42][Rga2][Cdc24]$$



➔ Cdc24 (and to some extent Rga2) boost the GTPase cycle of Cdc42, this is greater than the effect of crowding

➔ Synergy between Cdc24 and Rga2 (pos. $K'_{3,Cdc24,Rga2}$)

Synergistic regulation of the Cdc42 GTPase cycle through crowding, GEFs, GAPs, and scaffold proteins

Abstract Emergent properties of a system arise when the systems parts interact in a wider whole. An example of such an emergent system is the cell division protein network of *Saccharomyces cerevisiae*. Here the cell division control protein Cdc42 accumulates in a single spot at the cell membrane. Cdc42 is a membrane-binding Rho-type GTPase and a highly regulated protein, it's interacting with GEFs, GAPs, scaffold and other regulatory proteins. To shine more light on the emergent properties of the system, we investigated a process at the centre of Cdc42 - its GTPase cycle. We studied the entire GTPase cycle of Cdc42 *in vitro* and the effect of molecular crowding, the GEF Cdc24, GAP Rga2, scaffold protein Bem1, and combinations thereof, on it. We developed a mathematical model to describe the GTPase cycle and show that Cdc42 exhibits cooperativity, but exclude dimerisation as a cause. The GEF Cdc24 shows cooperativity as well, and our data suggests that it synergises with Rga2. Surprisingly, we also found that molecular crowding, even at μM concentrations, positively affects the Cdc42 GTPase cycle and interactions with its effector proteins.

4.1. Introduction

Emergent phenomena occur everywhere in nature, from the formation of bird flocks in the sky to small-scale intracellular processes. Although their size and manifestation can make them appear very distinct, they share that their properties do not arise because the system's parts possess these properties, but emerge because the parts interact as a wider whole. The fascinating yet also inherently difficult question underpinning these processes is, how?

An example of such an emergent system is the cell division protein network of *Saccharomyces cerevisiae*. Here the cell division control protein Cdc42 forms a simple pattern just before cell division; it accumulates in a single spot at the cell membrane. (Fig. 4.1a). Cdc42 is a membrane-binding Rho-type GTPase and a highly regulated protein: Cdc42's nucleotide state is affected by GDP/GTP exchange factors (GEFs) and GTP-activating proteins (GAPs). It can be extracted from membranes by the guanine nucleotide dissociation inhibitor (GDI) Rdi1, and interacts with p21 activated kinases, scaffold proteins, exocysts, and formins (Fig. 4.1b) (*Chiou et al. (2017)*). Some of these interactions are also influenced by Cdc42's nucleotide state. For example, *in vitro* data suggests that Bem1 preferably binds to Cdc42-GTP (*Bose et al. (2001)*), that Cdc24 binds stronger to nucleotide free Cdc42 than to Cdc42-GDP or Cdc42-GTP (*Zheng et al. (1995)*), and that Rdi1 has a higher affinity for membrane-bound Cdc42-GDP than for its GTP-bound form (*Johnson et al. (2009)*).

Dissecting the molecular interactions giving rise to Cdc42 accumulation through *in vivo* studies has turned out to be challenging, because of the high level of observed redundancy and inter-

Abbreviations:

AA	amino acid
BSA	Bovine serum albumin
CroCoDiLe	crowding, cooperativity, and dimerisation in luminescence experiments
GAP	GTPase activating protein
GDI	guanine nucleotide dissociation inhibitor
GEF	GDP/GTP exchange factor
MALS	multi-angle light scattering
PBR	polybasic region
SEC	size-exclusion chromatography

4

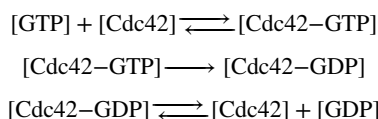
dependence between interactions. On the other hand, *in vitro* studies mostly focus on single reaction steps, such as the GTP hydrolysis by Cdc42 and the effect of GAPs (Zheng *et al.* (1993); Zhang *et al.* (1997); Zhang and Zheng (1998); Zhang *et al.* (1999, 2001)), the GDP/GTP exchange reaction in conjunction with GEFs (Zheng *et al.* (1994, 1995); Rapali *et al.* (2017)), or Cdc42 membrane binding and extraction by Rdi1 (Johnson *et al.* (2009, 2012); Das *et al.* (2012); Golding *et al.* (2019)). These studies are of great value, but focused only on a small aspect of the system and did not include how different proteins affect each other (and thus how emergent properties arise). This parameter interplay is of great importance, as has been pointed out for another emergent system - the Min protein system - before (Loose *et al.* (2008); Vecchiarelli *et al.* (2016, 2014); Miyagi *et al.* (2018); Kretschmer *et al.* (2017); Martos *et al.* (2013, 2015); Caspi and Dekker (2016))¹.

To explore emergent properties of the system, we investigated a process at the centre of Cdc42 - its GTPase cycle. We studied the entire GTPase cycle of Cdc42 and the effect of molecular crowding, the GEF Cdc24, GAP Rga2, scaffold protein Bem1, and combinations thereof, on it. We developed a mathematical model to describe the GTPase cycle. We show that Cdc42 exhibits cooperativity, and that this is likely not due to dimerisation. The GEF Cdc24 shows cooperativity as well, which we hypothesise to be linked to Cdc24 di- or oligomerisation and a release of its autoinhibition (Shimada *et al.* (2004); Mionnet *et al.* (2008)). Our data suggests that Cdc24 also synergises with Rga2. We further found that molecular crowding, even at μM concentrations, positively affects the GTPase cycle and Cdc42- effector protein interactions.

4.2. Results

4.2.1. GTPase activity of Cdc42

Cdc42 belongs to the group of GTPase proteins, meaning that they can hydrolyse GTP. This process involves three steps (Fig. 4.3a): (1) A GTP molecule from solution binds to Cdc42. (2) Cdc42 hydrolyses GTP. (3) Cdc42 releases GDP.



¹A more in-depth discussion on the Min protein system is given in Chapter 1.

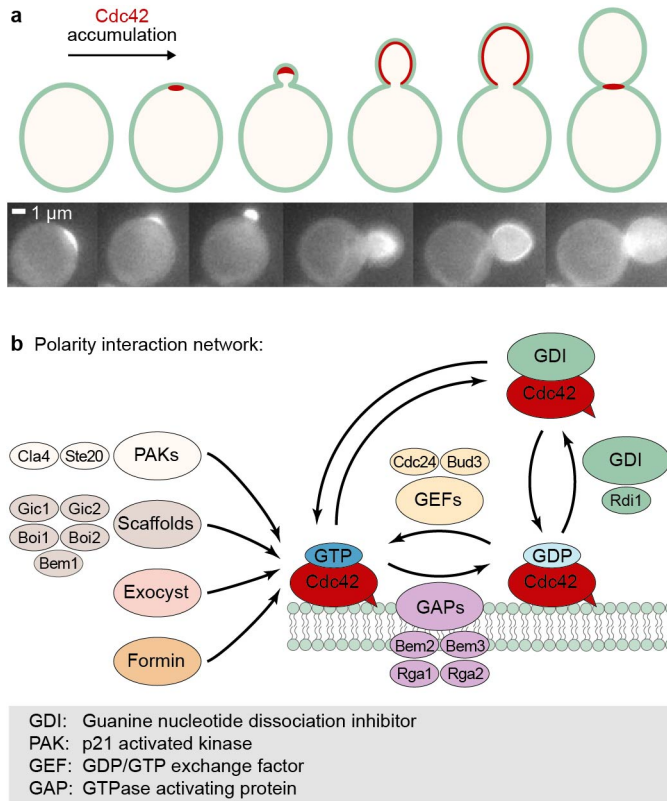


Figure 4.1. Polarity establishment in *Saccharomyces cerevisiae*. (a) An illustration of polarity establishment in the yeast cell cycle (top) and a montage of live cell spinning disk microscopy images of *sfGFP-Cdc42^{SW}* (bottom). Cdc42 is shown in red (illustration, top) or in white (microscopy images, bottom). (b) Illustration of the polarity interaction network around Cdc42: Cdc42's nucleotide state is regulated by GEFs and GAPs. It can be extracted from membranes by the GDI Rdi1, and also interacts with PAKs, scaffold proteins, exocysts and formins.

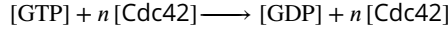
The GTP hydrolysis cycle can further be upregulated by effector proteins: GAPs have been shown to enhance GTP hydrolysis by Cdc42 (step 2), GEFs enhance the release of GDP from Cdc42 (step 3) (Martin (2015); Chiou et al. (2017)) and the scaffold Bem1 enhances the GEF activity of Cdc24 (Rapali et al. (2017)). To explore the regulation of the Cdc42 GTPase, we conducted GTPase assays using the Promega GTPase Glo™ assay. Here serial dilutions of Cdc42² (and effector proteins) were incubated with GTP for a certain time, after which the reactions were stopped and the amount of remaining GTP was measured (see materials and methods). Thus, we measured how much GTP got hydrolysed by Cdc42 proteins in a certain amount of time.

We first explored the GTPase activity of solely Cdc42, examining how GTP concentrations change for different Cdc42 concentrations over time. We performed experiments where we measured the amount of remaining GTP after incubation times of 1.5 h, 3 h, and 5 h. The graph of the

²In this chapter, all experiments were conducted with double-tagged Cdc42: H-Cdc42-F. To ensure that the purification tags do not affect the protein behaviour, we also conducted experiments using differently tagged constructs, including only N-terminally 6His-tagged Cdc42 (H-Cdc42:CTIS). Both double- and single-tagged constructs showed similar GTP hydrolysis cycling rates *k* and interactions with the GEF Cdc24, suggesting that the purification tags are not affecting protein dynamics (see Chapter 3).

amount of remaining GTP over time (Fig. 4.3b) shows that the GTP hydrolysis process follows an exponential decline³.

To quantitatively describe the GTPase reaction cycle, we coarse-grained the GTPase reaction steps with



We described the Cdc42 GTP hydrolysis data (Fig. 4.3b) with

$$[\text{GTP}]_t = [\text{GTP}]_{t_0} \exp(-k[\text{Cdc42}]^n t) \quad (4.1)$$

using $[\text{GTP}]_{t_0} = 100\%$, and fitted the data with

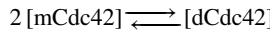
$$-\frac{1}{[\text{GTP}]} \frac{d[\text{GTP}]}{dt} = -\frac{d \ln[\text{GTP}]}{dt} = k[\text{Cdc42}]^n \quad (4.2)$$

resulting in the parameter values of $k=0.15 \pm 0.08 \mu\text{M}^{-1.65} \text{h}^{-1}$ and $n=1.65 \pm 0.10$ ($R^2=0.995$) (Appendix 4.4.1 Fig. 4.9). Our finding that $n>1$ suggests that cooperative effects between Cdc42 molecules are taking place.

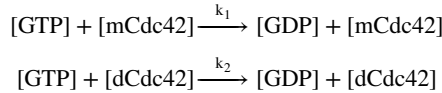
4.2.2. A Cdc42 GTPase activity model

To account for the non-linear effects we observed for Cdc42's GTP hydrolysis cycle, and to further explore its properties, we build a Cdc42 GTPase activity model. We included molecular crowding, Cdc42 dimerisation and other cooperative effects, and interactions with effector proteins. In the following we describe the reactions and assumptions the model is based on.

(1) We assume that Cdc42 can dimerise, as other small GTPases have been shown to dimerise (*Zhang and Zheng (1998); Zhang et al. (1999, 2001); Kang et al. (2010)*) (Fig. 4.2):



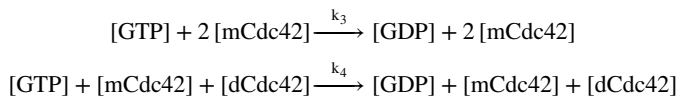
and both monomeric and dimeric Cdc42 can contribute to the overall GTP hydrolysis with different rates:



Assuming that the majority of Cdc42 is in its monomeric form ($[\text{mCdc42}] < C_d$, with C_d as the concentration at which half of the total Cdc42 is dimeric), we can approximate

$$\begin{aligned} [\text{dCdc42}] &= \frac{[\text{mCdc42}]^2}{2C_d} \\ [\text{mCdc42}] &\approx [\text{Cdc42}] - \frac{[\text{Cdc42}]^2}{C_d} \end{aligned} \quad (4.3)$$

(2) Next to cooperativity from dimerisation, cooperativity can also emerge when Cdc42 proteins come in close contact with each other - they can affect each other's behaviour without forming a stable homodimer, effectively functioning as an effector protein for themselves (Fig. 4.2):



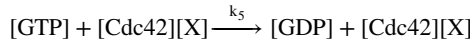
³We subsequently only performed measurements for incubation times of about 1.5 h for all other measurements.

(3) Molecular crowding⁴: Proteins can, simply by taking up space, affect the enzymatic activity and protein-protein interaction (*Kuznetsova et al. (2014)*) (Fig. 4.2). Crowding has been found to either increase or decrease reaction rates (*Kim and Yethiraj (2009)*). We model the effect of molecular crowding on reaction rates k_i through

$$k_i = k_i^*(1 + k_c[P]_{tot}) \quad (4.4)$$

where k_i^* is the protein-specific intrinsic rate, $[P]_{tot}$ is the total protein concentration, and k_c is the crowding parameter determining the magnitude and sign of the crowding effect.

(4) Effector proteins, such as GAPs and GEFs, affect the speed of the GTP hydrolysis cycle:



Here X is an effector protein.

Taking all these effects together, we can thus replace Eq. 4.2 with

$$-\frac{d\ln[\text{GTP}]}{dt} = k_1[\text{mCdc42}] + k_2[\text{dCdc42}] + k_3[\text{mCdc42}]^2 + k_4[\text{mCdc42}][\text{dCdc42}] + k_5[\text{Cdc42}][\text{X}] \quad (4.5)$$

Using Eq. 4.4 and Eq. 4.3, and considering only up to second-order terms, results in

$$-\frac{d\ln[\text{GTP}]}{dt} = k_1^*[\text{Cdc42}] + \left(\frac{k_2^*}{2C_d} + k_3^* - \frac{k_1^*}{C_d} + k_1^*k_c \right) [\text{Cdc42}]^2 + (k_5^* + k_1^*k_c)[\text{Cdc42}][\text{X}] = k'_1[\text{Cdc42}] + k'_2[\text{Cdc42}]^2 + k'_{3,X}[\text{Cdc42}][\text{X}] \quad (4.6)$$

where k'_1 refers to GTP hydrolysis cycling rates of monomeric Cdc42, k'_2 includes effects of crowding, cooperativity, and dimerisation (in short: CroCoDiLE: crowding, cooperativity, and dimerisation in luminescence experiments) and k'_3 represents the rate of Cdc42 - effector interaction plus crowding. We will refer to $-d\ln[\text{GTP}]/dt$ as 'relative GTP hydrolysis rate' in the following.

We used this model to fit Cdc42 GTP hydrolysis data (thus, $[\text{X}]=0$) (Fig. 4.3c), leading to $k'_1 = 0.075 \pm 0.004 \mu\text{M}^{-1}\text{h}^{-1}$ and $k'_2 = 0.081 \pm 0.006 \mu\text{M}^{-2}\text{h}^{-1}$ ($R^2 = 0.996$) ($n = 4$) (Tab. 4.1). k'_1 is only slightly smaller than k'_2 , again showing that the contribution of monomeric Cdc42 and that of the crocodile term is roughly equal, which is consistent with $n = 1.65 \pm 0.10$ as determined earlier (Eq. 4.2).

As k'_2 includes many effects, we wanted to unravel which of these are most plausible and/or dominating. In the following we will shine light on the effects of molecular crowding, Cdc42 dimerisation, and cooperativity on the Cdc42 GTPase cycle.

4.2.3. Assay variability

Before assessing how different factors influence the GTPase cycle, we need to account for assay variability, i.e. for the observation that the rates for Cdc42 can vary between assays (see Chapter 3). Possible reasons for this include small concentration differences introduced through pipetting of small volumes (as are required for this assay), temperature and shaker speed fluctuations during the incubation step, and/or intrinsic changes in the protein activities due to other external conditions. To account for this variance, we introduced the parameter c_{corr} . It maps all

⁴We here use a general definition of the term 'crowding', encompassing any non-specific interactions and effects that occur when molecules take up space.

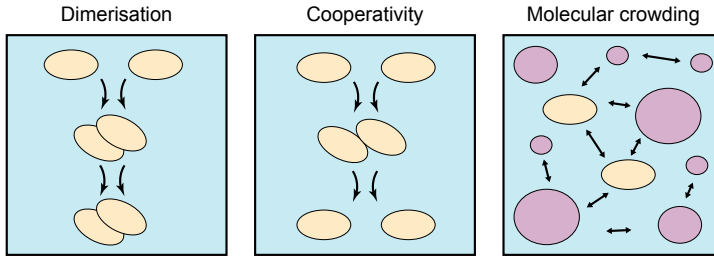


Figure 4.2. Schematic illustration of dimerisation, cooperativity, and molecular crowding. We distinguish dimerisation and cooperativity by the criterion of binding strength and duration: We speak of cooperativity if proteins bind very transiently and weakly to each other, i.e. they unbind very quickly after coming together. Protein dimers are stronger bound to each other and the dimeric state lasts longer. Nevertheless, we do not exclude that protein dimers can unbind again, this just occurs after a comparatively longer time than in the case of cooperativity. Molecular crowding: We here use a general definition of the term 'crowding', encompassing *any* non-specific interactions and effects that occur when molecules take up space. Molecular crowding can affect the system in various ways, it can enhance protein dimerisation or cooperativity, affect protein conformational changes and enzymatic activities, or form weak attractive interactions with the system's molecules.

factors that lead to variations between assays onto the Cdc42 concentration.

The assay data, including samples containing only Cdc42 and Cdc42 - (effector) protein mixtures, was fitted with

$$-\frac{d\ln[\text{GTP}]}{dt} = k'_1 c_{\text{corr}} [\text{Cdc42}] + k'_2 (c_{\text{corr}} [\text{Cdc42}])^2 + k'_{3,X} c_{\text{corr}} [\text{Cdc42}] [X] \quad (4.7)$$

to determine c_{corr} and $k'_{3,X}$ (using k'_1 and k'_2 determined earlier (Tab 4.1)). To ensure that we only consider data that displays a plausible Cdc42 behaviour, we only included assays with $0.5 < c_{\text{corr}} < 1.5$ in our subsequent analysis. Most data was within this range (Fig. 4.3e), confirming that the assay variability was not severe.

4.2.4. Molecular crowding

Next, we assessed if and how molecular crowding affects the GTP hydrolysis cycle of Cdc42 (i.e. if and how much it contributes to k'_2). We added Bovine serum albumin (BSA), a protein known to not interact with Cdc42, to assess if and how the presence of non-interacting proteins affects the GTP hydrolysis by Cdc42. Interestingly, additions of BSA (0.5-2 μM BSA to 1 μM Cdc42) leads to increased GTP hydrolysis rates of Cdc42 (Fig. 4.3f). Eq. 4.7 was used to determine the rate of BSA; $k'_{3,BSA} = 0.049 \pm 0.007 \mu\text{M}^{-2} \text{h}^{-1}$ ($n = 1$) (Tab. 4.2).

What does this mean? Previously, we determined the GTP hydrolysis cycling rates k'_1 and k'_2 of Cdc42. $k'_2 = 0.082 \pm 0.006 \mu\text{M}^{-2} \text{h}^{-1}$ represents the crocodile term, which is responsible for the non-linear behaviour and includes effects of crowding, cooperativity and dimerisation. $k'_{3,BSA}$ is about $0.6 \times k'_2$, suggesting that crowding is responsible for more than half of the non-linear affect. This implies that Cdc42 cooperativity and/or dimerisation play only a second-order role. We used BSA (66 kDa) as a crowding agent, which is roughly twice the size of Cdc42 (29 kDa). Crowding effects are governed by the hydrodynamic radius of a protein which must not necessarily scale with the proteins molecular weight. As a simple approximation we assume here that they do: BSA is about twice the size of Cdc42, thus the volume-filling crowding effect of 1 μM BSA molecule would correspond to that of 2 μM Cdc42 molecules. Considering this, $k'_{3,BSA}$ would only be half

of our measured value, and thus account for a third of the non-linear effect. Fig. 4.3g shows a comparison of the Cdc42 behaviour (rhombus and blue dashed line) and the crowding effect⁵ (green dashed line): For $k'_{3,BSA} = 0.049 \pm 0.007 \mu\text{M}^{-2}\text{h}^{-1}$ the non-linearity of Cdc42 is bigger than the median of the crowding effect, but only slightly above its 95% confidence interval line. When taking the size difference of Cdc42 and BSA into account ($k'_{3,BSA} = 0.025 \pm 0.004 \mu\text{M}^{-2}\text{h}^{-1}$), Cdc42's non-linear behaviour with concentration is significantly above the crowding-effect.

From this assay we can not determine the mechanism through which molecular crowding is affecting the GTPase activity of Cdc42, but we can speculate based on literature findings: Molecular crowding can increase the activity of an enzyme (*Liao et al. (2008)*), enhance protein oligomerisation (*Kuznetsova et al. (2014)*) and affect small-molecule substrates, such as GTP (*Aumiller et al. (2014)*). It is thus possible that BSA, by taking up space, is increasing the likelihood for Cdc42 molecules to dimerise and/or to engage in other cooperative behaviours. Crowding would then not reduce the relevance of Cdc42 cooperativity/ dimerisation, but facilitate it. On the other hand, the mechanism of crowding could also not involve increasing Cdc42 cooperativity/ dimerisation. For example, it can affect Cdc42 or GTP in such a way that any step of the GTPase cycle happens faster. In support of this is the finding that high concentrations of crowding agents enhance the GDP/GTP exchange of the small GTPase Ras (*Liao et al. (2008)*). Effects on GTP are less likely: crowding agents can form weak attractive interactions with small molecules, but these interactions were shown to reduce (not increase) enzymatic activity (*Aumiller et al. (2014)*).

In conclusion, crowding increases the Cdc42 GTP hydrolysis speed and partially explains its non-linear increase with Cdc42 concentration. It is possible that crowding enhances Cdc42 dimerisation/ cooperativity, or that it affects the reaction cycle in another way, thus minimising the role that Cdc42 dimerisation/ cooperativity plays. Further research on the effect of crowding agents on specific steps of the GTPase cycle and higher crowder concentrations is required to elucidate how crowding specifically affects the GTPase cycle. The use of other crowding reagents is recommended as well, to ensure the effect is not BSA specific.

4.2.5. Cdc42 dimerisation and cooperativity

Given that molecular crowding does not fully explain k'_2 , we explored if Cdc42 can form dimers. Cdc42 belongs to the group of small GTPases, of which some have been shown to dimerise or oligomerise (Appendix 4.4.2 Tab. 4.3). Dimerisation has been linked to the polybasic region (PBR), a short unstructured region of mostly positively charged amino acids at the protein's C-terminus. Different GTPases have similar, yet slightly distinct PBR sequences and it has been shown that partial removal of the PBR impedes dimerisation. An illustration of this is given in Appendix 4.4.2 Tab. 4.3. Yeast Cdc42 has the PBR sequence that has neither been linked to dimerisation or to its absence. As the direct relation between the PBR sequences and protein dimerisation is still largely unknown, it is difficult to say, based on the PBR sequence, if Cdc42 in principle can dimerise. *In vivo* data suggests that it does not (*Kang et al. (2010)*), but the absence of Cdc42 dimers *in vivo* does not necessarily exclude their existence *in vitro*⁶.

To investigate if Cdc42 can dimerise *in vitro*, we ran purified Cdc42 sample on a size-exclusion

⁵The contribution of the crowding effect was calculated using $k'_{1,Cdc42}$, $k'_{2,Cdc42} = k'_{3,BSA}$, and the concentration of Cdc42.

⁶Cdc42 occupies a central role in the yeast cell cycle and has a lot of binding partners (*Daalman et al. (2020)*). Thus, the presence of Cdc42 dimers can get lost (considering the amount of other complexes it is part of). Cdc42 dimerisation was assessed through the fluorescence signal of two Cdc42-YFP fusions with YFP truncations: One Cdc42 copy was fused to the N-terminal part of YFP, the other Cdc42 copy to the C-terminal part. Fluorescence appears when both YFP fragments are brought together through association of two Cdc42 molecules (*Kang et al. (2010)*). Hence, only dimeric Cdc42 leads to a YFP signal, monomeric Cdc42 and Cdc42 in hetero-complexes does not. If only a small fraction of Cdc42 dimers are

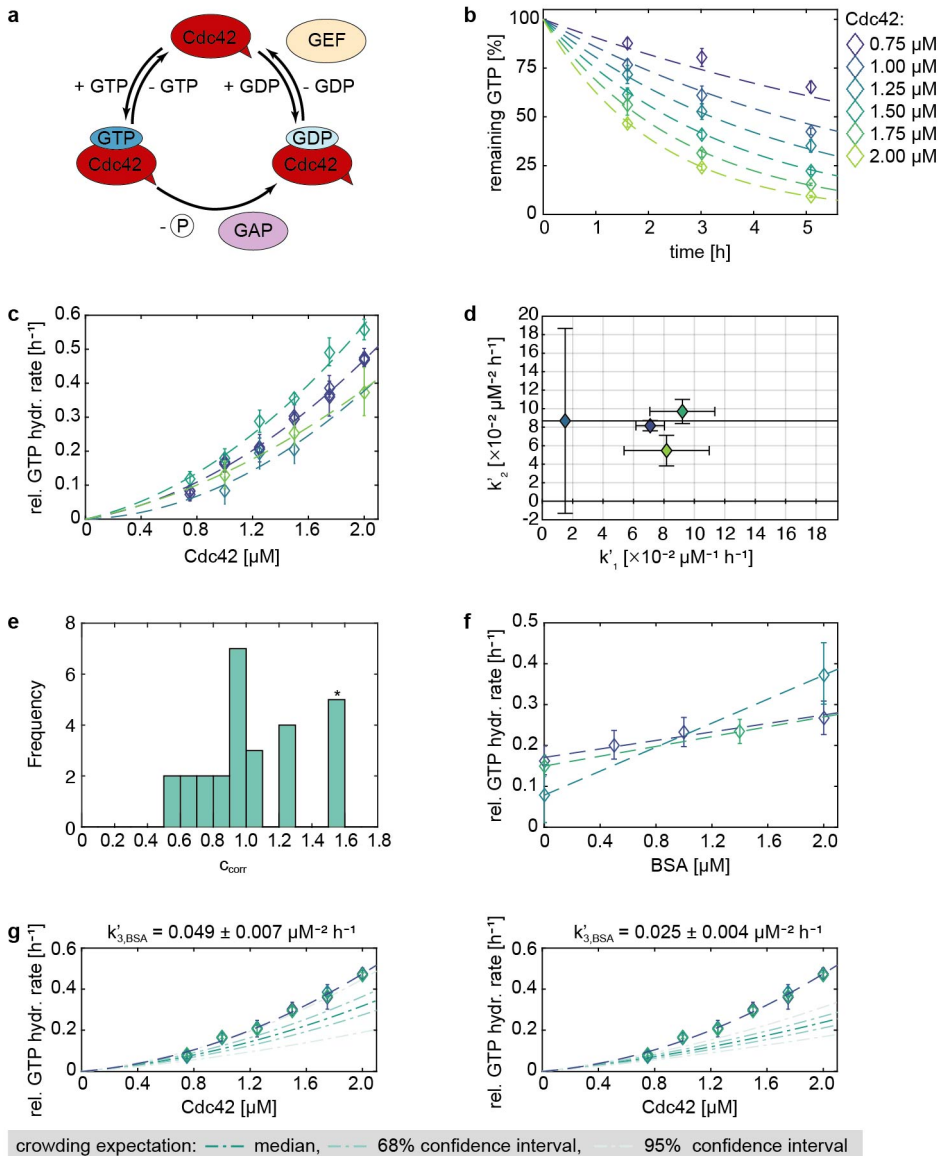


Figure 4.3. Cdc42's GTPase activity and effects of crowding. (a) Schematic illustration of the GTPase cycle of Cdc42. (b) GTP hydrolysis by Cdc42: in GTPase assays the GTP concentration declines exponentially with time. (c) The relative GTP hydrolysis rate of Cdc42 scales non-linearly with the Cdc42-concentration. Different colours denote separate experiments. (d) GTP hydrolysis cycling rates k_1' and k_2' of Cdc42 (determined from graphs shown in (c)). (e) Frequency of correction factors c_{corr} (with $0.5 < c_{\text{corr}} < 1.5$) throughout the entire data set. c_{corr} values of all experiments are stated in Appendix 4.4.3 Tab. 4.5 and Tab. 4.10. *: c_{corr} belongs to reference measurements of preliminary data in Appendix 4.4.4 and was included even though it was above the threshold of 1.5. (f) Effect of the crowding reagent BSA on the relative GTP hydrolysis rate of 1 μM Cdc42. Different colours denote separate experiments. (g) Relative GTP hydrolysis rate of Cdc42 in comparison to expected effect of crowding, based on the assumption that one Cdc42 molecules takes up the same space as one BSA molecules (top) or that it takes up half the space (bottom). (c,f,g) The "relative GTP hydrolysis rate" refers to $-d\ln[\text{GTP}]/dt$ in Eq. 4.6. (b,c,f,g) Fits are depicted as dashed lines.

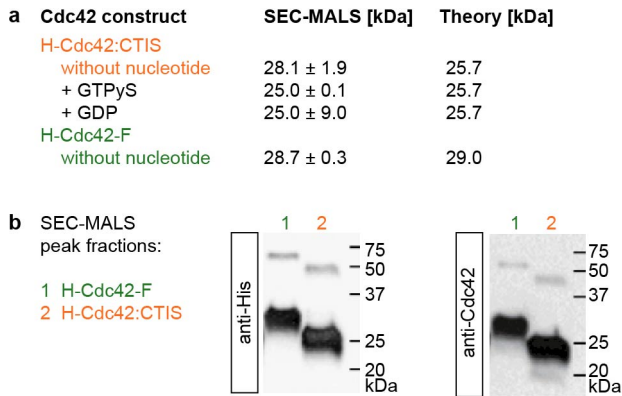


Figure 4.4. Cdc42 dimerisation. (a) Cdc42 does not dimerise *in vitro*: Comparison of Cdc42 molecular weight determined by SEC-MALS and based on the amino acid sequence. (b) Cdc42 forms dimers in denaturing conditions: anti-His and anti-Cdc42 Western Blots of SEC-MALS peak fractions.

chromatography (SEC) column and used multi-angle light scattering (MALS) to determine the molecular weight of the protein in each peak (Fig. 4.3a). Cdc42 ran in one peak and the SEC-MALS molecular weight corresponded to that of a monomer. This was independent of if single- or double-tagged Cdc42 was used or if Cdc42 was in its GDP- or GTP-bound state. We subsequently analysed the protein of these peak fractions by anti-His and anti-Cdc42 Western Blotting (Fig. 4.3b). Interestingly, the Blots show bands of the size of a monomer and a dimer, suggesting that the protein has dimerisation capacity. It is possible that Cdc42 can only form very transient and weakly bound Cdc42 dimers. Such complexes would not sustain themselves under the constant flow under which SEC is performed. However, we only (though consistently) observed Cdc42 dimers under denaturing conditions (see Chapter 3). This can be an artefact of the denaturing conditions that has no translation to the behaviour of the folded protein, or mean that Cdc42 has some, still unexplored, potential to dimerise.

Next to dimerisation, two weakly and transiently bound Cdc42 molecules can also affect each other through cooperativity (Fig. 4.2). They can in principle act as a GAP or GEF towards each other or increase the re-binding of GTP. The self-stimulating GAP activities of Rho-GTPases were studied before through assays measuring the amount of released phosphate of single GTP hydrolysis steps. *S. cerevisiae* Cdc42 was found to not act as a GAP towards itself (Zhang *et al.* (1999)). Nevertheless, cooperativity could still take place through (1) enhancing the GDP release and GTP binding step, and (2) affecting the GTP hydrolysis step to such a small extend that it was not observable in the GTP hydrolysis assays. We observed a small non-linear contribution to the Cdc42 GTP hydrolysis cycling rate ($n = 1.65 \pm 0.10$ (Eq. 4.2) or $k'_2 = 0.082 \pm 0.006 \mu\text{M}^{-2} \text{h}^{-1}$ (Eq. 4.6)). This contribution might be difficult to measure, especially if it is distributed among several steps (and thus the contribution of each single step is even smaller).

We found that it is unlikely that Cdc42 forms dimers, and suspect that cooperativity takes place. However, the origin of the cooperative contribution is still elusive.

Cdc42-Cdc42 homodimers (compared to Cdc42-effector protein heterodimers), not enough YFP signal might be generated to observe these homodimers.

4.2.6. Regulation of the GTPase activity of Cdc42 through the GEF Cdc24 and scaffold protein Bem1

We next assessed how different effector proteins affect the Cdc42 GTPase cycle. We first examined the effect of Cdc24 and Bem1. Cdc24 is a GEF; it enhances the release of GDP from Cdc42 (Zheng *et al.* (1994)). The scaffold protein Bem1 is involved in many protein complexes (Daalman *et al.* (2020)), and has also been shown to boost the GEF activity of Cdc24 *in vitro* (Rapali *et al.* (2017)).

To ensure that the proteins are properly functioning, we tested the binding of Bem1 to Cdc24 (Zheng *et al.* (1995); Butty *et al.* (2002)) and to Cdc42 (Bose *et al.* (2001)) with Flag-pulldown experiments. Here Flag-tagged Bem1 (H-Bem1-F) and Cdc42 and Cdc24 constructs that don't contain a Flag-tag (S-Cdc42-H, Cdc24-H), were incubated and mixed with anti-Flag affinity gel. Flag-tagged Bem1 can bind to the gel. Cdc42 or Cdc24, however, as they do not contain a Flag-tag, can not. After several rounds of washing, the proteins were eluted. If Cdc42 or Cdc24 was eluted as well, it must be because it was bound to Bem1 (Fig. 4.5a). Similar to observations by Zheng *et al.* (Zheng *et al.* (1995)), we observed a strong binding between Bem1 and Cdc24 (Fig. 4.5b). The elution fraction contained so high amounts of Cdc24 that it was visible on SDS-Page. The binding was also specific; Bem1 did not pull down Ovalbumin and Cdc24 did not bind to the anti-Flag affinity gel. We also observed binding between Bem1 and Cdc42 (Fig. 4.5c). It was weaker in comparison to the Bem1-Cdc24 interaction (Cdc42 could only be detected using Western Blotting) and showed some non-specificity: Cdc42 (without Bem1) stuck slightly to the anti-Flag affinity gel, but to a significantly lesser extent than in the presence of Bem1. We tested the binding of Bem1 to Cdc42 pre-loaded without nucleotide, with GTP γ S, and with GDP. Surprisingly, we observed binding interactions with all Cdc42 species. The intensities of the Western Blot signal for Cdc42 varied with the nucleotide type, but also per experiment: In one experiment more Cdc42-GDP (than Cdc42-GTP or nucleotide free Cdc42) bound to Bem1, but in another experiment it was nucleotide-free Cdc42 (Fig. 4.5c). We therefore can not quantify the binding differences of Cdc42 variants to Bem1 from this data. Binding of Bem1 to all Cdc42 species contrasts previous findings showing Bem1 binding to GTP-bound, but not to GDP-bound, Cdc42 (Bose *et al.* (2001)). It is possible that our pre-loading step of Cdc42 was not sufficient or that the difference lies in the distinct experimental conditions these assays were conducted in⁷. In conclusion, this pulldown data shows that Bem1 can bind to both Cdc24 and Cdc42, illustrating that the protein binding sites are functional.

We conducted GTPase assays with Cdc42 and Cdc24 (Fig. 4.6a). Cdc24 is highly active; the addition of sub- μ M concentrations of Cdc24 to 1 μ M Cdc42 is sufficient to boost the reaction cycle significantly, and the effect of Cdc24 is far above that of crowding ($k_{3,Cdc24} = 3.656 \pm 0.23 \mu\text{M}^{-3} \text{h}^{-1}$ in comparison to $k'_{3,BSA} = 0.049 \pm 0.007 \mu\text{M}^{-2} \text{h}^{-1}$) (Fig. 4.6d, Tab. 4.2).

Further, the data suggests that the GTP decline does not depend linearly on the Cdc24 concentration (Eq. 4.7), but is better approximated by a quadratic term:

$$-\frac{d\ln[\text{GTP}]}{dt} = k'_1 c_{\text{corr}}[\text{Cdc42}] + k'_2 (c_{\text{corr}}[\text{Cdc42}])^2 + k'_{3,Cdc24} c_{\text{corr}}[\text{Cdc42}][\text{Cdc24}]^2 \quad (4.8)$$

This suggests cooperativity. Previous work showed that Cdc24 has the capability to oligomerise via its DH domain (Mionnet *et al.* (2008)). We expect dimers and oligomers to have an increased

⁷A detailed discussion is given in Chapter 3.

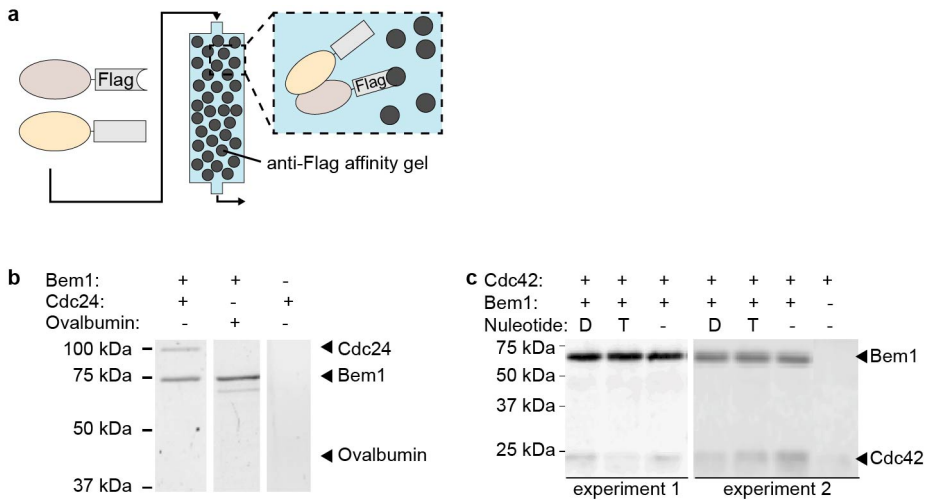


Figure 4.5. Bem1-Cdc24 and Bem1-Cdc42 binding. (a) Schematic illustration of Flag-pull-down experiments. (b) SDS-Page of elution fractions of Flag-pull-down experiments with H-Bem1-F, Cdc24-H, and Ovalbumin. (c) Anti-His Western Blots of elution fractions of two Flag-pull-down experiments with H-Bem1-F and S-Cdc42-H preloaded with no nucleotide, GDP (D), or GTP γ S (T).

GEF activity⁸. This could, for example, be facilitated by Cdc24's C-terminal PB1-domain, which has been suggested to reduce Cdc24's GEF activity through intramolecular interactions (*Shimada et al. (2004)*). Cdc24 oligomerisation could interfere with this self-interaction and thereby increase the proteins GEF activity.

In contrast to Cdc24, Bem1 does not increase the GTP hydrolysis cycling speed of Cdc42 (Fig. 4.6b), the effect of Bem1 on Cdc42 was only slightly above that of the crowding agent BSA (Fig. 4.6e). For this estimation we approximated that one Bem1 molecule takes up the same space as one BSA molecule. Both proteins are roughly equal in size (Bem1: 70 kDa, BSA: 66 kDa), but could still have unequal hydrodynamic radii. It is thus possible the effect of Bem1 on Cdc42 is purely due to crowding (assuming BSA is smaller than Bem1), or that Bem1 has a very weak enhancing effect (assuming BSA is bigger than Bem1). Given that so-far Bem1 has not been associated with directly affecting the Cdc42 GTPase cycle, and that it has been shown to not stimulate GDP/GTP exchange (*Rapali et al. (2017)*), it is likely that the effect of Bem1 on Cdc42 in this assay is due to crowding.

We then studied the impact of Cdc24 in conjunction with Bem1 on the Cdc42 GTPase cycle (Fig 4.6c) and calculated the Cdc42-Cdc24, Cdc42-Bem1, and Cdc42-Cdc24-Bem1 interaction rates $k'_{3,Cdc24}$, $k'_{3,Bem1}$, and $k'_{3,Cdc24,Bem1}$ using:

⁸*In vitro* work with Cdc24 peptides, consisting only of Cdc24's DH + PH domain, showed that these peptide exhibit GEF activity that was not changed when oligomerisation was inhibited (through mutations) or amplified (*Mionnet et al. (2008)*). These findings would exclude that Cdc24 oligomers exhibit an increased GEF activity. However, one has to be careful when applying these findings to full-size Cdc24: For one, not full size protein, but only peptides were used. Other domains that are not directly involved in oligomerisation or GEF function can still affect these properties. For example, the PB1 domain was suggested to reduce Cdc24 GEF activity in a self-inhibitory fashion (*Shimada et al. (2004)*). Next, samples representing a heightened oligomerisation state were produced through addition of an additional oligomerisation domain to the peptides. This domain was not related to Cdc24 and could be triggered to oligomerise through the addition of a chemical. It is thus questionable if the GEF activity of these oligomerised peptides relates to the GEF activity of oligomeric Cdc24.

$$\begin{aligned}
-\frac{d\ln[\text{GTP}]}{dt} = & k'_1 c_{\text{corr}}[\text{Cdc42}] + k'_2 (c_{\text{corr}}[\text{Cdc42}])^2 \\
& + k'_{3,\text{Cdc24}} c_{\text{corr}}[\text{Cdc42}][\text{Cdc24}]^2 \\
& + k'_{3,\text{Bem1}} c_{\text{corr}}[\text{Cdc42}][\text{Bem1}] \\
& + k'_{3,\text{Cdc24,Bem1}} c_{\text{corr}}[\text{Cdc42}][\text{Bem1}][\text{Cdc24}]^2
\end{aligned} \tag{4.9}$$

Here $k'_{3,\text{Cdc24,Bem1}}$ describes the contribution of Cdc24 in conjunction with Bem1. If this rate is greater than zero, the two proteins together have a greater effect on Cdc42 than their separate contributions - a synergy arises. This could happen for example through the formation of a Cdc24-Bem1 complex. If the term is negative, they antagonise each other. Fig. 4.6f (and Tab. 4.2) give an overview of the rates. The individual contributions of Cdc24 and Bem1 in the three-protein assay (Cdc42 + Cdc24 + Bem1) are about the same as those in two-protein assays (Cdc42 + Cdc24, Cdc42 + Bem1) and the synergistic term is $k'_{3,\text{Cdc24,Bem1}} = -0.500 \pm 0.788 \mu\text{M}^{-4} \text{h}^{-1}$ (Tab. 4.2). Because of the large error of $k'_{3,\text{Cdc24,Bem1}}$ no considerable conclusions can be drawn; the proteins could not interact, have a weak synergy, or weakly antagonise each other. Previous *in vitro* experiments showed that Bem1 enhances Cdc24's GEF activity (*Rapali et al. (2017)*). We therefore expect to see a positive $k'_{3,\text{Cdc24,Bem1}}$. The fact that we determined $k'_{3,\text{Cdc24,Bem1}}$ to be close to zero could have two explanations: (1) At least one of our proteins is not functional and they are therefore not interacting. (2) Our proteins are fully functional, but assay-related matters make the effect of Bem1 not detectable in the GTPase assay.

We did GTPase assays on Cdc42 and on the Cdc42-Cdc24 interaction, illustrating that the proteins are functional. Flag-pulldown experiments also showed that Bem1 binds to Cdc24 and Cdc42. However, we used a Flag-tagged Bem1 construct (H-Bem1-F) for the pulldown experiments, but a Strep-tagged Bem1 construct (S-Bem1-H) for the GTPase assays. We cannot exclude that this construct or purification batch is nonfunctional⁹. We had conducted a few, although less thorough, GTPase assays with Cdc24 and Flag-tagged Bem1 (H-Bem1-F) in the past (Appendix 4.4.4). These preliminary experiments gave a weak positive synergistic term ($k'_{3,\text{Cdc24,H-Bem1-F}} = 0.354 \pm 0.091 \mu\text{M}^{-4} \text{h}^{-1}$) (Appendix 4.4.4 Fig. 4.10, Tab. 4.10). The $k'_{3,\text{Cdc24,H-Bem1-F}}$ of these assays is positive and within the error range of $k'_{3,\text{Cdc24,S-Bem1-H}}$, suggesting that S-Bem1-H is functional. Hence, the GEF enhancing effect of Bem1 might be difficult to observe in GTPase assays even though it was in GEF assays by *Rapali et al. (2017)* (from now on referred to as GEF assays). How is this possible?

Our data revealed a non-linear concentration-dependence of the Cdc24 rate (Fig. 4.6a) starting at around 0.1-0.2 μM . In GEF assays the Cdc24 concentration was 60 nM (*Rapali et al. (2017)*). At 60 nM Cdc24 could be less active, and Bem1 can have a greater impact on its GEF activity. This would be especially true if the non-linearity is based on the release of Cdc24 autoinhibition through dimerisation. The autoinhibition is thought to arise from an intramolecular interaction of Cdc24's PB1 domain, and Bem1 is suspected to release this autoinhibition through binding to Cdc24's PB1 domain (*Shimada et al. (2004)*). For Cdc42-Cdc24-Bem1 assays we used Cdc24 concentrations of the non-linear rate regime. In this regime the autoinhibition of Cdc24 could already be released through the formation of Cdc24 dimers. Bem1 is then expected to only affect the remaining Cdc24 monomers, and thus to overall have a significantly smaller or not observable

⁹We conducted Flag-pulldown experiments with S-Bem1-H. However, because S-Bem1-H was partially sticking to the Flag-affinity gel, pulldown experiments with F-Cdc24-H and H-Cdc42-F are non-conclusive. Strep-pulldown experiments with S-Bem1-H are also not viable, because the Strep-II tag has a (too) low affinity for Strep-Tactin to bind sufficient protein.

effect on the GTPase cycle (Fig. 4.7) This hypothesis can be further contextualised, or challenged, by considering literature findings on the Cdc24/Bem1 binding strengths and dynamics. A discussion is given in Appendix 4.4.5.

Another distinguishing factor between the GEF and GTPase assays are the therein used protein ratios: In GEF assays Cdc42:Cdc24:Bem1 concentrations of 9.0:0.06:5.0 μM were used. In contrast, our GTPase assays were performed using ratios of 1.0:0.3:1.4 μM . The Cdc42/Cdc24 (Bem1/Cdc24) ratio in the GEF assays is thus 150 (83), whereas in our GTPase assays it's 3 (5). Hence, GEF assays contain 50x less Cdc24 per Cdc42 and about 16x more Bem1 per Cdc24 than GTPase assays. As GEF assays have less Cdc24 per Cdc42 available, and more Bem1 to boost Cdc24's GEF activity, GEF boosting effects of Bem1 might be more visible in this Cdc24-limited system (than in our system with more abundant Cdc24). This implies that the GEF-boosting effect of Bem1 depends on the Cdc24 concentration. GTPase and GEF assays using a wider range of protein ratios will reveal if and how Cdc24's GEF activity is affected by Cdc24 autoinhibition and the protein Bem1.

Lastly, the rate $k'_{3,Cdc24,Bem1}$ also includes the effects of crowding (Eq. 4.6). We assessed how crowding affects Cdc42 (Fig. 4.3g), but did not conduct tests on the effect of crowding on the Cdc42-Cdc24 and Cdc42-Bem1 system. To ensure that Cdc24-Bem1 synergy represented in $k'_{3,Cdc24,Bem1}$ is indeed due to the Cdc24-Bem1 interaction, this rate needs to be greater than $k'_{3,Cdc24,BSA}$ and $k'_{3,Bem1,BSA}$ ¹⁰. For this more experiments are required.

Taken together, the data shows that Cdc24 exhibits a strong GEF activity that involves second-order Cdc24-concentration terms, and lightly indicates that Bem1 might boost Cdc24's GEF activity.

¹⁰The influence of Bem1 on Cdc24 could be based on crowding in our GTPase assays. This calls into question if the effect of Bem1 in GEF assays is also due to crowding. In GTPase assays Bem1 alone affects the Cdc42 GTPase cycle (likely due to its crowding properties). Rapali *et al.*, however, only detected an effect of Bem1 on Cdc42 when Cdc24 was present, but not in its absence (Rapali *et al.* (2017)). Hence, the GEF stimulating effect of Bem1 in GEF assays is expected to not be due to crowding.

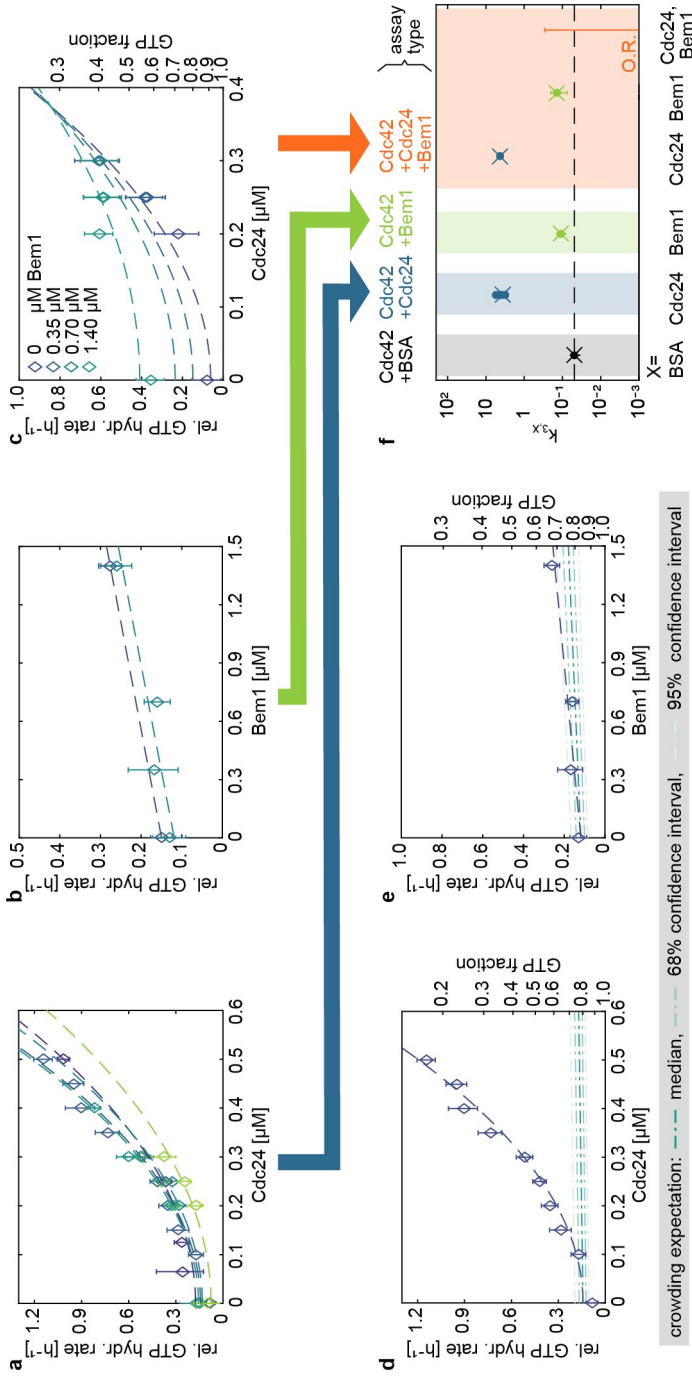


Figure 4.6. Regulation of the GTPase activity of Cdc42 through the GEF Cdc24 and scaffold protein Bem1. (a) The relative GTP hydrolysis rate in Cdc42-Cdc24 assays scales non-linearly with the Cdc24-concentration (1 μM Cdc42). Different colours denote separate experiments. (b) Effect of Bem1 on the relative GTP hydrolysis rate of 1 μM Cdc42. Different colours denote separate experiments. (c) Effect of Cdc24 and Bem1 on the relative GTP hydrolysis rate of 1 μM Cdc42. (d,e) Relative GTP hydrolysis rate of Cdc42-Cdc24 assays (d) and Cdc42-Bem1 assays (e) in comparison to expected effect of crowding, based on the assumption that one Cdc24/Bem1 molecule takes up the same space as one BSA molecule. (f) Summary of Cdc42 - effector interaction rates $k'_{3,x}$ and k'_{3,x_1,x_2} of two- and three-protein assays. Values are summarised in Tab. 4.2. (a-e) The "relative GTP hydrolysis rate" refers to $-d[\ln[GTP]/dt$ in Eq. 4.6. Fits are depicted as dashed lines. Abbreviations: O. R.: Data point is out of plotting range.

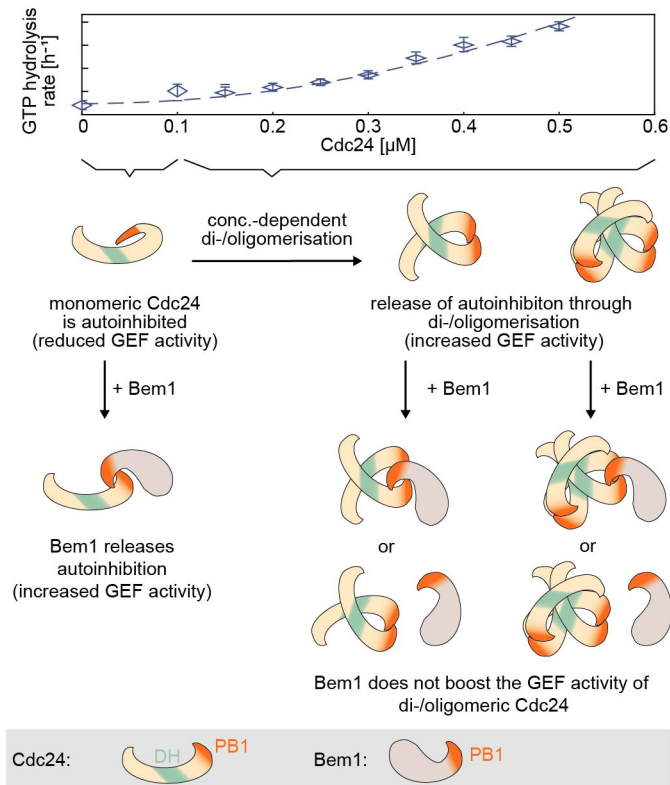


Figure 4.7. Speculative model of the concentration-dependent Cdc24-Bem1 interaction: At low concentrations (e.g. 0-0.1 μM) Cdc24 is monomeric. It has a lower GEF activity due to intramolecular interactions of its PB1 domain (*Shimada et al. (2004)*). Addition of Bem1 releases the autoinhibition through the formation of a Cdc24-Bem1 heterodimer (via their PB1 domains). With increasing Cdc24 concentration (e.g. above 0.1 μM) Cdc24 forms more and more di- and oligomers, via its DH domain (*Mionnet et al. (2008)*). The autoinhibition of Cdc24 is released through this process and its GEF activity increases. Addition of Bem1 leads to Bem1-Cdc24 complexes (or not). Because Cdc24's autoinhibition is already released (and it already has an increased GEF activity) effects of Bem1 are non-existent or minor.

4.2.7. Regulation of the GTPase activity of Cdc42 through GAPs Rga2 and Bem3

Besides GEFs, GAPs also speed up the GTPase cycle, through directly increasing the speed of the GTP hydrolysis step. We tested the GAP activity of Bem3 and Rga2. Against expectation (*Zheng et al. (1993)*; *Smith et al. (2002)*), both proteins show effects similar to, or only weakly above the BSA/crowding level (Fig. 4.8a,b,d,e). Later analysis revealed that both protein were partially degraded at the time of usage (Appendix 4.4.6 Fig. 4.11 a). This explains the weak effects we observed. Rga2 showed less degradation than Bem3, and in turn had a bigger effect on Cdc42 (Fig. 4.8f): $k'_{3,Rga2} = 0.251 \pm 0.033 \mu\text{M}^{-2} \text{h}^{-1}$ (Tab. 4.2). Its effect is about 5x above crowding expectation, assuming Rga2 and BSA have the same hydrodynamic radius. Rga2 has about 2x the molecular weight of BSA, hence a 1:1 comparison to BSA likely underestimates the crowding effect of Rga2. Nevertheless, given that $k'_{3,Rga2} \approx 5 \times k'_{3,BSA}$ we still expect Rga2 to have a GAP effect on Cdc42.

4.2.8. Interplay of the the GAP Rga2 and GEF Cdc24 in the regulation of the GTPase activity of Cdc42

GEFs and GAPs act on different stages of the GTPase cycle: GEFs affect the GDP release step, and GAPs enhance the GTP hydrolysis step (Fig. 4.3a). To test if there are synergistic effects when both proteins are present, we conducted GTPase experiments in which three proteins are present: Cdc42, Cdc24, and Rga2 (Fig. 4.8c). Similar to Cdc42-Cdc24-Bem1 assays, we determined the Cdc42-Cdc24, Cdc42-Rga2, and Cdc42-Cdc24-Rga interaction rates k'_3 using

$$\begin{aligned}
 -\frac{d\ln[\text{GTP}]}{dt} = & k'_1 c_{\text{corr}} [\text{Cdc42}] + k'_2 (c_{\text{corr}} ([\text{Cdc42}])^2 \\
 & + k'_{3,\text{Cdc24}} c_{\text{corr}} [\text{Cdc42}][\text{Cdc24}]^2 \\
 & + k'_{3,\text{Rga2}} c_{\text{corr}} [\text{Cdc42}][\text{Rga2}] \\
 & + k'_{3,\text{Cdc24,Rga2}} c_{\text{corr}} [\text{Cdc42}][\text{Rga2}][\text{Cdc24}]^2
 \end{aligned} \tag{4.10}$$

The contributions of the individual proteins stayed in the three-protein assay similar to those in the two-protein assays, and the interaction term is $k'_{3,\text{Cdc24,Rga2}} = 13.805 \pm 2.847 \mu\text{M}^{-4} \text{h}^{-1}$ (Fig. 4.8f, Tab. 4.2). This suggests that synergy between both proteins arises.

$k'_{3,\text{Cdc24,Rga2}}$ already includes the effect of crowding. In this assay the crowding contribution should be significant because the Rga2 protein sample contained a portion of degraded protein (Appendix 4.4.6 Fig. 4.11a) that is basically acting as a crowding agent. We did a (preliminary) test to assess the effect of crowding on the Cdc42-Cdc24 system (Appendix 4.4.6 Fig. 4.11b): here the addition of equimolar amounts of BSA (instead of Rga2) lead to the same boost in the GTPase cycle, revealing that crowding indeed has to be factored in. It is thus questionable if the perceived synergy between Rga2 and Cdc24 (or Bem1 and Cdc24) is (mainly) due to crowding or due to protein-specific interactions. Further experiments on the effect of crowding in a three-protein system, as well as experiments with non-degraded Rga2 are necessary to work out the explicit contributions of these two factors.

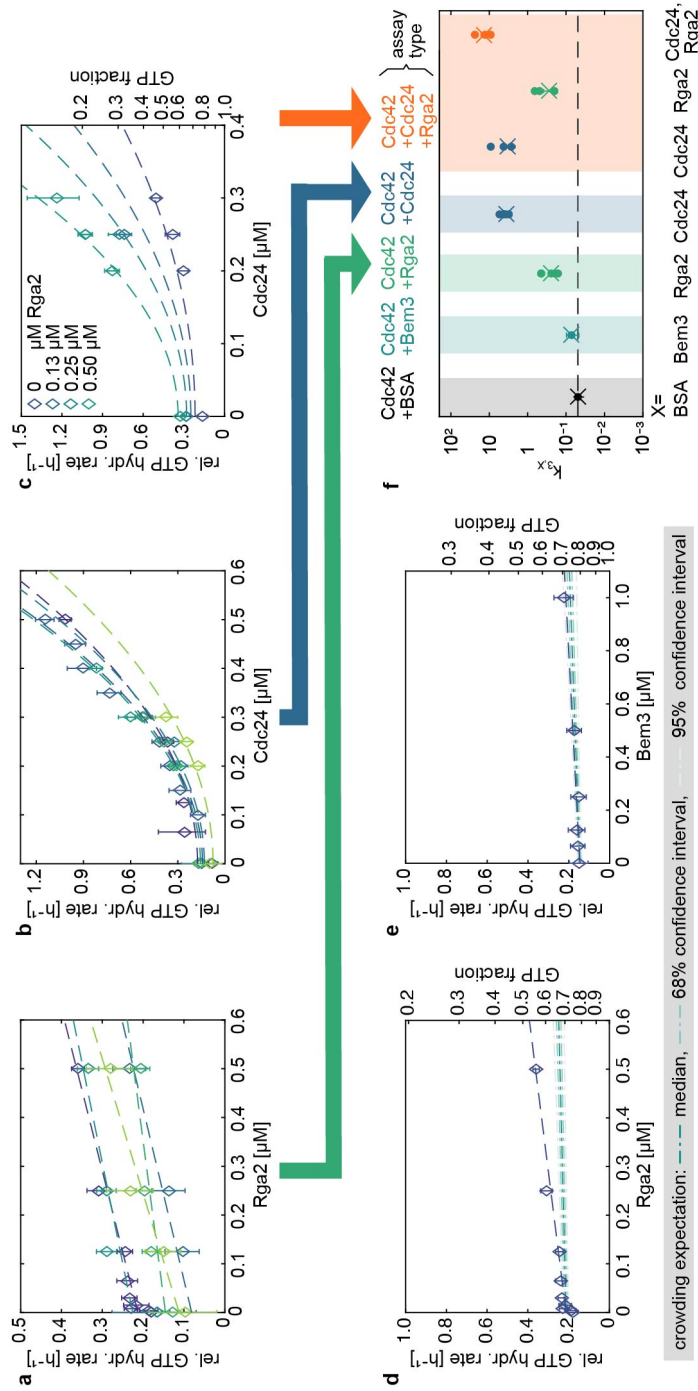


Figure 4.8. Regulation of the GTPase activity of Cdc42 through the GEF Cdc24 and GAPs Bem3 and Rga2. (a) Effect of Rga2 on the relative GTP hydrolysis rate of $1 \mu\text{M}$ Cdc42. Different colours denote separate experiments. (b) The relative GTP hydrolysis rate in Cdc42-Cdc24 assays increases non-linearly with the Cdc24 concentration ($1 \mu\text{M}$ Cdc42). Different colours denote separate experiments. (c) Effect of Cdc24 and Rga2 on the relative GTP hydrolysis rate of $1 \mu\text{M}$ Cdc42. (d,e) Relative GTP hydrolysis rate of Cdc42-Rga2 assays (d) and Cdc42-Bem3 assays (e) in comparison to expected effect of crowding, based on the assumption that one Rga2/Bem3 molecule takes up the same space as one BSA molecule. (f) Summary of Cdc42 - effector interaction rates $k'_{3,x}$ and $k'_{3,x} x_5$ of two- and three-protein assays. Values are summarised in Tab. 4.2. (a-e) The "relative GTP hydrolysis rate" refers to $-d \ln[\text{GTP}]/dt$ in Eq. 4.6. Fits are depicted as dashed lines.

Table 4.1. GTP hydrolysis cycling rates k_1 and k_2 of Cdc42 (H-Cdc42-F, purification 2). All values are given in Appendix 4.4.3 Tab. 4.4. Abbreviations: Σ : pooled estimate.

Exp	k_1 [$\times 10^{-2} \mu\text{M}^{-1} \text{h}^{-1}$]	k_1 std. err. [$\times 10^{-2} \mu\text{M}^{-1} \text{h}^{-1}$]	k_2 [$\times 10^{-2} \mu\text{M}^{-2} \text{h}^{-1}$]	k_2 std. err. [$\times 10^{-2} \mu\text{M}^{-2} \text{h}^{-1}$]
Σ (n=4)	0.075	0.004	0.081	0.006

Table 4.2. Cdc42 - effector protein X interaction rates k_{3,X_1} , k_{3,X_2} , and k_{3,X_1,X_2} of two- and three-protein assays. The stated values belong to assays in which H-Cdc42-F (purification 2), Cdc24-H (purification 2), S-Bem1-H, partially degraded H-Rga2-F, or partially degraded H-Bem3-F were used. All values are given in Appendix 4.4.3 Tab. 4.5 and Tab. 4.6. *: The values are based on one experiment, but additional experiments that showed similar rates were conducted. (Rates of these experiments did not have a standard error and could therefore not be used for pooling.) Abbreviations: degr.: partially degraded, Σ : pooled estimate.

Exp	Effector protein X_1	Effector protein X_2	k_{3,X_1} [$\mu\text{M}^{-3} \text{h}^{-1}$]	k_{3,X_1} std. err. [$\mu\text{M}^{-3} \text{h}^{-1}$]	k_{3,X_2} [$\mu\text{M}^{-2} \text{h}^{-1}$]	k_{3,X_2} std. err. [$\mu\text{M}^{-2} \text{h}^{-1}$]	k_{3,X_1,X_2} [$\mu\text{M}^{-4} \text{h}^{-1}$]	k_{3,X_1,X_2} std. err. [$\mu\text{M}^{-4} \text{h}^{-1}$]
Σ (n=6)	Cdc24		3.656	0.231				
E38F *		BSA			0.049	0.007		
E38Q *		Bem1			0.111	0.029		
Σ (n=5)		Rga2 (degr.)			0.251	0.033		
E38D		Bem3 (degr.)			0.072	0.013		
E38L	Cdc24	Bem1	4.254	0.739	0.139	0.064	-0.500	0.788
Σ (n=3)	Cdc24	Rga2 (degr.)	3.289	1.134	0.278	0.108	13.805	2.847

4.3. Discussion

To shed more light on emerging properties of the yeast polarity protein system, we studied the GTPase cycle of Cdc42 and the effect of molecular crowding, the GEF Cdc24, GAP Rga2, scaffold protein Bem1, and combinations thereof, on the GTPase cycle of Cdc42. What did we learn about Cdc42 regulation and its emergent properties?

Our data suggests that Cdc42 is highly tunable; its GTP hydrolysis cycling speed can distinctively be upregulated by GEFs, GAPs, and molecular crowding. This effect seems to be further enhanced if combinations of these factors are present. The GTP hydrolysis cycling rate also increased non-linearly with the Cdc42 and Cdc24 concentration. A synergistic upregulation of Cdc42 thus seems to arise when more than one protein species and/or crowding is present, and when certain proteins (Cdc42 and Cdc24 for example) are present at elevated concentrations. This way of regulating Cdc42 GTPase activity could be a resourceful and thus advantageous way of regulation; if regulatory factors have a synergistic interplay, wide ranges of upregulation can be achieved through a small amount of components. This synergy also implies that Cdc42 has a significantly higher GTPase activity at the polarity spot, where it is surrounded by many effector proteins. We suspect the strong upregulation at the site of bud emergence and the rather low baseline activity at other sites to have a cellular purpose, and imagine it is contributing to Cdc42 accumulation.

The non-linear concentration dependence of the GTPase cycling rate was stronger for Cdc24 in comparison to Cdc42 (sub- μM for Cdc24, μM for Cdc42), suggesting that the Cdc24 concentration has a significant impact on the system. The Cdc24-dosage sensitivity is in agreement with *in vivo* and *in silico* evidence: Timed release of Cdc24 from the nucleus (thus suddenly increasing the effective Cdc24 concentration) is known to be part of the polarity trigger *in vivo* (**Shimada et al. (2000)**). And a theoretical study showed that Cdc42 accumulation requires a certain Cdc24 concentration in the cell (**Klünder et al. (2013)**).

We also observed that molecular crowding, even at μM concentrations, affected the Cdc42 GTPase cycle and interactions between Cdc42 and its effector proteins. The fact that crowding has such a significant impact on the GTPase cycle adds another regulatory layer onto Cdc42 accumulation: its activity is not only affected by other regulatory proteins, but also by the density of its environment. If certain areas in the cell, for example the polarity spot, show a higher level of crowding, the GTPase cycling speed of Cdc42 will be increased in this particular area. This further emphasises how dynamic Cdc42's properties are, and how dependent its activity (and potentially functionality) is on its environment. It should not be seen as a static player in the polarity network, but as a protein that itself has dynamic properties. We are not the first to point out dynamic properties of the yeast polarity system. *In vivo* studies showed that the polarity spot is dynamic (**Wedlich-Soldner et al. (2004)**; **Gao et al. (2011)**) and that cellular components are highly connected and exhibit lots of interactions (**Costanzo et al. (2016)**).

Our data highlights the parameter interplay in the polarity system, and shows that the properties of the proteins are context-dependent. This implies that they should be studied in such a way. For example, kinetic *in vitro* studies might be more meaningful when conducted in various environments and where the effect of crowding is investigated. Further, potential synergy between proteins and other effectors should be explored.

We set out to gain further knowledge on how Cdc42 accumulation emerges by studying the Cdc42 GTPase cycle. We found that molecular crowding can have a significant effect on the system (and thus potentially on Cdc42 accumulation), and that effector proteins used in combination show

a synergy, although it is not clear whether this is due to the crowding effect or due to protein-specific properties. To gain more detailed knowledge, more experiments on these interactions and on the crowding effect are required. For example, the use of a wider range of crowding concentrations and reagents, and its impact on Cdc42 effector protein interaction, will show how and when crowding effects matter. For this, a more accurate determination of the hydrodynamic radii of the proteins involved is required. Further, the GEF/GAP synergy can be better characterised through (1) the use of GAP proteins that show no partial degradation, and (2) the use of broader concentration regimes. Knowledge of at which concentrations these effects saturate will also help to contextualise these findings. Lastly, additional experiments that only illuminate the GTP hydrolysis or GEF reaction step would point to which GTPase cycle step is most affected by which factor.

4

4.4. Appendix

4.4.1. Appendix: Cdc42 GTPase activity

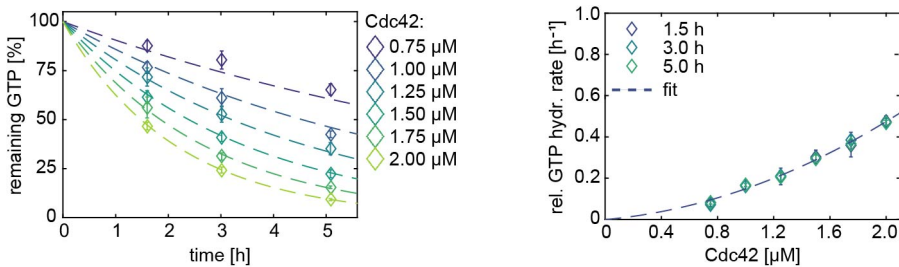


Figure 4.9. GTP hydrolysis by Cdc42. In GTPase assays the GTP concentration declines exponentially with time (left). The relative GTP hydrolysis rate of Cdc42 scales non-linearly with the Cdc42-concentration: a fit of the data with Eq. 4.2 results in the parameter values of $k=0.15\pm 0.08 \mu\text{M}^{-1.65} \text{h}^{-1}$ and $n=1.65\pm 0.10$ ($R^2=0.995$) (right). The "relative GTP hydrolysis rate" refers to $-d\ln[\text{GTP}]/dt$.

4.4.2. Appendix: Influence of the PBR on the dimerisation of GTPases

Table 4.3. Amino acid (AA) sequences of the C-terminal region of selected small GTPases in relation to the ability of these GTPases to dimerise/ oligomerise. The PBR and other basic AAs (K: lysine, R: arginine) are highlighted in bold. Abbreviations: *S.c.*: *S. cerevisia*, *H.s.*: *H. sapiens*, WT: wild-type, M: mutant.

Protein	Type	C-term. AA sequ.	State	Exp. cond.	Reference
<i>S.c.</i> Cdc42	WT	PVI KKSKK CAIL	unknown monomer	<i>in vitro</i> <i>in vivo</i>	<i>Kang et al. (2010)</i>
<i>H.s.</i> Cdc42	WT	PEP KKSRR CVLL	dimer	<i>in vitro</i>	<i>Zhang and Zheng (1998)</i>
<i>H.s.</i> Cdc42	M	PEP KKSKR CVLL	dimer	<i>in vitro</i>	<i>Zhang et al. (1999)</i>
<i>H.s.</i> Cdc42	M	PEP KK	monomer	<i>in vitro</i>	<i>Zhang and Zheng (1998)</i>
<i>H.s.</i> Rac1	WT	PVK KRKRK CLLL	oligomer	<i>in vitro</i>	<i>Zhang et al. (2001)</i>
<i>H.s.</i> Rac1	M	PVP KKSRR CVLL	oligomer	<i>in vitro</i>	<i>Zhang et al. (2001)</i>
<i>H.s.</i> Rac1	M	PVK QQQQQ CVLL	monomer	<i>in vitro</i>	<i>Zhang et al. (2001)</i>
<i>H.s.</i> Rac1	M	PVK K	monomer	<i>in vitro</i>	<i>Zhang et al. (2001)</i>
<i>H.s.</i> Rac2	WT	PTR QKRA CSLL	dimer	<i>in vitro</i>	<i>Zhang and Zheng (1998)</i>
<i>H.s.</i> RhoA	WT	RRG KKKSG CLVL	dimer	<i>in vitro</i>	<i>Zhang and Zheng (1998)</i>
<i>H.s.</i> RhoA	M	RRG KKKRG CLVL	dimer	<i>in vitro</i>	<i>Zhang et al. (1999)</i>
<i>H.s.</i> RhoA	M	RRG K	monomer	<i>in vitro</i>	<i>Zhang and Zheng (1998)</i>
<i>S.c.</i> Rsr1	WT	SQQ KKKKK NASTCTIL	dimer	<i>in vivo</i>	<i>Kang et al. (2010)</i>
<i>S.c.</i> Rsr1	M	SQQ SSSSS NASTCTIL	monomer	<i>in vivo</i>	<i>Kang et al. (2010)</i>

4.4.3. Appendix: GTP hydrolysis cycling rates (data set A)

Table 4.4. GTP hydrolysis cycling rates k_1 and k_2 of Cdc42 (H-Cdc42-F, purification 2). Abbreviations: Σ : pooled estimate.

Exp.	k_1 [$\times 10^{-2} \mu\text{M}^{-1} \text{h}^{-1}$]	k_1 std. err. [$\times 10^{-2} \mu\text{M}^{-1} \text{h}^{-1}$]	k_2 [$\times 10^{-2} \mu\text{M}^{-2} \text{h}^{-1}$]	k_2 std. err. [$\times 10^{-2} \mu\text{M}^{-2} \text{h}^{-1}$]	R ² (fit)
E38ABC	0.071	0.009	0.082	0.006	0.996
E38E	0.015	1.000×10^{12}	0.087	0.100	0.588
E38G	0.092	0.021	0.097	0.013	0.990
E38Q	0.082	0.028	0.055	0.017	0.982
Σ	0.075	0.004	0.081	0.006	

Table 4.5. Cdc42 - effector protein X interaction rates $k_{3,X}$ of two-protein assays. The stated values belong to assays in which H-Cdc42-F (purification 2), Cdc24-H (purification 2), S-Bem1-H, BSA (purification 2), partially degraded H-Rga2-F, or partially degraded H-Bem3-F were used. Values were used for pooling if a standard error was available. * When X = Cdc24, the unit of $k_{3,X}$ is [$\mu\text{M}^{-3} \text{h}^{-1}$]. Abbreviations: degr.: partially degraded, N.A.: not available, Σ : pooled estimate.

Effector protein X	Exp.	c_{corr}	c_{corr} std. err.	$k_{3,X}$ [$\mu\text{M}^{-2} \text{h}^{-1}$] *	$k_{3,X}$ std. err. *	R ² (fit)	Used for pooling?
Cdc24	E38D	1.075	0.096	3.121	0.120	0.993	yes
Cdc24	E38E	0.941	0.113	4.460	0.224	0.980	yes
Cdc24	E38J	0.889	0.268	4.165	1.109	0.815	yes
Cdc24	E38L	0.998	0.089	4.252	0.228	0.993	yes
Cdc24	E38M	1.024	0.047	3.794	0.134	0.996	yes
Cdc24	E38T	0.550	0.211	5.482	1.019	0.900	yes
Cdc24	Σ			3.656	0.231		
BSA	E38F	1.059	0.068	0.049	0.007	0.936	yes
BSA	E38K	0.623	0.037	0.235	N.A.	N.A.	no
BSA	E38L	0.971	0.056	0.062	N.A.	N.A.	no
BSA	Σ			0.049	0.007		
Bem1	E38L	0.971	0.056	0.093	N.A.	N.A.	no
Bem1	E38Q	0.830	0.110	0.111	0.029	0.826	yes
Bem1	Σ			0.111	0.029		
Rga2 (degr.)	E38G	1.220	0.074	0.246	0.025	0.928	yes
Rga2 (degr.)	E38J	0.638	0.193	0.446	0.155	0.716	yes
Rga2 (degr.)	E38M	1.266	0.150	0.191	0.098	0.483	yes
Rga2 (degr.)	E38N	0.952	0.091	0.164	0.069	0.612	yes
Rga2 (degr.)	E38T	0.799	0.110	0.453	0.089	0.896	yes
Rga2 (degr.)	Σ			0.251	0.033		
Bem3 (degr.)	E38D	0.955	0.060	0.072	0.013	0.863	

Table 4.6. Cdc42 - effector protein X interaction rates k_{3,X_1} , k_{3,X_2} , and k_{3,X_1,X_2} of three-protein assays. The stated values belong to assays in which H-Cdc42-F (purification 2), Cdc24-H (purification 2), S-Bem1-H, or partially degraded H-Rga2-F were used. Abbreviations: degr.: partially degraded, Σ : pooled estimate.

Effector protein X_1	Effector protein X_2	Exp.	C_{corr}	C_{corr} std. err.	k_{3,X_1} [$\mu\text{M}^{-3} \text{h}^{-1}$]	k_{3,X_1} std. err.	k_{3,X_2} [$\mu\text{M}^{-2} \text{h}^{-1}$]	k_{3,X_2} std. err.	k_{3,X_1,X_2} [$\mu\text{M}^{-4} \text{h}^{-1}$]	k_{3,X_1,X_2} std. err.	R^2 (fit)
Cdc24	Rga2 (degr.)	E38J	0.570	0.319	9.283	1.733	0.662	0.253	23.952	4.735	0.976
Cdc24	Rga2 (degr.)	E38M	1.238	0.133	2.714	0.470	0.203	0.086	13.102	1.962	0.969
Cdc24	Rga2 (degr.)	E38T	0.746	0.243	4.281	1.276	0.496	0.226	9.365	4.055	0.929
Cdc24	Rga2 (degr.)	Σ			3.289	1.134	0.278	0.108	13.805	2.847	
Cdc24	Bem1	E38L	0.999	0.244	4.254	0.739	0.139	0.064	-0.500	0.788	0.848

4.4.4. Appendix: Cdc42 - Cdc24 - Bem1 interaction (data set B)

We did not observe a (strong) GEF boosting effect of the Bem1 construct S-Bem1-H (data set A, discussed in the main text). The reason for this can be that this Bem1 construct lacked its ability to interact with Cdc24 or Cdc42. Another Bem1-construct, H-Bem1-F, had been used to verify these interactions (Fig. 4.5a,b). We also used H-Bem1-F for some preliminary experiments on the Cdc42-Cdc24-Bem1 interaction, which are discussed here (data set B):

An overview of which constructs were used in which data sets is given in Tab. 4.7.

First we determined the rates of Cdc42 (Fig. 4.10a) and those of the Cdc42-BSA, Cdc42-Cdc24, Cdc42-Bem1, and Cdc42-BSA interaction (Fig. 4.10): They all are similar to, but distinctively lower, than the rates of protein batches in the main text (Tab. 4.8 and Tab. 4.9). All proteins used here originate from a different batch than those used in data set A. We already observed that different purification batches can have different rates (see Chapter 3), therefore the occurrence of lower rates seems not problematic.

We then analysed the Cdc42-Cdc24-Bem1 interaction data (Fig. 4.10c). The contributions of the individual proteins ($k'_{3,Cdc24}$ and $k'_{H-Bem1-F}$) in the three-protein assay are similar to those in the two-protein assays, and the interaction term is slightly positive ($k'_{3,Cdc24,H-Bem1-F} = 0.354 \pm 0.091 \mu\text{M}^{-4} \text{h}^{-1}$ (Tab. 4.10)). It is bigger, but within the error range of $k'_{3,Cdc24,S-Bem1-H}$. As both protein constructs show the same trend, we presume that S-Bem1-H is also functional. H-Bem1-F could still have a slightly higher GEF boosting activity than S-Bem1-H. This could be, similar to Cdc42 and Cdc24, due to batch activities, or due to presence of different purification tags.

In conclusion, the data of both Bem1 constructs indicates that the GEF enhancing effect of Bem1 is difficult to observe in GTPase assays.

Table 4.7. Overview of the protein constructs used in data set A and B. Abbreviations: P1: Purification batch 1, P2: Purification batch 2.

	Data set A (main text)	Data set B (this appendix)
Cdc42	H-Cdc42-F (P2)	H-Cdc42-F (P1)
BSA	BSA (P2)	BSA (P1)
Cdc24	Cdc24-H (P2)	Cdc24-H (P1)
Bem1	S-Bem1-H	H-Bem1-F

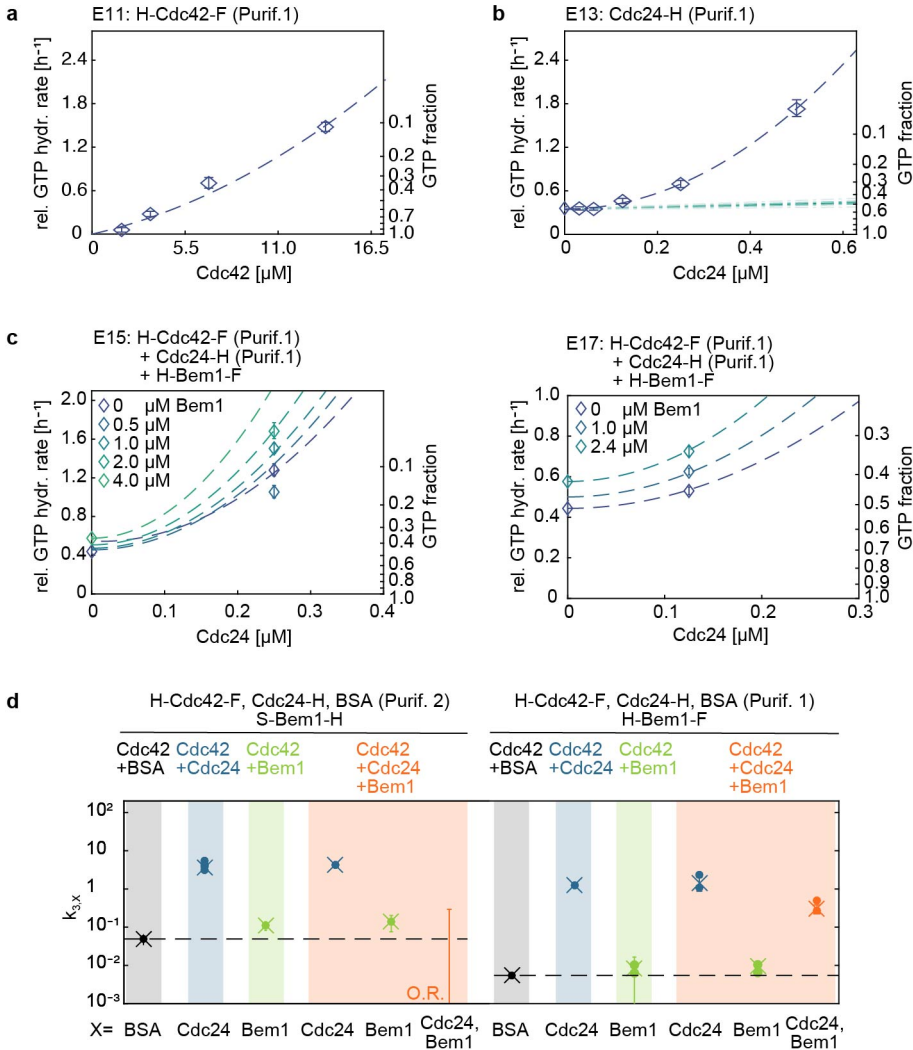


Figure 4.10. Preliminary data of the Cdc42-Cdc24-Bem1 interaction (data set B, Tab. 4.7). The experiment numbers of these data are indicated on top. (a) The relative GTP hydrolysis rate of Cdc42 scales non-linearly with the Cdc42-concentration. (b) The relative GTP hydrolysis rate in Cdc42-Cdc24 assays scales non-linearly with the Cdc24-concentration (7 μ M Cdc42). (c) Effect of Cdc24 and Bem1 on the relative GTP hydrolysis rate of 7 μ M Cdc42. (c) Summary of Cdc42 - effector interaction rates $k'_{3,x}$ and k'_{3,x_1,x_2} of two- and three-protein assays. Experiments discussed in the main text (data set A, left) are compared to those from this additional data set B (right, data from a-c). Values are summarised in Tab. 4.8, Tab. 4.9, and Tab. 4.10. (a-c) The "relative GTP hydrolysis rate" refers to $-d\ln[\text{GTP}]/dt$ in Eq. 4.6. Fits are depicted as dashed lines. Abbreviations: O. R.: Data point is out of plotting range.

Table 4.8. Comparison of the Cdc42 GTP hydrolysis cycling rates k_1 and k_2 obtained from data set A and B. Abbreviations: P1: purification 1 (data set B, discussed in this appendix), P2: purification 2 (data set A, discussed in the main text), Σ : pooled estimate.

Data set	Protein	Exp.	k_1 [$\times 10^{-2} \mu\text{M}^{-1} \text{h}^{-1}$]	k_1 std. err.	k_2 [$\times 10^{-2} \mu\text{M}^{-2} \text{h}^{-1}$]	k_2 std. err.
B	Cdc42 (P1)	E11	0.058	0.028	0.004	0.002
A	Cdc42 (P2)	Σ (n=4)	0.075	0.004	0.081	0.006

Table 4.9. Comparison of the Cdc42 - effector protein X interaction rates $k_{3,X}$ (two-protein assays) obtained from data set A and B. *: When X = Cdc24, the unit of $k_{3,X}$ is [$\mu\text{M}^{-3} \text{h}^{-1}$]. **: The values are based on one experiment, but additional experiments that showed similar rates were conducted. (Rates of these experiments did not have a standard error and could therefore not be used for pooling.) Abbreviations: P1: purification 1, P2: purification 2., N.A.: not available, Σ : pooled estimate.

Data set	Effector protein X	Exp.	c_{corr}	c_{corr} std. err.	$k_{3,X}$ [$\mu\text{M}^{-2} \text{h}^{-1}$] *	$k_{3,X}$ std. err. *	R ² (fit)
B	Cdc24 (P1)	E13	1.276	1.210	1.241	0.065	0.998
A	Cdc24 (P2)	Σ (n=6)			3.656	0.231	
B	H-Bem1-F	E15	1.53	1.27	0.006	N.A.	
B	H-Bem1-F	E17	1.55	1.27	0.10	N.A.	
B	H-Bem1-F	Σ (n=2)			0.008	N.A.	
A	S-Bem1-H	E38Q **			0.111	0.029	
B	BSA (P1)	E15	1.55	1.27	0.005	N.A.	
A	BSA (P2)	E38F**			0.049	0.007	

Table 4.10. Comparison of the Cdc42 - effector protein X interaction rates k_{3,X_1} , k_{3,X_2} , and k_{3,X_1,X_2} (three-protein assays) obtained from data set A and B. Abbreviations: P1: purification 1, P2: purification 2, Σ : pooled estimate.

Data set	Effector protein X_1	Effector protein X_2	Exp.	C_{corr}	C_{corr} std. err.	k_{3,X_1} [$\mu\text{M}^{-3} \text{h}^{-1}$]	k_{3,X_1} std. err.	k_{3,X_2} [$\mu\text{M}^{-2} \text{h}^{-1}$]	k_{3,X_2} std. err.	k_{3,X_1,X_2} [$\mu\text{M}^{-4} \text{h}^{-1}$]	k_{3,X_1,X_2} std. err.	R^2 (fit)
B	Cdc24 (P1)	H-Bem1-F	E15	1,541	1,286	2,340	0,444	0,006	0,004	0,584	0,385	0,965
B	Cdc24 (P1)	H-Bem1-F	E17	1,549	1,272	1,083	0,273	0,010	0,002	0,318	0,152	0,979
B	Cdc24 (P1)	H-Bem1-F	Σ (n=2)			1,426	0,560	0,010	0,002	0,354	0,091	
A	Cdc24 (P2)	S-Bem1-H	E38L	0,999	0,244	4,254	0,739	0,139	0,064	-0,500	0,788	0,848

4.4.5. Appendix: The GEF enhancing effect of Bem1

Our data suggested that the GEF enhancing effect of Bem1 is difficult to observe in GTPase assays (even though it was observed in GEF assays by Rapali *et al.* (Rapali *et al.* (2017))). One difference is that we used a significantly higher Cdc24 concentration in the GTPase assay than was used in the GEF assay. We speculated that Bem1 only has a GEF-enhancing effect on Cdc24 when it is in its monomeric and autoinhibited state, which is at low concentrations. We also speculated that at high concentrations Cdc24 releases the autoinhibition through the formation of homo-dimers or oligomers, and Bem1 no longer boosts its GEF activity (Fig. 4.7).

We can contextualise, or challenge, this speculation further by considering the Cdc24/Bem1 binding strengths and dynamics: In pulldown experiments from cell lysates only 6% of Cdc24 was found to be oligomeric, suggesting that these complexes are very dynamic (Mionnet *et al.* (2008)). Cdc24-Bem1 complexes, on the other hand, are stable and persistent and can survive multiple washing steps in pulldown experiments (Zheng *et al.* (1995) and Fig. 4.6b).

Given the dynamic nature of Cdc24 dimers, we thus expect to always have a pool of Cdc24 dimers and monomers. Bem1 then competes with a monomeric Cdc24 for another monomeric Cdc24. If two Cdc24 molecules form a dimer, this dimer likely falls apart quite quickly. If a Bem1-Cdc24 complex forms, it will likely persist. Over time Bem1 will then bind to all existing monomers, depleting the monomeric Cdc24 pool (that has a lower GEF activity). We hypothesise three scenarios:

(1) Bem1 increases the overall GEF activity of Cdc24: If both Bem1-Cdc24 and Cdc24-Cdc24 dimers have a similarly enhanced GEF activity, Bem1 increases the pool of Cdc24 with a higher GEF activity. This should increase the overall GTPase cycling speed.

(2) The effect of Bem1 is modulated by the GEF concentration: If the GEF activity of Cdc24 dimers is significantly higher than that of Cdc24-Bem1 dimers, Bem1 decreases the GEF activity of the Cdc24 population (through taking Cdc24 monomers out of the Cdc24 monomer - dimer pool). Bem1 has a modulating effect: At low Cdc24 concentrations (where Cdc24 is monomeric) it boosts the overall Cdc24 GEF activity, whereas at higher Cdc24 concentrations (where some Cdc24 is dimeric) it reduces the GEF activity of the Cdc24 population.

(3) Bem1 has no effect: If at a given Cdc24 concentration the Cdc24 pool does not consist of a mixture of monomers and dimers, but only of Cdc24 dimers, then all Cdc24 molecules have an enhanced GEF activity. In addition, if both Bem1-Cdc24 and Cdc24-Cdc24 dimers have a similarly enhanced GEF activity, then Bem1 still reduces the pool of Cdc24 dimers (through formation of Cdc24-Bem1 dimers), but the overall pool of Cdc24 with increased GEF activity does not change. Bem1 does not affect the GTPase cycling speed.

Given that we do not know the monomer/dimers ratio at our Cdc24 concentration, and that we do not know if Bem1-Cdc24 complexes have a stronger or weaker GEF activity compared to Cdc24 homodimers, it is difficult to say which of these hypotheses are most likely. Additional GEF assays (as done by Rapali *et al.*) can be used to quantify the GEF activities of Cdc24 and Cdc24-Bem1 dimers. The concentration-dependence of Cdc24 dimer formation, in conjunction with the influence of Bem1 on this dimer pool, can be studied through mass photometry (Refeyn). Here the molecular weight distribution of proteins and protein complexes is measured in solution.

4.4.6. Appendix: GAPs

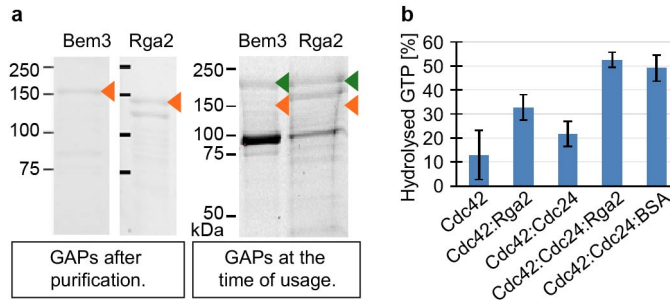


Figure 4.11. Cdc42-GAP interaction. (a) SDS-Page of GAPs (Bem3 and Rga2, ~120-130 kDa) after purification and at the time of usage. The molecular weight of the full-length protein is indicated by an orange arrow. At the time of usage a significant portion of GAPs was degraded and no band at ~130 kDa could be observed (orange arrow). However, higher bands were present (green arrow). In the SDS-Page gels of proteins after purification, Bem3 has one band and Rga2 has two bands at ~130 kDa. This pattern also shows up in the SDS-Page at the time of usage, but at a bigger size (~200 kDa, green arrow). It is possible that in this SDS-Page these are the full-length proteins that run at a bigger size than expected. (b) GTPase assay, showing the amount of hydrolysed GTP for various protein mixtures, using one or several of the following proteins in stated concentration: 1 μM Cdc42 (H-Cdc42-F, purification 2), 0.5 μM Rga2 (H-Rga2-F, partially degraded), 0.2 μM Cdc24 (Cdc24-H, purification 2), 0.5 μM BSA (purification 2).

Contributions and acknowledgements

R. van der Valk constructed the plasmids of protein constructs. Proteins were expressed and purified by S. Tschirpke, F. Shamsi, and F. van Opstal. S. Tschirpke conducted GTPase assays, Flag-pulldown experiments, Western Blots, and analysed the data thereof. The development of the GTPase model, the fitting and further analysing of the GTPase data was done by W. Daalman. The results were discussed by S. Tschirpke and W. Daalman. Figure preparation and writing of this chapter was done by S. Tschirpke.

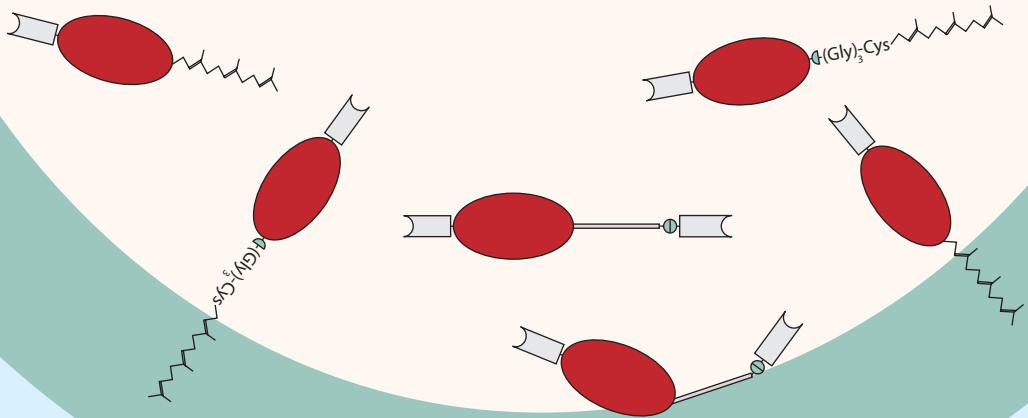
We thank D. McCusker (University of Bordeaux) for the plasmid pDM272 and N. Dekker (TU Delft) for the plasmid pET28a-His-mcm10-Sortase-Flag.

5

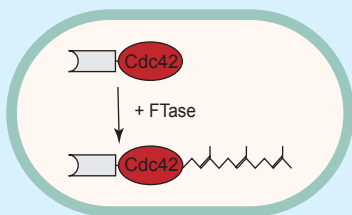
Don't wish it was easier, wish you were better.
Don't wish for less problems, wish for more skills.

— Jim Rohn

Approaches for Cdc42 with membrane-binding capabilities

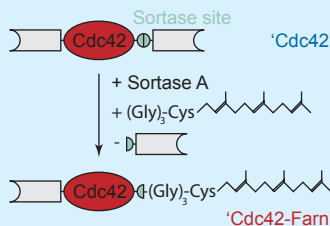


Co-expression of FTase and Cdc42 in *E. coli*



extremely low yield of farnesylated Cdc42

Sortase-mediated *in vitro* farnesylation



low-medium yield

Alternative membrane binding domain

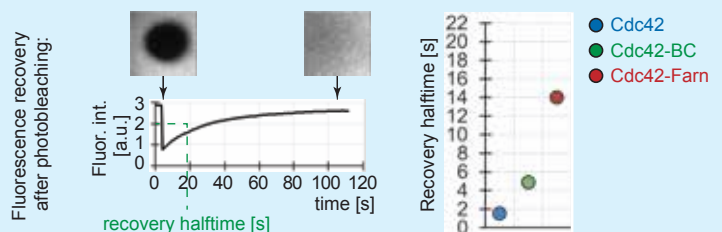


Cdc42 with Bem1 basic cluster (BC) membrane binding domains (51 AA) (Meca *et al.* 2019)

'Cdc42-BC'

high yield

Membrane binding properties:



- ➔ Cdc42-BC binds very transiently to the membrane
- ➔ Farnesylated Cdc42 binds strongest

Approaches for Cdc42 with membrane-binding capabilities

Abstract Small GTPases are highly conserved proteins and control cell polarisation in most eukaryotes. In *Saccharomyces cerevisiae*, polarity establishment is controlled by the membrane-binding GTPase Cdc42, and is initiated by its accumulation on the membrane at the site of bud emergence. Cdc42 binds to membranes through a lipid tail that it acquires through post-translational prenylation: through thioether linkage a hydrophobic iso-prenoid lipid group (farnesyl or geranyl-geranyl) is added to Cdc42's C-terminal CAAX box. Because of its central position in the yeast polarity system, Cdc42 is an interesting candidate for *in vitro* studies. However, obtaining prenylated Cdc42 remains a challenge and available methods are not accessible for everyone. In order to make the use of membrane-binding Cdc42 for *in vitro* experiments more widely accessible, we here show and compare three complementary approaches for producing it; (1) Sortase-mediated *in vitro* farnesylation of Cdc42, (2) *E. coli*-based farnesylation of Cdc42, and (3) Cdc42 with Bem1 basic cluster (BC) membrane binding domains (*Meca et al. (2019)*). We show that Sortase-mediated farnesylation of Cdc42 works robustly. The reaction product can easily be separated from the other reaction components through a purification-tag based strategy. The farnesylation does not interfere with the protein's GTPase activity and GEF interaction and preliminary data suggests that this protein binds strongly to membranes. *E. coli*-based farnesylation of Cdc42 works, but leads to <1% farnesylated protein. We are currently exploring further optimisation steps to increase the yield. Addition of BC domains to the C-terminus of Cdc42 encompasses the easiest approach; Cdc42 can be purified in a high yield in a single purification step. BC domains do not alter Cdc42's GTPase activity nor interaction with the GEF Cdc24, but seem to only bind weakly to membranes.

5.1. Introduction

Small GTPases are highly conserved proteins and control cell polarisation in most eukaryotes (*Diepeveen et al. (2018)*). In *Saccharomyces cerevisiae*, polarity establishment is controlled by the membrane-binding Rho-family GTPase Cdc42, and initiated by its accumulation at the site of bud emergence. Cdc42 cycles between a GTP- and a GDP-bound form, which is highly regulated through interactions with GDP/GTP exchange factors (GEFs), GTPase activating proteins (GAPs), guanine nucleotide dissociation inhibitors (GDIs), scaffold proteins, and other regulatory proteins. Cdc42 binds to membranes through a lipid tail that it acquires through post-translational prenylation. Accumulation of Cdc42 on the membrane is driven by at least two interconnected regulatory feedback loops; a reaction-diffusion system, and the actin cytoskeleton (*Martin (2015)*; *Chiou et al. (2017)*).

Given the number of Cdc42 interactors and interconnection of the regulatory mechanisms, *in vivo* studies can give insights into general mechanisms, but fail to give precise knowledge on the

Abbreviations:

AA	amino acid
BC	basic cluster
DMSO	dimethyl sulfoxide
FRAP	fluorescence recovery after photobleaching
FTase	farnesyltransferase
GAP	GTPase activating protein
GDI	guanine nucleotide dissociation inhibitor
GEF	GDP/GTP exchange factor
GGTase I	geranylgeranyl-transferase type I
HIC	hydrophobic interaction chromatography
His-AC	His affinity chromatography
PBR	polybasic region
SEC	size-exclusion chromatography
SLB	supported lipid bilayer

5

molecular reactions that lead to the observed phenomena (*Vendel et al. (2019)*). *In vitro* studies, where cellular functions are reconstituted using purified components, allow the disentanglement of ongoing reactions, but face another obstacle: prenylated Cdc42 needs to be purified.

How is Cdc42 prenylated *in vivo*? The C-terminus of Cdc42 contains the so-called CAAX box, consisting of a cysteine (C), two aliphatic amino acids (A), and a variable amino acid (X). At this position the native protein is post-translationally prenylated: through thioether linkage a hydrophobic isoprenoid lipid group (15-Carbon farnesyl or 20-carbon geranyl-geranyl) is added to the cysteine, after which the other three amino acids are cleaved and the cysteine is carboxymethylated (*Caplin et al. (1994)*; *Coxon and Rogers (2003)*). This prenyl group is responsible for anchoring Cdc42 to the membrane, and is covered by the GDI Rdi1 to make Cdc42 cytosolic (*Koch et al. (1997)*). Two proteins, farnesyltransferase (FTase), and geranylgeranyl-transferase type I (GGTase I), are responsible for attaching a prenyl group to Cdc42. They differ in their affinity for Cdc42's CAAX box, thereby leading to a mixed pool of Cdc42 with a geranyl-geranyl or farnesyl tail in *S. cerevisiae* (*Caplin et al. (1994)*).

Purification of prenylated Cdc42 can not be done using standard *Escherichia coli*-based expression systems, because prenylation is a post-translational modification, for which the machinery is absent in *E. coli*. It therefore remains a challenge. *In vitro* studies can be limited to the use of unprenylated Cdc42 (*Kozminski et al. (2003)*; *Zhang and Zheng (1998)*; *Zhang et al. (2000)*) or cell lysates (*Bose et al. (2001)*). These studies are valuable, but by design neglect any effect of the membrane and its composition, the membrane-bound conformation of Cdc42, and an influence of Cdc42's modified C-terminal region (including prenylation-dependent Rdi1-binding), on the studied interactions with other proteins.

Previous *in vitro* studies with prenylated Cdc42 obtained the protein using (1) insect cell expression systems (Fig. 5.1b) (*Zheng et al. (1994, 1995)*; *Zhang and Zheng (1998)*; *Zhang et al. (1999)*; *Kozminski et al. (2003)*; *Johnson et al. (2009, 2012)*), (2) through purification of membrane-bound Cdc42 from yeast (Fig. 5.1a) (*Das et al. (2012)*; *Rapali et al. (2017)*), or (3) through *in vitro* prenylation of purified unprenylated Cdc42 from *E. coli* (Fig. 5.1e) (*Golding et al. (2019)*). These three methods are powerful tools, but may not be accessible for everyone. Insect cell expression sys-

tems require culturing facilities that are not available at every research location, purification from yeast remains not as reproducible as needed, and *in vitro* prenylation of Cdc42 requires additional purification and testing of the GGTase I enzyme, whose activity might vary among different purification batches. In order to make the use of membrane-binding Cdc42 for *in vitro* experiments more widely accessible, we here show and compare three complementary approaches for producing it; (1) Sortase-mediated *in vitro* farnesylation of Cdc42 (Fig. 5.1f), (2) farnesylation of Cdc42 in *E. coli* (Fig. 5.1c) (as established previously for GBP1 (*Fres et al. (2010)*)), and (3) Cdc42 with Bem1 basic cluster (BC) membrane binding domains (Fig. 5.1d) (*Meca et al. (2019)*).

We show that Sortase-mediated farnesylation of Cdc42 works robustly. The reaction product can easily be separated from the other reaction components through a purification-tag based strategy. The farnesylation does not interfere with the protein's GTPase activity and GEF interaction. Our preliminary data suggests that this protein binds strongly to membranes. *E. coli*-based farnesylation of Cdc42 works, but leads to <1% farnesylated protein. We are currently exploring further optimisation steps to increase the yield. The easiest approach was to add BC domains to the C-terminus of Cdc42. Here Cdc42 could be purified in a high yield in a single purification step. BC domains do not alter Cdc42's GTPase activity nor interaction with the GEF Cdc24, but seem to only bind weakly to membranes.

5.2. Results

5.2.1. Methods for creating membrane-binding Cdc42

Sortase-mediated *in vitro* farnesylation of Cdc42

We set out to find an *in vitro* prenylation method for Cdc42, as this approach does not require special cell culturing expertises and bacterial expressed Cdc42 can be used. Prenylation of Cdc42 *in vivo* is performed by FTases and GGTases, that can also be purified and used for prenylation *in vitro* (*Golding et al. (2019)*). We aimed for a method that does not require the additional purification of one or more enzymes, to decrease the workload of this method; the protein purification often requires extensive optimisation and activities of purified enzymes often vary among purification batches and thus need to be tested and quantified for every batch.

Sortase A (which we will refer to as 'Sortase' in the following), a transpeptidase enzyme from *Staphylococcus aureus*, is widely used for protein labelling, easy to purify and commercially available. Sortase recognises the LPXTG motif (with L: leucine, P: proline, X: variable amino acid, T: threonine, G: glycine) in a substrate and cleaves between the threonine and glycine. If an oligoglycine probe is present, an amide bond between threonine (substrate) and glycine (probe) gets formed. If no oligoglycine probe is present, the reaction terminates after the cleavage step. Sortase has almost no requirements for the structure or sequence of the probe (as long as it contains oligoglycine), and even accepts a wide range of non-proteinaceous molecules, like fluorescent dyes, fatty acids, nucleic acids, or polymers (*Pritz et al. (2007)*; *Antos et al. (2017)*; *Popp and Ploegh (2011)*). This makes it a valuable candidate for our purposes. Further, *Antos et al.* used Sortase to attach C14-C24 lipid chains (*Antos et al. (2008)*), that partially resemble farnesyl or geranylgeranyl in their hydrophobic properties, to proteins in a high yield, and showed that these fusions were able to localise to the plasma membrane.

We purified Cdc42 with a C-terminal Sortase recognition motif from *E. coli*, synthesised H₂N-Gly₃-cysteamine-farnesyl ('farnesyl peptide', see materials and methods)¹, and used a Sortase mutant

¹By that time peptides with farnesyl modification were commercially not available yet, though several companies offer them by now.

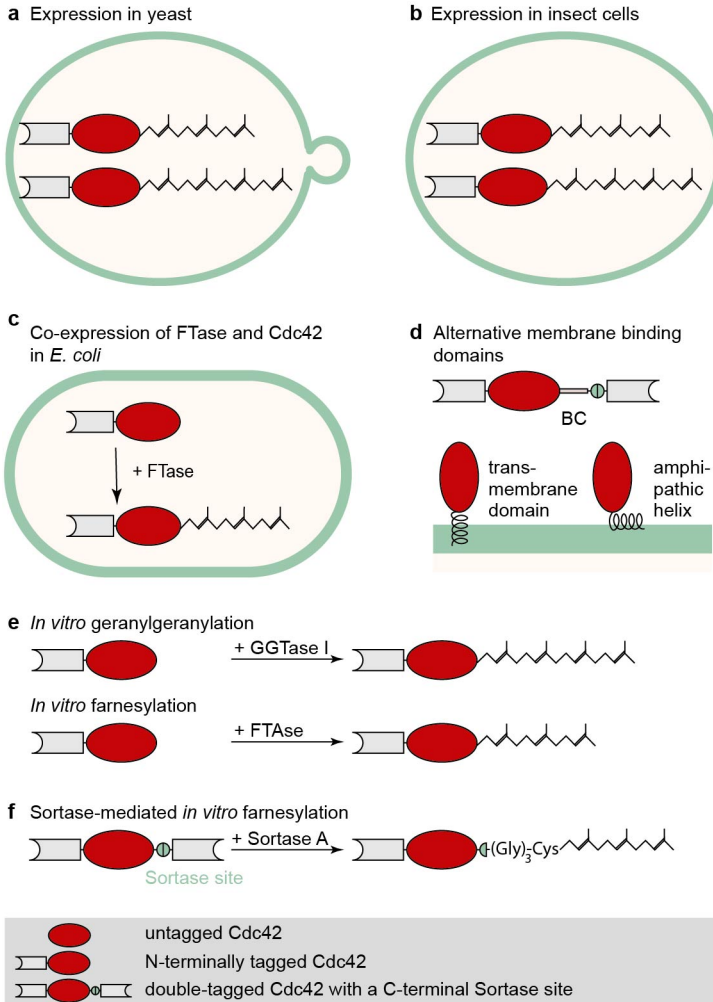


Figure 5.1. Schematic overview of available methods for obtaining prenylated Cdc42. (a) Expression of Cdc42 in yeast cells leads to a mixed pool of farnesylated and geranylgeranylated Cdc42, that can be purified from the membrane fraction (*Das et al. (2012)*). (b) Expression of Cdc42 in insect cells (for example Sf9 or Sf21) can also result in both prenylation products (e.g. *Zheng et al. (1994)*). (c) Co-expression of the FTase and Cdc42 produces farnesylated Cdc42 in *E. coli* (this work, and established previously for GBP1 (*Fres et al. (2010)*)). (d) Cdc42 constructs with alternative membrane binding domains, such as the basic clusters from Bem1 (BC) (this work, and *Meca et al. (2019)*), an amphipathic helix or a transmembrane domain (*Bendezú et al. (2015)*). (e) *In vitro* geranylgeranylation or farnesylation of bacterial expressed Cdc42 (*Golding et al. (2019)*). (f) Sortase-mediated *in vitro* farnesylation of bacterial expressed Cdc42 (this work).

with improved catalytic properties (*Chen et al. (2016)*, available from BPS Bioscience) for the labelling reactions (Fig. 5.1f).

To optimise reaction conditions, we carried out screens using Bem1 (S-Bem1-H) or Cdc42 (S-Cdc42-H) and Alexa488 peptide (Fig. 5.2a). Initially we used the intended reaction components (Cdc42 and farnesyl peptide), and monitored product formation using anti-farnesyl Western Blotting, but an eight condition screen ² revealed that all conditions showed false-positive and false-negative bands for farnesyl (data not shown). Considering the wide use and probe tolerances of Sortase, we assumed that the general trends of Cdc42/Bem1 Alexa488-peptide condition screens are applicable to reactions of Cdc42 and farnesyl peptide. We tested reactions with Sortase : protein : Alexa peptide ratios of 1:100:1000, 2:100:1000 and 2:100:2000 with reaction times of 60-120 min (at room temperature) and 24-72 h (at 4°C). Labelled and unlabelled protein are of roughly the same size and run at the same height on SDS-Page. We monitored the formation of labelled protein through the Alexa488-signal of the protein bands on SDS-Page (Fig. 5.2b). The more intense the signal, the more protein got labelled (Bem1 band at 70 kDa and Cdc42 band at 25 kDa). Cdc42 and Bem1 Alexa488-peptide screens showed the same trends: Increasing amounts of Sortase enzyme, peptide probe, and reaction time lead to an increased signal, and thus increased product formation. Reactions carried out for 24-72 h at 4°C showed a higher amount of product than those conducted at room temperature for 60-90 min. The most product got formed for reactions carried out for 72 h at 4°C at a 2:100:2000 molar ratio of Sortase : protein : Alexa peptide. For the reaction of Cdc42 with farnesyl peptide we used this condition, and even higher Sortase and peptide concentrations to further boost product formation (Fig. 5.2b). We considered even longer incubation times as they might increase the yield, but decided against it as this also increases the chances for protein degradation and aggregation.

The activity of Sortase was reported to be unaffected by up to 20% (v/v) content of dimethyl sulfoxide (DMSO) and polyethylene glycol in the reaction solution and to show decreased activity by solvent concentrations of 40% (*Pritz et al. (2007)*). We further investigated the effect of methanol, as alcoholic solvents might be present in traces in the synthesised farnesyl peptide. In alignment with previous findings, contents of up to 10% methanol did not affect the labelling reaction at all (Appendix 5.4.1 Fig. 5.7).

²We tried a combination of two primary antibodies, two secondary antibodies, and two detection kit solutions that previously were successfully used to detect farnesyl (*Kennedy et al. (2019)*; *Li et al. (2020)*).

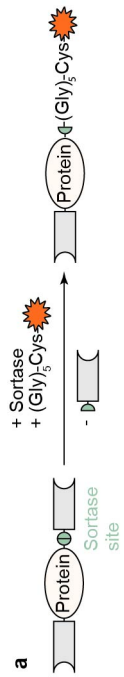


Figure 5.2. Sortase-mediated labelling of Cdc42 and Bem1 with Alexa488- and farnesyl-peptide. (a) Schematic illustration of the Sortase-mediated labelling reaction of double-tagged protein (Cdc42 or Bem1) with Alexa-peptide. (b) Condition screen of the labelling reaction of Bem1 (S-Bem1-H, 70 kDa) or Cdc42 (S-Cdc42-H, 29 kDa) with Alexa488 peptide, using stated temperatures, Sortase : peptide (Srt:P:Peptide) ratios, and incubation times. SDS-Page of the Alexa488-signal are shown.

We next used the Sortase reaction to ligate farnesyl peptide to Cdc42 (Fig. 5.3a). We considered two schemes for the purification of the reaction product (= farnesylated Cdc42); (1) based on the presence and absence of purification tags, and (2) based on the hydrophobicity of the final product. Route 1 worked reproducibly and is described below. Route 2 worked only partially and is discussed in Appendix 5.4.2.

Route 1: Cdc42 with an N-terminal Flag-tag and C-terminal 6His-tag (F-Cdc42-H) was labelled with farnesyl peptide using molar reaction ratios of Sortase : Cdc42 : farnesyl peptide of 4:100:20'000. During the labelling reaction the Sortase enzyme can cleave off Cdc42's C-terminal tag and ligate farnesyl peptide to the protein (Fig. 5.3a). The final reaction mixture therefore contains three Cdc42 species: unreacted protein (F-Cdc42-H, 29 kDa), reacted but not labelled protein (F-Cdc42 (28 kDa)), and labelled protein (F-Cdc42-Farn (28.5 kDa)), in addition to Sortase (22 kDa, but with an apparent size of 30 kDa), cleaved C-terminal tags, and remaining farnesyl peptide (Farn) (Fig. 5.3b). First size exclusion chromatography (SEC) was used to separate reactants and products by size. Considering the protein sizes, SEC separates a mixture of the three Cdc42 species and Sortase enzyme (peak 1) from remaining farnesyl and cleaved 6His-tag peptides (peak 2) (Fig. 5.3b). Of the proteins in SEC peak 1, both Sortase and unreacted protein are 6His-tagged, and the reacted protein is only Flag-tagged. It can therefore further be purified through His affinity chromatography (His-AC). The SEC peak fraction was loaded repeatedly on a nickel column and the flow-through was collected (Fig. 5.3b).

All reaction and purification steps were analysed by SDS-Page and Western Blotting (anti-His and anti-Flag) (Fig. 5.3c). SDS-Page showed that the reaction mixture pre-reaction (0 h) contained a protein band around the size of ~30 kDa, and that both the reaction mixture post-reaction (72 h), SEC peak, and His-AC flow-through, had an additional proteins species of ~27 kDa. (Unreacted protein has a size of 29 kDa, Cdc42 with a cleaved-off 6His-tag is 28 kDa, and protein reacted with farnesyl peptide is 28.5 kDa.) The change in electromobility shift after the reaction was a greater than expected. This could be due to altered electromobility properties of farnesylated protein. Western Blotting showed that the ~30 kDa protein species has a 6His- and a Flag-tag, confirming that it is unreacted protein (F-Cdc42-H). The 27 kDa species only has a Flag-tag, indicating that it is reacted protein (F-Cdc42 (28 kDa) or F-Cdc42-Farn (28.5 kDa)). The 30 kDa species of the His-AC flow-through shows almost no signal in the anti-His Blot, even though in the SEC lane it does, and the two bands have the same intensity on SDS-Page and in the anti-Flag Blot. This could indicate that the 30 kDa species after SEC is in fact made out of two species that show the same electromobility shift behaviour. It is possible that these are unreacted protein (H-Cdc42-F) and reacted but not ligated protein (H-Cdc42), and that the 27 kDa band is reacted protein that got ligated to farnesyl (H-Cdc42-Farn) which runs at a lower than expected size due to its hydrophobic tail.

After all clean-up steps, we obtained 0.6-6 nmol of labelled protein, which translates to a labelling efficiency of 1-10%. We prepared a sample for mass-spectroscopy, but the sample amount was below the amount needed (data not shown). We are currently investigating the use of MALDI-TOF mass-spectroscopy, which requires significantly smaller sample amounts, for analysis. A fraction of the sample was used to perform assays to assess the properties of the labelling product.

To obtain a fluorescent version of farnesylated Cdc42, we performed a labelling reaction of F-Cdc42-mNeon-H with farnesyl peptide, and used the clean-up steps described (SEC followed by His-AC, Appendix 5.4.3 Fig. 5.9).

Taken together, a Sortase-mediated reaction can be used to attach a farnesyl-group to bacterial expressed Cdc42 in a straightforward fashion. The reaction works robustly and can also be em-

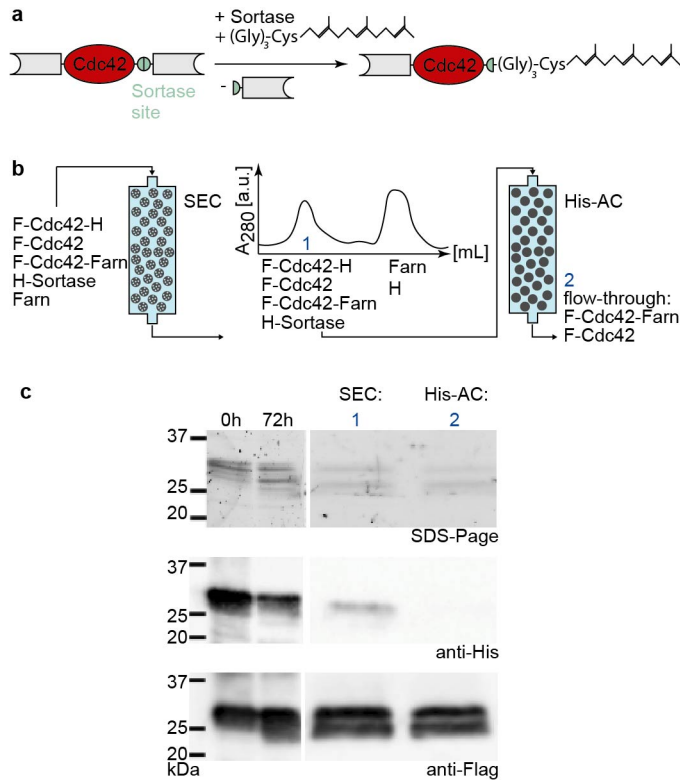


Figure 5.3. Sortase-mediated labelling of Cdc42 and Bem1 with Alexa488- and farnesyl-peptide. (a) Schematic illustration of the Sortase-mediated labelling reaction of double-tagged Cdc42 with farnesyl peptide. (b) Clean-up procedure for the labelling reaction of Cdc42 (F-Cdc42-H) with farnesyl-peptide (Farn): after an incubation of 72 h size exclusion chromatography (SEC) is used to separate unreacted farnesyl peptide (Farn) and cleaved purification tags (H) from proteins (1), which get loaded onto a His affinity chromatography (His-AC) column. Labelled protein (F-Cdc42-Farn) and reacted but unlabelled protein (F-Cdc42) do not bind to the column due to the absence of a 6His-tag (2). (c) SDS-Page and Western Blots of the reaction mixture pre-reaction (0 h), post-reaction (72 h), of the SEC peak (1) and His-AC flow-through (2).

ployed for fluorophore-protein fusions. The final product can be separated from other reaction mixture components through use of purification tags, making this approach a viable option for scientists from a non-biochemistry background.

Farnesylation of Cdc42 in *E. coli*

Most proteins, no matter which organisms they originate from, can be expressed and purified from *E. coli*. This bacteria species is easy to manipulate, low in maintenance, grows fast, and lyses under relatively mild conditions. Proteins expressed in a foreign host are also less likely to bind to, and co-purify, one of their natural binding partners. Despite these advantages, the use of bacterial expression systems is in general limited to post-translationally unmodified proteins, as the *E. coli* machinery lacks the enzymes responsible for these modifications. However, attempts have been made to introduce such enzymes into the bacterium (*Sugase et al. (2008)*). Farnesylation of the human Guanylate-binding protein GBP1 was achieved through co-expression of the α and β subunit of the human FTase (FTase- α , FTase- β) in *E. coli* (*Fres et al. (2010)*).

In yeast, farnesylation of Cdc42 is also carried out by an FTase (*Gomez et al. (1993)*). The substrate specificity of FTases is mainly determined by the sequence of the targets CAAX box, and the CAAX sequence preference of mammalian FTases has been found to be nearly identical to that of the yeast enzyme (*Caplin et al. (1994)*; *Reid et al. (2004)*). Following *Fres et al.*, we here also introduced FTase- α and FTase- β into *E. coli* (*Fres et al. (2010)*) to test if prenylated Cdc42 can be produced by a bacterial expression system (Fig. 5.1c). We decided to try out farnesylation first, as gernylgeranylation requires a larger machinery.

Cdc42's natural CA₁A₂X sequence in yeast is CAIL. The leucine at position four gives the protein a higher affinity for binding to the GGTase I compared to the FTase (*Caplin et al. (1994)*). In general, FTases prefer valine (V), isoleucine (I), or leucine (L) on the A₂ position, and methionine (M), serine (S), or glutamine (Q) on the last position of the CAAX box (*Caplin et al. (1994)*; *Houglund et al. (2010)*; *Reid et al. (2004)*). In order to optimise for high farnesylation, we designed four Cdc42 constructs with CAAX sequences that matched these criteria and also showed high kinetic values in *in vitro* farnesylation screens with peptide substrates (*Caplin et al. (1994)*; *Houglund et al. (2009, 2010)*); CTIS, CAIM, CALQ, CSIM.

To optimise the expression of all involved proteins, we carried out expression screens for (1) the FTase alone, (2) Cdc42 alone, and (3) Cdc42 in presence of the FTases, and analysed expression levels through anti-His Western Blotting³ (Fig. 5.4). Three expression conditions were chosen: 'f': a strong and fast expression at elevated temperatures, induced by a high amount of IPTG (3 h at 37°C with 1 mM IPTG). 's': a low and slow expression at lower temperatures, induced by a smaller amount of IPTG (18 h at 18°C with 0.2 mM IPTG). 'AI': a self-inducing combined approach (3 h at 37°C + 18 h at 18°C) (*Studier (2005)*).

We tested the expression levels of the FTase by using a 6His-tagged FTase- α subunit (H-FTase- α) and co-expressing it with untagged FTase- β (Fig. 5.4a). All conditions show a band at ~50 kDa in the anti-His Western Blot, corresponding to H-FTase- α (45 kDa). One or two lower bands are visible as well, likely representing products of degradation or of prematurely terminated translations of FTase- α . The expression of FTase- β can not be assessed (as FTase- β is not 6His-tagged), but we assume they are equal to that of FTase- α . These results indicate that the FTase expresses well in all conditions.

We tested how Cdc42 constructs with farnesylation-optimised CAAX sequences express. We used H-Cdc42:CAIA as a control for a construct with a CAAX sequence that does not favour farnesylation. In absence of FTase, all Cdc42 constructs (26 kDa) express well - intense bands at 25 kDa are visible in the anti-His Western Blot⁴ in all conditions (Fig. 5.4c). The expression levels seem mostly unaffected by the specific CAAX sequences.

Next, we investigated the effects of co-expressing Cdc42 and FTase. Less Cdc42-CTIS expresses in presence of FTase compared to absence of FTase (Fig. 5.4b). This is both true when the 6His-tagged and the untagged FTase versions are used. Of the tested expression conditions, 'f' seem to produce the most Cdc42 (both in absence and presence of FTase). The Blots of H-Cdc42:CTIS in presence of H-FTase- α /FTase- β show again two bands at 50 and 40 kDa, corresponding to H-FTase- α . Thus, co-expression of Cdc42:CTIS and FTase in *E. coli* is viable. We examined the effect of Cdc42's CAAX sequence on protein expression levels in cells with both Cdc42 and H-FTase-

³Initially we intended to monitor Cdc42 farnesylation using anti-farnesyl Western Blotting, but an eight condition screen (combination of two primary antibodies, two secondary antibodies, and two detection kit solutions that were successfully used to detect farnesyl previously (*Kennedy et al. (2019)*; *Li et al. (2020)*)) revealed that all conditions showed false-positive and false-negative bands for farnesyl (data not shown).

⁴The bands at 50 kDa correspond to Cdc42 dimers that form in denaturing conditions (see Chapter 3 and 4).

α /FTase- β (Fig. 5.4d) or FTase- α /FTase- β (Fig. 5.4e). The Blots show bands for Cdc42 and for H-FTase- α (Fig. 5.4d), illustrating that co-expression of H-FTase- α /FTase- β and all Cdc42 constructs is possible. The intensity of the H-FTase- α bands is not influenced by the CAAX sequence of Cdc42. Hence, Cdc42 does not influence the expression of FTase. We assume that this also applies for the untagged FTase and Cdc42. However, the distinct CAAX sequences seem to influence Cdc42 expression levels: In presence of tagged and untagged FTase- α /FTase- β , H-Cdc42:CAIA expresses best in condition 'f', and H-Cdc42:CSIM and H-Cdc42:CTIS express best in condition 's' and 'AI' (Fig. 5.4d)⁵.

As farnesylation levels are not known, it is difficult to predict if the differences in Cdc42 expression in presence of FTase correspond to differences in Cdc42 farnesylation levels. It is surprising that the CAAX sequences are only influencing Cdc42 expression levels in presence of FTases and that they do not influence the expression of FTase. FTase has a low affinity for the CAAX sequence CAIA. We thus expect H-Cdc42:CAIA to not, or only to a very limited extent, get farnesylated. In presence of FTase, a very small (Fig. 5.4e, condition 'AI') or a medium amount (Fig. 5.4d, condition 'AI') of H-Cdc42:CAIA expresses and more of H-Cdc42:CTIS expresses. If there is a correlation between expression levels and farnesylation, we therefore would assume that high expression levels mean high farnesylation (otherwise we would expect H-Cdc42:CAIA to express way stronger than all other Cdc42 constructs).

We expressed H-Cdc42:CSIM (condition 's' and 'AI') and H-Cdc42:CTIS (condition 'AI'), as they exhibited a high expression level in 'AI' in presence of FTase (Fig. 5.4e), and purified Cdc42 using His-AC. The protein was dialysed and prepared for mass-spectroscopy (see materials and methods). Of all purified H-Cdc42:CSIM (condition 's' and 'AI'), less than 0.1% was farnesylated. The sample of H-Cdc42:CTIS (condition 'AI') precipitated during dialysis. In the soluble fraction less than 0.1%, and in protein in the pellet 5% was farnesylated (Appendix 5.4.5 Fig. 5.11), yielding in total less than 1% farnesylated protein. It illustrates that the CAAX sequence indeed influences farnesylation, but that the Cdc42 expression levels might not that strongly correlate with farnesylation levels.

We showed that in principle *E. coli* can be engineered to produce prenylated Cdc42, but that further optimisation is necessary to bring the yield to a worthwhile level. So-far we only purified and analysed the soluble protein fraction. If farnesylation is occurring, most farnesylated Cdc42 might as well bind to membranes and be in the membrane fraction after lysis. For further research we will be investigating if and how much Cdc42 is in the membrane fraction and if this Cdc42 is farnesylated. What other optimisation is possible? We already altered Cdc42's CAAX sequence to make it more farnesylation prone. Directly upstream of the CAAX box is the polybasic region (PBR), which consists of five mostly basic amino acids (AAs). The PBR is a common feature of prenylated GTPases and affects the FTase's affinity for the protein (*Hicks et al. (2005); Williams (2003)*). Even though the PBR is a common feature, its sequence varies amongst GTPases. For example, yeast Cdc42 has the PBR sequence KKS₂KK and that of human Cdc42 is KKS₂RR. Here we integrated human FTase in *E. coli* to farnesylate yeast Cdc42. The CAAX sequence preferences of yeast FTase have been found to be nearly identical to the preferences of the mammalian enzyme (*Caplin et al. (1994); Reid et al. (2004)*), suggesting that the protein origin is not that important. The human and yeast PBR are also quite similar. However, single mutations in the PBR have been

⁵The different expression conditions can not be directly compared to each other, as the images are from distinct Western Blots. To compare the expression levels of the three conditions, see Fig. 5.4b. Here three conditions are shown in the same blot (for H-Cdc42:CTIS).

shown to have the capacity to significantly influence protein behaviour (*Zhang et al. (1999)*). To test if this is the case for FTase's affinity for yeast Cdc42, we are generating a Cdc42 version with the PBR of human Cdc42 (KKSRR). Another reason for the low farnesylation yield could be that the CAAX box is not that accessible to the FTase. We are therefore also generating Cdc42 versions where a short linker is placed either upstream of the PBR or in-between PBR and CAAX box, or where the C-terminal region of Cdc42 (PBR and CAAX box) is replaced by the C-terminal region of the GTPase GBP1. The latter approach alters Cdc42 the most, but GBP1 has been successfully and reproducibly been farnesylated in *E. coli* (*Fres et al. (2010)*, work (in preparation) by A. Jacobi group (TU Delft)). It thus might give most insight into whether the C-terminal region of Cdc42 is hindering farnesylation and if farnesylation of Cdc42 in *E. coli* is viable.

Cdc42 with BC domains

The farnesyl or geranylgeranyl tail in Cdc42 is mainly responsible for anchoring the protein to the membrane (*Peurois et al. (2018)*). If membrane-binding is the main objective of adding a post-translational modification to the protein, any other membrane-binding modification may also be sufficient. Earlier work in fission yeast by Bendezu *et al.* showed that cells in which prenylated Cdc42 got replaced with a Cdc42 allele with a prenylation independent membrane binding mechanism (Cdc42 with a transmembrane domain from the protein Psy1, or Cdc42 with an amphipathic helix from the protein Rit, Fig. 5.1d) polarised and showed viability (*Bendezú et al. (2015)*). We considered testing if such constructs are viable alternatives for prenylated Cdc42 for *in vitro* experiments, but disregarded them, as proteins with transmembrane domains are typically difficult to purify, and purified Cdc42 with the amphipathic helix had previously shown folding issues (data (in preparation) by P. Schwille group (MPI Martinsried)).

Recently, Meca *et al.* introduced another membrane-binding Cdc42 construct: here, the membrane-binding property originates from the so-called basic cluster (BC) region of the yeast protein Bem1 (*Meca et al. (2019)*). The BCs are a 23 to 74 AAs long unstructured region of mostly positively charged AAs, that are responsible for anchoring Bem1 to negatively charged membranes *in vitro*. It was shown that cells containing a fusion of Cdc42 with the first part of the BC region (26 AA) are viable and polarise, suggesting that the membrane binding capability of the BC region is sufficient to mimic those of the prenyl group.

Adding the BCs as membrane binding domain, rather than adding a transmembrane domain, might also be advantageous in another way: The BCs are mainly positively charged, thereby resembling the PBR (that is also associated with membrane-binding (*Johnson et al. (2012)*)). Thereby the C-terminal addition of BCs to Cdc42 may simply extend its positively charged C-terminal region without introducing other properties to it (as an amphipathic helix might do).

We designed a Cdc42 construct similar to Meca *et al.* (*Meca et al. (2019)*), where two out of three BC regions (51 AA) got inserted into the protein's C-terminus in between the PBR and the CAAX box (Fig. 5.1d). The protein expressed in similar yield as other Cdc42 constructs in *E. coli* and could be purified in a one-step His affinity chromatography. We also expressed a fluorescent version, 'Cdc42-mNeon-BC' (Appendix 5.4.4 Fig. 5.10).

5.2.2. Properties of the protein constructs

We tested three approaches for producing a membrane-binding Cdc42: (1) Sortase-mediated *in vitro* farnesylation of Cdc42, (2) farnesylation of Cdc42 in *E. coli* (*Fres et al. (2010)*), and (3) Cdc42 with BC domains (*Meca et al. (2019)*).

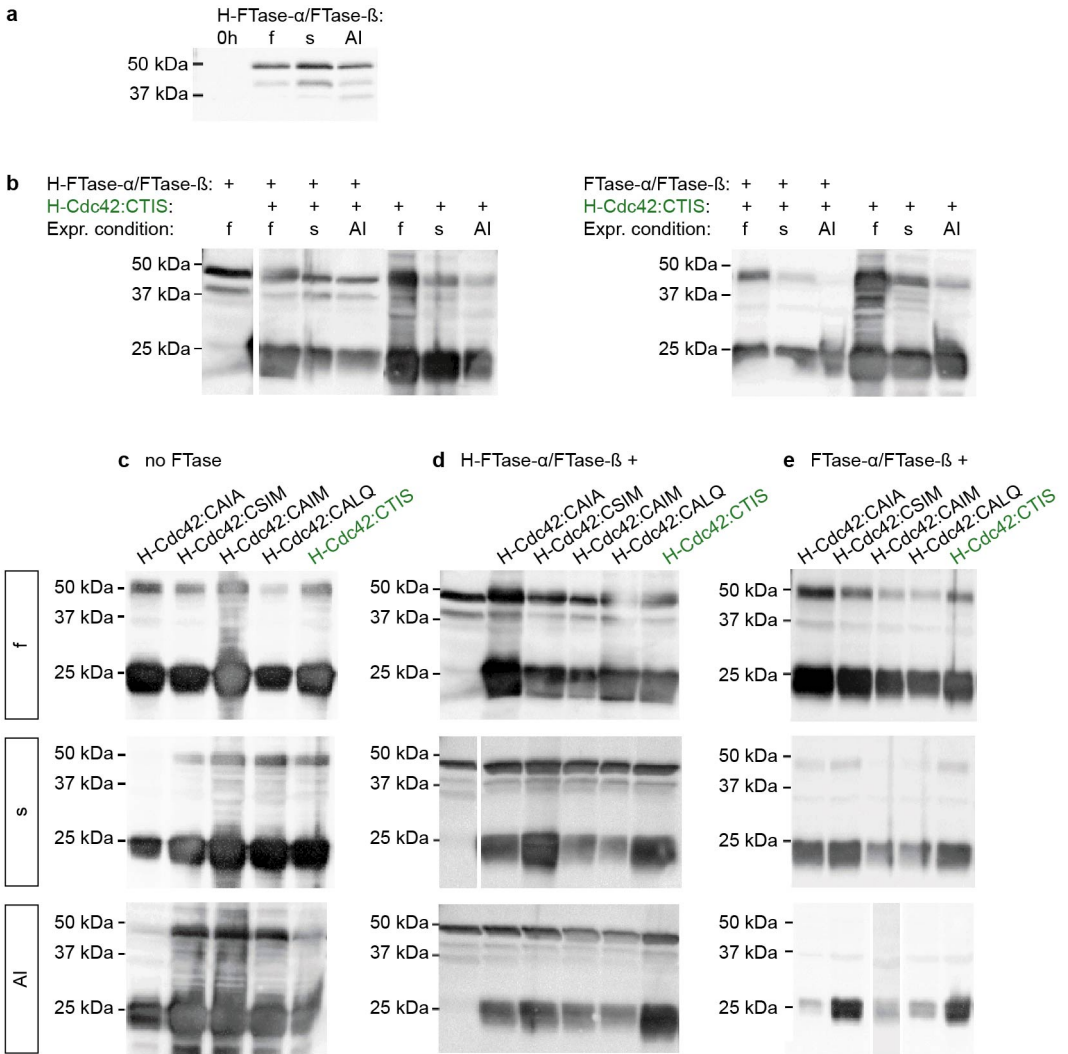


Figure 5.4. Farnesylation of Cdc42 in *E. coli*. Expression screens (condition 'f', 's', and 'AI'), monitored by anti-His Western Blotting, of (a) H-FTase- α in presence of untagged FTase- β , (b) H-Cdc42:CTIS in presence and absence of H-FTase- α /FTase- β (left) or FTase- α /FTase- β (right), (c) Cdc42 constructs with different CAAX sequences, (d) Cdc42 constructs with different CAAX sequences in presence of H-FTase- α /FTase- β , and (e) Cdc42 constructs with different CAAX sequences in presence of FTase- α /FTase- β .

Approach (2) lead to so little farnesylated Cdc42 that we could not further explore its properties. Approach (1) resulted in a small amount of potentially farnesylated protein, and (3) lead to the biggest amount of protein. We hence used proteins obtained from (1) and (3) to conduct experiments that assess the protein's properties: Cdc42's GTPase activity, interaction with the GEF proteins Cdc24, and, most importantly, its ability to bind to membranes.

Cdc42 GTPase activity and interaction with GEF Cdc24

Cdc42 is a GTPase and can therefore hydrolyse GTP. To test if the proteins are functional, we performed GTPase assays using the Promega GTPase Glo™ assay. Here serial dilutions of Cdc42 were incubated with GTP for a certain time, after which the reactions were stopped and the amount of remaining GTP was measured (see materials and methods). Thus, how much GTP got hydrolysed by Cdc42 proteins in a certain amount of time was measured. To quantitatively compare the GTPase activity of Cdc42 obtained from the different approaches, we determined GTP hydrolysis cycling rates k . These rates encompass the entire GTPase cycle, which can be described in three steps (Fig. 5.5a): (1) Cdc42 binds to a free GTP. (2) GTP gets hydrolysed by Cdc42. (3) Cdc42 releases GDP.

If one construct shows decreased rates k it would indicate that at least one of these steps is happening at a slower speed - potentially indicating that the membrane-binding modification is interfering with the GTPase functionality of Cdc42.

Previous measurements had shown that in the experiment the amount of remaining GTP declines exponentially with time (see Chapter 3, 4). Thus, the GTP hydrolysis cycling rates of Cdc42 can be determined by using an exponential fit

$$\begin{aligned} [\text{GTP}]_t &= [\text{GTP}]_{t_0} \exp(-K[\text{Cdc42}]t) \\ &\text{with } [\text{GTP}]_{t_0} = 100\%, \\ &\text{and } K = k_1'[\text{Cdc42}] + k_2'[\text{Cdc42}]^2 \end{aligned} \quad (5.1)$$

where k_1 describes the GTP hydrolysis cycling rate of a single Cdc42 molecule and k_2 includes any effects due to crowding, cooperativity, and Cdc42 dimerisation⁶.

We further assessed the Cdc42-Cdc24 interaction. Cdc24 is a GEF, meaning it boosts the release of GDP from Cdc42 (GTPase cycle step (3), Fig. 5.5a) and thereby increases the cycling speed of the GTPase cycle. Cdc42:Cdc24 mixtures, as well as samples containing only Cdc42, were incubated with GTP and subsequent the amount of remaining GTP was measured.

We had observed that rates for Cdc42 can vary slightly between assays. Possible reasons for this include small concentration differences introduced through pipetting of small volumes (as are required for this assay), temperature and shaker speed fluctuations during the incubation, and/or intrinsic changes in the Cdc42 activity due to other external conditions. To account for this variance, we introduced the parameter c_{corr} that maps all factors that lead to variations between assays onto the Cdc42 concentration. The assay data, including samples containing only Cdc42 and Cdc42 - Cdc24 mixtures, was fitted with Eq. 5.1 using

$$K = k_1 c_{corr} [\text{Cdc42}] + k_2 (c_{corr} [\text{Cdc42}])^2 + k_3 c_{corr} [\text{Cdc42}][\text{Cdc24}]^2 \quad (5.2)$$

to determine c_{corr} and k_3 (using k_1 and k_2 values determined from Cdc42 serial dilutions earlier (Eq. 5.1)).

⁶For a more in-depth description of the fitting model, see Chapter 4.

We determined the rates k_1 , k_2 , and k_3 and correction factor c_{corr} for Cdc42 with BCs (S-Cdc42-BC-H) and compared them to the 'unmodified' Cdc42 construct (S-Cdc42-H) (Fig. 5.5b). The GTP hydrolysis cycling rates k_1 and k_2 for both constructs are very similar to each other and the correction factors are close to one, showing that the GTPase activities of the constructs are similar and that the protein activity did not vary a lot between GTPase assays. The Cdc42-Cdc24 interaction rate k_3 of S-Cdc42-BC-H seems a bit higher, but still within error, of that of S-Cdc42-H. This highlights that the BCs indeed do not interfere with the GTPase functionality and GEF interaction of Cdc42.

We also assessed the GTPase properties of F-Cdc42-Farn (the product of the Sortase-mediated reaction) in comparison to F-Cdc42-H (the educt of that reaction). The concentration of F-Cdc42-Farn was estimated to be 30-300 nM. Because of the low concentration, and because 95% of the reaction product was used for the (unsuccessful) mass-spectroscopy analysis, we could not determine the rates as done for Cdc42 with BC domains. Instead, a GTPase assay with 10 nM and 100 nM F-Cdc42-H, and 10-100 nM F-Cdc42-Farn, both with and without Cdc24, and an incubation time of 15 h was done (Fig. 5.5c). Due to the low concentrations, no GTP hydrolysis could be measured in absence of Cdc24 (data not shown). In presence of Cdc24, 100 nM F-Cdc42-H hydrolysed 35% of the total GTP and 10 nM hydrolysed 25%. F-Cdc42-H hydrolysed 35% of the total GTP. This suggests that the F-Cdc42-Farn concentration in the assay is closer to 100 than to 10 nM, that it is a functional GTPase and that it interacts with Cdc24. It seems that addition of the farnesyl group to Cdc42 (through the Sortase-mediated reaction) did not alter its properties significantly. More precise measurements using higher concentrations would be needed to confirm this indication. Previously we had observed that the presence of any protein can lead to a decrease in remaining GTP concentration (up to about -5% remaining GTP in 1.5 h), simulating a GTPase activity that is not real. To ensure that the decline in remaining GTP was indeed because of Cdc42's GTPase activity, we added a control sample containing only Cdc24 (Fig. 5.5c). Cdc24 alone, even though it is not a GTPase, lead to 20% hydrolysed GTP. This value is higher than previously observed ones, but within reason considering the longer incubation time used in this compared to other GTPase assays (15 h vs. 1-1.5 h). In presence of Cdc42, a significantly higher amount of GTP got hydrolysed, implying that claims from this data are genuine.

Taken together, this data suggests that the BC domain and the farnesyl group do not alter Cdc42's GTPase properties and interaction with the GEF Cdc24.

Membrane binding capability of Cdc42 constructs

To test how strongly the Cdc42 constructs can bind to membranes, we conducted fluorescence microscopy experiments using Cdc42 versions where the fluorescent protein mNeogreen is appended to a solvent-exposed loop of Cdc42 (*Bendezú et al. (2015)*). The binding between Cdc42 and a supported lipid bilayer (SLB), mimicing the composition of the yeast plasma membrane (75% phosphatidylcholine, 20% phosphatidylserine, 5% phosphatidylinositol 4,5-bisphosphate (*Meca et al. (2019)*)) was determined using total internal reflection fluorescence microscopy and fluorescence recovery after photobleaching (FRAP): an area of the SLB got bleached and the recovery of fluorescent signal of that area got measured (Fig. 5.6). Recovery occurs from the sides of the bleached patch due to membrane-diffusion and from the centre due to binding of previously unbound fluorescent Cdc42 molecules. These can only bind if the Cdc42 molecules from the bleached area have unbound and "made space" on the membrane for new molecules to bind. Thus, the longer the recovery takes, the longer the bleached Cdc42 molecules were bound to the

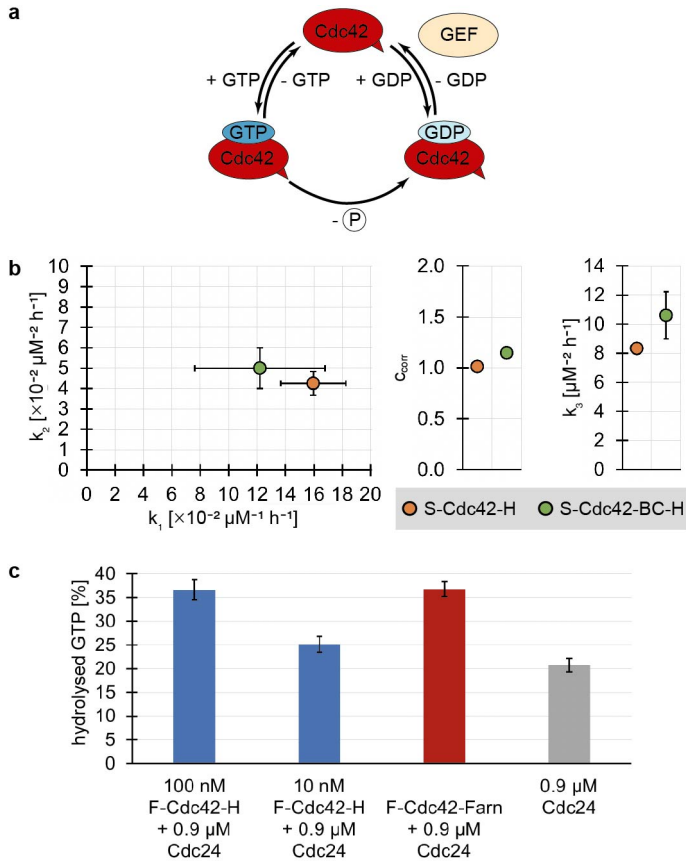


Figure 5.5. GTPase activity of Cdc42 constructs. (a) Schematic illustration of the GTPase cycle. (b) GTP hydrolysis cycling rates (k_1 , k_2), assay variability correction factor C_{corr} , and Cdc42-Cdc24 interaction rate (k_3) of S-Cdc42-H and S-Cdc42-BC-H. (c) GTPase activity of F-Cdc42-H and F-Cdc42-Farn. Amount of hydrolysed GTP after an incubation of 15.25 h, using 5 μM GTP and stated protein concentrations.

membrane. To quantify this, we determined the recovery halftime, representing the amount of time it takes for the membrane to recover to its half-maximal value (see materials and methods).

We first determined the recovery rate of the SLB (using an SLB was supplemented with fluorescently modified lipids), to ensure the lipid is fluid (Fig. 5.6). We next assessed FRAP of the mNeonGreen signal from protein samples on a non-fluorescent SLB. The signal of the Cdc42-mNeonGreen samples was significantly weaker than that of the SLB, and the extend of bleaching as well (Fig. 5.6), suggesting that the protein did not strongly interact with the membrane. We determined the recovery halftimes from these FRAP curves. As the the bleaching was not very strong, and the recovery did not follow exactly an exponential, the recovery halftimes can only be seen as a rough indication of how strongly the proteins bound to the membrane. The recovery of the protein signal after bleaching was in all cases faster than that of the SLB, suggesting that the recovery is not only due to membrane-diffusion but also due to exchange of bleached and not-bleached Cdc42 molecules. Cdc42 without added membrane-binding moieties (F-Cdc42-mNeon-H) recovered very fast (1.5 s, $n=1$), Cdc42 with BCs (S-Cdc42-mNeon-BC-H) only minimally

slower (4.9 ± 0.6 s, $n=4$), and Cdc42 with a farnesyl group (F-Cdc42-mNeon-Farn) was the slowest (14 s, $n=1$, Fig. 5.6). Addition of the latter to a previously recoverable membrane lead also to non-recoverable membrane (data not shown, $n=3$). This preliminary data suggests that only the farnesyl moieties can bind Cdc42 to the membrane, and that the BC domains do not, or only very weakly, facilitate membrane binding for Cdc42. The interaction between the farnesyl group and membrane could also explain why most membranes (3 out of 4) were non-recoverable. Insertion of many Cdc42-bound farnesyl groups into a membrane could reduce its fluidity, eliminating recovery from membrane-diffusion. If bleached membrane-bound Cdc42 molecules can not release from the membrane, which could be reinforced through a changes in the membrane structure, no fluorescent Cdc42 molecules can bind, and the fluorescent signal from this membrane patch does not recover.

Further, the behaviour of F-Cdc42-mNeon-Farn is a strong indication that the Sortase-mediated labelling of F-Cdc42-H/ F-Cdc42-mNeon-H with farnesyl peptide worked. Analysis by Western Blotting had revealed that the C-terminal 6His-tag of (most) Cdc42 had been cleaved during the reaction (Fig. 5.3c and Appendix 5.4.3 Fig. 5.9), leaving two possibilities: the product of the labelling reaction is (1) the cleavage product (F-Cdc42/ F-Cdc42-mNeon) or (2) the labelled protein (F-Cdc42-Farn/ F-Cdc42-mNeon-Farn). The cleavage product is expected to behave similarly to Cdc42, as it has no membrane-binding domain. The only difference between both would be the absence of the 6His-tag in case of the cleavage product. The absence of this tag should not significantly enhance membrane binding, but rather reduce it. We used a lipid composition that lead to a slightly negatively charged membrane. The 6His-tag is positively charged, meaning its presence is expected to increase membrane binding. The cleavage product, which does not contain a 6His-tag, should therefore have an even smaller recovery halftime than unmodified Cdc42. We observed a 10x longer recovery halftime for the reaction product of the Sortase-mediated reaction, which would imply that the reaction product is indeed the labelled protein F-Cdc42-mNeon-Farn.

In conclusion, our data suggests that only Cdc42 with a farnesyl group, but not with BC domains, binds to membranes. More experiments are still required to better quantify these findings. We are therefore currently conducting additional quartz crystal microbalance with dissipation monitoring experiments.

5.3. Discussion

We set out to make the use of membrane-binding Cdc42 for *in vitro* experiments more widely accessible by applying and comparing three complementary approaches for producing it; (1) Sortase-mediated *in vitro* farnesylation of Cdc42, (2) farnesylation of Cdc42 in *E. coli*, and (3) Cdc42 with BC domains (*Meca et al. (2019)*).

All three methods yielded protein, and showed different strengths and drawbacks:

(1) Sortase-mediated labelling of Cdc42 with farnesyl peptide is a robust reaction, but has a rather low labelling efficiency ($\approx 10\%$). The reaction product could easily be separated from the other reaction components using a purification-tag based strategy. The labelling did not interfere with the protein's GTPase activity and GEF interaction. Although we still need to confirm that during the reaction indeed a farnesyl group got appended, we know from Western Blotting that the C-terminal tag got cleaved. Most importantly, preliminary data suggests that this protein binds to membranes.

(2) *E. coli*-based farnesylation lead to a very small amount of farnesylated protein ($<1\%$). Even

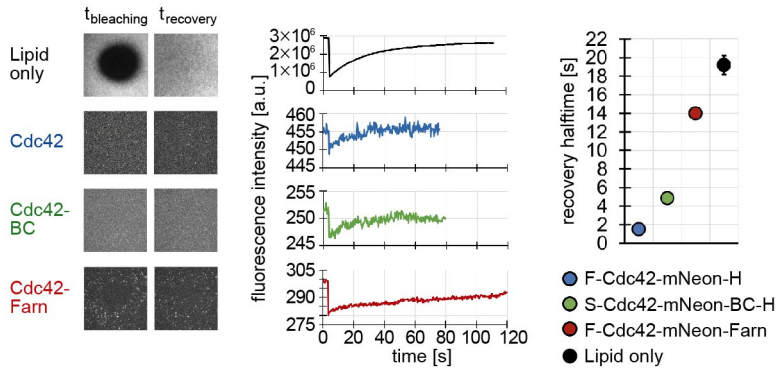


Figure 5.6. Membrane binding properties of Cdc42 constructs: Fluorescent images, FRAP curves, and recover half-time of a fluorescent SLB and of fluorescent Cdc42 on a SLB (F-Cdc42-mNeon-H, S-Cdc42-mNeon-BC-H, F-Cdc42-mNeon-Farn). The membrane composition was chosen to resemble that of the yeast plasma membrane: 75% phosphatidylcholine, 20% phosphatidylserine, 5% phosphatidylinositol 4,5-bisphosphate (*Meca et al. (2019)*). Number of experiments: n=1 (H-Cdc42-F), n=4 (S-Cdc42-BC-H), n=1 for 14 s and n=3 for non-recoverable (F-Cdc42-Farn), n=5 (lipid only).

though the protein could easily be purified in a single-step reaction, separation of farnesylated and unmodified Cdc42 might be a challenge, as not all HIC columns can separate the two protein species (*Fres et al. (2010)*). We also encountered this issue of HIC when trying to separate reaction products of the Sortase-mediated farnesylation reaction: The reaction products eluted in two strongly overlapping peaks, with in turn overlapped with the broad peak unmodified Cdc42 displayed (Appendix 5.4.2 Fig. 5.8). In the Sortase-mediated reaction this problem can be circumvented by switching to a purification-tag based strategy. This is not possible for the *E. coli*-based farnesylation approach. It therefore might be challenging to isolate the farnesylated fraction in this method. A way to sidestep this problem would be to drastically increase the yield (80-95%) so that only a tiny fraction of purified Cdc42 is not farnesylated. As this fraction binds only very weakly to membranes, it is possible to use the entire batch (of 80-95% farnesylated Cdc42, 20-5% not farnesylated Cdc42) for studies involving Cdc42 membrane binding. We are currently exploring further optimisation steps to increase the yield.

(3) The easiest approach was to add BC domains to the C-terminus of Cdc42. Here Cdc42 can be purified in a high yield in a single AC purification step. BC domains do not alter Cdc42's GTPase activity nor interaction with the GEF Cdc24, but seem to bind only extremely weakly to membranes.

We set out to find easier and more reliable approaches for producing membrane-binding Cdc42. Off the three methods tested, the Sortase-mediated reaction seems to be the best candidate; it worked robustly and produced labelled protein that could easily be purified and bound strongly to membranes. The yield of 10% was not very high, but a reaction condition with a higher yield could be found through additional screens. The main challenge is to find a fast analysis method determining the amount of farnesylated protein that does not require purification steps. We explored several anti-farnesyl Western Blot conditions, but found no good match. Thus, establishing a working anti-farnesyl Western Blot protocol might be the biggest factor that can facilitate improved Sortase-mediated farnesylation. The Sortase-mediated approach has biggest potential to be expanded to the other form of Cdc42 prenylation: geranyl geranylation. Sortase was

shown to accept a wide range of peptide probes (*Popp and Ploegh (2011)*), making it likely that the same reaction conditions and yields of Sortase-mediated farnesylation can be applied to a Sortase-mediated geranyl geranylation reaction. The proposed clean-up steps do not involve any specific properties of the labelling group, and are therefore applicable to any Sortase-mediated reaction. The Sortase-based approach can also be used to easily engineer the Cdc42 membrane binding strength by appending various lipid chains to the protein. In contrast to the Sortase-mediated approach, *E. coli*-based farnesylation still faces the challenge of a unacceptably low yield (<1%). If the yield could drastically be improved, for example through the proposed C-terminal modifications, this method would be a highly competitive way for Cdc42 farnesylation; both protein expression and farnesylation are done in one step and only one protein purification step is needed. However, it could still not be as easily expanded to other prenylation forms, as *E. coli* would need to be engineered to include the required machinery. Lastly, the approach of Cdc42 with BC domains is by far the easiest and gives protein in the highest yield. However, the protein is not very useful for Cdc42 membrane studies, as the membrane binding behaviour of Cdc42 with BC domains is way more similar to Cdc42 without any membrane binding domains than it is to farnesylated Cdc42. It could be used if explicitly a very weak binding is desired.

We described three orthogonal methods of creating Cdc42 with membrane binding capabilities. Both the Sortase- and BC domain-based approach involve C-terminal modifications on Cdc42. (If mentioned C-terminal changes increase the yield in the *E. coli*-based approach, then this applies to all three methods.) Cdc42's 'natural' C-terminal region includes the PBR directly followed by the CAAX box, to which the prenyl group is appended. For Sortase-mediated farnesylation a Sortase recognition motif was placed directly after the CAAX box. To this motif the farnesyl peptide is ligated, spacing eight additional AAs between the farnesyl group and the C-terminal AA that is naturally farnesylated. Cdc42 with BC domains has 51 AA long unstructured region placed between the PBR and CAAX box. These linker or unstructured regions do not influence the membrane binding or protein's GTPase activity itself ⁷, but could potentially separate the two functions. Cdc42 has a GDP- and GTP-bound conformation. If the nucleotide state affects the position of the membrane binding group, the placement of a linker region (Sortase- and *E. coli*-based approach) or the replacement the farnesyl group with a large unstructured region (BC domains) could disrupt this connection. This could result in Cdc42 behaving in a way that is distinct from Cdc42 *in vivo*, placing a huge limitation on the usefulness of these approaches. One way to test if the introduced modifications affect Cdc42 behaviour would be to introduce similar modifications (e.g. a linker region between the protein CAAX box) to Cdc42 *in vivo* and to observe the effects on the cellular level or on the localisation of Cdc42. Strong defects would indicate that a necessary functional connection got broken.

⁷We base our conclusion that C-terminal modifications downstream of the PBR are not influencing Cdc42's GTPase activity on two observations: (1) Cdc42-BC showed a similar GTP hydrolysis cycling and Cdc42-Cdc24 interaction rates as Cdc42 without these domains. (2) Cdc42 with various C-terminal tags showed similar GTP hydrolysis cycling and Cdc42-Cdc24 interaction rates as a Cdc42 construct that did not have a C-terminal modification (see Chapter 3).

5.4. Appendix

5.4.1. Appendix: Effect of methanol on Sortase-mediated reactions

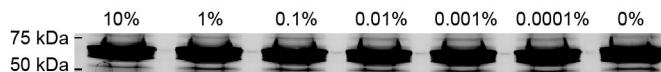


Figure 5.7. Sortase-mediated labelling of Bem1 with Alexa488 peptide. SDS-Page showing the fluorophore signal. Concentrations of up to 10% methanol do not affect the Sortase-mediated labelling Bem1 (H-Bem1-F, 75 kDa) with Alexa488 peptide.

5.4.2. Appendix: SEC and HIC as clean-up strategy for Sortase-mediated reaction products

Cdc42 with an N-terminal 6His-tag and C-terminal Flag-tag (H-Cdc42-F) was labelled with farnesyl peptide, using molar reaction ratios of Sortase : Cdc42 : farnesyl peptide of 2:100:2000 (Fig. 5.8a). During the labelling reaction the Sortase enzyme can cleave Cdc42's C-terminal tag and ligate farnesyl peptide to the protein. The final reaction mixture therefore contains three Cdc42 species (unreacted protein (H-Cdc42-F, 29 kDa), reacted but not labelled protein (H-Cdc42, 26 kDa), and labelled protein (H-Cdc42-Farn, 26.5 kDa), in addition to Sortase (22 kDa, but with an apparent size of 30 kDa), cleaved C-terminal tags, and remaining farnesyl peptide (Farn) (Fig. 5.8b).

As a first step, size exclusion chromatography (SEC) was used to separate reactants and products by size. Considering the proteins' sizes, SEC separates a mixture of the three Cdc42 species and Sortase enzyme (peak 1) from remaining peptide and cleaved 6His/Flag-tag peptides (peak 2) (Fig. 5.8b).

The final product was further purified using its hydrophobic properties: farnesyl is a very hydrophobic molecule, therefore farnesylated Cdc42 should bind way stronger to a hydrophobic material in comparison to unfarnesylated Cdc42 and Sortase. SEC peak 1 was loaded onto a hydrophobic interaction chromatography (HIC) column. After rounds of washing, the sample was eluted using a gradient elution. The elution profile showed two strongly overlapping peaks, indicating the presence of two distinct species (Fig. 5.8d). This is in partial agreement with findings by Fres *et al.* (Fres *et al.* (2010)), who observed that different Butyl Sepharose column variants were more or less able to separate farnesylated from unfarnesylated protein.

All reaction and purification steps were analysed by SDS-Page and Western Blotting (Fig. 5.8c,e). SDS-Page showed that the reaction mixture pre-reaction (0 h) contained proteins of ~29 and ~32 kDa, whereas the reaction mixture post-reaction (72 h) contained three proteins species (~ 27, 25, and 23 kDa) (Fig. 5.8c). Unlabelled protein has a size of 29 kDa and is observed to sometimes run in double bands, thus confirming the bands observed in the pre-reaction sample. Cdc42 with a cleaved-off Flag-tag is 26 kDa, and protein reacted with farnesyl peptide is 26.5 kDa. The latter two species would not be distinguishable on SDS-Page, except if one species runs at a different size than expected. Labelled Cdc42 has the highly hydrophobic farnesyl tail, which could influence its electromobility shift behaviour on SDS-Page. The observed reduced sizes in the post-reaction sample indicate that most protein underwent the labelling reaction, but that different products got formed, which also all seem to run at a slightly lower size than expected. After separation via SEC the main protein peak contained proteins of two sizes, a small fraction

of ~26 kDa and a at least 20× larger fraction of 23 kDa⁸. All fractions of the HIC elution showed one band at 23 kDa (Fig. 5.8e). The 26 kDa band matches the size of reacted and labelled protein (H-Cdc42 and H-Cdc42-Farn), the 23 kDa band does not match with of the size any expected protein species. Analysis via Western Blotting revealed that the 23 kDa protein species in both SEC and HIC fractions has a His-tag, whereas the ~26 kDa species has both a His- and a Flag-tag. Surprisingly, this observation was also true for the HIC fractions, where on SDS-Page only the lower 23 kDa band was visible. A combined blot (using both anti-His and anti-Flag primary antibodies) confirmed the presence of two bands in the HIC fractions (Fig. 5.8e). These findings suggest that both unreacted protein (H-Cdc42-F) and reacted proteins (H-Cdc42, H-Cdc42-Farn) are present throughout the SEC and HIC purification process, and that the ratio of unreacted:reacted protein is at least 1:20. These findings cannot distinguish between farnesylated Cdc42 and Cdc42 where solely the Flag-tag got cut off, and do not explain why suddenly unreacted protein runs at a lower than expected size on SDS-Page, or how a protein of a lower size can have both N- and C-terminal purification tags. To test if Cdc42 by itself can bind to the HIC column, we ran a HIC purification protocol using only a small amount of Cdc42. Cdc42 eluted in one broad peak (Fig. 5.8d), but ran at its expected size on SDS-Page (data not shown).

5

Taken together, these findings suggest that during the reaction the majority of purified protein reacted with Sortase, leading to two protein species of an apparent size of 26 and 23 kDa, with the majority being 23 kDa. Both can bind to a HIC column and but are distinct in their elution profile and in the presence/absence of a C-terminal Flag-tag. However, hydrophobicity seems to not be sufficient to separate labelled from unlabelled protein. The farnesylation of the 23 kDa species would further need to be confirmed by mass-spectroscopy. This analysis could not be performed due to a too low yield of final product.

⁸The estimation was done from integrated band intensities. As the signal of the 23 kDa band was slightly oversaturated, the real ratio is even higher.

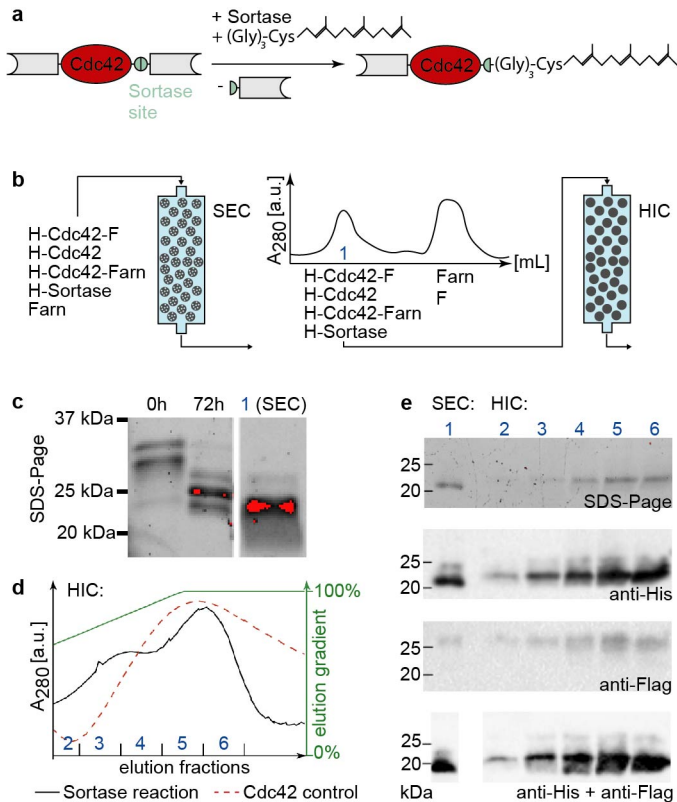


Figure 5.8. Sortase-mediated labelling of Cdc42 with farnesyl-peptide. (a) Schematic illustration of the Sortase-mediated labelling reaction of double-tagged Cdc42 with farnesyl peptide. (b) Clean-up procedure for the labelling reaction of Cdc42 (H-Cdc42-F) with farnesyl peptide (Farn): after an incubation of 72 h size exclusion chromatography (SEC) is used to separate unreacted farnesyl-peptide (Farn) and cleaved purification tags (F) from proteins (1), which get loaded onto a hydrophobic interaction chromatography (HIC) column. (c) SDS-Page of the reaction mixture pre-reaction (0 h) and post-reaction (72 h), and SEC peak (1). (d) The HIC elution profile of SEC peak 1 (black line, fractions 2-6), in comparison with the elution profile of a Cdc42 control (dashed red line). (e) SDS-Page, anti-His, anti-Flag, and a combined anti-His + anti-Flag Western Blot of the SEC peak (1) and HIC fractions (2-6).

5.4.3. Appendix: Sortase-mediated farnesylation of Cdc42-mNeonGreen

To obtain a fluorescent version of farnesylated Cdc42, we performed a labelling reaction of F-Cdc42-mNeon-H with farnesyl peptide. The reaction mixture was separated by SEC and His-AC and analysed by SDS-Page and Western blotting (Fig. 5.9). Surprisingly, the final product fraction (His-AC FT) still contained protein with a C-terminal 6His-tag. Given the decreased signal of the band after His-AC compared to the band after SEC in the anti-His Western blot, it is likely that still His-tagged protein makes only a small portion of the overall protein. It is possible that reacted (F-Cdc42-mNeon, F-Cdc42-mNeon-Farn) and unreacted protein (F-Cdc42-mNeon-H) formed oligomers, thereby sterically hindering unreacted protein from binding to the nickel column, as a similar behaviour was observed during the purification process of Cdc42-mNeonGreen.

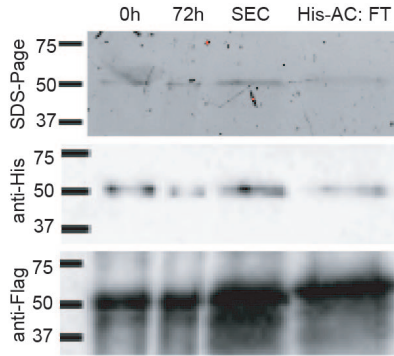


Figure 5.9. Sortase-mediated labelling of Cdc42-mNeon (F-Cdc42-mNeon-H) with farnesyl peptide: SDS-Page and Western Blots (anti-His, anti-Flag) of the reaction mixture pre-reaction (0 h) and post-reaction (72 h), after size exclusion chromatography (SEC), and the flow-through of His affinity chromatography (His-AC: FT).

5

5.4.4. Appendix: Cdc42-BC

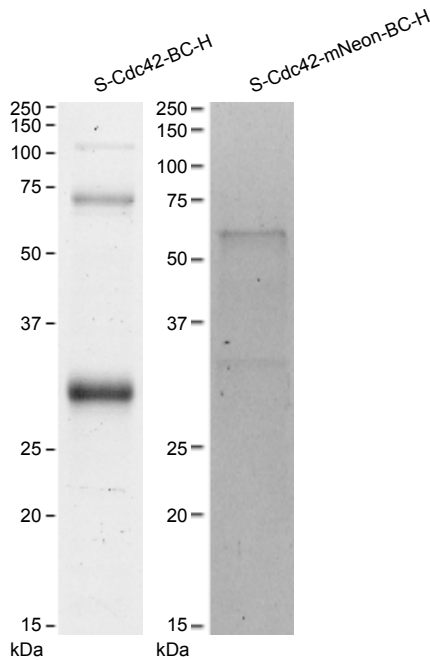


Figure 5.10. SDS-Page showing purified Cdc42-BC (33 kDa, left) and Cdc42-mNeon-BC (61 kDa, right). The higher bands in Cdc42-BC are likely dimers and trimers of the protein.

5.4.5. Appendix: Mass spectroscopy analysis of Cdc42 from the *E. coli*-based farnesylation approach

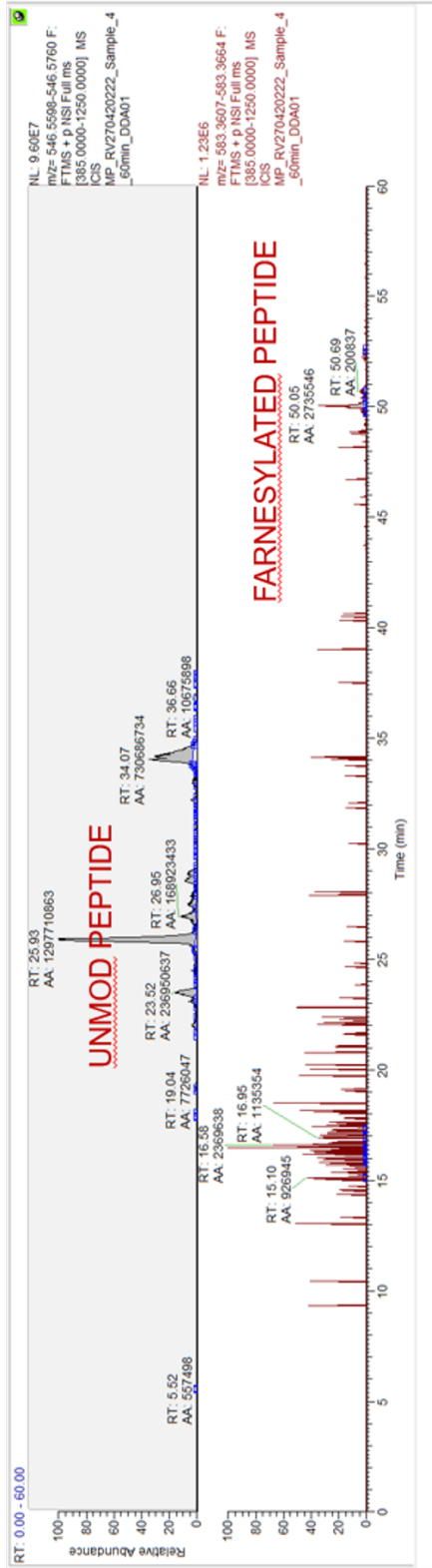


Figure 5.11. Mass spectrometry peaks of the pellet fraction of farnesylated H-Cdc42:CTIS (expressed with condition 'A').

Contributions and acknowledgements

R. van der Valk constructed the plasmids of protein constructs. Proteins were expressed and purified by S. Tschirpke and F. van Opstal. B. Spitzbarth (Rienk Eelkema group, TU Delft) synthesised farnesyl peptide. S. Tschirpke conducted Sortase labelling and clean-up experiments and GTPase assays, and analysed the data thereof. The modelling and fitting of the GTPase data was done by W. Daalman. F. van Opstal conducted expression tests and Western Blots, which were analysed by S. Tschirpke. Samples for mass-spectroscopy were prepared by R. van der Valk. S. Farooq did microscopy experiments and analysed the data thereof. Figure preparation and writing of this chapter was done by S. Tschirpke.

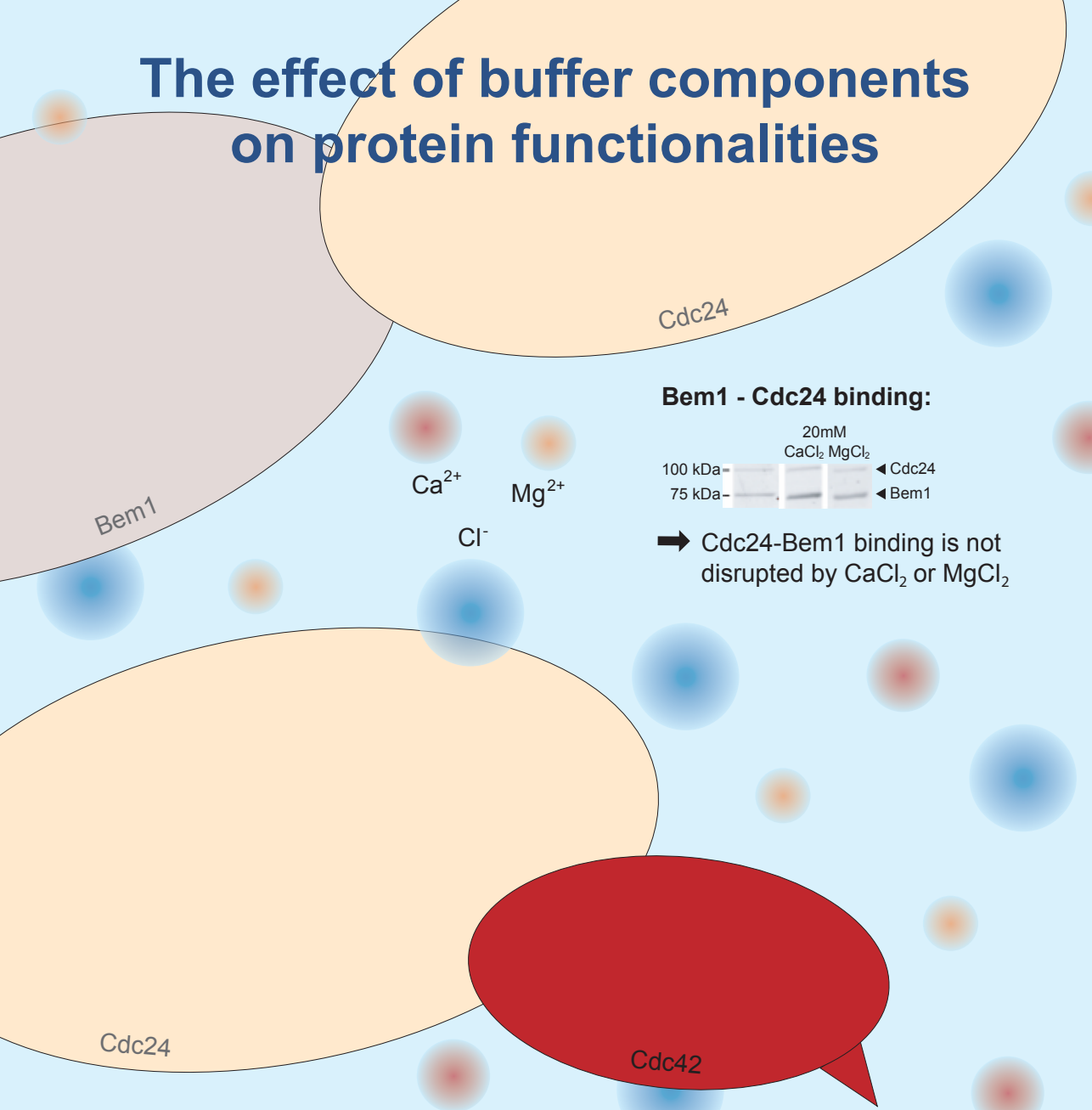
We thank M. Pabst for doing mass-spectroscopy with our samples and A. Jacobi, C. de Agrela Pinto, and T. Kuhm for their help with the *E. coli* based farnesylation system. We thank D. McCusker (University of Bordeaux) for the plasmid pDM272, A. Jacobi (TU Delft) for the plasmid pAJLD0063 and N. Dekker (TU Delft) for the plasmid pET28a-His-mcm10-Sortase-Flag.

6

Science is not about being right, it's about figuring out how things work.

— Lisa Feldman Barrett

The effect of buffer components on protein functionalities



Cdc24

Bem1

Cdc24

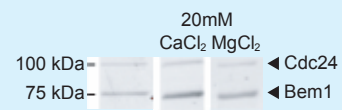
Cdc42

Ca²⁺

Mg²⁺

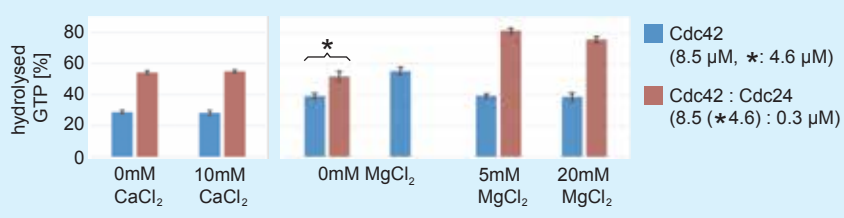
Cl⁻

Bem1 - Cdc24 binding:



➔ Cdc24-Bem1 binding is not disrupted by CaCl₂ or MgCl₂

Cdc42 GTPase activity:



- ➔ CaCl₂ does not affect the Cdc42 GTPase activity or Cdc24 activity
- ➔ MgCl₂ reduces the GTPase activity of Cdc42 but is required for full activity of Cdc24 (which boosts the GTPase activity of Cdc42)

The effect of buffer components on protein functionalities

Abstract In this thesis I show our efforts towards establishing a minimal system for Cdc42-based polarity establishment, consisting of three proteins: the small GTPase Cdc42, the GEF Cdc24, and the scaffold protein Bem1. To achieve this, (1) protein interactions need to be verified through biochemical assays, (2) proteins need to be fluorescently labelled, and (3) all proteins need to be combined to observe their dynamics using microscopy. These experiments need to be conducted in a buffer, which ideally would fulfill the requirements of all steps. Then time-consuming and potentially activity-altering dialysis steps can be omitted and data from biochemical and microscopy data can be compared quantitatively. It has been shown that some of these reactions require Mg^{2+} and Ca^{2+} , but also that the Cdc24-Bem1 interaction is inhibited by 2 mM $CaCl_2$ (Zheng *et al.* (1995)). To gain more knowledge about the effects of $MgCl_2$ and $CaCl_2$, we conducted experiments to test if and how much these ions influence Cdc42's GTPase activity, the Cdc42-Cdc24, and Bem1-Cdc24 interaction. We show, contrary to previous findings (Zheng *et al.* (1995)), that Ca^{2+} (up to 20 mM) does not disrupt the Bem1-Cdc24 interaction. Calcium also does not influence the GTPase activity of Cdc42. Mg^{2+} , on the other hand, reduces Cdc42's intrinsic GTPase activity, and is required for the GEF activity of Cdc24. From this data we conclude that a buffer with the composition 50 mM Tris-HCl (pH=7.5), 100 mM NaCl, 10 mM $MgCl_2$ will be suitable to conduct our *in vitro* experiments leading towards the reconstitution. This buffer can be supplemented with $CaCl_2$ to accommodate labelling reactions, and calcium would not need to be removed as it did not show inhibitory effects towards protein activities and interactions.

6

6.1. Introduction

Molecular biologists thrive to unravel the reactions and interactions of cellular components and to understand the broader mechanisms arising from these interactions. To gain such knowledge, cells can be manipulated and the effects of these manipulations on the whole cellular machinery can be observed (*in vivo* experiments), and specific components can be isolated and studied in detail outside the cellular environment (*in vitro* studies). In order for these *in vitro* studies to be meaningful, they need to keep the components in an environment that mimicks that of the cell/ the cytosol. The cytosol is filled with water molecules, proteins, DNA, RNA, lipids, other biological species, and ions (e.g. Na^+ , K^+ , Ca^{2+} , Mg^{2+} , Cu^{2+} , Zn^{2+} , and Cl^-), and has a pH of ~ 7.2 (Orij *et al.* (2009); Alberts *et al.* (2014)). The buffer needs to resemble at least partially these conditions, and needs to attain to the requirements of *all* involved components.

Common buffers in protein biochemistry are Tris or phosphate based, they buffer the pH between 7 and 8, and often contain mM amounts of salts with Na^+ , K^+ , and Cl^- . Other ions, such as Ca^{2+} , Mg^{2+} , Cu^{2+} , Zn^{2+} , are added when required, for example when they function as a co-factor of an enzyme (Alberts *et al.* (2014)).

We aim to establish a minimal system for Cdc42-based polarity establishment, consisting of three proteins: the small GTPase Cdc42, the GDP/GTP exchange factor (GEF) Cdc24, and the scaffold protein Bem1. All proteins are interacting with each other, Cdc42-Cdc24, Cdc42-Bem1, Cdc24-Bem1, and Cdc42 exhibits GTPase activity. In order to establish a minimal system, (1) these protein interactions need to be verified through biochemical assays, (2) Cdc24 and Bem1 need to be fluorescently labelled in a Sortase-mediated reaction, for which in a first step a small polyglycine peptide is linked to the fluorophore (maleimide reaction), and (3) all proteins need to be combined to observe their dynamics using microscopy. The proteins also contain an Enterokinase cleave site that allows to cleave their N-terminal purification tag. The ideal buffer fulfills the requirements of all of these reactions, as then time-consuming and potentially activity-altering intermediate dialysis steps can be omitted.

From literature it is known that the Cdc42-Cdc24 interaction requires Mg^{2+} (Zhang *et al.* (2000)), that the Cdc24-Bem1 interaction is inhibited by 2 mM $CaCl_2$ (Zheng *et al.* (1995)), that Sortase A requires $CaCl_2$ (Antos *et al.* (2017)), that the maleimide reaction is best performed at pH 7.2-7.5 (Nanda and Lorsch (2014); Liu *et al.* (2018)), and that Enterokinase requires $CaCl_2$ as well and can tolerate up to 100 mM NaCl (New England Biolabs (2022)). Further, only sub-mM amounts of $CaCl_2$ can be dissolved in phosphate buffers, excluding them as an option. All three proteins have been purified previously and were shown to be functional in a buffer of 20 mM Tris-HCl (pH=8.0), 150 mM NaCl, supplemented with 5-10 mM $MgCl_2$ (Rapali *et al.* (2017)).

6

Considering this, an ideal buffer can be made up from 50 mM Tris-HCl (pH=7.5), 100 mM NaCl, 5-10 mM $MgCl_2$, and can be supplemented with $CaCl_2$ to accommodate Sortase and Enterokinase activity. For assays requiring a Cdc24-Bem1 interaction, $CaCl_2$ would need to be removed, although it is unknown if amounts below 2 mM would still be inhibiting the interaction. To gain more knowledge about the effects of $MgCl_2$ and $CaCl_2$, we conducted experiments to test if and how much these salts influence Cdc42's GTPase activity, the Cdc42-Cdc24, and Bem1-Cdc24 interaction. For completeness, the effect on the Bem1-Cdc42 interaction should have been tested as well. This was not done as the Bem1-Cdc42 interaction was generally weak and not as robustly observable as the other interactions (see Chapter 3), and as no Mg^{2+} or Ca^{2+} -specific effects were reported previously.

We show, contrary to previous findings (Zheng *et al.* (1995)), that Ca^{2+} (up to 20 mM) does not disrupt the Bem1-Cdc24 interaction. Calcium also does not influence the GTPase activity of Cdc42. Mg^{2+} , on the other hand, reduces Cdc42's intrinsic GTPase activity (contradicting Zhang *et al.* (2000)), and is required for the GEF activity of Cdc24 (in agreement with Zhang *et al.* (2000)). From this data we conclude that a buffer with the composition 50 mM Tris-HCl (pH=7.5), 100 mM NaCl, 10 mM $MgCl_2$ will be suitable to conduct our *in vitro* experiments leading towards the reconstitution. This buffer can be supplemented with $CaCl_2$ to accommodate Sortase and Enterokinase activity, and according to our data and contrary to previous findings (Zheng *et al.* (1995)), calcium would not need to be removed as it did not show inhibitory effects towards protein activities and interactions.

Abbreviations:

GEF GDP/GTP exchange factor
PBR polybasic region

6.2. Results

6.2.1. Cdc42 GTPase activity and Cdc42-Cdc24 interaction

We conducted GTPase assays to study the effect of Ca^{2+} and Mg^{2+} on the GTPase activity of Cdc42 and the Cdc42-Cdc24 interaction: Proteins were incubated with GTP at 30°C for 90 min, after which the reaction was stopped and the amount of remaining GTP was measured (see materials and methods). Cdc42 has an intrinsic GTPase activity that gets boosted through its interaction with Cdc24, which helps to speed up the release of the hydrolysis product GDP.

Measurements showed that Ca^{2+} , up to a concentration of 10 mM, did affect neither of these processes (Fig. 6.1a). Magnesium ions had an unexpected effect on Cdc42: Cdc42 hydrolysed more GTP in absence of Mg^{2+} than when it was added, but the amount of hydrolysed GTP did not change with increasing Mg^{2+} concentrations (5-20 mM) (Fig. 6.1b). This shows that Mg^{2+} decreases the intrinsic GTPase activity of Cdc42 and that this effect does not increase at concentrations above 5 mM. This observation is contrary to previous findings. In an experiment by Zhang *et al.* Cdc42 was pre-loaded with GTP and the amount of released phosphate after a single hydrolysis step was measured (Zhang *et al.* (2000)). In presence of 5 mM MgCl_2 , more phosphate got released, indicating that magnesium ions boost the intrinsic GTP hydrolysis speed of Cdc42. It is possible that the observed differences of the effect of MgCl_2 are due to (1) differences in protein constructs, or (2) assay boundaries.

(1) Zhang *et al.* used human Cdc42 of which the last seven C-terminal amino acids were removed (Zhang *et al.* (2000)). It is unlikely that the different genetic backgrounds of the Cdc42 construct cause the contrary behaviour, as Cdc42 is a highly conserved and human Cdc42 shows an 80% sequence identity to yeast Cdc42 (Diepeveen *et al.* (2018)). It is more likely that the altered C-terminal region of Zhang *et al.*'s construct modified its behaviour. Cdc42's C-terminus consists of the poly-basic region (PBR, five amino acids) directly followed by the CAAX box (four amino acids). The CAAX box is responsible for protein prenylation, and the PBR was shown to be involved in Cdc42 dimerisation, which can self-enhance Cdc42's GTP hydrolysis rate (Zhang and Zheng (1998); Zhang *et al.* (1999)). As the PBR was shown to influence the GTP hydrolysis dynamics of Cdc42, it is possible that magnesium ions' effect on the hydrolysis behaviour of a protein with an intact PRB is different than on a protein without it. It is also possible that our construct, which is both N- and C-terminally tagged, showed a tag-related unusual behaviour. This, however, is unlikely, as Cdc42 constructs with different tags showed roughly the same GTPase activity. Tags therefore are unlikely to influence Cdc42's GTP hydrolysis dynamics (see Chapter 3).

(2) Zhang *et al.* measured the release of phosphate in a single-step GTP hydrolysis reaction (Zhang *et al.* (2000)). In the GTPase assay, we determined the amount of remaining GTP after many GTP hydrolysis cycles. A full cycle consists of Cdc42 binding to GTP, the hydrolysis of GTP, and the release of bound GDP. Both assays measure two distinct things; Zhang *et al.* measures the effect of Mg^{2+} on the GTP hydrolysis step, and the GTPase assay measures the effect on the overall GTP hydrolysis cycle. It is therefore possible that both assays depict the effect of Mg^{2+} : It speeds up GTP hydrolysis, but could slow down GDP release or GTP binding to such an extent that the overall cycling speed decreases. Further experiments on single reaction steps and on the entire GTPase cycle are needed to reveal the detailed workings of Mg^{2+} on the GTPase properties of fullsize and mutant Cdc42.

We further tested how magnesium affects the Cdc24-Cdc42 interaction (Fig. 6.1c). In accordance with previous findings (Zhang *et al.* (2000)), we found that the GEF activity of Cdc24 is vastly diminished in absence of magnesium. In presence of it we found no concentration dependency

between 5-20 mM.

6.2.2. Bem1-Cdc24 interaction

We conducted Flag-pulldown assays to study the effect of Ca^{2+} and Mg^{2+} on the Bem1-Cdc24 interaction. Bem1 and Cdc24, of which only Bem1 has a Flag-tag, got incubated with anti-Flag affinity gel. Flag-tagged Bem1 can bind to the gel and Cdc24 (lacking a Flag-tag) can not. After several rounds of washing, the proteins were eluted. If Cdc24 was eluted as well, it must have been bound to Flag-tagged Bem1. We tested if Cdc24 can bind to Flag gel, but it got washed off after one round of washing (Fig. 6.1d). The same held true for the nonspecific binding of a protein (Ovalbumin) to Flag-tagged Bem1 (Fig. 6.1d).

We tested if Ca^{2+} or Mg^{2+} affect Cdc24-Bem1 binding (Fig. 6.1d). Zheng *et al.* showed that 2 mM CaCl_2 could disrupt the binding of Cdc24 to N-terminally GST-tagged Bem1 (in a GST-pulldown experiment, similar to our Flag-pulldown experiment) (Zheng *et al.* (1995)). However, our findings reproducibly suggest that neither Ca^{2+} nor Mg^{2+} , up to a concentration of 20 mM, disrupt the binding of the two proteins. Bem1 and Cdc24 bind to each other via their C-terminal PB1 domain (Peterson *et al.* (1994); Zheng *et al.* (1995); Ogura *et al.* (2009)). It might be that the bulky GST-tag (26 kDa), that was previously used, at least partially destabilises the PB1-PB1 interaction, thereby making it more susceptible to the effect of Ca^{2+} . Although it is questionable if a N-terminal tag could disrupt the interaction of C-terminal domains to such an extent. We are still puzzled by our findings. Comparative experiments using Flag- and GST-tagged Bem1 could reveal if the GST-tag can destabilise Cdc24-Bem1 binding.

6

6.3. Discussion

In this chapter we discuss our considerations for determining the buffer composition of our main buffer - the buffer in which all proteins are stored and all experiments are conducted in. We did so by considering the requirements of the protein and enzymes involved and by conducting experiments to verify and further quantify literature findings.

It might seem like a waste of time to settle on one final buffer composition, and to investigate how specific buffer components affect the reactions, as most buffers used in biochemical assays are similar to each other and are generally considered to not affect the experiment much. This, however, is not always true. Reconstitution experiments of multi-component systems require a high level of control and tuning - if only a few reactions do not take place, or to a lesser extent than expected, the entire system might not produce the desired outcome. It would then be tedious and time-consuming to disentangle if this is because certain reactions do not take place as assumed, or because the components involved are simply not sufficient to reconstitute the desired process (i.e. the model behind the reconstitution idea is incorrect).

Keeping all involved components (in this case proteins) in the same buffer has therefore several advantages: intermediate dialysis steps can be avoided, during which proteins can precipitate, lose their or get a reduced activity (see Chapter 3). This allows a higher level of reproducibility and thereby easier troubleshooting in the reconstitution experiment. It also makes different biochemical assays more relatable to each other; the same amounts of salts are present in each experiment, and salt concentrations can modulate interaction strengths of protein. For example, increasing concentrations of MgCl_2 and NaCl have been found to increasingly inhibit the

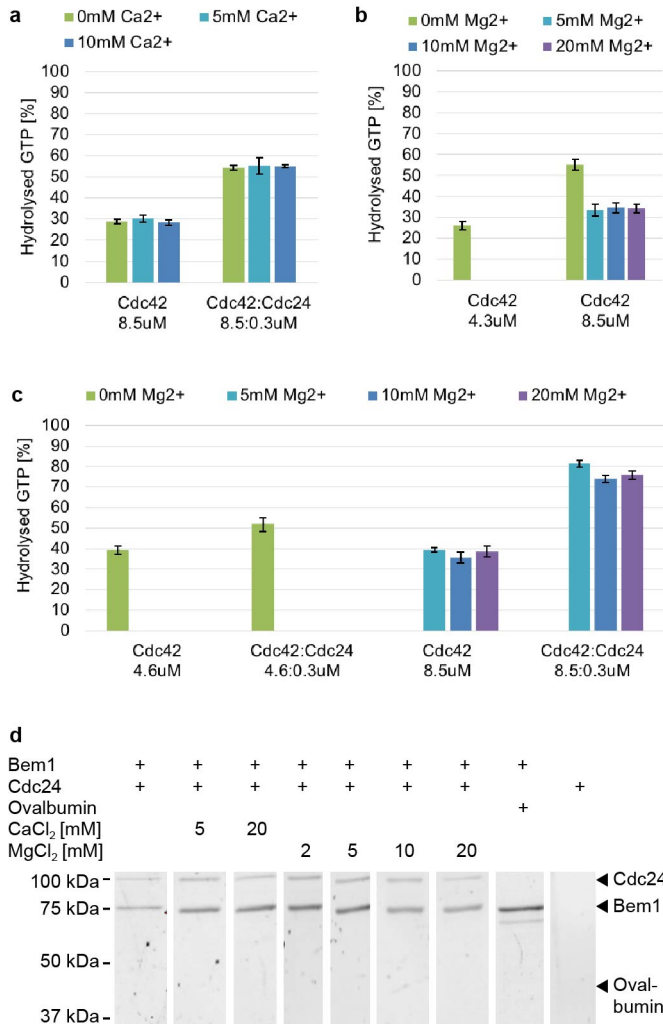


Figure 6.1. Effect of Ca²⁺ and Mg²⁺ on protein-protein interactions: (a-c) GTPase assay measuring the amount of hydrolysed GTP after incubation (30 °C, 90 min) of stated protein concentrations (H-Cdc42-F, Cdc24-H) with 5 μM GTP. CaCl₂, up to 10 mM, does not influence Cdc42's intrinsic GTPase activity or the GEF activity of Cdc24 (a). In absence of MgCl₂ Cdc42 shows an increased GTPase activity. The GTPase activity reducing effect of Mg²⁺ shows no concentration-dependency between 5 and 20 mM (b). In absence of MgCl₂ Cdc24's GEF activity is significantly reduced. It requires Mg²⁺, but is not concentration-dependent between 5 and 20 mM (c). (d) SDS-Page of elution fractions of Flag-pulldown experiments with H-Bem1-F (70 kDa), Cdc24-H (98 kDa), Ovalbumin (44 kDa) in absence and presence of CaCl₂ or MgCl₂. Neither CaCl₂ nor MgCl₂ (both up to 20 mM), effect Cdc24-Bem1 binding.

oligomerisation of the small GTPase Rac1 (*Zhang et al. (2001)*).

Conducting experiments to verify and further quantify literature findings (regarding the effect of buffer components) can further reveal that these finding might not be applicable to (1) your specific constructs, and/or (2) your experimental condition.

We showed in a Flag-pulldown experiment that the Bem1-Cdc24 interaction is not disrupted by CaCl_2 (up to 20 mM), contradicting a similar GST-pulldown experiment by Zheng *et al.* (*Zheng et al. (1995)*). It is possible that the 26 kDa GST-tag sterically weakens the Bem1-Cdc24 interaction, making it way more susceptible to calcium. In comparison, we used proteins tagged with a < 3 kDa Flag- and 6His-tag. It is also possible that the tags introduced by us strengthened the Bem1-Cdc24 interaction: the PB1 domain is located on the C-terminus of both Cdc24 and Bem1. On this terminus our Bem1 construct has a Flag-tag (which has overall a negative charge) and our Cdc24 construct has a 6His-tag (which is positively charged). It would be possible that after Cdc24-Bem1 binding these tags support the interaction, making it less susceptible to calcium. The exact cause for the discrepancy between both experiments still needs to be determined, and the biological implication needs to be resolved. However, the finding that calcium does not inhibit the Bem1-Cdc24 interaction in our case is valuable itself, as it shows that small amounts of calcium, that could be introduced by labelling-reactions, do not stringently need to be removed as they do not affect the interactions.

6

Our experiments also revealed that Cdc42 hydrolysed more GTP in absence of magnesium compared to when it was added, contrary to findings by Zhang *et al.* (*Zhang et al. (2000)*). It is again possible that this discrepancy was the result of the different constructs used, or that it shed light on a property of the Cdc42 GTPase cycle: Zhang *et al.* measured the effect of Mg^{2+} on the GTP hydrolysis step, and the GTPase assay measured the effect on the overall GTP hydrolysis cycle. Magnesium could speed up the GTP hydrolysis step and slow down GDP release and/or GTP binding to such an extend that the overall cycling speed decreases. Further research is needed to illuminate how magnesium tunes the Cdc42 GTPase cycle: for example, if the decrease in GTP hydrolysis in the GTPase assay happens at a critical concentration of magnesium, or if it scales linearly with the magnesium concentration. Experiments disentangling the steps of the GTPase cycle - GTP binding, GTP hydrolysis, GDP realease - are also needed to further understand which step magnesium is affecting, and thereby to explain the discrepancy between our findings and those of Zhang *et al.*

Taken together, our finding highlight that the buffer composition matters and that buffer components can influence critical steps in a reconstituted system. Considering and discussing the buffers of experiments is a crucial point still lacking in most biochemical investigations, but one that can be especially relevant when dealing with complex multi-component systems (such as reconstitutions).

Contributions and acknowledgements

R. van der Valk constructed the plasmids of protein constructs. Proteins were expressed and purified by S. Tschirpke and F. van Opstal. S. Tschirpke conducted the experiments, data analysis, figure preparation, and writing of this chapter.

We thank D. McCusker (University of Bordeaux) for the plasmid pDM272 and N. Dekker (TU Delft) for the plasmid pET28a-His-mcm10-Sortase-Flag.

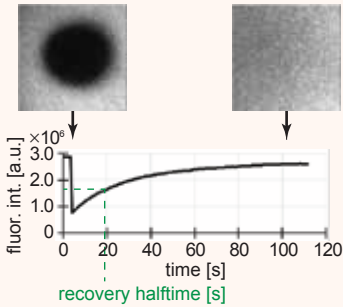
7

I am rather low today about all my experiments, — everything has been going wrong — the fan-tails have picked the feathers out of the Pouters in their Journey home — the fish at the Zoological Gardens after eating seeds would spit them all out again — Seeds will sink in salt-water — all nature is perverse and will not do as I wish it, and just at present I wish I had the old Barnacles to work at and nothing new.

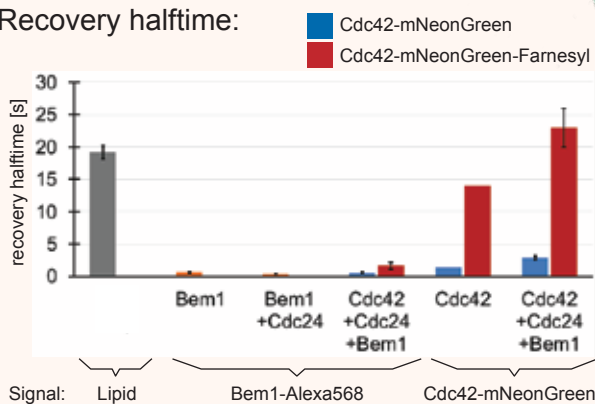
— Letter from Charles Darwin to W. D. Fox (May 7th 1855)

Preliminary data and outlook

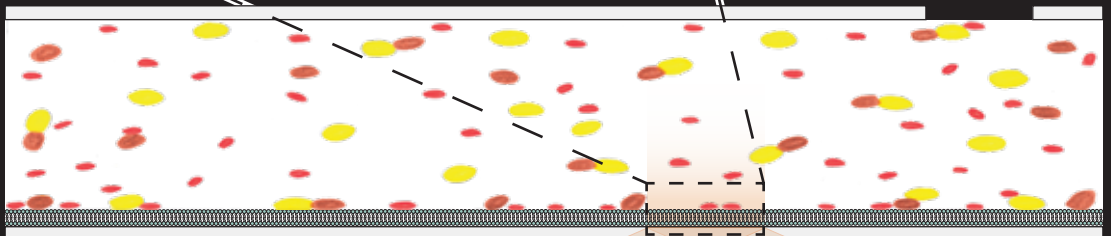
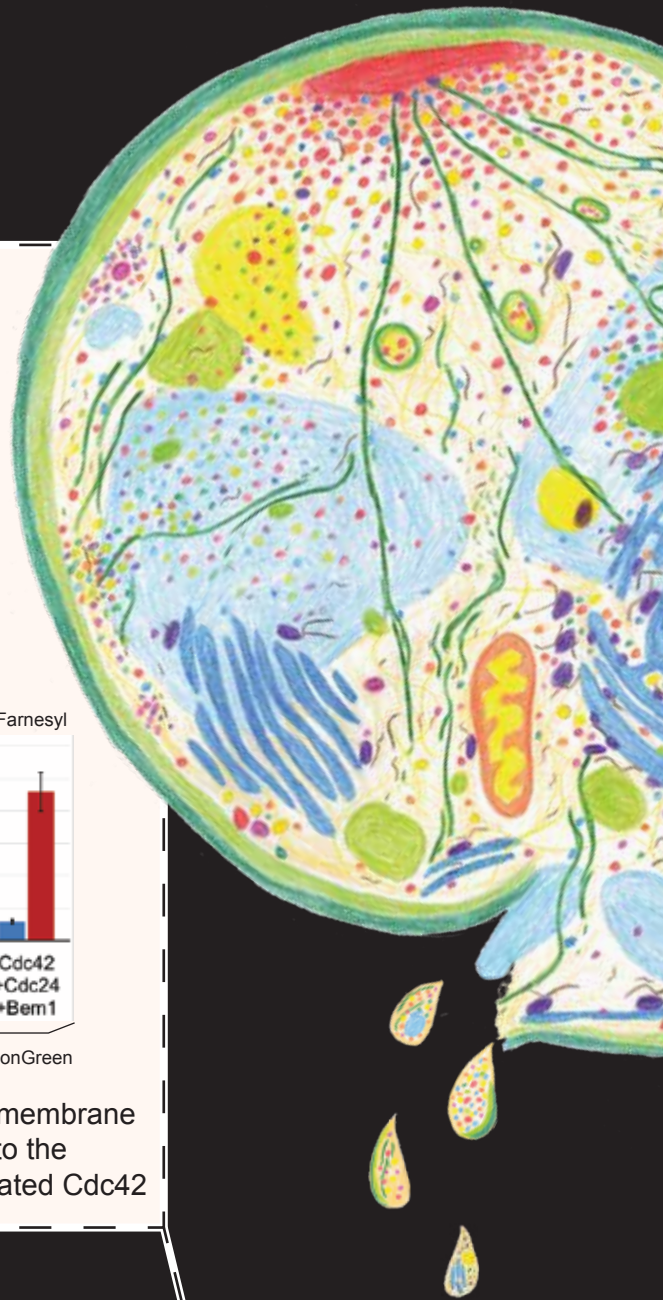
Fluorescence recovery after photo-bleaching:



Recovery half-time:



- ➔ Proteins bind very transiently to the membrane
- ➔ Farnesylated Cdc42 binds stronger to the membrane than Bem1 or unfarnesylated Cdc42



Protein dynamics on a supported lipid bilayer

TIRF microscopy

Preliminary data and outlook

Polarity establishment refers to the first step in cell division of *Saccharomyces cerevisiae*, where the cell division control protein Cdc42 accumulates in a spot (i.e. a very simplistic pattern) at the side of cell division. Cdc42 is a membrane-binding Rho-type GTPase and highly regulated, interacting with GDP/GTP exchange factors (GEFs), GTP-activating proteins (GAPs), a guanine nucleotide dissociation inhibitor (GDI), and scaffold and other regulatory proteins (*Chiou et al. (2017)*). The exact molecular mechanisms leading to Cdc42 accumulation are still not entirely understood, and several pathways have been proposed (*Goryachev and Leda (2017)*).

In this thesis I describe our steps towards reconstituting Cdc42-based polarity establishment in a minimal *in vitro* system (*Vendel et al. (2019)*). It is based on theoretical work that predicts that Cdc42, Bem1, and Cdc24 are sufficient to form Cdc42-based patterns on a spherical lipid membrane through a reaction-diffusion mechanism (*Klunder et al. (2013)*). We set out to realise such a system experimentally. In this chapter I present our ongoing work towards that goal: we added the three proteins on a supported lipid bilayer (SLB) and observed their behaviour by total internal reflection fluorescence (TIRF) microscopy (Fig. 7.1). We also conducted fluorescence recovery after photobleaching (FRAP) experiments to assess the membrane binding dynamics: here an area of the SLB got bleached and the recovery of fluorescent signal of that area got measured. We determined the recovery halftime, representing the amount of time it takes for the signal to recover to its half-maximal value (Fig. 7.6).

We started by investigating the protein - membrane interaction of a single protein; Bem1 labelled with Alexa-568. On a very simple SLB consisting of only DOPC (1,2-dioleoyl-sn-glycero-3-phosphocholine) Bem1 aggregated in clusters on the membrane and interfered with the membrane fluidity: after bleaching, the fluorescent signal did not recover (Fig. 7.3). Recovery should occur from the sides of the bleached patch due to membrane-diffusion and from the centre due to binding of previously unbound fluorescently labelled proteins. These can only bind if the proteins from the bleached area have unbound and "made space" on the membrane for new proteins to bind. The longer the recovery takes, the longer the bleached proteins were bound to the membrane. The recovery of an SLB (using an SLB was supplemented with fluorescently modified lipids) takes about 20 s (Fig. 7.2). Given that the Bem1 signal did not recover at all, we concluded that Bem1 did not unbind from the membrane and that its binding to the membrane disrupted the fluidity of the membrane. This indicates protein unfolding and a malfunctioning interaction. The yeast plasma membrane does not consist of only PC (phosphatidylcholine). Hence the usage of a SLB mimicking that lipid composition of the plasma membrane is better suited. Literature statements about this composition are not in complete agreement with each other, stating varying lipid ratios (Tab. 7.1). The commonality between these statements is the presence of about 20% PS (phosphatidylserine), 5% PI, PIP2, or PI4P (PI: phosphatidylinositol, PI4P: phosphatidylinositol 4-phosphate, PIP2: phosphatidylinositol 4,5-bisphosphate), and about 30% of a sterol (cholesterol or ergosterol). PI, PIP2, and PI4P are structurally similar and only differ in their amount of phosphate groups, and PI4P is the precursor of PIP2 *in vivo*. The second commonality is that all membrane compositions have an overall slightly negative charge (Tab. 7.1). Given that, we continued using SLBs consisting of 75:20:5 M% PC:PS:PIP2 (*Meca et al. (2019)*). This composition mimics the yeast plasma membrane composition in its main components and charge,

Abbreviations:

BC	basic cluster
DOPC	1,2-dioleoyl-sn-glycero-3-phosphocholine
FRAP	fluorescence recovery after photobleaching
GAP	GTPase activating protein
GDI	guanine nucleotide dissociation inhibitor
GEF	GDP/GTP exchange factor
PA	phosphatic acid
PC	phosphatidylcholine
PE	phosphatidylethanolamine
PI	phosphatidylinositol
PI4P	phosphatidylinositol 4-phosphate
PIP2	phosphatidylinositol 4,5-bisphosphate
PS	phosphatidylserine
SLB	supported lipid bilayer
TIRF	total internal reflection fluorescence (microscopy)

7

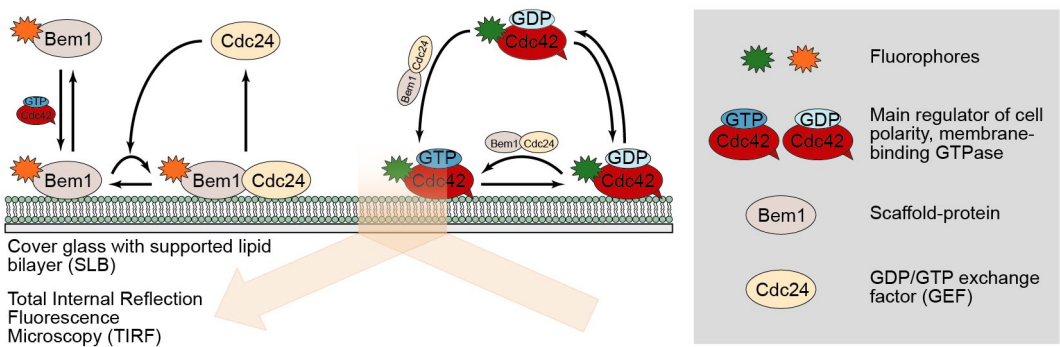


Figure 7.1. A minimal system for reconstituting Cdc42-based polarity establishment in *S. cerevisiae*. Illustration of the reactions and feedback loops the minimal system is comprised of (based on and modified from Klünder *et al.* (2013)): GTP-bound Cdc42 is recruiting Bem1 to the membrane. Membrane-bound Bem1 recruits the GEF Cdc24 to the membrane and forms a heterodimeric complex with it. The resulting localised concentrations of Cdc24 can lead to enhanced nucleotide exchange rates of Cdc42, thus increasing the local Cdc42-GTP concentration. The model implicitly includes the effects of GAPs and the GDI as well. GAPs increase Cdc42's GTP hydrolysis rate and the GDI extracts Cdc42 from the membrane. Both thus reduce the local Cdc42-GTP concentration and counterbalance the positive feedback of Cdc24-Bem1, thereby leading to pattern formation of membrane-bound Cdc42.

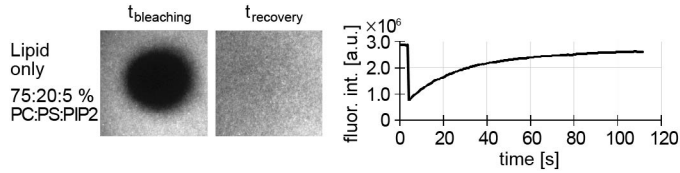


Figure 7.2. TIRF microscopy images and FRAP curve of the lipid signal of an SLB (75:20:5 %M DOPC:DOPS:PIP2).

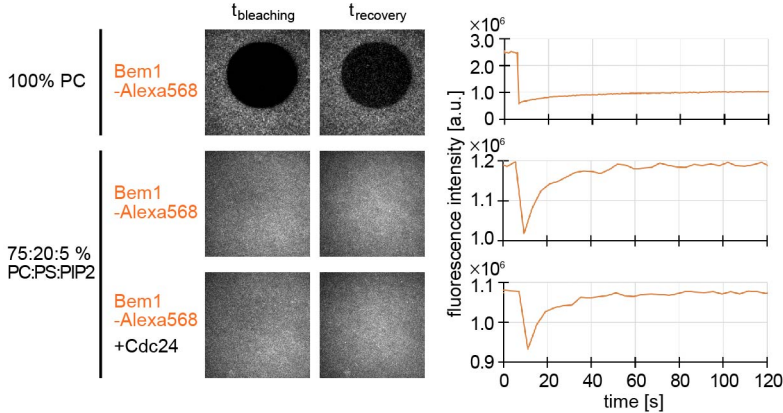


Figure 7.3. TIRF microscopy images and recovery curves of Bem1-Alexa568 on an SLB made of 100% DOPC (top), made of DOPC, DOPS, and PIP2 (middle), and in presence of Cdc24 on an SLB made of DOPC, DOPS, and PIP2 (bottom). The following protein constructs (in stated concentrations) were used: S-Bem1-Alexa568 (1.5 nM), Cdc24-H (0.5 nM).

and is rather simple and thus experimentally less challenging.

The change in SLB composition had a direct impact on the Bem1 behaviour: Bem1 stopped aggregating and the recovery of the fluorescent signal after bleaching happened immediately (Fig. 7.3). We determined the recovery halftimes from these FRAP curves. As the bleaching was not very strong, and the recovery did not follow exactly an exponential, the recovery halftimes can only be seen as a rough indication of how strongly the proteins bound to the membrane. The recovery of the Bem1 signal after bleaching was in about 20x faster than that of the SLB (Fig. 7.6), suggesting that the recovery is not only due to membrane-diffusion but mostly due to exchange of bleached with not-bleached Bem1 molecules. It also means that Bem1 does not significantly bind to the SLB. This is surprising, *Meca et al.* showed in membrane flotation assays that about 90% of Bem1 binds to liposomes of our lipid composition (*Meca et al. (2019)*). Their experiments concluded that an N-terminal unstructured region of mostly positively charged amino acids (the 'basic cluster' (BC) domains) is responsible for the strong binding of Bem1 to a negatively charged membrane (of the same composition we used). We conducted two additional membrane binding assays to assess Bem1-membrane binding: membrane flotation assays (in accordance to the protocol by *Meca et al. (2019)*), and quartz crystal microbalance with dissipation monitoring experiments. Both did not show a strong binding of Bem1 to the membrane (data not shown). We are therefore still puzzled by the discrepancy in results.

We next added protein mixtures to the SLB. The results of these experiments are still in their

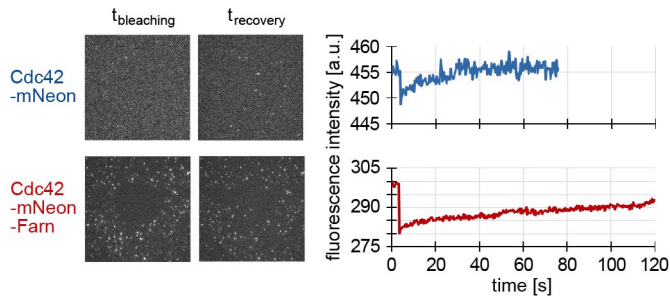


Figure 7.4. TIRF microscopy images and FRAP curves of unfarnesylated and farnesylated Cdc42-mNeon on an SLB (75:20:5 %M DOPC:DOPS:PIP2). The following protein constructs (in stated concentrations) were used: F-Cdc42-mNeon-Farn (1.5 nM), F-Cdc42-mNeon-H (1.5 nM).

early phase and very preliminary, as we were still struggling with the protein - membrane system and sometimes proteins got stuck on the membrane. The addition of Cdc24 to Bem1 did not change the Bem1 membrane binding dynamics, Bem1 still bound very transiently (Fig. 7.3). We also assessed the binding of Cdc42-mNeonGreen (*Bendezú et al. (2015)*) to the membrane. We tested two fluorescent Cdc42 constructs: Cdc42-mNeonGreen without a membrane-binding domain (Cdc42-mNeon), and Cdc42-mNeonGreen to which a farnesyl tail got appended in a Sortase-mediated reaction (Cdc42-mNeon-Farn). Cdc42-mNeon had a recovery half-time of ~ 2 s and Cdc42-mNeon-Farn one of 14 s (Fig. 7.4,7.6). Addition of the latter to a previously recoverable membrane also resulted in a non-recoverable membrane. This suggests that only the farnesyl group can bind Cdc42 to the membrane¹. The interaction between the farnesyl group and membrane could also explain why most membranes (3 out of 4) were non-recoverable. Insertion of many Cdc42-bound farnesyl groups into a membrane could reduce its fluidity, eliminating recovery from membrane-diffusion. If bleached membrane-bound Cdc42 molecules can not release from the membrane, which could be reinforced through a changes in the membrane structure, no fluorescent Cdc42 molecules can bind, and the fluorescent signal from this membrane patch does not recover.

We then added mixtures of all three proteins, Bem1-Alexa568, Cdc24, and Cdc42-mNeonGreen to the SLB. We used Bem1:Cdc24:Cdc42 ratios of 1.5:0.5:1.5 nM. Here Bem1 and Cdc24 levels are comparatively high. We choose this initial ratio because model predictions suggested that Cdc42 polarisation *in vivo* only occurs above certain Cdc24 and Bem1 levels (*Klünder et al. (2013)*). We monitored both the Alexa-568 (Bem1) and mNeonGreen (Cdc42) signal in these three-protein systems (Fig. 7.5). In all cases, no Cdc42 patterns formed over the time course of 3 h. We thus investigated the protein dynamics via FRAP: Bem1 stayed very dynamic and the recovery half-time from FRAP curves did not change significantly (compared to those of Bem1 alone) (Fig. 7.6). The Cdc42-mNeon-Farn signal recovered slightly slower in presence of Bem1 and Cdc24 (compared to their absence), indicating stronger or longer membrane binding (Fig. 7.6). It also seemed less aggregated and the recovery curve followed more of an exponential curve, suggesting that the system behaved better (Fig. 7.5b). We suspect that Bem1/Cdc24 interactions lead to less aggre-

¹We observed Cdc42-mNeon-Farn (75:20:5% PC:PS:PIP2 SLB) and Bem1 (100% PC SLB) sticking to membranes, concluding that one indicates membrane binding, whereas the other suggests an issue with the protein membrane interaction. We concluded that sticking of Bem1 to a membrane of PC indicates a malfunction of the interaction, because Bem1 is not known to strongly bind to membranes *in vivo* (*Gao et al. (2011)*) or to PC *in vitro* (*Meca et al. (2019)*). Farnesylated proteins, on the other hand, bind stronger to membranes, and can thus be expected to stick to them.

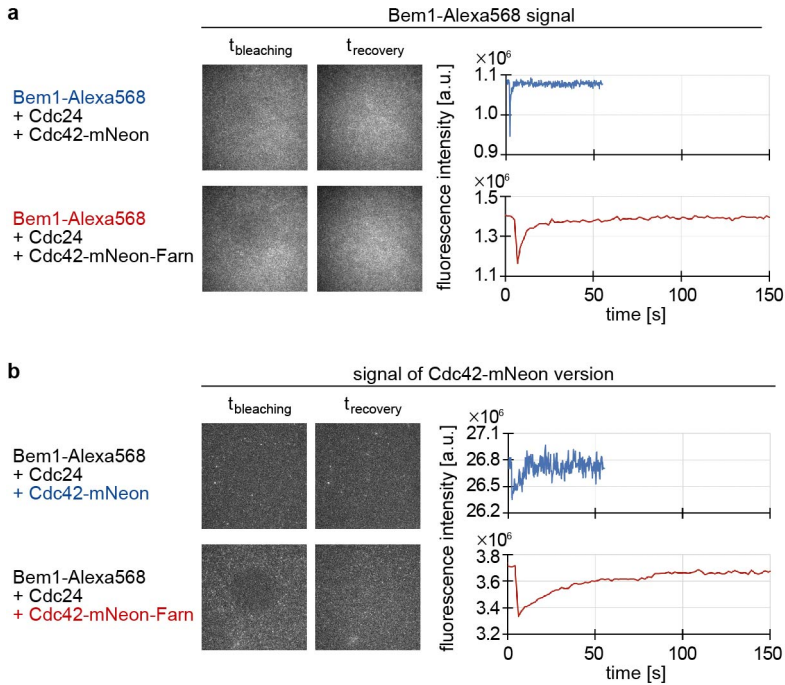


Figure 7.5. TIRF microscopy images and FRAP curves of proteins on an SLB (75:20:5 %M DOPC:DOPS:PIP2). Recovery of the Bem1-Alexa568 signal (a) and Cdc42-mNeonGreen signal (b) in a three protein assay. The following protein constructs (in stated concentrations) were used: S-Bem1-Alexa568 (1.5 nM), Cdc24-H (0.5 nM), F-Cdc42-mNeon-Farn (1.5 nM), F-Cdc42-mNeon-H (1.5 nM).

gation of Cdc42. The slower recovery of the Cdc42-mNeon-Farn signal in presence of Bem1 and Cdc24 could mean that Bem1 and Cdc24 are recruiting Cdc42 to the membrane, and by this keeping it longer there and/or increasing the binding strength. Our measurements are not controlled enough to definitively say that this is indeed true, and more experiments are required.

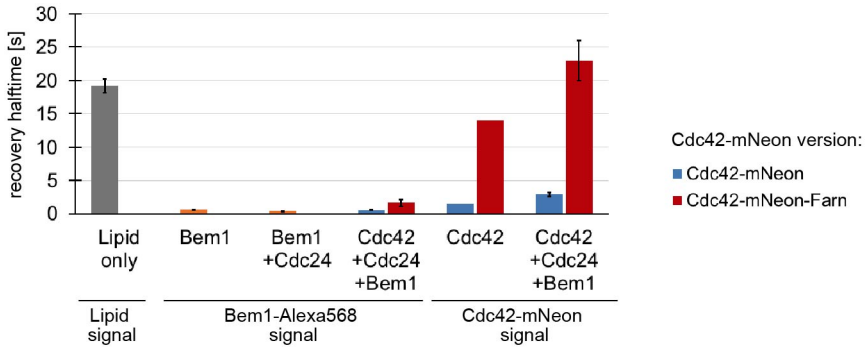


Figure 7.6. Recovery halftimes, determined from FRAP curves shown in Fig. 7.2-7.5.

We here showed our first preliminary data on reconstituting Cdc42-based polarity establishment in a minimal *in vitro* system. The data shows that at the used protein concentrations no patterns form. To achieve Cdc42 accumulation, several steps have to be taken:

1. We were still struggling with the protein - membrane system, and in some samples proteins randomly accumulated on the membrane. If this behaviour was not the norm in the tested condition, we excluded those samples. This however means that we still need to control the the system better, and understand what leads to this behaviour and how to avoid it.
2. When adding all three proteins together, we only used one ratio and a very low concentration. As reaction-diffusion systems are parameter sensitive, a change in concentration and ratio regime can significantly alter the emergent behaviour of the system. It is likely that concentrations in the low nM regime are significantly too low and that higher nM or μ M amounts are required (as were for two other reaction-diffusion systems: *Loose et al. (2008)*; *Bezjak et al. (2020)*).

In conjunction with that, it is useful to screen the parameter regime computationally using rates determined experimentally. This reveals if certain protein concentrations or ratios are critical for Cdc42 pattern formation, if additional proteins need to be added (e.g. a GAP or GDI), or if changes in the experimental setup are required.

3. The model our minimal system is based on includes a double-positive feedback in which (1) membrane-bound Cdc42-GTP recruits Bem1, and (2) the Cdc24-Bem1 complex recruits more Cdc42-GTP to the membrane. If one of these assumptions is not true, we will not see Cdc42 pattern formation. It is thus useful to verify these feedback loops experimentally: We can use our system of the three proteins on an SLB as before, but now we bind a Strep-tagged protein species to biotinylated SLBs. We then observe if the other protein species are recruited from the cytosol to the membrane (Fig. 7.7). We expect that membrane-bound Cdc42 recruits Bem1 and/or a Bem1-Cdc24 complex to the membrane, and that membrane-bound Cdc24 (and Bem1) recruits Cdc42 to the membrane.

If these assumptions are not true, the model should be adapted and new ways of feedback need to be explored and tested.

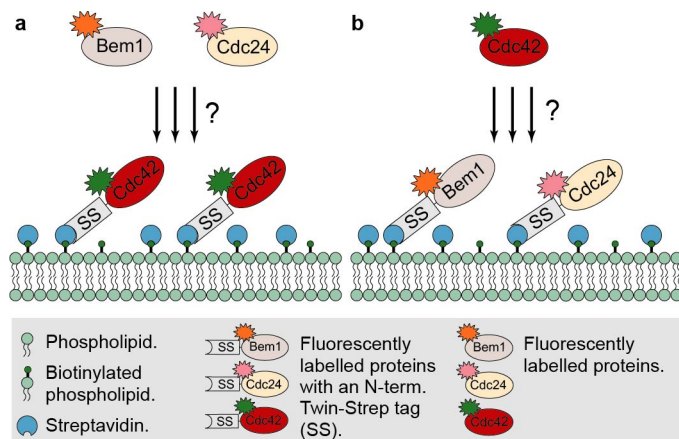


Figure 7.7. Illustration of an experimental approach to test if the in the model (Klünder *et al.* (2013), Fig. 7.1) assumed feedback or recruitment loops are occurring in the *in vitro* system. Supported lipid bilayers (SLBs), containing biotinylated phospholipids, are coated with streptavidin. (a) Fluorescent Strep-tagged (SS) Cdc42 can bind with its tag to streptavidin and can thereby be tethered to the SLB. Through the addition of fluorescently labelled Bem1 and Cdc24, which both do not contain a Strep-tag, Cdc42's ability to recruit Bem1 and Cdc24 to the membrane can be tested. (b) In the same fashion Strep-tagged Bem1 and Cdc24 can be tethered to SLBs. Cdc42 (without a Strep-tag) is proposed to be recruited to the membrane.

Contributions and acknowledgements

R. van der Valk constructed the plasmids of protein constructs. Proteins were expressed and purified by S. Tschirpke and F. van Opstal. S. Tschirpke conducted Sortase-labelling experiments. S. Farooq did microscopy experiments and analysed the data thereof. N. Hettema conducted membrane flotation assays and quartz crystal microbalance with dissipation monitoring experiments. Figure preparation and writing of this chapter was done by S. Tschirpke.

We thank D. McCusker (University of Bordeaux) for the plasmid pDM272 and N. Dekker (TU Delft) for the plasmid pET28a-His-mcm10-Sortase-Flag.

Table 7.1. Lipid composition of the yeast plasma membrane, according to literature. Values are stated as molar percentage. Abbreviations: PC: phosphatidylcholine (Change: 0), PE: phosphatidylethanolamine (Change: 0), PS: phosphatidylserine (Change: -1), PA: phosphatic acid (Change: -1), PI: phosphatidylinositol (Change: -1), PI4P: phosphatidylinositol 4-phosphate (Change: -2), PIP2: phosphatidylinositol 4,5-bisphosphate (Change: -3).

Lipid	<i>Meca et al. (2019)</i>	<i>Meca et al. (2019)</i>	<i>Johnson et al. (2012)</i>	<i>Zinser et al. (1991)</i>	<i>Van Meer et al. (2008)</i>
PC	75	35		14	5
PS	20	20	25	25	10
PE			35	14	10
PA				3	
PI/PIP2/PI4P	5 PIP2 or PI4P	5 PIP2 or PI4P	5 PI or PIP2	14 PI	10 PI
Ergosterol		40		30	50
Cholesterol			35		
Average charge	-0.35/-0.30	-0.35/-0.30	-0.30/-0.40	-0.42	-0.20

8

If you think about the history of science, which sciences got solved first? Or where did we make progress? The first science to really make good progress was astronomy – which

I would think is kind of surprising at first, given that the moon and the stars and the planets are very far from us – are very remote. And you might think: Why shouldn't biology be the subject where we made the most progress? It's very important: medicine, helping sick people, prolonging life, all of that. And it's because it's intrinsically complex!

Whereas astronomy, if you think about it, has a lot going for it: the motions of the planets are very repetitive and regular, the moon is very predictable. It's very slow. It doesn't change that much from night to night. And it's very observable, you can just look up there and see what's going on and make measurements - pretty decent ones. It's

at a timescale where it's not too fast and not too slow for naked eye observation - whereas the processes in the body are so fast sometimes and the molecules or the cells involved are so small, that biology is just intrinsically really hard! It's in the nature of

biology that it's much harder... it's very complex, there are lots of parts. Also keep in mind that there is lots of diversity in biology: my genes are different than yours, even though we're both human beings – our molecules are the same, but we're configured differently. In physics it's not like that: any two electrons anywhere in the universe are

absolutely indistinguishable – there is no diversity of subatomic particles. There are different particles – electrons are different from protons – but every electron is completely the same in every respect as every other electron; same charge, same mass. They never

break, they never age, they never *chip*. In that way physics is really simple. Whereas haemoglobin molecules could all be a little bit different. There is also a lot of noise in

biology – a lot of randomness, that is just because of molecular jiggling. It's just inherently chaotic. So it's really hard, and it's going to keep us occupied for a while, but still, it is ultimately chemistry and physics.

— Steven Strogatz

Conclusion and discussion: *why, how, and what?*

In this thesis I describe our work towards a minimal system for Cdc42-based polarity establishment in *Saccharomyces cerevisiae*. I start by introducing minimal systems on the example of the Min protein system in *Escherichia coli*, and illustrate how such a system could look like for *S. cerevisiae*. I show *our* progress towards such a reconstitution: We start by examining Cdc42. We explore the effect of purification tags on its expression levels, GTPase activity, and interaction with the GDP/GTP exchange factor (GEF) Cdc24. We then investigate the GTPase cycle of Cdc42 more closely. We build a model to characterise its kinetics, including the effect of molecular crowding, the GEF Cdc24, GTPase activating protein (GAP) Rga2, scaffold protein Bem1, and combinations thereof, on it. We continue by discussing our attempts on establishing easily accessible methods for Cdc42 prenylation, and examine the effect of buffer components on protein functions. We close with showing our first steps on building a reconstitution and discuss steps that still need to be taken.

In this thesis I start with *why*: *why* do minimal systems matter? To answer this question I explore the Min protein system in *E. coli*, for which a minimal system has been established (**Loose et al. (2008)**). Here the proteins MinD and MinE oscillate between the cell poles *in vivo* and form wave-like patterns on a supported lipid bilayer *in vitro*. Reconstitution work played a key role in elucidating the mechanism of the patterning process of the Min proteins. It showed that parameters (such as confinement geometry, protein ratios, temperature, and membrane composition) and their interplay strongly affect the system, and helped to refine *in silico* models of the system. I continue with *how*: *how* can we build a minimal system for Cdc42-based polarity establishment? What matters at the core? The Min protein system showed that despite the small number of components involved such systems are complex and dynamic in nature; in different parameter regimes the system forms different patterns. Work on Cdc42 polarity emphasised protein ratios and their rates as parameters affecting Cdc42 dynamics (**Klunder et al. (2013)**). Given this innate complexity and sensitivity, (1) a high level of control over the components involved is required, and (2), multidisciplinary research examining the system from any angles is needed to fully understand all its layers. To facilitate this, proteins and methods involved need to be accessible for researchers from many fields.

(1) We build the fundamentals for a reconstitution by examining Cdc42 in great detail. We learned that the Cdc42 GTPase activity shows cooperativity and that it is affected by molecular crowding. The GEF Cdc24 shows cooperativity as well, and we suspect this is due to dimerisation (**Mionnet et al. (2008)**; **Shimada et al. (2004)**). We also found a potential synergy between the GEF Cdc24 and GAP Rga2, and maybe even between Cdc24 and the scaffold Bem1 (**Rapali et al. (2017)**). Such

Abbreviations:

GAP GTPase activating protein
GEF GDP/GTP exchange factor

fundamental knowledge of a protein allows a higher level of control over it. These observations also question a static view of protein properties. The GEF rate of Cdc24, for example, is not a specific number, but depends non-linearly on the concentration and the surrounding environment (e.g. the presence of other proteins and/or crowding). Thus, the properties of proteins might better be viewed as dynamic. This questions if *in vitro* assays examining only a small number of conditions are useful. How much can these assays tell us about the system and the protein? How much can these results deceive us to believe that a protein or protein system has these properties in all/most conditions when in fact it might only have them in a few cases? This calls for research that shows several conditions, states boundary conditions, and shows under which conditions an effect appears and when it fades.

(2) We set out to make Cdc42 more accessible for researchers from a non-biochemical background. We discuss protein construct design and assessed the effect of purification tags, showing that N- and C-terminal 6His-, Flag-, and Strep-II-tags do not affect the protein expression and function. The Twin-Strep-tag, however, impedes protein expression and/or functionality if placed at a protein's N-terminus, but has no effect when placed on the C-terminus. We extend our analysis towards the expression behaviour of fluorescent Cdc42 versions, showing how strongly and with which level of degradation variously tagged Cdc42-sfGFP and Cdc42-mNeonGreen sandwich-fusions (**Bendezú et al. (2015)**) express. We further explore and compare easily accessible prenylation methods for Cdc42. Of these, prenylation via a Sortase-mediated reaction seems most useful. In this work we openly share otherwise not discussed technical details and do not exclude approaches that did not work. In doing so we aspire to make working with these proteins more accessible and lower the barrier of entry, thus encouraging research from non-biochemical backgrounds. We call for more sharing of such details, for research showing what did and what did not work, so that the published work can be continued and expanded on. The gained knowledge should not be kept secret and be used to keep an advantage over other researchers. We also call for more collaboration between groups and between groups of different fields. Dynamic biological systems are inherently complex and difficult to work with and benefit from many lenses. A simple example illustrating this is our knowledge of proteins: Research from the fields of e.g. biology, biochemistry, structural biology, genetics, physics, computer science (e.g. the development of alpha fold) are contributing to our understanding of proteins, and the knowledge is collected in large databases. We could not have gotten to our current level of understanding with work from only a single field.

There is, of course, a trade-off between depth and speed. New discoveries enhance science and novel studies that do not consider all details are valuable. Detailed studies take time, are more expensive, and are slower in discovering new ideas. But they also lead to fundamental and deep knowledge, they help discover knowledge that is "between the lines". This knowledge is needed to move from understanding a system to building something new (e.g. a minimal system) with it. Both approaches are needed. We found, however, that there seems to be a lack of deep fundamental knowledge about *S. cerevisiae* proteins. We believe that this deficit contributed to us finding results that are contradicting previous studies: Our Flag-pulldown experiments on Bem1-Cdc42 binding and on the effect of calcium on the Bem1-Cdc24 interaction did not reproduce previous GST-pulldowns (**Zheng et al. (1995)**; **Bose et al. (2001)**). The effect of magnesium on the GTPase activity of our full-length Cdc42 construct did not match that on a Cdc42-mutant lacking seven C-terminal amino acids (**Zhang et al. (2000)**). One explanation for this is that we are experiencing experimental issues we have not discovered yet. Another is that there are experi-

mental differences that are not discussed or have not been explored. Our call for more in depth knowledge still holds true even when the origin of our contradicting results is us experiencing experimental issues: We followed the assay's protocol and did controls. Yet we still do not know why we could not reproduce previous findings. This suggests that there are unknown or not discussed details.

I want to close with *what*: *what* is the the future of minimal systems? Minimal systems, or reconstituted systems with a higher complexity, are needed. "Simple" *in vitro* experiments might not be sufficient to cover the complexity and dynamic nature of many biological systems, as they (often) investigate a component outside of its cellular context. Reconstitutions, however, are much harder to realise. To build more and to enhance the field, more collaborations, in-depth knowledge, easier and reproducible experimental tools, and accessible communication of large amounts of information are needed. The community will also need to address the question of which details matter most and which do not. Minimal systems should also be used as a starting point to build more elaborate reconstitutions that consider even more complexity, and to understand the ongoing processes from multiple lenses. By doing so intricate *in vivo* questions can be approached one component at a time.

Zooming in again, *what* is the future of a minimal system for Cdc42-based polarity establishment? In this thesis I showed our progress towards building a minimal system. We established the fundamentals and outlined the steps that still need to be taken. While doing so, we can compare our system to, and learn from, established reconstitutions. Examples are the Min protein system ([Loose et al. \(2008\)](#)) and the Rab protein system ([Bezelj et al. \(2020\)](#)). From a reconstituted Cdc42 system, we can learn details about the mechanism leading to Cdc42 accumulation and how protein concentration changes or additions affect the system. To expand on that, this minimal system should also be used to apply additional perspectives to the Cdc42 system: Our work suggests that protein properties are dynamic and depend much on the context/environment of the system. Instead of describing the system in terms of its components it could be seen in terms of its (changing) properties (that are distributed among its components). As an example, properties leading to phase separation can be applied to explain Cdc42 accumulation. Describing a system in terms of its properties moves our interpretation away from the "biological" view of proteins with specific attributes. Instead, proteins have many context-dependent properties. It also contributes to a more integrated view on Cdc42 accumulation. Instead of answering the question of which process drives Cdc42 accumulation, it answers to which extend do which processes combined lead to Cdc42 accumulation. This questions whether Cdc42 accumulation *in vivo* should be thought of arising through distinct feedback loops ([Chiou et al. \(2017\)](#)), or whether the system is an interconnected whole. Reconstituted systems are good starting points to build integrated/multi-faceted models of biological processes, because they still allow for a high level of control over the components involved. Here specific model predictions can be tested.

What could we learn from a multi-faceted view on Cdc42 accumulation? This more integrated view might be needed to explain the complex processes happening *in vivo*. [Laan et al.](#) conducted evolution experiments showing that *S. cerevisiae* compensates for the deletion of Bem1 through the stepwise deletion of Bem2, Bem3, and Nrp1 ([Laan et al. \(2015\)](#)). How the deletion of three proteins compensates for the loss of Bem1 remains elusive, and likely can not be explained through a single lens.

Bibliography

- Agarwal V**, Diethelm S, Ray L, Garg N, Awakawa T, Dorrestein PC, Moore BS. Chemoenzymatic Synthesis of Acyl Coenzyme A Substrates Enables in Situ Labeling of Small Molecules and Proteins. *Organic Letters*. 2015; 17(18):4452–4455. doi: [10.1021/acs.orglett.5b02113](https://doi.org/10.1021/acs.orglett.5b02113).
- Alberts B**, Johnson A, Walter P, Raff M, Lewis J, Roberts K. *Molecular Biology of the Cell*. 6 ed. New York: Garland Science; 2014.
- Altschuler SJ**, Angenent SB, Wang Y, Wu LF. On the spontaneous emergence of cell polarity. *Nature*. 2008; 454(7206):886–889. doi: [10.1016/j.jacc.2007.01.076.White](https://doi.org/10.1016/j.jacc.2007.01.076.White).
- Antos JM**, Ingram J, Fang T, Pishesha N, Truttmann MC, Ploegh HL. Site-Specific Protein Labeling via Sortase-Mediated Transpeptidation. *Current Protocols in Protein Science*. 2017 8; 89(1):1–15. <https://onlinelibrary.wiley.com/doi/10.1002/cpps.38>, doi: [10.1002/cpps.38](https://doi.org/10.1002/cpps.38).
- Antos JM**, Miller GM, Grotenbreg GM, Ploegh HL. Lipid modification of proteins through sortase-catalyzed transpeptidation. *Journal of the American Chemical Society*. 2008; 130(48):16338–16343. doi: [10.1021/ja806779e](https://doi.org/10.1021/ja806779e).
- Arjunan SNV**, Tomita M. A new multicompartmental reaction-diffusion modeling method links transient membrane attachment of *E. coli* MinE to E-ring formation. *Systems and Synthetic Biology*. 2010; 4(1):35–53. doi: [10.1007/s11693-009-9047-2](https://doi.org/10.1007/s11693-009-9047-2).
- Arumugam S**, Petrášek Z, Schwille P. MinCDE exploits the dynamic nature of FtsZ filaments for its spatial regulation. *Proceedings of the National Academy of Sciences*. 2014; 111(13):E1192–E1200. <http://www.pnas.org/lookup/doi/10.1073/pnas.1317764111>, doi: [10.1073/pnas.1317764111](https://doi.org/10.1073/pnas.1317764111).
- Aumiller WM**, Davis BW, Hatzakis E, Keating CD. Interactions of macromolecular crowding agents and cosolutes with small-molecule substrates: Effect on horseradish peroxidase activity with two different substrates. *Journal of Physical Chemistry B*. 2014; 118(36):10624–10632. doi: [10.1021/jp506594f](https://doi.org/10.1021/jp506594f).
- Bender A**, Pringle JR. Use of a screen for synthetic lethal and multicopy suppressor mutants to identify two new genes involved in morphogenesis in *Saccharomyces cerevisiae*. *Molecular and Cellular Biology*. 1991; 11(3):1295–1305. <http://mcb.asm.org/lookup/doi/10.1128/MCB.11.3.1295>, doi: [10.1128/MCB.11.3.1295](https://doi.org/10.1128/MCB.11.3.1295).
- Bendezú FO**, Vincenzetti V, Vavylonis D, Wyss R, Vogel H, Martin SG. Spontaneous Cdc42 Polarization Independent of GDI-Mediated Extraction and Actin-Based Trafficking. *PLoS Biology*. 2015; 13(4):1–30. doi: [10.1371/journal.pbio.1002097](https://doi.org/10.1371/journal.pbio.1002097).
- Bezeljak U**, Loya H, Kaczmarek B, Saunders TE, Loose M. Stochastic activation and bistability in a Rab GTPase regulatory network. *Proceedings of the National Academy of Sciences*. 2020 3; 117(12):6540–6549. <https://pnas.org/doi/full/10.1073/pnas.1921027117>, doi: [10.1073/pnas.1921027117](https://doi.org/10.1073/pnas.1921027117).
- Bi E**, Lutkenhaus J. FtsZ ring structure associated with division in *Escherichia coli*. *Nature*. 1991; 354(6349):161–164. <http://www.nature.com/doi/10.1038/354161a0>, doi: [10.1038/354161a0](https://doi.org/10.1038/354161a0).
- Bi E**, Park HO. Cell polarization and cytokinesis in budding yeast. *Genetics*. 2012; 191(2):347–387. doi: [10.1534/genetics.111.132886](https://doi.org/10.1534/genetics.111.132886).
- de Boer PAJ**, Crossley RE, Hand AR, Rothfield LI. The MinD protein is a membrane ATPase required for the correct placement of the *Escherichia coli* division site. *The EMBO journal*. 1991; 10(13):4371–4380. <https://www-embopress-org.tudelft.idm.oclc.org/doi/abs/10.1002/j.1460-2075.1991.tb05015.x>.

- de Boer PAJ**, Crossley RE, Rothfield LI. A division inhibitor and a topological specificity factor coded for by the minicell locus determine proper placement of the division septum in *E. coli*. *Cell*. 1989; 56(4):641–649. doi: 10.1016/0092-8674(89)90586-2.
- Bonny M**, Fischer-friedrich E, Loose M, Schwille P, Kruse K. Membrane Binding of MinE Allows for a Comprehensive Description of Min-Protein Pattern Formation. *PLoS Computational Biology*. 2013; 9(12):e1003347. doi: 10.1371/journal.pcbi.1003347.
- Bose I**, Irazoqui JE, Moskow JJ, Bardes ES, Zyla TR, Lew DJ. Assembly of scaffold-mediated complexes containing Cdc42p, the exchange factor Cdc24p, and the effector Cla4p required for cell cycle-regulated phosphorylation of Cdc24p. *J Biol Chem*. 2001; 276(10):7176–7186. <http://www.ncbi.nlm.nih.gov/pubmed/11113154>, doi: 10.1074/jbc.M010546200.
- Boulter E**, Garcia-Mata R, Guilluy C, Dubash A, Rossi G, Brennwald PJ, Burrridge K. Regulation of Rho GTPase crosstalk, degradation and activity by RhoGDI1. *Nat Cell Biol*. 2010; 12(5):477–483. <http://www.ncbi.nlm.nih.gov/pubmed/20400958>, doi: 10.1038/ncb2049.
- Butty AC**, Perrinjaquet N, Petit A, Jaquenoud M, Segall JE, Hofmann K, Zwahlen C, Peter M. A positive feedback loop stabilizes the guanine-nucleotide exchange factor Cdc24 at sites of polarization. *EMBO J*. 2002; 21(7):1565–1576. <http://www.ncbi.nlm.nih.gov/pubmed/11927541>, doi: 10.1093/emboj/21.7.1565.
- Caplin BE**, Hettich LA, Marshall MS. Substrate characterization of the *saccharomyces cerevisiae* protein farnesyltransferase and type-I protein geranylgeranyltransferase. *Biochimica et Biophysica Acta (BBA)/Protein Structure and Molecular*. 1994; 1205(1):39–48. doi: 10.1016/0167-4838(94)90089-2.
- Caspi Y**, Dekker C. Mapping out Min protein patterns in fully confined fluidic chambers. *eLife*. 2016 11; 5:1–27. <https://elifesciences.org/articles/19271>, doi: 10.7554/eLife.19271.
- Chant J**, Herskowitz I. Genetic control of bud site selection in yeast by a set of gene products that constitute a morphogenetic pathway. *Cell*. 1991; 65(7):1203–1212. doi: 10.1016/0092-8674(91)90015-Q.
- Chen H**, Kuo CC, Kang H, Howell AS, Zyla TR, Jin M, Lew DJ. Cdc42p regulation of the yeast formin Bni1p mediated by the effector Gic2p. *Mol Biol Cell*. 2012; 23(19):3814–3826. <http://www.ncbi.nlm.nih.gov/pubmed/22918946>, doi: 10.1091/mbc.E12-05-0400.
- Chen L**, Cohen J, Song X, Zhao A, Ye Z, Feulner CJ, Doonan P, Somers W, Lin L, Chen PR. Improved variants of SrtA for site-specific conjugation on antibodies and proteins with high efficiency. *Scientific Reports*. 2016 8; 6(1):31899. <http://www.nature.com/articles/srep31899>, doi: 10.1038/srep31899.
- Chiou Jg**, Balasubramanian MK, Lew DJ. Cell Polarity in Yeast. *Annual Review of Cell and Developmental Biology*. 2017 8; 33:77–101. <https://doi.org/10.1146/annurev-cellbio-100616-060856>, doi: 10.1146/annurev.cellbio.15.1.365.
- Cini E**, Lampariello LR, Rodriguez M, Taddei M. Synthesis and application in SPSS of a stable amino acid isostere of palmitoyl cysteine. *Tetrahedron*. 2009; 65(4):844–848. <http://dx.doi.org/10.1016/j.tet.2008.11.033>, doi: 10.1016/j.tet.2008.11.033.
- Corbin BD**, Yu XC, Margolin W. Exploring intracellular space: Function of the Min system in round-shaped *Escherichia coli*. *EMBO Journal*. 2002; 21(8):1998–2008. doi: 10.1093/emboj/21.8.1998.
- Costanzo M**, VanderSluis B, Koch EN, Baryshnikova A, Pons C, Tan G, Wang W, Usaj M, Hanchard J, Lee SD, Pelechano V, Styles EB, Billmann M, van Leeuwen J, van Dyk N, Lin ZY, Kuzmin E, Nelson J, Piotrowski JS, Srikumar T, et al. A global genetic interaction network maps a wiring diagram of cellular function. *Science*. 2016 9; 353(6306):aaf1420–aaf1420. <https://www.sciencemag.org/lookup/doi/10.1126/science.aaf1420>, doi: 10.1126/science.aaf1420.
- Cox AD**, Der CJ. Protein prenylation: more than just glue? *Current Opinion in Cell Biology*. 1992; 4(6):1008–1016. doi: 10.1016/0955-0674(92)90133-W.

- Coxon FP, Rogers MJ.** The role of prenylated small GTP-binding proteins in the regulation of osteoclast function. *Calcified Tissue International*. 2003; 72(1):80–84. doi: 10.1007/s00223-002-2017-2.
- Cytrynbaum EN, Marshall BDL.** A multistranded polymer model explains MinDE dynamics in *E. coli* cell division. *Biophysical Journal*. 2007; 93(4):1134–1150. doi: 10.1529/biophysj.106.097162.
- Daalman WKG, Sweep E, Laan L.** The Path towards Predicting Evolution as Illustrated in Yeast Cell Polarity. *Cells*. 2020; 9(12). doi: 10.3390/cells9122534.
- Dajkovic A, Lan G, Sun SX, Wirtz D, Lutkenhaus J.** MinC Spatially Controls Bacterial Cytokinesis by Antagonizing the Scaffolding Function of FtsZ. *Current Biology*. 2008; 18(4):235–244. doi: 10.1016/j.cub.2008.01.042.
- Das A, Slaughter BD, Unruh JR, Bradford WD, Alexander R, Rubinstein B, Li R.** Flippase-mediated phospholipid asymmetry promotes fast Cdc42 recycling in dynamic maintenance of cell polarity. *Nature Cell Biology*. 2012; 14(3):304–310. <http://www.nature.com/doifinder/10.1038/ncb2444>, doi: 10.1038/ncb2444.
- De Boer PAJ, Crossley RE, Rothfield LI.** Roles of MinC and MinD in the Site-Specific Septation Block Mediated by the MinCDE System of *Escherichia coli*. *Journal of Bacteriology*. 1992; 174(1):63–70. <https://doi-org.tudelft.idm.oclc.org/10.1128/jb.174.1.63-70.1992>.
- DerMardirossian C, Bokoch GM.** GDIs: central regulatory molecules in Rho GTPase activation. *Trends Cell Biol*. 2005; 15(7):356–363. <http://www.ncbi.nlm.nih.gov/pubmed/15921909>, doi: 10.1016/j.tcb.2005.05.001.
- Diepeveen ET, Gehrman T, Pourquié V, Abeel T, Laan L.** Patterns of conservation and diversification in the fungal polarization network. *Genome Biology and Evolution*. 2018; 10(August):evy121–evy121. <http://dx.doi.org/10.1093/gbe/evy121>, doi: 10.1093/gbe/evy121.
- Dong Y, Pruyne D, Bretscher A.** Formin-dependent actin assembly is regulated by distinct modes of Rho signaling in yeast. *J Cell Biol*. 2003; 161(6):1081–1092. <http://www.ncbi.nlm.nih.gov/pubmed/12810699>, doi: 10.1083/jcb.200212040.
- Douglas ME, Diffley JFX.** Recruitment of Mcm10 to sites of replication initiation requires direct binding to the minichromosome maintenance (MCM) complex. *Journal of Biological Chemistry*. 2016; 291(11):5879–5888. doi: 10.1074/jbc.M115.707802.
- Dovas A, Couchman JR.** RhoGDI: multiple functions in the regulation of Rho family GTPase activities. *Biochemical Journal*. 2005 8; 390(1):1–9. <http://www.ncbi.nlm.nih.gov/pubmed/16083425><https://portlandpress.com/biochemj/article/390/1/1/41925/RhoGDI-multiple-functions-in-the-regulation-of-Rho>, doi: 10.1042/BJ20050104.
- Dransart E, Morin A, Cherfils J, Olofsson B.** Uncoupling of inhibitory and shuttling functions of rho GDP dissociation inhibitors. *Journal of Biological Chemistry*. 2005; 280(6):4674–4683. <http://www.ncbi.nlm.nih.gov/pubmed/15513926>, doi: 10.1074/jbc.M409741200.
- Drew DA, Osborn MJ, Rothfield LI.** A polymerization-depolymerization model that accurately generates the self-sustained oscillatory system involved in bacterial division site placement. *Proceedings of the National Academy of Sciences USA*. 2005; 102(17):6114–6118. <http://www.ncbi.nlm.nih.gov/pubmed/15840714> 5Cn<http://www.ncbi.nlm.nih.gov/sites/entrez>, doi: 10.1073/pnas.0502037102.
- Dubendorf JW, Studier FW.** Controlling basal expression in an inducible T7 expression system by blocking the target T7 promoter with lac repressor. *Journal of Molecular Biology*. 1991; 219(1):45–59. doi: 10.1016/0022-2836(91)90856-2.
- Evangelista M, Blundell K, Longtine MS, Chow CJ, Adames N, Pringle JR, Peter M, Boone C.** Bni1p, a yeast formin linking cdc42p and the actin cytoskeleton during polarized morphogenesis. *Science*. 1997; 276(5309):118–122. <http://www.ncbi.nlm.nih.gov/pubmed/9082982>.
- Fange D, Elf J.** Noise-induced min phenotypes in *E. coli*. *PLoS Computational Biology*. 2006; 2(6):0637–0648. doi: 10.1371/journal.pcbi.0020080.

- Fischer-Friedrich E**, Meacci G, Lutkenhaus J, Chaté H, Kruse K. Intra- and intercellular fluctuations in Min-protein dynamics decrease with cell length. *Proceedings of the National Academy of Sciences of the United States of America*. 2010; 107(14):6134–6139. doi: [10.1073/pnas.0911708107](https://doi.org/10.1073/pnas.0911708107).
- Fischer-Friedrich E**, Van Yen RN, Kruse K. Surface waves of Min-proteins. *Physical Biology*. 2007; 4(1):38–47. doi: [10.1088/1478-3975/4/1/005](https://doi.org/10.1088/1478-3975/4/1/005).
- Freisinger T**, Klünder B, Johnson J, Müller N, Pichler G, Beck G, Costanzo M, Boone C, Cerione RA, Frey E, Wedlich-Söldner R. Establishment of a robust single axis of cell polarity by coupling multiple positive feedback loops. *Nature Communications*. 2013 6; 4(1):1–11. <http://www.nature.com/articles/ncomms2795>, doi: [10.1038/ncomms2795](https://doi.org/10.1038/ncomms2795).
- Fres JM**, Müller S, Praefcke GJK. Purification of the CaaX-modified, dynamin-related large GTPase hGBP1 by coexpression with farnesyltransferase. *Journal of Lipid Research*. 2010; 51(8):2454–2459. doi: [10.1194/jlr.D005397](https://doi.org/10.1194/jlr.D005397).
- Fu X**, Shih YL, Zhang Y, Rothfield LI. The MinE ring required for proper placement of the division site is a mobile structure that changes its cellular location during the *Escherichia coli* division cycle. *Proceedings of the National Academy of Sciences of the United States of America*. 2001; 98(3):980–985. doi: [10.1073/pnas.98.3.980](https://doi.org/10.1073/pnas.98.3.980).
- Gao JT**, Guimera R, Li H, Pinto IM, Sales-Pardo M, Wai SC, Rubinstein B, Li R. Modular coherence of protein dynamics in yeast cell polarity system. *Proceedings of the National Academy of Sciences*. 2011; 108(18):7647–7652. <http://www.pnas.org/cgi/doi/10.1073/pnas.1017567108>, doi: [10.1073/pnas.1017567108](https://doi.org/10.1073/pnas.1017567108).
- Gibson DG**, Young L, Chuang RY, Venter JC, Hutchison CA, Smith HO. Enzymatic assembly of DNA molecules up to several hundred kilobases. *Nature Methods*. 2009; 6(5):343–345. doi: [10.1038/nmeth.1318](https://doi.org/10.1038/nmeth.1318).
- Golding AE**, Visco I, Bieling P, Bement WM. Extraction of active RhoGTPases by RhoGDI regulates spatiotemporal patterning of RhoGTPases. *eLife*. 2019 10; 8:1–26. <https://elifesciences.org/articles/50471>, doi: [10.7554/eLife.50471](https://doi.org/10.7554/eLife.50471).
- Gomez R**, Goodman LE, Tripathy SK, O'Rourke E, Manne V, Tamanoi F. Purified yeast protein farnesyltransferase is structurally and functionally similar to its mammalian counterpart. *Biochemical Journal*. 1993; 289(1):25–31. doi: [10.1042/bj2890025](https://doi.org/10.1042/bj2890025).
- Goryachev AB**, Leda M. Many roads to symmetry breaking: molecular mechanisms and theoretical models of yeast cell polarity. *Molecular Biology of the Cell*. 2017 2; 28(3):370–380. <https://www.molbiolcell.org/doi/10.1091/mbc.e16-10-0739>, doi: [10.1091/mbc.e16-10-0739](https://doi.org/10.1091/mbc.e16-10-0739).
- Goryachev AB**, Pokhilko AV. Dynamics of Cdc42 network embodies a Turing-type mechanism of yeast cell polarity. *FEBS Letters*. 2008; 582(10):1437–1443. <http://www.ncbi.nlm.nih.gov/pubmed/18381072>, doi: [10.1016/j.febslet.2008.03.029](https://doi.org/10.1016/j.febslet.2008.03.029).
- Guimaraes CP**, Witte MD, Theile CS, Bozkurt G, Kundrat L, Blom AEM, Ploegh HL. Site-specific C-terminal and internal loop labeling of proteins using sortase-mediated reactions. *Nature Protocols*. 2013; 8(9):1787–1799. doi: [10.1038/nprot.2013.101](https://doi.org/10.1038/nprot.2013.101).
- Halatek J**, Brauns F, Frey E. Self-organization principles of intracellular pattern formation. *Philosophical Transactions of the Royal Society B: Biological Sciences*. 2018 5; 373(1747):20170107. doi: [10.1098/rstb.2017.0107](https://doi.org/10.1098/rstb.2017.0107).
- Halatek J**, Frey E. Rethinking pattern formation in reaction-diffusion systems. *Nature Physics*. 2018; 14(5):507–514. <http://dx.doi.org/10.1038/s41567-017-0040-5>, doi: [10.1038/s41567-017-0040-5](https://doi.org/10.1038/s41567-017-0040-5).
- Halatek J**, Frey E. Highly Canalized MinD Transfer and MinE Sequestration Explain the Origin of Robust MinCDE-Protein Dynamics. *Cell Reports*. 2012; 1(6):741–752. <http://dx.doi.org/10.1016/j.celrep.2012.04.005>, doi: [10.1016/j.celrep.2012.04.005](https://doi.org/10.1016/j.celrep.2012.04.005).

- Hale CA**, Meinhardt H, de Boer PAJ. Dynamic localization cycle of the cell division regulator MinE in *Escherichia coli*. *The EMBO journal*. 2001; 20(7):1563–72. <http://embojnl.embopress.org/content/20/7/1563.abstract>, doi: 10.1093/emboj/20.7.1563.
- Hartwell LH**, Mortimer RK, Culotti J, Culotti M. Genetic control of the cell division cycle in yeast: V. Genetic analysis of *cdc* mutants. *Genetics*. 1973; 74(2):267–286. doi: 74(2): 267–286.
- Hicks KA**, Hartman HL, Fierke CA. Upstream polybasic region in peptides enhances dual specificity for prenylation by both farnesyltransferase and geranylgeranyltransferase type I. *Biochemistry*. 2005; 44(46):15325–15333. doi: 10.1021/bi050951v.
- Hoffmann M**, Schwarz US. Oscillations of Min-proteins in micropatterned environments: a three-dimensional particle-based stochastic simulation approach. *Soft Matter*. 2014; 10(14):2388–2396. <http://xlink.rsc.org/?DOI=C3SM52251B>, doi: 10.1039/C3SM52251B.
- Hopp TP**, Prickett KS, Price VL, Libby RT, March CJ, Pat Cerretti D, Urdal DL, Conlon PJ. A Short Polypeptide Marker Sequence Useful for Recombinant Protein Identification and Purification. *Bio/Technology*. 1988; 6(10):1204–1210. <https://doi.org/10.1038/nbt1088-1204>, doi: 10.1038/nbt1088-1204.
- Houglund JL**, Hicks KA, Hartman HL, Kelly RA, Watt TJ, Fierke CA. Identification of Novel Peptide Substrates for Protein Farnesyltransferase Reveals Two Substrate Classes with Distinct Sequence Selectivities. *Journal of Molecular Biology*. 2010; 395(1):176–190. <http://dx.doi.org/10.1016/j.jmb.2009.10.038>, doi: 10.1016/j.jmb.2009.10.038.
- Houglund JL**, Lamphear CL, Scott SA, Gibbs RA, Fierke CA. Context-dependent substrate recognition by protein farnesyltransferase. *Biochemistry*. 2009; 48(8):1691–1701. doi: 10.1021/bi801710g.
- Howard M**, Rutenberg AD. Pattern Formation inside Bacteria: Fluctuations due to the Low Copy Number of Proteins. *Physical Review Letters*. 2003 3; 90(12):128102–1. <https://link.aps.org/doi/10.1103/PhysRevLett.90.128102>, doi: 10.1103/PhysRevLett.90.128102.
- Howard M**, Rutenberg AD, de Vet S. Dynamic Compartmentalization of Bacteria: Accurate Division in *E. Coli*. *Physical Review Letters*. 2001 12; 87(27):278102–1. <https://link.aps.org/doi/10.1103/PhysRevLett.87.278102>, doi: 10.1103/PhysRevLett.87.278102.
- Howell AS**, Jin M, Wu CF, Zyla TR, Elston TC, Lew DJ. Negative feedback enhances robustness in the yeast polarity establishment circuit. *Cell*. 2012; 149(2):322–333. <http://www.sciencedirect.com/science/article/pii/S009286741200342X>.
- Hsieh CW**, Lin TY, Lai HM, Lin CC, Hsieh TS, Shih YL. Direct MinE-membrane interaction contributes to the proper localization of MinDE in *E. coli*. *Molecular Microbiology*. 2010; 75(2):499–512. doi: 10.1111/j.1365-2958.2009.07006.x.
- Hu Z**, Gogol EP, Lutkenhaus J. Dynamic assembly of MinD on phospholipid vesicles regulated by ATP and MinE. *Proceedings of the National Academy of Sciences of the United States of America*. 2002; 99(10):6761–6766. <http://www.pubmedcentral.nih.gov/articlerender.fcgi?artid=124476&tool=pmcentrez&rendertype=abstract>, doi: 10.1073/pnas.102059099.
- Hu Z**, Lutkenhaus J. Topological regulation of cell division in *Escherichia coli* involves rapid pole to pole oscillation of the division inhibitor MinC under the control of MinD and MinE. *Molecular Microbiology*. 1999; 34(1):82–90. doi: 10.1046/j.1365-2958.1999.01575.x.
- Hu Z**, Lutkenhaus J. Analysis of MinC reveals two independent domains involved in interaction with MinD and FtsZ. *Journal of Bacteriology*. 2000; 182(14):3965–3971. doi: 10.1128/JB.182.14.3965-3971.2000.
- Hu Z**, Lutkenhaus J. Topological Regulation of Cell Division in *E. coli*: Spatiotemporal Oscillation of MinD Requires Stimulation of Its ATPase by MinE and Phospholipid. *Molecular Cell*. 2001; 7(6):1337–1343. [https://doi.org/10.1016/S1097-2765\(01\)00273-8](https://doi.org/10.1016/S1097-2765(01)00273-8).

- Hu Z**, Lutkenhaus J. A conserved sequence at the C-terminus of MinD is required for binding to the membrane and targeting MinC to the septum. *Molecular Microbiology*. 2003; 47(2):345–355. doi: [10.1046/j.1365-2958.2003.03321.x](https://doi.org/10.1046/j.1365-2958.2003.03321.x).
- Hu Z**, Saez C, Lutkenhaus J. Recruitment of MinC, an inhibitor of Z-ring formation, to the membrane in *Escherichia coli*: Role of minD and minE. *Journal of Bacteriology*. 2003; 185(1):196–203. doi: [10.1128/JB.185.1.196-203.2003](https://doi.org/10.1128/JB.185.1.196-203.2003).
- Huang J**, Cao C, Lutkenhaus J. Interaction between FtsZ and inhibitors of cell division. *Journal of Bacteriology*. 1996; 178(17):5080–5085. doi: [10.1128/jb.178.17.5080-5085.1996](https://doi.org/10.1128/jb.178.17.5080-5085.1996).
- Huang KC**, Meir Y, Wingreen NS. Dynamic structures in *Escherichia coli*: Spontaneous formation of MinE rings and MinD polar zones. *Proceedings of the National Academy of Sciences*. 2003; 100(22):12724–12728. <http://www.pnas.org/cgi/doi/10.1073/pnas.2135445100>, doi: [10.1073/pnas.2135445100](https://doi.org/10.1073/pnas.2135445100).
- Irazaqui JE**, Gladfelter AS, Lew DJ. Scaffold-mediated symmetry breaking by Cdc42p. *Nature Cell Biology*. 2003 12; 5(12):1062–1070. <http://www.ncbi.nlm.nih.gov/pubmed/14625559><http://www.nature.com/articles/ncb1068>, doi: [10.1038/ncb1068](https://doi.org/10.1038/ncb1068).
- Ivanov V**, Mizuuchi K. Multiple modes of interconverting dynamic pattern formation by bacterial cell division proteins. *Proceedings of the National Academy of Sciences of the United States of America*. 2010; 107(18):8071–8078. doi: [10.1073/pnas.0911036107](https://doi.org/10.1073/pnas.0911036107).
- Johnson JL**, Erickson JW, Cerione RA. New Insights into How the Rho Guanine Nucleotide Dissociation Inhibitor Regulates the Interaction of Cdc42 with Membranes. *Journal of Biological Chemistry*. 2009 8; 284(35):23860–23871. <http://www.ncbi.nlm.nih.gov/pubmed/19581296><https://linkinghub.elsevier.com/retrieve/pii/S0021925818608130>, doi: [10.1074/jbc.M109.031815](https://doi.org/10.1074/jbc.M109.031815).
- Johnson JL**, Erickson JW, Cerione RA. C-terminal Di-arginine motif of Cdc42 protein is essential for binding to phosphatidylinositol 4,5-bisphosphate-containing membranes and inducing cellular transformation. *Journal of Biological Chemistry*. 2012; 287(8):5764–5774. doi: [10.1074/jbc.M111.336487](https://doi.org/10.1074/jbc.M111.336487).
- Kang PJ**, Béven L, Hariharan S, Park HO. The Rsr1/Bud1 GTPase interacts with itself and the Cdc42 GTPase during bud-site selection and polarity establishment in budding yeast. *Molecular Biology of the Cell*. 2010; 21(17):3007–3016. doi: [10.1091/mbc.E10-03-0232](https://doi.org/10.1091/mbc.E10-03-0232).
- Kang PJ**, Lee ME, Park HO. Bud3 activates Cdc42 to establish a proper growth site in budding yeast. *Journal of Cell Biology*. 2014; 206(1):19–28. doi: [10.1083/jcb.201402040](https://doi.org/10.1083/jcb.201402040).
- Karsenti E**. Self-organization in cell biology: A brief history. *Nature Reviews Molecular Cell Biology*. 2008; 9(3):255–262. <http://www.ncbi.nlm.nih.gov/pubmed/18292780>, doi: [10.1038/nrm2357](https://doi.org/10.1038/nrm2357).
- Kennedy K**, Cobbold SA, Hanssen E, Birnbaum J, Spillman NJ, McHugh E, Brown H, Tilley L, Spielmann T, McConville MJ, Ralph SA. Delayed death in the malaria parasite *Plasmodium falciparum* is caused by disruption of prenylation-dependent intracellular trafficking. *PLoS Biology*. 2019; 17(7):1–28. <http://dx.doi.org/10.1371/journal.pbio.3000376>, doi: [10.1371/journal.pbio.3000376](https://doi.org/10.1371/journal.pbio.3000376).
- Kerr Ra**, Levine H, Sejnowski TJ, Rappel WJ. Division accuracy in a stochastic model of Min oscillations in *Escherichia coli*. *Proceedings of the National Academy of Sciences of the United States of America*. 2006; 103(2):347–352. doi: [10.1073/pnas.0505825102](https://doi.org/10.1073/pnas.0505825102).
- Kim JS**, Yethiraj A. Effect of macromolecular crowding on reaction rates: A computational and theoretical study. *Biophysical Journal*. 2009; 96(4):1333–1340. <http://dx.doi.org/10.1016/j.bpj.2008.11.030>, doi: [10.1016/j.bpj.2008.11.030](https://doi.org/10.1016/j.bpj.2008.11.030).
- Klünder B**, Freisinger T, Wedlich-Söldner R, Frey E. GDI-Mediated Cell Polarization in Yeast Provides Precise Spatial and Temporal Control of Cdc42 Signaling. *PLoS Computational Biology*. 2013 12; 9(12):e1003396. <https://dx.plos.org/10.1371/journal.pcbi.1003396>, doi: [10.1371/journal.pcbi.1003396](https://doi.org/10.1371/journal.pcbi.1003396).

- Koch G**, Tanaka K, Masuda T, Yamochi W, Nonaka H, Takai Y. Association of the Rho family small GTP-binding proteins with Rho GDP dissociation inhibitor (Rho GDI) in *Saccharomyces cerevisiae*. *Oncogene*. 1997; 15(4):417–422. doi: [10.1038/sj.onc.1201194](https://doi.org/10.1038/sj.onc.1201194).
- Koppelman CM**, Den Blaauwen T, Duursma MC, Heeren RMA, Nanninga N. *Escherichia coli* Minicell Membranes Are Enriched in Cardiolipin. *Journal of Bacteriology*. 2001; 183(20):6144–6147. doi: [10.1128/JB.183.20.6144](https://doi.org/10.1128/JB.183.20.6144).
- Kozminski KG**, Beven L, Angerman E, Tong AHY, Boone C, Park HO. Interaction between a Ras and a Rho GTPase Couples Selection of a Growth Site to the Development of Cell Polarity in Yeast. *Molecular Biology of the Cell*. 2003; 14(12):4958–4970. <https://doi.org/10.1091/mbc.e03-06-0426>, doi: [10.1091/mbc.E03](https://doi.org/10.1091/mbc.E03).
- Kozubowski L**, Saito K, Johnson JM, Howell AS, Zyla TR, Lew DJ. Symmetry-Breaking Polarization Driven by a Cdc42p GEF-PAK Complex. *Current Biology*. 2008 11; 18(22):1719–1726. <http://www.ncbi.nlm.nih.gov/pubmed/19013066><https://linkinghub.elsevier.com/retrieve/pii/S0960982208012955>, doi: [10.1016/j.cub.2008.09.060](https://doi.org/10.1016/j.cub.2008.09.060).
- Kretschmer S**, Harrington L, Schwille P. Reverse and forward engineering of protein pattern formation. *Philosophical Transactions of the Royal Society B: Biological Sciences*. 2018 5; 373(1747):20170104. <https://royalsocietypublishing.org/doi/10.1098/rstb.2017.0104>, doi: [10.1098/rstb.2017.0104](https://doi.org/10.1098/rstb.2017.0104).
- Kretschmer S**, Schwille P. Pattern formation on membranes and its role in bacterial cell division. *Current Opinion in Cell Biology*. 2016 2; 38:52–59. <http://dx.doi.org/10.1016/j.cub.2016.02.005><https://linkinghub.elsevier.com/retrieve/pii/S0955067416300126>, doi: [10.1016/j.cub.2016.02.005](https://doi.org/10.1016/j.cub.2016.02.005).
- Kretschmer S**, Zieske K, Schwille P. Large-scale modulation of reconstituted Min protein patterns and gradients by defined mutations in MinEs membrane targeting sequence. *PLOS ONE*. 2017; 12(6):e0179582. <https://doi.org/10.1371/journal.pone.0179582>.
- Kruse K**. A dynamic model for determining the middle of *Escherichia coli*. *Biophysical Journal*. 2002; 82(2):618–627. doi: [10.1016/S0006-3495\(02\)75426-X](https://doi.org/10.1016/S0006-3495(02)75426-X).
- Kuznetsova I**, Turoverov K, Uversky V. What Macromolecular Crowding Can Do to a Protein. *International Journal of Molecular Sciences*. 2014 12; 15(12):23090–23140. <http://www.mdpi.com/1422-0067/15/12/23090>, doi: [10.3390/ijms151223090](https://doi.org/10.3390/ijms151223090).
- Laan L**, Koschwanetz JH, Murray AW. Evolutionary adaptation after crippling cell polarization follows reproducible trajectories. *eLife*. 2015 10; 4:1–18. <https://elifesciences.org/articles/09638>, doi: [10.7554/eLife.09638](https://doi.org/10.7554/eLife.09638).
- Lackner LL**, Raskin DM, de Boer PAJ. ATP-dependent interactions between *Escherichia coli* Min proteins and the phospholipid membrane in vitro. *Journal of Bacteriology*. 2003; 185(3):735–749. doi: [10.1128/JB.185.3.735-749.2003](https://doi.org/10.1128/JB.185.3.735-749.2003).
- Laemmli UK**. Cleavage of structural proteins during the assembly of the head of bacteriophage T4. *Nature*. 1970; 227:680–685. <https://doi-org.tudelft.idm.oclc.org/10.1038/227680a0>.
- Laloux G**, Jacobs-Wagner C. How do bacteria localize proteins to the cell pole? *Journal of Cell Science*. 2014; 127(1):11–19. <http://jcs.biologists.org/cgi/doi/10.1242/jcs.138628>, doi: [10.1242/jcs.138628](https://doi.org/10.1242/jcs.138628).
- Layton AT**, Savage NS, Howell AS, Carroll SY, Drubin DG, Lew DJ. Modeling Vesicle Traffic Reveals Unexpected Consequences for Cdc42p-Mediated Polarity Establishment. *Current Biology*. 2011 2; 21(3):184–194. <https://linkinghub.elsevier.com/retrieve/pii/S0960982211000352>, doi: [10.1016/j.cub.2011.01.012](https://doi.org/10.1016/j.cub.2011.01.012).
- Li M**, Min W, Wang J, Wang L, Li Y, Zhou N, Yang Z, Qian Q. Effects of mevalonate kinase interference on cell differentiation, apoptosis, prenylation and geranylgeranylation of human keratinocytes are attenuated by farnesyl pyrophosphate or geranylgeranyl pyrophosphate. *Experimental and Therapeutic Medicine*. 2020 2; 19:2861–2870. <http://www.spandidos-publications.com/10.3892/etm.2020.8569>, doi: [10.3892/etm.2020.8569](https://doi.org/10.3892/etm.2020.8569).

- Liao JM**, Mo ZY, Wu LJ, Chen J, Liang Y. Binding of calcium ions to Ras promotes Ras guanine nucleotide exchange under emulated physiological conditions. *Biochimica et Biophysica Acta - Proteins and Proteomics*. 2008; 1784(11):1560–1569. <http://dx.doi.org/10.1016/j.bbapap.2008.08.009>, doi: 10.1016/j.bbapap.2008.08.009.
- Liu L**, Boyd S, Kavoussi M, Winkler DD. Receptor with the Cry1Ab Toxin of *Bacillus thuringiensis*. *Journal of Proteomics Bioinformatics*. 2018; 11(4):104–110. doi: 10.4172/jpb.1000474.Interaction.
- Loose M**, Fischer-Friedrich E, Herold C, Kruse K, Schwille P. Min protein patterns emerge from rapid rebinding and membrane interaction of MinE. *Nature Structural and Molecular Biology*. 2011; 18(5):577–583. <http://dx.doi.org/10.1038/nsmb.2037>, doi: 10.1038/nsmb.2037.
- Loose M**, Fischer-Friedrich E, Ries J, Kruse K, Schwille P. Spatial Regulators for Bacterial Cell Division Self-Organize into Surface Waves in Vitro. *Science*. 2008; 320(5877):789–792. <http://www.sciencemag.org/cgi/doi/10.1126/science.1154413>, doi: 10.1126/science.1154413.
- Loose M**, Kruse K, Schwille P. Protein Self-Organization: Lessons from the Min System. *Annual Review of Biophysics*. 2011; 40(1):315–336. <http://www.annualreviews.org/doi/10.1146/annurev-biophys-042910-155332>, doi: 10.1146/annurev-biophys-042910-155332.
- Mannik J**, Driessen R, Galajda P, Keymer JE, Dekker C. Bacterial growth and motility in sub-micron constrictions. *Proceedings of the National Academy of Sciences*. 2009; 106(35):14861–14866. <http://www.pnas.org/cgi/doi/10.1073/pnas.0907542106>, doi: 10.1073/pnas.0907542106.
- Männik J**, Wu F, Hol FJH, Bisicchia P, Sherratt DJ, Keymer JE, Dekker C. Robustness and accuracy of cell division in *Escherichia coli* in diverse cell shapes. *Proceedings of the National Academy of Sciences*. 2012; 109(18):6957–6962. <http://www.pnas.org/cgi/doi/10.1073/pnas.1120854109>, doi: 10.1073/pnas.1120854109.
- Martin SG**. Spontaneous cell polarization: Feedback control of Cdc42 GTPase breaks cellular symmetry. *BioEssays*. 2015; 37(11):1193–1201. doi: 10.1002/bies.201500077.
- Martos A**, Petrasek Z, Schwille P. Propagation of MinCDE waves on free-standing membranes. *Environmental Microbiology*. 2013; 15(12):3319–3326. doi: 10.1111/1462-2920.12295.
- Martos A**, Raso A, Jiménez M, Petrášek Z, Rivas G, Schwille P. FtsZ Polymers Tethered to the Membrane by ZipA Are Susceptible to Spatial Regulation by Min Waves. *Biophysical Journal*. 2015 5; 108(9):2371–2383. <https://linkinghub.elsevier.com/retrieve/pii/S0006349515002921>, doi: 10.1016/j.bpj.2015.03.031.
- Mazel T**. Crosstalk of cell polarity signaling pathways. *Protoplasma*. 2017; 254:1241–1258. <http://link.springer.com/article/10.1007/s00709-017-1075-2>.
- Meacci G**, Kruse K. Min-oscillations in *Escherichia coli* induced by interactions of membrane-bound proteins. *Physical Biology*. 2005; 2(2):89–97. doi: 10.1088/1478-3975/2/2/002.
- Meacci G**, Ries J, Fischer-Friedrich E, Kahya N, Schwille P, Kruse K. Mobility of Min-proteins in *Escherichia coli* measured by fluorescence correlation spectroscopy. *Physical Biology*. 2006; 3(4):255–263. doi: 10.1088/1478-3975/3/4/003.
- Meca J**, Massoni-Laporte A, Martinez D, Sartorel E, Loquet A, Habenstein B, McCusker D. Avidity-driven polarity establishment via multivalent lipid-GTPase module interactions. *The EMBO Journal*. 2019; 38(3):1–19. doi: 10.15252/embj.201899652.
- Meinhardt H**, de Boer PAJ. Pattern formation in *Escherichia coli*: a model for the pole-to-pole oscillations of Min proteins and the localization of the division site. *Proceedings of the National Academy of Sciences of the United States of America*. 2001; 98(25):14202–7. <http://www.ncbi.nlm.nih.gov/pubmed/11734639%5Cnhttp://www.pubmedcentral.nih.gov/articlerender.fcgi?artid=PMC64659>, doi: 10.1073/pnas.251216598.

- Mileykovskaya E**, Dowhan W. Visualization of Phospholipid Domains in Escherichia coli by Using the Cardiolipin-Specific Fluorescent Dye 10- N -Nonyl Acridine Orange. *Journal of Bacteriology*. 2000; 182(4):1172–1175. <http://www.pubmedcentral.nih.gov/articlerender.fcgi?artid=94398&tool=pmcentrez&rendertype=abstract>, doi: 10.1128/JB.182.4.1172-1175.2000.Updated.
- Mileykovskaya E**, Dowhan W. Role of membrane lipids in bacterial division-site selection. *Current Opinion in Microbiology*. 2005; 8(2):135–142. doi: 10.1016/j.mib.2005.02.012.
- Mileykovskaya E**, Fishov I, Fu X, Corbin BD, Margolin W, Dowhan W. Effects of phospholipid composition on MinD-membrane interactions in vitro and in vivo. *Journal of Biological Chemistry*. 2003; 278(25):22193–22198. doi: 10.1074/jbc.M302603200.
- Mionnet C**, Bogliolo S, Arkowitz RA. Oligomerization regulates the localization of Cdc24, the Cdc42 activator in Saccharomyces cerevisiae. *Journal of Biological Chemistry*. 2008; 283(25):17515–17530. doi: 10.1074/jbc.M800305200.
- Miyagi A**, Ramm B, Schwille P, Scheuring S. High-Speed Atomic Force Microscopy Reveals the Inner Workings of the MinDE Protein Oscillator. *Nano Letters*. 2018; 18(1):288–296. doi: 10.1021/acs.nanolett.7b04128.
- Mondal S**, Hsiao K, Goueli SA. A Homogenous Bioluminescent System for Measuring GTPase, GTPase Activating Protein, and Guanine Nucleotide Exchange Factor Activities. *Assay and Drug Development Technologies*. 2015; 13(8):444–455. doi: 10.1089/adt.2015.643.
- Naider FR**, Becker JM. Synthesis of prenylated peptides and peptide esters. *Biopolymers*. 1997; 43(1):3–14. doi: 10.1002/(SICI)1097-0282(1997)43:1<3::AID-BIP2>3.0.CO;2-Z.
- Nanda JS**, Lorsch JR. Labeling of a Protein with Fluorophores Using Maleimide Derivatization. In: *Methods in Enzymology*, vol. 536, 1 ed. Elsevier Inc.; 2014.p. 79–86. <http://dx.doi.org/10.1016/B978-0-12-420070-8.00007-6>, doi: 10.1016/B978-0-12-420070-8.00007-6.
- New England Biolabs**, Protocol for use with Enterokinase, light chain (P8070); 2022. <https://international.neb.com/protocols/2018/04/05/protocol-for-use-with-enterokinase-light-chain-p8070>.
- Ogura K**, Tandai T, Yoshinaga S, Kobashigawa Y, Kumeta H, Ito T, Sumimoto H, Inagaki F. NMR Structure of the Heterodimer of Bem1 and Cdc24 PB1 Domains from Saccharomyces Cerevisiae. *Journal of Biochemistry*. 2009; 146(3):317–325. <http://www.ncbi.nlm.nih.gov/pubmed/19451149>, doi: 10.1093/jb/mvp075.
- Olins PO**, Devine CS, Rangwala SH, Kavka KS. The T7 phage gene 10 leader RNA, a ribosome-binding site that dramatically enhances the expression of foreign genes in Escherichia coli. *Gene*. 1988; 73(1):227–235. [https://doi.org/10.1016/0378-1119\(88\)90329-0](https://doi.org/10.1016/0378-1119(88)90329-0).
- Orij R**, Postmus J, Beek AT, Brul S, Smits GJ. In vivo measurement of cytosolic and mitochondrial pH using a pH-sensitive GFP derivative in Saccharomyces cerevisiae reveals a relation between intracellular pH and growth. *Microbiology*. 2009; 155(1):268–278. doi: 10.1099/mic.0.022038-0.
- Osawa M**, Anderson DE, Erickson HP. Reconstitution of Contractile FtsZ Rings in Liposomes. *Science*. 2008 5; 320(5877):792–794. <https://www.science.org/doi/10.1126/science.1154520>, doi: 10.1126/science.1154520.
- Park KT**, Wu W, Battaile KP, Lovell S, Holyoak T, Lutkenhaus J. The min oscillator uses MinD-dependent conformational changes in MinE to spatially regulate cytokinesis. *Cell*. 2011; 146(3):396–407. <http://dx.doi.org/10.1016/j.cell.2011.06.042>, doi: 10.1016/j.cell.2011.06.042.
- Pavin N**, Paljetak HC, Krstic V. Min-protein oscillations in Escherichia coli with spontaneous formation of two-stranded filaments in a three-dimensional stochastic reaction-diffusion model. *Physical Review E - Statistical, Nonlinear, and Soft Matter Physics*. 2006; 73(2):1–5. doi: 10.1103/PhysRevE.73.021904.
- Pédrelacq JD**, Cabantous S, Tran T, Terwilliger TC, Waldo GS. Engineering and characterization of a superfolder green fluorescent protein. *Nature Biotechnology*. 2006; 24(1):79–88. doi: 10.1038/nbt1172.

- Peterson J**, Zheng Y, Bender L, Myers A, Cerione RA, Bender A. Interactions between the bud emergence proteins Bem1p and Bem2p and Rho- type GTPases in yeast. *Journal of Cell Biology*. 1994; 127(5):1395-1406. doi: [10.1083/jcb.127.5.1395](https://doi.org/10.1083/jcb.127.5.1395).
- Peurois F**, Peyroche G, Cherfils J. Small GTPase peripheral binding to membranes: Molecular determinants and supramolecular organization. *Biochemical Society Transactions*. 2018; 47(1):13-22. doi: [10.1042/BST20170525](https://doi.org/10.1042/BST20170525).
- Popp MWL**, Ploegh HL. Making and breaking peptide bonds: Protein engineering using sortase. *Angewandte Chemie - International Edition*. 2011; 50(22):5024-5032. doi: [10.1002/anie.201008267](https://doi.org/10.1002/anie.201008267).
- Pritz S**, Wolf Y, Kraetke O, Klose J, Bienert M, Beyermann M. Synthesis of Biologically Active Peptide Nucleic Acid - Peptide Conjugates by Sortase-Mediated Ligation. *The Journal of Organic Chemistry*. 2007 5; 72(10):3909-3912. <https://pubs.acs.org/doi/10.1021/jo062331i>, doi: [10.1021/jo062331i](https://doi.org/10.1021/jo062331i).
- Rapali P**, Mitteau R, Braun C, Massoni-Laporte A, Ünü C, Bataille L, Arramon FS, Gygi SP, McCusker D. Scaffold-mediated gating of Cdc42 signalling flux. *eLife*. 2017 3; 6:1-18. <https://elifesciences.org/articles/25257>, doi: [10.7554/eLife.25257](https://doi.org/10.7554/eLife.25257).
- Raskin DM**, de Boer PAJ. The MinE ring: an FtsZ-independent cell structure required for selection of the correct division site in *E. coli*. *Cell*. 1997; 91(5):685-694. doi: [10.1016/S0092-8674\(00\)80455-9](https://doi.org/10.1016/S0092-8674(00)80455-9).
- Raskin DM**, de Boer PAJ. MinDE-dependent pole-to-pole oscillation of division. *Journal of Bacteriology*. 1999; 181(20):6419-6424.
- Raskin DM**, de Boer PAJ. Rapid pole-to-pole oscillation of a protein required for directing division to the middle of *Escherichia coli*. *Proceedings of the National Academy of Sciences*. 1999 4; 96(9):4971-4976. <https://pnas.org/doi/full/10.1073/pnas.96.9.4971>, doi: [10.1073/pnas.96.9.4971](https://doi.org/10.1073/pnas.96.9.4971).
- Reid ST**, Terry KL, Casey PJ, Beese LS. Crystallographic analysis of CaaX prenyltransferases complexed with substrates defines rules of protein substrate selectivity. *Journal of Molecular Biology*. 2004; 343(2):417-433. doi: [10.1016/j.jmb.2004.08.056](https://doi.org/10.1016/j.jmb.2004.08.056).
- Renner LD**, Weibel DB. Cardiolipin microdomains localize to negatively curved regions of *Escherichia coli* membranes. *Proceedings of the National Academy of Sciences*. 2011; 108(15):6264-6269. <http://www.pnas.org/cgi/doi/10.1073/pnas.1015757108>, doi: [10.1073/pnas.1015757108](https://doi.org/10.1073/pnas.1015757108).
- Renner LD**, Weibel DB. MinD and MinE interact with anionic phospholipids and regulate division plane formation in *Escherichia coli*. *Journal of Biological Chemistry*. 2012; 287(46):38835-38844. doi: [10.1074/jbc.M112.407817](https://doi.org/10.1074/jbc.M112.407817).
- Rico AI**, Krupka M, Vicente M. In the beginning, *Escherichia coli* assembled the proto-ring: An initial phase of division. *Journal of Biological Chemistry*. 2013; 288(29):20830-20836. doi: [10.1074/jbc.R113.479519](https://doi.org/10.1074/jbc.R113.479519).
- Rowland SL**, Fu X, Sayed MA, Zhang Y, Cook WR, Rothfield LI. Membrane redistribution of the *Escherichia coli* MinD protein induced by MinE. *Journal of Bacteriology*. 2000; 182(3):613-619. doi: [10.1128/JB.182.3.613-619.2000](https://doi.org/10.1128/JB.182.3.613-619.2000).
- Rowlett VW**, Margolin W. The bacterial divisome: ready for its close-up. *Philosophical Transactions of the Royal Society B: Biological Sciences*. 2015; 370(1679):20150028. <http://rstb.royalsocietypublishing.org/lookup/doi/10.1098/rstb.2015.0028>, doi: [10.1098/rstb.2015.0028](https://doi.org/10.1098/rstb.2015.0028).
- Rubinstein B**, Slaughter BD, Li R. Weakly nonlinear analysis of symmetry breaking in cell polarity models. *Physical Biology*. 2012 8; 9(4):045006. <https://iopscience.iop.org/article/10.1088/1478-3975/9/4/045006>, doi: [10.1088/1478-3975/9/4/045006](https://doi.org/10.1088/1478-3975/9/4/045006).
- Sartorel E**, Unlu C, Jose M, Aurélie ML, Meca J, Sibarita JB, McCusker D. Phosphatidylserine and GTPase activation control Cdc42 nanoclustering to counter dissipative diffusion. *Molecular Biology of the Cell*. 2018; 29(11):1299-1310. doi: [10.1091/mbc.E18-01-0051](https://doi.org/10.1091/mbc.E18-01-0051).

- Savage NS**, Layton AT, Lew DJ. Mechanistic mathematical model of polarity in yeast. *Molecular Biology of the Cell*. 2012; 23(10):1998–2013. <http://www.molbiolcell.org/cgi/doi/10.1091/mbc.E11-10-0837>, doi: 10.1091/mbc.E11-10-0837.
- Schmidt TGM**, Batz L, Bonet L, Carl U, Holzapfel G, Kiem K, Matulewicz K, Niermeier D, Schuchardt I, Stanar K. Development of the Twin-Strep-tag® and its application for purification of recombinant proteins from cell culture supernatants. *Protein Expression and Purification*. 2013; 92(1):54–61. <http://dx.doi.org/10.1016/j.pep.2013.08.021>, doi: 10.1016/j.pep.2013.08.021.
- Schweizer J**, Loose M, Bonny M, Kruse K, Monch I, Schwille P. Geometry sensing by self-organized protein patterns. *Proceedings of the National Academy of Sciences*. 2012; 109(38):15283–15288. <http://www.pnas.org/cgi/doi/10.1073/pnas.1206953109>, doi: 10.1073/pnas.1206953109.
- Shahravan SH**, Qu X, Chan IS, Shin JA. Enhancing the specificity of the enterokinase cleavage reaction to promote efficient cleavage of a fusion tag. *Protein Expression and Purification*. 2008; 59(2):314–319. <https://www.ncbi.nlm.nih.gov/pmc/articles/PMC3624763/pdf/nihms412728.pdf>, doi: 10.1016/j.pep.2008.02.015.Enhancing.
- Shaner NC**, Lambert GG, Chammas A, Ni Y, Cranfill PJ, Baird MA, Sell BR, Allen JR, Day RN, Israelsson M, Davidson MW, Wang J. A bright monomeric green fluorescent protein derived from *Branchiostoma lanceolatum*. *Nature Methods*. 2013; 10(5):407–409. doi: 10.1038/nmeth.2413.
- Shih YL**, Fu X, King GF, Le T, Rothfield LI. Division site placement in *E. coli*: Mutations that prevent formation of the MinE ring lead to loss of the normal midcell arrest of growth of polar MinD membrane domains. *EMBO Journal*. 2002; 21(13):3347–3357. doi: 10.1093/emboj/cdf323.
- Shih YL**, Huang KF, Lai HM, Liao JH, Lee CS, Chang CM, Mak HM, Hsieh CW, Lin CC. The N-Terminal Amphipathic Helix of the Topological Specificity Factor MinE Is Associated with Shaping Membrane Curvature. *PLoS ONE*. 2011 6; 6(6):e21425. <https://dx.plos.org/10.1371/journal.pone.0021425>, doi: 10.1371/journal.pone.0021425.
- Shih YL**, Kawagishi I, Rothfield LI. The MreB and Min cytoskeletal-like systems play independent roles in prokaryotic polar differentiation. *Molecular Microbiology*. 2005; 58(4):917–928. doi: 10.1111/j.1365-2958.2005.04841.x.
- Shimada Y**, Gulli MP, Peter M. Nuclear sequestration of the exchange factor Cdc24p by Far1 regulates cell polarity during mating. *Nature Cell Biology*. 2000; 2:117–124. <https://doi-org.tudelft.idm.oclc.org/10.1038/35000073>.
- Shimada Y**, Wiget P, Gulli MP, Bi E, Peter M. The nucleotide exchange factor Cdc24p may be regulated by auto-inhibition. *EMBO Journal*. 2004; 23(5):1051–1062. doi: 10.1038/sj.emboj.7600124.
- Slaughter BD**, Smith SE, Li R. Symmetry Breaking in the Life Cycle of the Budding Yeast. *Cold Spring Harbor Perspectives in Biology*. 2009 9; 1(3):a003384–a003384. <http://cshperspectives.cshlp.org/lookup/doi/10.1101/cshperspect.a003384>, doi: 10.1101/cshperspect.a003384.
- Slaughter BD**, Das A, Schwartz JW, Rubinstein B, Li R. Dual Modes of Cdc42 Recycling Fine-Tune Polarized Morphogenesis. *Developmental Cell*. 2009; 17(6):823–835. <http://dx.doi.org/10.1016/j.devcel.2009.10.022>, doi: 10.1016/j.devcel.2009.10.022.
- Slaughter BD**, Unruh JR, Das A, Smith SE, Rubinstein B, Li R. Non-uniform membrane diffusion enables steady-state cell polarization via vesicular trafficking. *Nature Communications*. 2013 6; 4(1):1380. <http://www.nature.com/articles/ncomms2370>, doi: 10.1038/ncomms2370.
- Sloat BF**, Adams A, Pringle JR. Roles of the CDC24 gene product in cellular morphogenesis during the *Saccharomyces cerevisiae* cell cycle. *Journal of Cell Biology*. 1981; 89(3):395–405. doi: 10.1083/jcb.89.3.395.
- Smith GR**, Givan SA, Cullen P, Sprague GF. GTPase-Activating Proteins for Cdc42. *Eukaryotic Cell*. 2002 6; 1(3):469–480. <https://journals.asm.org/doi/10.1128/EC.1.3.469-480.2002>, doi: 10.1128/EC.1.3.469-480.2002.

- Smith SE**, Rubinstein B, Pinto IM, Slaughter BD, Unruh JR, Li R, Mendes Pinto I, Slaughter BD, Unruh JR, Li R, Pinto IM, Slaughter BD, Unruh JR, Li R. Independence of symmetry breaking on Bem1-mediated autocatalytic activation of Cdc42. *Journal of Cell Biology*. 2013; 202(7):1091–1106. <http://www.ncbi.nlm.nih.gov/pubmed/24062340>, doi: 10.1083/jcb.201304180.
- Stevenson BJ**, Ferguson B, De Virgilio C, Bi E, Pringle JR, Ammerer G, Sprague Jr GF. Mutation of RGA1, which encodes a putative GTPase-activating protein for the polarity-establishment protein Cdc42p, activates the pheromone-response pathway in the yeast *Saccharomyces cerevisiae*. *Genes and Development*. 1995; 9(23):2949–2963. <http://www.ncbi.nlm.nih.gov/pubmed/7498791>.
- Studier FW**. Protein production by auto-induction in high density shaking cultures. *Protein expression and purification*. 2005; 41(1):207–234. doi: 10.1016/j.pep.2005.01.016.
- Studier FW**, Moffatt BA. Use of bacteriophage T7 RNA polymerase to direct selective high-level expression of cloned genes. *Journal of Molecular Biology*. 1986 5; 189(1):113–130. <https://linkinghub.elsevier.com/retrieve/pii/0022283686903852>, doi: 10.1016/0022-2836(86)90385-2.
- Suefuji K**, Valluzzi R, RayChaudhuri D. Dynamic assembly of MinD into filament bundles modulated by ATP, phospholipids, and MinE. *Proceedings Of The National Academy Of Sciences Of The United States Of America*. 2002; 99(26):16776–16781. doi: 10.1073/pnas.262671699.
- Sugase K**, Landes MA, Wright PE, Martinez-Yamout M. Overexpression of post-translationally modified peptides in *Escherichia coli* by co-expression with modifying enzymes. *Protein Expression and Purification*. 2008; 57(2):108–115. doi: 10.1016/j.pep.2007.10.018.
- Szeto TH**, Rowland SL, Habrukowich CL, King GF. The MinD membrane targeting sequence is a transplantable lipid-binding helix. *Journal of Biological Chemistry*. 2003; 278(41):40050–40056. doi: 10.1074/jbc.M306876200.
- Szeto TH**, Rowland SL, King GF. The dimerization function of MinC resides in a structurally autonomous C-terminal domain. *Journal of Bacteriology*. 2001; 183(22):6684–6687. doi: 10.1128/JB.183.22.6684-6687.2001.
- They M**, Racine V, Piel M, Pépin A, Dimitrov A, Chen Y, Sibarita JB, Bornens M. Anisotropy of cell adhesive microenvironment governs cell internal organization and orientation of polarity. *Proceedings of the National Academy of Sciences of the United States of America*. 2006; 103(52):19771–19776. doi: 10.1073/pnas.0609267103.
- Tostevin F**, Howard M. A stochastic model of Min oscillations in *Escherichia coli* and Min protein segregation during cell division. *Physical Biology*. 2006; 3(1):1–12. doi: 10.1088/1478-3975/3/1/001.
- Touhami A**, Jericho M, Rutenberg AD. Temperature Dependence of MinD Oscillation in *Escherichia coli* : Running Hot and Fast. *Journal of Bacteriology*. 2006; 188(21):7661–7667. doi: 10.1128/JB.00911-06.
- Turing AM**. The Chemical Basis of Morphogenesis. *Philosophical Transactions of the Royal Society of London*. 1952; 237(641):37–72. <http://links.jstor.org/sici?sici=0080-4622%2819520814%29237%3A641%3C37%3ATCBOM%3E2.0.CO%3B2-I>.
- Van Meer G**, Voelker DR, Feigenson GW. Membrane lipids: Where they are and how they behave. *Nature Reviews Molecular Cell Biology*. 2008; 9(2):112–124. doi: 10.1038/nrm2330.
- Varma A**, Huang KC, Young KD. The Min system as a general cell geometry detection mechanism: Branch lengths in Y-shaped *Escherichia coli* cells affect Min oscillation patterns and division dynamics. *Journal of Bacteriology*. 2008; 190(6):2106–2117. doi: 10.1128/JB.00720-07.
- Vecchiarelli AG**, Li M, Mizuuchi M, Hwang LC, Seol Y, Neuman KC, Mizuuchi K. Membrane-bound MinDE complex acts as a toggle switch that drives Min oscillation coupled to cytoplasmic depletion of MinD. *Proceedings of the National Academy of Sciences*. 2016; 113(11):E1479–E1488. <http://www.pnas.org/lookup/doi/10.1073/pnas.1600644113>, doi: 10.1073/pnas.1600644113.

- Vecchiarelli AG**, Li M, Mizuuchi M, Mizuuchi K. Differential affinities of MinD and MinE to anionic phospholipid influence Min patterning dynamics in vitro. *Molecular Microbiology*. 2014; 93(3):453–463. doi: [10.1111/mmi.12669](https://doi.org/10.1111/mmi.12669).
- Vendel KJA**, Tschirpke S, Shamsi F, Dogterom M, Laan L. Minimal in vitro systems shed light on cell polarity. *Journal of Cell Science*. 2019; 132(4):1–21. doi: [10.1242/jcs.217554](https://doi.org/10.1242/jcs.217554), doi: [10.1242/jcs.217554](https://doi.org/10.1242/jcs.217554).
- Vicente M**, Rico AI. The order of the ring: Assembly of Escherichia coli cell division components. *Molecular Microbiology*. 2006; 61(1):5–8. doi: [10.1111/j.1365-2958.2006.05233.x](https://doi.org/10.1111/j.1365-2958.2006.05233.x).
- Watson LJ**, Rossi G, Brennwald P. Quantitative analysis of membrane trafficking in regulation of Cdc42 polarity. *Traffic*. 2014; 15(12):1330–1343. doi: [10.1111/tra.12211](https://doi.org/10.1111/tra.12211).
- Wedlich-Soldner R**, Li R. Spontaneous cell polarization: undermining determinism. *Nature Cell Biology*. 2003 4; 5(4):267–270. <http://www.ncbi.nlm.nih.gov/pubmed/12669070><http://www.nature.com/articles/ncb0403-267>, doi: [10.1038/ncb0403-267](https://doi.org/10.1038/ncb0403-267).
- Wedlich-Soldner R**, Wai SC, Schmidt T, Li R. Robust cell polarity is a dynamic state established by coupling transport and GTPase signaling. *Journal of Cell Biology*. 2004 9; 166(6):889–900. <https://rupress.org/jcb/article/166/6/889/51279/Robust-cell-polarity-is-a-dynamic-state>, doi: [10.1083/jcb.200405061](https://doi.org/10.1083/jcb.200405061).
- WEDLICHOLDNER R**, LI R. Closing the loops: new insights into the role and regulation of actin during cell polarization. *Experimental Cell Research*. 2004 11; 301(1):8–15. <http://www.ncbi.nlm.nih.gov/pubmed/15501439><https://linkinghub.elsevier.com/retrieve/pii/S0014482704004562>, doi: [10.1016/j.yexcr.2004.08.011](https://doi.org/10.1016/j.yexcr.2004.08.011).
- Wessel D**, Flügge UI. A method for the quantitative recovery of protein in dilute solution in the presence of detergents and lipids. *Analytical Biochemistry*. 1984; 138(1):141–143. doi: [10.1016/0003-2697\(84\)90782-6](https://doi.org/10.1016/0003-2697(84)90782-6).
- Wettmann L**, Kruse K. The Min-protein oscillations in Escherichia coli : an example of self-organized cellular protein waves. *Philosophical Transactions of the Royal Society B: Biological Sciences*. 2018 5; 373(1747):20170111. <https://royalsocietypublishing.org/doi/10.1098/rstb.2017.0111>, doi: [10.1098/rstb.2017.0111](https://doi.org/10.1098/rstb.2017.0111).
- Williams CL**. The polybasic region of Ras and Rho family small GTPases: a regulator of protein interactions and membrane association and a site of nuclear localization signal sequences. *Cellular Signalling*. 2003 12; 15(12):1071–1080. <https://linkinghub.elsevier.com/retrieve/pii/S0898656803000986>, doi: [10.1016/S0898-6568\(03\)00098-6](https://doi.org/10.1016/S0898-6568(03)00098-6).
- Witte K**, Strickland D, Glotzer M. Cell cycle entry triggers a switch between two modes of Cdc42 activation during yeast polarization. *eLife*. 2017 7; 6:1–27. <https://elifesciences.org/articles/26722>, doi: [10.7554/eLife.26722](https://doi.org/10.7554/eLife.26722).
- Woods B**, Lai H, Wu CF, Zyla TR, Savage NS, Lew DJ. Parallel Actin-Independent Recycling Pathways Polarize Cdc42 in Budding Yeast. *Current Biology*. 2016; 26(16):2114–2126. doi: [10.1016/j.cub.2016.06.047](https://doi.org/10.1016/j.cub.2016.06.047).
- Wu CF**, Lew DJ. Beyond symmetry-breaking: competition and negative feedback in GTPase regulation. *Trends in Cell Biology*. 2013 10; 23(10):476–483. <https://linkinghub.elsevier.com/retrieve/pii/S096289241300086X>, doi: [10.1016/j.tcb.2013.05.003](https://doi.org/10.1016/j.tcb.2013.05.003).
- Wu F**, Halatek J, Reiter M, Kingma E, Frey E, Dekker C. Multistability and dynamic transitions of intracellular Min protein patterns. *Molecular Systems Biology*. 2016 6; 12(6):873. <http://msb.embopress.org/lookup/doi/10.15252/msb.20156724>, doi: [10.15252/msb.20156724](https://doi.org/10.15252/msb.20156724).
- Wu F**, Van Schie BGC, Keymer JE, Dekker C. Symmetry and scale orient Min protein patterns in shaped bacterial sculptures. *Nature Nanotechnology*. 2015; 10(8):1–8. doi: [10.1038/nnano.2015.126](https://doi.org/10.1038/nnano.2015.126).
- Wu LJ**, Errington J. Nucleoid occlusion and bacterial cell division. *Nature Reviews Microbiology*. 2012; 10(1):8–12. <http://dx.doi.org/10.1038/nrmicro2671>, doi: [10.1038/nrmicro2671](https://doi.org/10.1038/nrmicro2671).

- Zhang B**, Zhang Y, Wang ZX, Zheng Y. The role of Mg²⁺ cofactor in the guanine nucleotide exchange and GTP hydrolysis reactions of Rho family GTP-binding proteins. *Journal of Biological Chemistry*. 2000; 275(33):25299–25307. doi: [10.1074/jbc.M001027200](https://doi.org/10.1074/jbc.M001027200).
- Zhang B**, Gao Y, Moon SY, Zhang Y, Zheng Y. Oligomerization of Rac1 GTPase Mediated by the Carboxyl-terminal Polybasic Domain. *Journal of Biological Chemistry*. 2001; 276(12):8958–8967. <http://dx.doi.org/10.1074/jbc.M008720200>, doi: [10.1074/jbc.M008720200](https://doi.org/10.1074/jbc.M008720200).
- Zhang B**, Wang ZX, Zheng Y. Characterization of the interactions between the small GTPase Cdc42 and its GTPase-activating proteins and putative effectors: Comparison of kinetic properties of Cdc42 binding to the Cdc42-interactive domains. *Journal of Biological Chemistry*. 1997; 272(35):21999–22007. doi: [10.1074/jbc.272.35.21999](https://doi.org/10.1074/jbc.272.35.21999).
- Zhang B**, Zhang Y, Collins CC, Johnson DI, Zheng Y. A built-in arginine finger triggers the self-stimulatory GTPase-activating activity of Rho family GTPases. *Journal of Biological Chemistry*. 1999; 274(5):2609–2612. doi: [10.1074/jbc.274.5.2609](https://doi.org/10.1074/jbc.274.5.2609).
- Zhang B**, Zheng Y. Negative regulation of Rho family GTPases Cdc42 and Rac2 by homodimer formation. *Journal of Biological Chemistry*. 1998; 273(40):25728–25733. doi: [10.1074/jbc.273.40.25728](https://doi.org/10.1074/jbc.273.40.25728).
- Zheng Y**, Bender A, Cerione RA. Interactions among proteins involved in bud-site selection and bud-site assembly in *Saccharomyces cerevisiae*. *Journal of Biological Chemistry*. 1995; 270(2):626–630. <http://www.ncbi.nlm.nih.gov/pubmed/7822288>.
- Zheng Y**, Cerione R, Bender A. Control of the yeast bud-site assembly GTPase Cdc42. Catalysis of guanine nucleotide exchange by Cdc24 and stimulation of GTPase activity by Bem3. *J Biol Chem*. 1994; 269(4):2369–2372. <http://www.ncbi.nlm.nih.gov/pubmed/8300560>.
- Zheng Y**, Harts MJ, Shinjosq K, Evansn T, Benderll A, Ceriones Ra. Biochemical Comparisons of the *Saccharomyces cerevisiae* Bem2 and Bem3 Proteins. *Journal of Biological Chemistry*. 1993; 268(33):24629–24634. [https://doi.org/10.1016/S0021-9258\(19\)74512-8](https://doi.org/10.1016/S0021-9258(19)74512-8).
- Zieske K**, Chwastek G, Schwille P. Protein Patterns and Oscillations on Lipid Monolayers and in Microdroplets. *Angewandte Chemie - International Edition*. 2016; 55(43):13455–13459. doi: [10.1002/anie.201606069](https://doi.org/10.1002/anie.201606069).
- Zieske K**, Schwille P. Reconstitution of pole-to-pole oscillations of min proteins in microengineered polydimethylsiloxane compartments. *Angewandte Chemie - International Edition*. 2013; 52(1):459–462. doi: [10.1002/anie.201207078](https://doi.org/10.1002/anie.201207078).
- Zieske K**, Schwille P. Reconstitution of self-organizing protein gradients as spatial cues in cell-free systems. *eLife*. 2014 10; 3:e03949. <https://elifesciences.org/articles/03949>, doi: [10.7554/eLife.03949](https://doi.org/10.7554/eLife.03949).
- Zinser E**, Sperka-Gottlieb CDM, Fasch EV, Kohlwein SD, Paltauf F, Daum G. Phospholipid synthesis and lipid composition of subcellular membranes in the unicellular eukaryote *Saccharomyces cerevisiae*. *Journal of Bacteriology*. 1991; 173(6):2026–2034. doi: [10.1128/jb.173.6.2026-2034.1991](https://doi.org/10.1128/jb.173.6.2026-2034.1991).

Acknowledgements

I'm not my best self when things are going the best or when things are going really badly. When things are going really, really well, I'm not my best self because my ego can get in the way. And when things are going really badly, I'm not my best self because my fear is getting in the way.

— Scott Belsky

Thank you
BN and
all former
& current
Laan-
lab
members:



Liedewij



Werner



Leila



Enzo



Marieke



Esangül



Christine



Miranda



Daphne



Julia



Renske



Ingar



Constant



Maaike



Laurie



Keije



Bram



Ezra



Albert



Pam

Thank you
to our
collaborators:



dr.
Rienk
Eelkema



Benjamin



Prof.
dr.
Erwin Frey



Laeschkin

Thank you
to my
committee:



dr.
L. Laan



dr.
A. Jakobi



dr. R.
Eelkema



Prof.
dr. M.
Loose

Thank
you!



Prof.
dr. Jan
Lipfert



NWO









friends
&
family



you!

 Ramon
  Fayerzeh
  Frank
  Shazia
  Nynke
  Els




 Reza
  Gregory
  Caspar
  Eveline
  Mathia
  Vlad

 Floor
  Valentina
  Thomas
  Wessel
  Zaida
  Thijs

 Aisha
  Antoine
  Germain
  Rosanne
  Pam
  Ilse

 Buddy
  all technicians @BN
  BN secretaries
  building personal
  all BN!

 Fridjof
  dr. Arjen Jakobi
  Cecilia
  Stefan
  Tanja

 Prof. dr. c. Dakker
  Prof. dr. E. Frey.
  Prof. dr. G. Koenderink



This work is not my work alone, and emerged due to the effort of many people:

Thank you Liedewij, for letting me embark on this journey, your many many ideas, support for my artistic and organisational endeavours, and your limitless optimism. Thank you for encouraging me to be more of my peculiar self and for letting me say no as often as I did.

Thank you to our collaborators:

Thank you dr. Rienk Elkeema and Benjamin, for creating the farnesyl peptide molecule we were in dire need of, it helped us address a the great challenge of Cdc42 prenylation. It's still not fully solved, but with your help we're on our way!

Thank you to the group of dr. Arjen Jakobi - to Arjen, Cecilia, Tanja, and Stefan - for your many, many ideas on and help with protein prenylation, dimerisation, GTPase activity, and other protein-related things.

Thank you Prof. dr. Erwin Frey, Laeschkir and Fridtjof, for explaining how the model our system is based on works, how to do a linear stability analysis and simulate the system in Comsol. I did not get far enough to fully utilise these skills, but it greatly helped my understanding of the system and will be of use in the future.

Thank you to the current and former members of the Laan-Lab: Thank you Liedewij, Leila, Enzo, Werner, Fayeze, Ramon, Frank, Shazia, Marieke, Nynke, Esengül, Els, Christine, Reza, Miranda, Gregory, Caspar, Eveline, Mathia, Vlad, Julia, Renske, Daphne, Valentina, Ingmar, Thomas, Floor, Wessel, Zaida, Thijs, Constant, Maaïke, Laurie, Keije, Aisha, Antoine, Germain, Rosanne, Pam, Ilse, Bram, Ezra, Albert, Pim, and Buddy, for the good times and open atmosphere.

Thank you Werner, for your in-depth knowledge about the yeast polarity system and the *in vivo* literature, for building a way more elaborate model for my *in vitro* data than I could have ever done, and for all the wonderful recommendations in Rotterdam.

Thank you Esengül, for showing me around and knowing everything about the department.

Thank you Marieke, for picking up the Buddy project and keeping it alive, and for joining me build him such a nice tiny lab.

Thank you to the *in vitro* group of the lab:

Thank you Fayeze, for pioneering the project and teaching me the basics of protein purification.

Thank you Ramon, for your no-question-is-a-bad-question attitude and help with all the big and small problems.

Thank you Shazia, for doing the microscopy part of this project, your amazing food, a couch in Delft, and the beautiful cover art.

Thank you Frank, for picking up the protein purification and keeping it going.

Thank you Nynke, for taking over the project. This baby is yours now, I hope it will develop well. I wish you best of luck (you might need some ;))!

Thank you to my students - Vlad, Julia, Daphne, and Renske - for sharing my interest, your eager to learn, and your contribution to the project.

Thank you BN, for the open and collaborative atmosphere.

Thank you to the technicians of BN: Thank you Theo, Eli, Ramon, and Cecilia, for helping me with the AKTA and other project issues. Thank you Jan and Anke, and all the other people involved, for keeping the machines and labs running. Thank you for keeping the shelves refilled, LB autoclaved, and all the other invisible things you are doing.

Thank you to the secretaries, for keeping BN and Liedewij organised and for planning Quo Vadis, the Kavli day, and other activities for us.

Thank you Joyce, and all other staff, for keeping the building in a nice state.

Thank you to my committee: Thank you dr. ir. L. Laan, dr. A. Jacobi, dr. R. Eelkema, Prof. dr. E. Frey, Prof. dr. M. Loose, Prof. dr. C. Dekker, and Prof. dr. G. H. Koenderink, for your time and effort in reading my manuscript, giving comments, and attending the defence.

Thank you dr. Jan Lipfert, for encouraging me to reach out to groups in Delft at the time I was looking for a PhD position, I am more than happy that I came here.

Thank you NWO for funding this project.

Thank you to my friends and family, and to *you* - whom I haven't mentioned yet.

Thank you for indulging me.

List of Publications

In this thesis

1. Kim J. A. Vendel*, **Sophie Tschirpke***, Fayeze Shamsi, Marileen Dogterom, Liedewij Laan, Minimal *in vitro* systems shed light on cell polarity, *J. Cell Sci.* **132** (2019).
* equally contributing authors

Other

1. Franziska Kriegel, Christian Matek, Tomas Drsata, Klara Kulenkampff, **Sophie Tschirpke**, Martin Zacharias, Filip Lankas, Jan Lipfert, The temperature dependence of the helical twist of DNA, *Nucleic Acids Res.* **46** (2018).

